

SOFT-COLLINEAR FACTORIZATION AND SUDAKOV
RESUMMATION OF HEAVY MESON DECAY
AMPLITUDES WITH EFFECTIVE FIELD THEORIES

A Dissertation

Presented to the Faculty of the Graduate School

of Cornell University

in Partial Fulfillment of the Requirements for the Degree of

Doctor of Philosophy

by

Björn Olaf Lange

January 2005

© 2005 Björn Olaf Lange

ALL RIGHTS RESERVED

SOFT-COLLINEAR FACTORIZATION AND SUDAKOV RESUMMATION OF
HEAVY MESON DECAY AMPLITUDES WITH EFFECTIVE FIELD
THEORIES

Björn Olaf Lange, Ph.D.

Cornell University 2005

Decays of the B meson into light and energetic particles are discussed. The calculation of the corresponding decay amplitudes is non-trivial in many respects. Strong interaction effects are always present and cannot be computed reliably using analytic techniques. However, besides the intrinsic energy scale Λ_{QCD} of Quantum Chromo Dynamics, there also exists a much larger scale, the b -quark mass m_b , at which perturbation theory can be applied. QCD-factorization is the idea of separating the contributions that arise at these different scales and performing a systematic expansion in the ratio Λ_{QCD}/m_b . Hard processes at the large scale can be computed using perturbation theory, while soft processes are encoded in non-perturbative structure functions. The observation that for many decay modes the same structure functions are needed make this a useful approach. However, factorization theorems need to be proved for every single decay, since some amplitudes do not factorize. The intent of this thesis is to study examples of factorizable and non-factorizable amplitudes in a systematic framework, by using effective field theory techniques.

The advancing precision of experimental measurements of B -decays make it necessary to improve the accuracy of theoretical predictions. To achieve this, it is

necessary to perform a resummation of Sudakov logarithms, which enter at every non-trivial order in perturbation theory.

In this thesis we present an introduction to Soft-Collinear Effective Theory, which can be used to prove (or disprove) factorization theorems to all orders in the strong coupling constant for some B decays into light and energetic particles. Specifically, the factorizable amplitudes for inclusive $B \rightarrow X_u l^- \bar{\nu}$ and exclusive $B^- \rightarrow \gamma l^- \bar{\nu}$ are calculated in renormalization-group improved perturbation theory to first non-trivial order. Form factors encoding the exclusive decay amplitudes for $\bar{B} \rightarrow P l^- \bar{\nu}$ and $B \rightarrow V l^- \bar{\nu}$ (P = light pseudoscalar meson, V = light vector meson) are studied and proved to be dominated by the non-factorizable Feynman mechanism.

BIOGRAPHICAL SKETCH

Bjorn O. Lange was born in Minden, Germany on the 24th of September, 1974, as the second son of the primary school teacher Christa Lange and the patent attorney Gerd Lange. He attended the primary school “Bierpohlschule” for four years, starting in 1981, and continued his education at the “Besselgymnasium” in Minden. In 1994 he graduated with the “Abitur” at the top of his class and was awarded the “Besselpreis” for extra-curriculum activities. After spending twelve months as a navigator in the German navy in fulfillment of his military service duties, he began his academic education at the university of Heidelberg, Germany, where he studied Physics. In 1998 he was awarded one year of full scholarship at Cornell University, where he enrolled in the PhD physics program on a non-degree status in the academic year 1998/99. After his return to Germany he finished the program in Heidelberg and received the degree “Diplom-Physiker” in 2001. In the fall of that year he came to Cornell as a regular graduate student. This document is the outcome of that course of action.

ACKNOWLEDGEMENTS

Many thanks to my collaborators of the past three years: Thomas Becher, Stefan Bosch, Richard Hill, Matthias Neubert, and Gil Paz. Much of the content of this thesis has been found in teamwork, and I am deeply indebted to them. I am especially grateful to my advisor Matthias Neubert for his encouragement, support, patience, and, most of all, for being an outstanding teacher.

The research has been supported by the National Science Foundation under Grant PHY-0098631.

TABLE OF CONTENTS

| | | |
|----------|-------------------------------|----------|
| 1 | Introduction | 1 |
| 1.1 | Preface | 1 |
| 1.2 | Methodology | 4 |
| 1.3 | Structure of Thesis | 8 |

Theory

| | | |
|----------|---|-----------|
| 2 | Soft-Collinear Effective Theory | 13 |
| 2.1 | General Considerations | 13 |
| 2.2 | Renormalization | 22 |
| 2.3 | SCET _I | 25 |
| 2.3.1 | Power Counting | 26 |
| 2.3.2 | Wilson lines | 29 |
| 2.3.3 | Gauge Transformations | 32 |
| 2.3.4 | Heavy-to-Collinear Currents | 33 |
| 2.4 | SCET _{II} | 36 |
| 2.4.1 | Gauge Transformations and Interaction Terms | 39 |
| 2.4.2 | Currents | 43 |
| 2.4.3 | Four-quark Operators | 50 |
| 2.4.4 | Decoupling transformation | 53 |
| 2.5 | Reparameterization Invariance | 56 |
| 3 | Structure Functions | 59 |
| 3.1 | The B -meson Light-Cone Distribution Amplitudes | 59 |
| 3.1.1 | Renormalization-Group Evolution | 62 |
| 3.1.2 | Asymptotic behaviour | 65 |
| 3.2 | The Shape Function | 67 |
| 3.2.1 | Renormalization-Group Evolution | 69 |
| 3.2.2 | Properties of the shape function | 76 |
| 3.2.3 | Moments of the scheme-independent function $\hat{S}(\hat{\omega}, \mu)$ | 81 |

Phenomenological Applications

| | | |
|----------|--|-----------|
| 4 | Inclusive Semileptonic Decays | 83 |
| 4.1 | Factorization theorem | 84 |
| 4.2 | Matching calculations | 88 |
| 4.2.1 | Hard functions | 89 |
| 4.2.2 | Jet function | 91 |
| 4.3 | Sudakov resummation | 92 |
| 4.4 | Differential decay rates and spectra | 95 |

| | | |
|----------|---|------------|
| 4.4.1 | Charged-lepton energy spectrum | 99 |
| 4.4.2 | Hadronic \mathbf{P}_+ spectrum | 101 |
| 4.4.3 | Hadronic invariant mass spectrum | 102 |
| 4.4.4 | Combined cuts on hadronic and leptonic invariant mass . . . | 104 |
| 4.5 | Model-independent relations between spectra | 106 |
| 4.6 | Numerical results | 108 |
| 4.6.1 | Shape-function mass and kinetic energy | 109 |
| 4.6.2 | Model shape functions | 110 |
| 4.6.3 | Predictions for decay spectra and event fractions | 112 |
| 4.7 | Charm background | 120 |
| 4.8 | Theoretical accuracy of a $ \mathbf{V}_{ub} $ measurement | 123 |
| 5 | Exclusive Radiative Decays | 127 |
| 5.1 | Proof of factorization | 129 |
| 5.2 | Calculation of the hard-scattering kernel | 133 |
| 5.3 | Resummation of large logarithms | 135 |
| 6 | Exclusive Semileptonic Decays | 142 |
| 6.1 | Heavy-to-light form factors at large recoil | 142 |
| 6.2 | Spin-symmetry and factorization | 145 |
| 6.3 | Matching calculations | 148 |
| 6.3.1 | Spin-symmetric contributions | 149 |
| 6.3.2 | Spin-symmetry breaking contributions | 158 |
| 6.4 | Physics of endpoint singularities – a toy model | 159 |
| 6.5 | Soft-collinear messengers and the soft overlap | 165 |
| 6.6 | Operator mixing and Sudakov logarithms | 170 |
| 6.7 | Factorization of spin-symmetry breaking effects | 176 |
| 7 | Conclusion | 178 |
| A | List of Abbreviations and Acronyms | 183 |
| | Bibliography | 184 |

LIST OF TABLES

| | | |
|-----|--|-----|
| 2.1 | Nomenclature for various momentum modes in SCET | 18 |
| 4.1 | Parameters and moments of the model shape functions at the intermediate scale. | 112 |
| 4.2 | Numerical predictions of event fractions for different experimental cuts. | 118 |
| 6.1 | Matching of flavor-changing currents from QCD onto SCET. | 150 |

LIST OF FIGURES

| | | |
|------|---|-----|
| 2.1 | An example for the method of regions. | 19 |
| 2.2 | Corresponding effective theory diagrams | 21 |
| 2.3 | One-loop SCET current diagrams. | 47 |
| 2.4 | One-loop SCET four-quark operator diagrams | 52 |
| 3.1 | One-loop diagrams for the calculation of the anomalous dimension of the B -meson light-cone distribution amplitude. | 63 |
| 3.2 | Left: The cusp in the Wilson line. Right: Poles in the complex plane | 66 |
| 3.3 | One-loop diagrams for the shape-function operator. | 69 |
| 4.1 | One-loop SCET diagrams of the forward current correlator. | 90 |
| 4.2 | Hadronic phase space for the light-cone variables P_- and P_+ | 97 |
| 4.3 | Phase-space constraints and weight functions for combined cuts on the hadronic and leptonic invariant mass | 105 |
| 4.4 | Weight function in the prototype relation | 108 |
| 4.5 | Shape function models under variation of its parameter settings. | 113 |
| 4.6 | Renormalization-group evolution of a model shape function. | 113 |
| 4.7 | Event fractions for a P_+ cut and for a hadronic invariant mass cut. | 114 |
| 4.8 | Event fraction for a cut on the charged-lepton energy. | 115 |
| 4.9 | Various different functional forms for the shape function. | 117 |
| 4.10 | Event fractions and charm background in a single plot. | 121 |
| 5.1 | One-loop diagrams in QCD | 133 |
| 5.2 | One-loop diagrams in SCET. | 134 |
| 5.3 | Sudakov resummation for the hard-scattering kernel. | 140 |
| 6.1 | Gluon exchange contributions to heavy-to-light form factors. | 143 |
| 6.2 | Diagrams with an extra gluon. | 156 |
| 6.3 | Subgraph study of endpoint singularities. | 160 |
| 6.4 | Endpoint singularities in a toy model. | 165 |
| 6.5 | An artist's view of the soft-collinear messenger contribution to the form factors. | 168 |
| 6.6 | Energy dependence of the Wilson coefficients $C_i(E, \mu)$ at next-to- leading order in RG-improved perturbation theory. | 176 |

CHAPTER 1

INTRODUCTION

1.1 Preface

The conscious and active interplay between the observation of Nature and its mathematical description is at the core of the physical sciences since the 16th century. In the quest of finding the ever-more fundamental processes, this interplay has led to emergence of the “Standard Model” in the second half of the 20th century. Our current theoretical understanding of elementary processes at energies testable through terrestrial experiments is based on the description within quantum field theories in combination with the gauge principle. The effects of electromagnetic, weak and strong nuclear forces through which the matter, quarks and leptons, interacts, is captured in a quantum field theory which is invariant under the gauge group $SU(3)_C \times SU(2)_L \times U(1)_Y$. The electromagnetic and weak forces are unified in the gauge group $SU(2)_L \times U(1)_Y$ around the energy scale of roughly 100 GeV. Below the electroweak scale this gauge group is spontaneously broken down to $U(1)_{\text{em}}$, which is the group of Quantum Electro Dynamics, and the W^\pm and Z bosons mediating the weak interactions become massive. In the most simple mechanism that breaks the electroweak symmetry, the Higgs mechanism or Glashow-Weinberg-Salam Model, masses are also given to quarks and leptons. Fermion masses are generated through Yukawa interactions with the Higgs field. Using global unitary transformations in flavor space, the Yukawa interactions are diagonalized to obtain the physical mass eigenstates. It can be chosen such that all up-type quarks (up, charm, top) are not rotated in flavor space, whereas the weak eigenstates of the down-type quarks (down, strange, bottom) are related to the mass eigenstates

through the unitary matrix V_{CKM} . Numerically, the Cabbibo-Kobayashi-Maskawa matrix V_{CKM} is found to be almost diagonal, as the non-diagonal entries, that allow for transitions between quarks of different generations, are small. Such transitions are mediated by the weak currents. Since the W^\pm and Z bosons have masses very close to the electroweak scale, it is possible to construct an effective theory for weak processes far below this scale. This theory is called the Fermi theory of weak interactions, or the weak effective Hamiltonian.

The theory of strong interactions is Quantum Chromo Dynamics (QCD), the non-abelian gauge theory of $SU(3)_C$. The condition to be renormalizable determines the Lagrangian (almost entirely) to be

$$\mathcal{L}_{\text{QCD}} = \sum_{\psi=u,d,\dots} \bar{\psi}(i\not{D} - m_\psi)\psi - \frac{1}{4} G_{\mu\nu}^a G^{a,\mu\nu}, \quad (1.1)$$

where $iD^\mu = i\partial^\mu + g_s A^\mu$ is the covariant derivative. We have suppressed any spinor indices and the color index a on the gluon field $A_\mu = A_\mu^a T^a$, which reflects the fact that it is a color-octet. The gluon field strength is $G_{\mu\nu}^a = \partial_\mu A_\nu^a - \partial_\nu A_\mu^a + g_s f^{abc} A_\mu^b A_\nu^c$. Finally, the generators of $SU(N)$ are denoted by t^a with $a = 1, \dots, N^2 - 1$, f^{abc} are the structure constants, and g_s is the strong coupling constant. Every procedure to renormalize the theory necessitates the introduction of a dimensionful parameter μ . It is generally thought of as the energy scale at which the theory is defined. The dependence of various quantities in the theory on this scale is governed by renormalization-group equations (RGEs), which can be calculated in perturbatively as long as the coupling is reasonably small compared to unity. Qualitatively, the strong coupling “constant” $g_s(\mu)$ is large for values of μ around the intrinsic QCD scale $\Lambda_{\text{QCD}} \sim 0.5 \text{ GeV}$, and tends asymptotically to zero for increasing μ . This effect is in contrast to the other sectors of the Standard Model and reflects the fact that quarks are confined in hadrons for low scales, but are “asymptotically

free” for highly energetic processes such as deep inelastic scattering at scales much larger than Λ_{QCD} .

All of the above is standard class-work and text-book material, which is why we do not feel the need to cite [1] and discuss the original works in great detail here.

Corrections to the Standard Model, generally referred to as “New Physics”, can be searched for in two complementary ways: in direct searches where new particles are produced and observed, or in indirect searches in which new particles enter as quantum corrections. The former method is obviously a very effective way to find New Physics, albeit a formidable financial endeavor. Indirect searches, on the other hand, require both precision measurements on the experimental side, as well as a level of theoretical Standard Model predictions that compares well with the experimental uncertainties. Only if both sides of the scientific medallion, the observation of Nature through High-Energy Experiments and its mathematical description within the Standard Model, are met with equal precision can we conclude on the validity of the underlying theory.

Needless to say, the knowledge of the parameter values entering the Standard Model is crucial for theoretical predictions to be reliable. The flavor sector is in this respect very challenging. In particular, the smallest of the CKM matrix elements, V_{ub} and V_{td} , are least well known, but are responsible for a wealth of phenomena, such as \mathcal{CP} violation. In general, the flavor sector of the Standard Model displays a broad spectrum of phenomena and mechanisms that need to be understood in order to engage in indirect searches for New Physics. Primarily one is interested in the study of flavor-changing heavy quark decays, which are governed by the weak interactions. However, it is the strong force that is responsible for the formation of

the hadrons that can be observed in experiments. The B meson is a unique system in that it is the simplest hadron containing a heavy quark. Simple, because it is a bound state of only one heavy and one light (anti-) quark. A heavy quark is favorable for New Physics searches, because flavor-changing processes from heavy particles of the third family to light particles of the first two families are very rare. If the Standard Model predicts a quantity to be small or even vanishing, the chances of observing New Physics are more pronounced. Even though top quarks are by far the heaviest, they are less suitable because they decay before hadronization can occur.

The broader aim of the “ B -physics community” is the study of weak decays of B mesons and the interpretation of the data collected at dedicated B factories, such as the BaBar, Belle and CLEO experiments. The major goals are to test the Standard Model, extract its fundamental parameters, explore the phenomenon of \mathcal{CP} violation, and to search for New Physics at higher energies. This quest will continue in the future with the help of the Large Hadron Collider and the LHCb detector in particular, as well as BTeV and possible High-Luminosity B factories. The theoretical challenge is the development and application of tools that enable us to control the effects from strong interactions. These theoretical tools include effective field theories, factorization theorems, symmetries, and heavy-quark expansions. It is our belief that the present work contributes a significant step toward meeting this challenge.

1.2 Methodology

The calculation of hadronic processes is extremely difficult because of our lack of understanding of the connection between quark and hadron properties at low-

energy scales. While it is possible to apply the perturbative technique to “hard” processes (for example $\alpha_s(m_b) \approx 0.22$), soft processes make it difficult for analytical methods to make reliable predictions, since the expansion in the coupling constant $\alpha_s(\mu) = g_s^2(\mu)/4\pi$ no longer converges. This puts some grave limitations on the amount of information about the quark level, that can be extracted from the hadronic level, and vice versa. Often times it is only possible to access such information if certain symmetries are present, such as the chiral symmetry for massless quarks, or the heavy-quark symmetry in the limit of infinite quark masses [2].

In the present work, we will concentrate on the subgroup of B decays into light particles only. We are thus facing the problem of having neither of the two symmetries mentioned above, but rather a system that involves both heavy and light quarks. As we shall see below, in some cases a certain “universality” emerges, that all soft processes are captured in a set of structure functions entering the calculation of factorizable decay amplitudes, regardless of the specific decay channel. To achieve this it is necessary to disentangle the short-distance effects associated with the large scale m_b , from the long-distance effects at the low scale Λ_{QCD} . This is the idea of QCD-factorization, as put forward by Beneke, Buchalla, Neubert, and Sachrajda [3, 4, 5, 6]. It states that factorizable amplitudes can be expressed in the heavy-quark limit and to all orders in perturbation theory as convolution integrals of a perturbatively calculable “hard-scattering kernel” with some of the universal structure functions, which are treated as input parameters, i.e. quantities that need to be extracted by other non-perturbative techniques or directly from experiment. For practical purposes they may simply be replaced by a model. We shall stress, however, that this would obviously introduce a model dependence to

the prediction, whereas QCD-factorization itself is a model independent property of QCD. We were careful to add the pronoun “factorizable” to the amplitudes in question, because not all processes share this feature. Factorization needs to be proved for every individual decay channel.

QCD-factorization combines the disentangling of physics effects from different energy scales with the idea of “naive factorization” of matrix elements. For a simple example of naive factorization consider the weak semileptonic decay amplitude of a neutral kaon into a charged pion and an electron-neutrino pair. The parton-level tree diagram mediating this decay is as follows: the strange quark couples to an up quark and an highly off-shell W boson, which in turn decays into a lepton-neutrino pair. After integrating out the W boson, the decay is mediated by $G_F V_{us}$ times a four-fermion operator. The matrix element of this operator can be factorized to all orders in the strong coupling constant into

$$\langle e^- \bar{\nu}_e \pi^+ | (\bar{l}\nu)_{V-A} (\bar{u}s)_{V-A} | \bar{K}^0 \rangle = \langle e^- \bar{\nu}_e | (\bar{l}\nu)_{V-A} | 0 \rangle \langle \pi^+ | (\bar{u}s)_{V-A} | \bar{K}^0 \rangle, \quad (1.2)$$

since gluons cannot couple to the lepton-neutrino pair. Note that this argument holds for any lepton-neutrino pair that is kinematically allowed, e.g. also for a muon-neutrino pair. The purely hadronic matrix element on the right-hand side is identified with a structure function called the transition form factor. Therefore equation (1.2) serves as a simple example of the “universality” mentioned above. Note also that an attempt to further factorize this hadronic matrix element must fail because of unsuppressed soft gluon exchange. The question of whether this is nevertheless possible for a $B \rightarrow \pi$ transition form factor (exchange $s \leftrightarrow b$ quarks and $K \leftrightarrow B$ states) in the limit of $m_b \rightarrow \infty$ is a very non-trivial one and will be addressed in this thesis. (The answer is that the form factor does *not* factorize. However, the study reveals many surprising properties of this quantity.)

To see how this might possibly work consider a different example, the non-leptonic $B \rightarrow D\pi$ decays in which the D meson picks up the spectator quark of the B meson, i. e. $\bar{B} \rightarrow D^+\pi^-$ and $B^- \rightarrow D^0\pi^-$ [7]. The spectator quark and the other light degrees of freedom inside the B meson can easily form a D meson after the weak $b \rightarrow c$ transition. The remaining two light quarks are very energetic. To form a pion they must carry momenta collinear to the pion momentum and must form a color-singlet state. Such an energetic “color-transparent” compact object can leave the decay region without interfering with the formation of the D meson. The decoupling of soft degrees of freedom from collinear ones therefore lies at the core of the color-transparency argument, and likewise of soft-collinear factorization.

Let us now turn to the question of energy scale separation. Perturbative effects are included in the hard-scattering kernel. In many processes one has to deal with multiple scales that enter the calculation. Typically, aside from a large scale E and the soft scale Λ_{QCD} there exists also an intermediate scale of order $\sqrt{E\Lambda_{\text{QCD}}}$. For the sake of the argument, let us simply state that two perturbative scales M_1 and M_2 enter the calculation of the hard-scattering kernel. Whereas one would naturally expand the kernel in the strong coupling constant $\alpha_s(\mu)$ if μ can be chosen close to either of the two scales, it could also happen that $\alpha_s(\mu)$ is multiplied by powers of the large logarithm $\ln M_1/M_2$, thus upsetting the expansion procedure. The effects of a single power of such a logarithm at one-loop order is well understood. However, double (Sudakov) logarithms appearing in the series $\alpha_s \ln^2 + \alpha_s^2 \ln^4 + \dots$ are more troublesome. A clean separation of scales requires the resummation of large logarithms to all orders in perturbation theory.

Both issues, the soft-collinear factorization and the separation of energy scales including Sudakov resummation, can be most elegantly addressed using effective

field theory technology. By definition the use of effective field theories achieves the separation of scales in that infra-red physics are reproduced in the matrix elements of effective operators, while ultra-violet physics effects give rise to Wilson coefficients. A resummation of large Sudakov logarithms is performed by solving the RGEs of effective operators and running Wilson coefficients from a high scale $\mu_h \sim M_1$ down to a low scale $\mu_i \sim M_2$.

The theories we have in mind are the familiar heavy-quark effective theory (HQET) and two versions of soft-collinear effective theory (SCET), called SCET_I and SCET_{II}. These theories have been proposed and pioneered in the year 2000 by Bauer, Pirjol, Stewart et. al. [8, 9, 10, 11], with further development by Beneke, Feldman, et. al. [12, 13] and Becher, Hill, Neubert, et. al. [14, 15, 16] as of today. (Here we refer to the major developments only. Many more researchers contributed as well and were not mentioned, for which we apologize.) These theories can be applied to any process in which soft particles interact with light but highly energetic particles such as heavy-to-light decays, deep inelastic scattering and jet physics. In the present thesis SCET will be used to prove (or disprove) QCD-factorization for some exemplary inclusive and exclusive B meson decays.

1.3 Structure of Thesis

The thesis is structured as follows:

We begin with a pedagogical introduction to SCET in Chapter 2. Since the theory is a relatively recent development within the Standard Model (its proposal dates only four years back), a comprehensive introduction on a basic level seems worthwhile. It should be understood that the presentation does not follow the chronology of development, but rather follows the logical steps in the construction

as understood in retrospect¹. As mentioned above, two different theories, called SCET_I and SCET_{II} , are needed in later Chapters. They differ in the field content and will be discussed separately. Conceptually, SCET_I is less complicated in that it contains only two distinct sectors of momentum modes, whereas SCET_{II} contains three and therefore displays a richer gauge structure. Before we address the two theories separately and in detail, a brief motivation and an outline of the general strategy is given. As a first application, we consider SCET currents and general four-quark operators, including their renormalization. These quantities are of special interest to any heavy-to-light decay process, in which a local operator product expansion (OPE) fails due to the appearance of soft and collinear singularities. We close this Chapter with a discussion on reparameterization invariance, which provides useful information on the structure of SCET operators and the large-scale dependence of their Wilson coefficients.

Hadronic matrix elements of low-energy effective operators cannot be calculated perturbatively. They define long-distance structure functions, whose precise functional form must be extracted by other means, for example Lattice QCD or directly from experiment. However, much can be learned apart from the functional form using perturbative techniques. For two structure functions, the B -meson light-cone distribution amplitude (LCDA) and the so-called shape function, such calculations are performed in Chapter 3. While LCDAs enter the factorization theorems of exclusive B decays, the shape function encodes the “Fermi motion” of the b quarks inside the B meson and is needed to factorize inclusive B decay ampli-

¹In particular we will not formulate SCET in the “label formalism” which was used in early papers by Bauer et. al. The formulation in position space, first used by Beneke et. al. and then by Neubert et. al., is equally intuitive but easier on the technical level. We will use the latter framework in this thesis.

tudes. Besides a study of renormalization properties of these structure functions, several novel constraints emerging from a moment analysis of the shape function are derived.

As a first application we factorize the decay amplitude for inclusive $\bar{B} \rightarrow X_u l^- \bar{\nu}$ in Chapter 4, using a two-step matching procedure $\text{QCD} \rightarrow \text{SCET}_I \rightarrow \text{HQET}$ at next-to-leading order in perturbation theory and leading power. Such a calculation is appropriate in the phase-space region of large energy and moderate invariant mass of the X_u system. (It would be possible to avoid this two-step matching procedure and apply a local operator product expansion instead, only if the X_u invariant mass is also large. Such a kinematic setup is, however, not suitable due to large backgrounds, see below.) The inclusive decay is, in a sense, simpler than exclusive ones because the more complicated theory SCET_{II} does not enter the computation. However, the matching calculation and subsequent resummation of Sudakov logarithms by analytically solving renormalization-group equations is far from trivial. To discriminate the background $\bar{B} \rightarrow X_c l^- \bar{\nu}$ decays it is necessary to restrict the kinematics to a subspace in phase-space by means of certain experimental cuts. We present results for event fractions that pass such cuts. To give a final numerical answer the functional form of the shape function is required. Here we adopt a model that is consistent with all constraints derived in the previous Chapter 3. One of the discussed methods of kinematic cuts, the P_+ cut, is theoretically favored and deserves a closer study. This is done at the end of this Section, including a thorough estimate of all theoretical uncertainties entering a $|V_{ub}|$ determination using this method.

In the remainder of this thesis we turn our attention to exclusive decays. In Chapter 5, the outlined methodology is applied to $B \rightarrow \gamma l^- \bar{\nu}$, which is one of

the simplest exclusive decay modes in that there are no hadrons in the final state. Still there is sensitivity to the light-cone structure of the B meson, because of the coupling of the high-energy photon to the soft spectator quark inside the heavy meson. Many techniques can be learned in this environment. With minor modifications they can then be applied to the hard-scattering term of such important decay amplitudes as the ones for $B \rightarrow K^* \gamma$ or $B \rightarrow \pi \pi$, etc. One of the important remaining contributions to the corresponding amplitudes involves $B \rightarrow M$ form factors, where M is some light meson. While it is not the goal of this thesis to study these difficult decay modes in all completeness, we wish to contribute by analyzing some of their ingredients in a clean environment.

For that reason we devote the Chapter 6 to analyse $B \rightarrow M$ form factors in the high recoil region, meaning that the light meson M is highly energetic. The underlying processes are $B \rightarrow \pi l^- \bar{\nu}$ and $B \rightarrow \rho l^- \bar{\nu}$. The calculation of these form factors using a two-step matching procedure $\text{QCD} \rightarrow \text{SCET}_I \rightarrow \text{SCET}_{II}$ reveals some almost expected outcomes (such as the fact that form factors do *not* factorize, and that form factors at large recoil are power suppressed quantities) and also some surprises. The most important one might be that, although going through SCET_I enables us to resum large *perturbative* logarithms, there exists a purely long-distance contribution for which the intermediate theory is without any physical significance. In other words, the non-perturbative “soft overlap” or Feynman mechanism (of lots of small momentum kicks to bring the spectator quark up to speed) exists and dominates over the hard-scattering picture. Furthermore we find that there are unsuppressed contributions from higher Fock states of both the B and M meson. More precisely, three-particle configurations (two quarks plus one gluon) contribute at the same power as two-particle ones. This is in contrast to

the previous understanding as found by e. g. light-cone sum rules. It is tempting to try to estimate the contribution of this effect; however, this would be accompanied by large uncertainties. Note also that we only perform the matching at tree-level, due to the complexity of the problem. A numerical analysis is therefore left for future work and will not be given here. Finally we conclude in Chapter 7.

CHAPTER 2

SOFT-COLLINEAR EFFECTIVE THEORY

2.1 General Considerations

Many processes in B -decay physics involve hadrons or jets of hadrons with energies much larger than their masses. The assumption, that underlies the construction of an effective field theory describing the dynamics of the process, is that the constituents of these hadrons or jets carry momenta collinear to the hadronic momenta. Consider a light but energetic hadron with momentum P^μ in the z -direction and invariant mass $P^2 = m_H^2$ much smaller than its energy E . We may decompose $P^\mu = (E - m_H^2/4E + \dots)n^\mu + (m_H^2/4E + \dots)\bar{n}^\mu$ with the light-like vectors $n^\mu = (1, 0, 0, 1)$ and $\bar{n}^\mu = (1, 0, 0, -1)$ satisfying $n^2 = \bar{n}^2 = 0$ and $n \cdot \bar{n} = 2$. Up to small corrections of order m_H^2/E^2 the coefficient of n^μ is given by the large energy E of the hadron. A natural description of these kind of momenta is given in terms of the light-cone decomposition

$$P^\mu = (n \cdot P) \frac{\bar{n}^\mu}{2} + (\bar{n} \cdot P) \frac{n^\mu}{2} + P_\perp^\mu. \quad (2.1)$$

Four-vectors are characterized by the scaling of the individual light-cone components. The three terms in (2.1) are referred to as P_+ , P_- and P_\perp . In other words, P_+ is a four-vector $P_+^\mu = (n \cdot P) \bar{n}^\mu/2$, etc. In the example above, we have $(P_+^\mu, P_-^\mu, P_\perp^\mu) = (\frac{m_H^2}{2E} \frac{\bar{n}^\mu}{2}, 2E \frac{n^\mu}{2}, 0) + \dots$ as the leading contributions. We assume that a parton inside this hadron carries momentum p^μ , which also points essentially in the n^μ direction, but it may also have non-vanishing momentum in the \bar{n} and perpendicular direction. Those are, however, dynamically generated and typically much smaller than the large minus component. By introducing a dimensionless scaling parameter λ we may characterize the order of the light-cone components

$p^\mu \sim (\lambda^2, 1, \lambda)$. The scaling of the “plus component” $p_+ \sim \lambda^2$ follows from the assumptions that the invariant mass of the constituent $p^2 = 2p_+ \cdot p_- + p_\perp^2$ is not larger than $O(\lambda^2)$. All the above assumptions are well justified for the processes described below. For example, consider a decay $B \rightarrow \pi$ in the kinematic situation where the B meson is at rest and the pion takes away almost half of the B -meson mass as kinetic energy $E \approx M_B/2$. The quarks and gluons inside the pion are massless, but off-shell by parametrically Λ_{QCD}^2 . Throughout this work, Λ_{QCD} denotes the soft QCD scale of non-perturbative physics. We would define $\lambda = \Lambda_{\text{QCD}}/E$ and assume $\bar{n} \cdot p = 2xE$ where x is a positive dimensionless variable less than (but of order) 1. Generally, the precise definition of the scaling parameter λ depends on the particular process and should be thought of as the ratio of two scales whenever we are facing a multi-scale problem. The effective theory is constructed around the systematic expansion in inverse powers of the larger of the two scales. We shall distinguish between labels and dynamical components. While large momentum components appear as labels and are not altered by soft interactions (only by collinear interactions), the remaining ones are dynamical. This is similar to the notion of the velocity label v and “residual” momentum k in the HQET expansion $p_b = m_b v + k$ [2]. For the sake of simplicity, we will not write out explicitly the label v on heavy quark fields or the label En on collinear fields. In fact, we will not use the label formalism of earlier papers, and keep the large momentum dependence explicit.

The relevant degrees of freedom of SCET are such that for any given perturbative process in QCD involving the kind of momenta described above, each infra-red contribution is reproduced by the effective fields. In this spirit, SCET is founded on the method of regions [17]. However, the approach of going through the effec-

tive theory allows for a systematic power counting already at the beginning of a calculation.

There is a certain spin-symmetry realized in the large energy limit. This can be understood when decomposing the collinear QCD spinor ψ_c into two separate fields ξ and η , which are both two-component spinors and subject to the constraints $\not{n}\xi = 0$ and $\not{\bar{n}}\eta = 0$. One defines

$$\xi = \frac{\not{n}\not{\bar{n}}}{4}\psi_c, \quad \eta = \frac{\not{\bar{n}}\not{n}}{4}\psi_c. \quad (2.2)$$

The power counting associated with these two-component spinor fields is chosen such that propagation of the fields do not enter the power counting of any given diagram, i.e. count as unity. Denoting the time-ordered product by T , the propagator reads

$$\langle 0|T\{\psi_i(x), \bar{\psi}_j(y)\}|0\rangle = \int \frac{d^4p}{(2\pi)^4} \frac{i\not{p}_{ij}}{p^2 + i\epsilon} e^{-ip \cdot (x-y)}. \quad (2.3)$$

When assuming collinear momentum scaling $\sim (\lambda^2, 1, \lambda)$, the integration measure $d^4p = \frac{1}{2}dp_+dp_-d^2p_\perp$ scales like $O(\lambda^4)$, and $p^2 \sim O(\lambda^2)$. It follows that the individual fields count as $\xi \sim O(\lambda)$ and $\eta \sim O(\lambda^2)$. In the limit of large energy, the 4-component QCD spinors ψ_c reduce to a two-component spinor ξ , thus giving rise to a reduced Dirac basis. This is the manifestation of large-energy spin-symmetry [18]. Similarly, analyzing the gluon propagator in covariant gauge

$$\langle 0|T\{A_c^\mu(x), A_c^\nu(y)\}|0\rangle = \int \frac{d^4p}{(2\pi)^4} \frac{i}{p^2 + i\epsilon} \left[-g^{\mu\nu} + (1 + \alpha) \frac{p^\mu p^\nu}{p^2} \right] e^{-ip \cdot (x-y)} \quad (2.4)$$

reveals that A_c^μ counts in its light-cone components like the momentum p^μ itself.

After the identification of the small component η , the SCET-Lagrangian, which contains only the leading collinear field ξ , is constructed by integrating out η . Let

ψ_c be the full QCD quark field which carries collinear momentum.

$$\mathcal{L}_q^{\text{QCD}} = \bar{\psi}_c i \not{D} \psi_c = (\bar{\xi} + \bar{\eta}) \left(in \cdot D \frac{\not{n}}{2} + i \bar{n} \cdot D \frac{\not{n}}{2} + i \not{D}_\perp \right) (\xi + \eta) \quad (2.5)$$

The small component η is integrated out by solving its equation of motion $\delta \mathcal{L}_q^{\text{QCD}} / \delta \bar{\eta} = 0$. The solution is

$$\eta = -\frac{\not{n}}{2} \frac{1}{i \bar{n} \cdot D + i\epsilon} i \not{D}_\perp \xi. \quad (2.6)$$

The SCET Lagrangian is therefore identical to the QCD Lagrangian, but boosted to a reference frame in which the fields carry collinear momenta. As a result, the collinear Lagrangian is exact to all orders in λ and not renormalized [12]. At this stage we have

$$\mathcal{L}_c = \bar{\xi} \frac{\not{n}}{2} \left(in \cdot D + i \not{D}_\perp \frac{1}{i \bar{n} \cdot D + i\epsilon} i \not{D}_\perp \right) \xi. \quad (2.7)$$

Note that the Lagrangian itself scales like λ^4 , which is consistent with the action $S = \int d^4x \mathcal{L}_c \sim O(1)$ since the integration measure $d^4x \sim O(\lambda^{-4})$ for collinear momenta. The factor $\bar{n} \cdot D$ in the denominator is symbolic. After the introduction of Wilson lines, it leads to an integration of the fields along the n direction. This point will be explained later on in more detail. We have also inserted a $+i\epsilon$ prescription, which is an arbitrary choice and not dictated by the QCD Lagrangian [12]. This regulator is necessary for practical purposes but bears no physical implications. From now on we will omit this prescription in the notation and only refer to it explicitly when needed.

The next step toward a consistent power counting is to achieve a “homogeneous” scaling in λ , i.e. an expansion. In the above formulation, D denotes the full covariant derivative, which means that the gluon fields can carry any momentum. As mentioned before, the strategy for the construction of SCET is to assign an independent effective field for each momentum configuration that contributes

to a given process at leading power. Depending on the process, there can be many. Typically, we work in a reference frame in which there are “soft” momenta present, e.g. fields that carry momenta with small light-cone components. The largest soft mode that is kinematically allowed to couple to a collinear field without changing its momentum scaling is an “ultrasoft” field with momentum $\sim (\lambda^2, \lambda^2, \lambda^2)$. Let us assume for the moment, and for the sake of simplicity, that only these two momentum configurations contribute. (Such a theory is called SCET_I .) It is then necessary to split up $iD^\mu = i\partial^\mu + A_c^\mu + A_{us}^\mu$. The subscripts c and us label the collinear and ultrasoft fields, respectively. Ultrasoft gluons scale like ultrasoft momenta, and it is therefore necessary to expand the Lagrangian in powers of λ for a homogeneous scaling. This, and also the so-called “multipole expansion” below, provide a rigorous definition of leading and subleading Lagrangians in terms of inverse powers of the large scale E .

Many ingredients of SCET, including the definition of the expansion parameter λ in terms of physical quantities, and the number and nature of degrees of freedom in the effective theory, depend on the particular process that is analyzed. In the next sections we will construct two different theories called SCET_I and SCET_{II} , suitable for inclusive and exclusive heavy-to-light decays. The heavy system provides for a natural reference frame in which to carry out the calculations, namely its rest frame. The constituents of the heavy system contain both heavy and light soft fields. In the effective theory, the mass of the heavy system is a large scale and should not enter the low-energy description. This is provided by the heavy-quark effective theory, which will be part of SCET. In the decay applications considered here, the b -quark mass m_b and the large energy E of the collinear fields will be of the same order.

Table 2.1: Nomenclature for various momentum modes. Quark fields carrying these momenta scale according to the last column, whereas gluon fields scale in their light-cone components like the corresponding momenta. The effective field theories will contain a subset of these fields, depending on the application.

| Name | Abbreviation | Momentum scaling $[E]$ | mom. squared $[E^2]$ | Fermion field scaling |
|----------------|--------------|---------------------------------------|-------------------------|--------------------------|
| hard | h | $(1, 1, 1)$ | 1 | |
| hard-collinear | hc | $(\lambda, 1, \lambda^{1/2})$ | λ | $\lambda^{1/2}$ |
| collinear | c | $(\lambda^2, 1, \lambda)$ | λ^2 | λ |
| soft | s | $(\lambda, \lambda, \lambda)$ | λ^2 | $\lambda^{3/2}$ |
| soft-collinear | sc | $(\lambda^2, \lambda, \lambda^{3/2})$ | λ^3 | λ^2 |
| ultrasoft | us | $(\lambda^2, \lambda^2, \lambda^2)$ | λ^4 | λ^3 |

Before going into detail, let us set the nomenclature for the various fields and their scaling. The names are tied to the scaling in λ , regardless of the physical definition of λ . They are listed in Table 2.1. Not all fields listed here will be included in the final low-energy theory. Nevertheless, it is convenient to define a set of momentum modes which allow to address contributions to processes as they are found by the method of regions. This can be demonstrated in the following example [15]: Consider a scalar triangle graph in the kinematic setup where the external momenta are $l^\mu \sim (\lambda, \lambda, \lambda)$ soft, $p^\mu \sim (\lambda^2, 1, \lambda)$ collinear, and $q^\mu = (l - p)^\mu \sim (\lambda, 1, \lambda)$ hard-collinear, as shown in Fig. 2.1. (q^μ is called a hard-collinear momentum even though the perpendicular component is smaller than $\sqrt{\lambda}$. Only the first two components, “plus” and “minus” are of importance.) One defines the

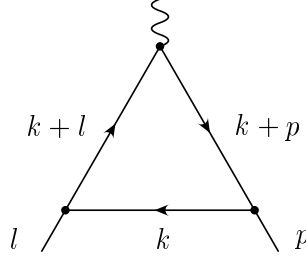


Figure 2.1: An Example: Scalar triangle graph with external momenta l (soft) and p (collinear). The loop momentum is denoted k .

loop integral

$$I = i\pi^{-d/2}\mu^{4-d} \int d^d k \frac{1}{(k^2 + i0) [(k+l)^2 + i0] [(k+p)^2 + i0]} \quad (2.8)$$

in $d = 4 - 2\epsilon$ space-time dimensions and analyzes it for arbitrary external momenta obeying the above scaling relations. It will be convenient to define the invariants

$$L^2 \equiv -l^2 - i0, \quad P^2 \equiv -p^2 - i0, \quad Q^2 \equiv -(l-p)^2 - i0 = 2l_+ \cdot p_- - i0 + \dots, \quad (2.9)$$

which scale like $L^2 \sim \lambda^2$, $P^2 \sim \lambda^2$, and $Q^2 \sim \lambda$. (This P has nothing to do the momentum defined in (2.1), where P served as an example for the light-cone decomposition of a 4-vector.) The exact result is

$$I = \frac{1}{Q^2} \left[\ln \frac{Q^2}{L^2} \ln \frac{Q^2}{P^2} + \frac{\pi^2}{3} + O(\lambda) \right]. \quad (2.10)$$

The next step is to reproduce the result using the method of regions [17], which means that one assumes a certain scaling for the loop momentum k and expands the integrand in powers of λ *before* performing the integration. Going through the list of modes in Table 2.1 we find leading power contributions for k being hard-collinear, collinear, soft, and soft-collinear. The individual regions give the

following contributions [15]:

$$\begin{aligned}
I_{\text{HC}} &= i\pi^{-d/2} \mu^{4-d} \int d^d k \frac{1}{(k^2 + i0) (k^2 + 2k_- \cdot l_+ + i0) (k^2 + 2k_+ \cdot p_- + i0)} \\
&= \frac{\Gamma(1+\epsilon)}{Q^2} \left(\frac{1}{\epsilon^2} + \frac{1}{\epsilon} \ln \frac{\mu^2}{Q^2} + \frac{1}{2} \ln^2 \frac{\mu^2}{Q^2} - \frac{\pi^2}{6} \right) + O(\epsilon), \tag{2.11}
\end{aligned}$$

$$\begin{aligned}
I_{\text{C}} &= i\pi^{-d/2} \mu^{4-d} \int d^d k \frac{1}{(k^2 + i0) (2k_- \cdot l_+ + i0) [(k+p)^2 + i0]} \\
&= \frac{\Gamma(1+\epsilon)}{Q^2} \left(-\frac{1}{\epsilon^2} - \frac{1}{\epsilon} \ln \frac{\mu^2}{P^2} - \frac{1}{2} \ln^2 \frac{\mu^2}{P^2} + \frac{\pi^2}{6} \right) + O(\epsilon). \tag{2.12}
\end{aligned}$$

$$\begin{aligned}
I_{\text{S}} &= i\pi^{-d/2} \mu^{4-d} \int d^d k \frac{1}{(k^2 + i0) [(k+l)^2 + i0] (2k_+ \cdot p_- + i0)} \\
&= \frac{\Gamma(1+\epsilon)}{Q^2} \left(-\frac{1}{\epsilon^2} - \frac{1}{\epsilon} \ln \frac{\mu^2}{L^2} - \frac{1}{2} \ln^2 \frac{\mu^2}{L^2} + \frac{\pi^2}{6} \right) + O(\epsilon). \tag{2.13}
\end{aligned}$$

$$\begin{aligned}
I_{\text{SC}} &= i\pi^{-d/2} \mu^{4-d} \int d^d k \frac{1}{(k^2 + i0) (2k_- \cdot l_+ + l^2 + i0) (2k_+ \cdot p_- + p^2 + i0)} \\
&= \frac{\Gamma(1+\epsilon)}{Q^2} \left(\frac{1}{\epsilon^2} + \frac{1}{\epsilon} \ln \frac{\mu^2 Q^2}{L^2 P^2} + \frac{1}{2} \ln^2 \frac{\mu^2 Q^2}{L^2 P^2} + \frac{\pi^2}{6} \right) + O(\epsilon). \tag{2.14}
\end{aligned}$$

A couple of comments are in order.

(i) It is a simple check to add all the above contributions and find that they indeed reproduce the full result $I = I_{\text{HC}} + I_{\text{C}} + I_{\text{S}} + I_{\text{SC}}$.

(ii) Each individual integral is, of course, Lorentz invariant. In this sense Lorentz invariance was never broken by picking a particular frame. Had we picked a different reference frame, for example the Breit frame, the results would not change. However, we would have found different momentum modes that contribute. Clearly, we could perform a boost to this frame before evaluating the integrals, thus finding a different set of momentum modes. In the example of the Breit frame, the formerly soft leg l becomes collinear in the \bar{n} direction (anti-collinear), and the collinear momentum p stays collinear in the n direction. Leading contributions would come from hard loop momenta (formerly hard-collinear), anticollinear

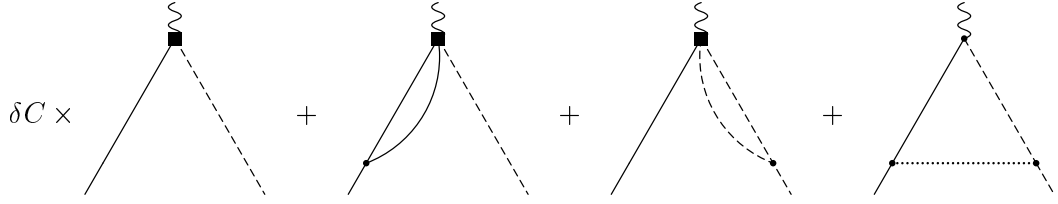


Figure 2.2: Corresponding contributions in the effective low-energy theory. δC denotes a Wilson coefficient, the solid lines are soft fields, the dashed lines collinear, and the dotted line soft-collinear.

(formerly soft), collinear (formerly collinear) and ultrasoft (formerly soft-collinear). It is therefore not only the physical process that defines which modes must be included in the effective theory, but also the frame in which we choose to work. One further point can be made by boosting the frame even further, such that the formerly collinear momenta become soft. Clearly, the formerly soft momenta then become collinear in the \bar{n} direction and we find the following “symmetry” (this is, of course, nothing else but Lorentz invariance): The contribution from soft and collinear loop momenta are related to each other under the simultaneous exchange of soft and collinear external momenta and the interchange of n and \bar{n} . However, if a heavy quark is present there is a preferred Lorentz frame, namely the rest frame of the heavy quark, and the above symmetry is broken.

(iii) We went through a lengthy discussion of the various contributions to the full theory diagram. The benefit is the separation of short- and long-distance physics. The strategy for constructing a low-energy effective theory is to let the collinear, soft, and soft-collinear contributions be reproduced by exchange of collinear, soft, and soft-collinear fields, while the hard-collinear contribution in this case will be absorbed into a Wilson coefficient. In fact, the sum of the collinear, soft, and soft-collinear integrals is free of infra-red singularities, which are regular-

ized by keeping the external legs off-shell (e.g. the sum is free of $\ln(\mu^2/L^2)$ and $\ln(\mu^2/P^2)$). The view of associating the infra-red contributions with diagrams in the effective theory is depicted in Fig. 2.2. Note that when a soft gluon connects to a collinear line it will lead to a (hard-collinear) off-shell mode, which will be integrated out. Therefore the soft gluon emerges out of the vertex in the figure. A similar argument applies to the collinear gluon. A deeper investigation of this point will follow in later sections and lead to Wilson lines. Here we wish to stress the close connection between the method of regions and the idea of constructing SCET as a low-energy effective theory.

Before beginning the discussion of SCET_I in greater detail, note that the same (physical) momentum modes may have different names, depending on the (physical) definition of the expansion parameter λ . Consider, for example, a momentum $p \sim (\Lambda_{\text{QCD}}, E, \sqrt{E\Lambda_{\text{QCD}}})$ with some scales $E \gg \Lambda_{\text{QCD}}$. This mode can be called collinear when defining $\lambda = \sqrt{\Lambda_{\text{QCD}}/E}$. It can, however, also be called hard-collinear when defining $\lambda = \Lambda_{\text{QCD}}/E$. Similarly, a momentum $l \sim (\Lambda_{\text{QCD}}, \Lambda_{\text{QCD}}, \Lambda_{\text{QCD}})$ might be called ultrasoft or soft for $\lambda = \sqrt{\Lambda_{\text{QCD}}/E}$ or $\lambda = \Lambda_{\text{QCD}}/E$, respectively.

2.2 Renormalization

For consistency we review the main strategies of renormalization using dimensional regularization [19] in $4 - 2\epsilon$ space-time dimensions. This scheme has already been adopted in the previous section and will be used throughout this work. As apparent in (2.11), for example, loop integrals which are logarithmically divergent in four dimensions become finite for $\epsilon \neq 0$. The general strategy is to absorb terms that diverge in the limit $\epsilon \rightarrow 0$ into factors that relate bare quantities to renormalized

ones. In the end, renormalized quantities are finite for $\epsilon \rightarrow 0$ and have meaningful relations to physical observables.

Since the action $\int d^{4-2\epsilon}x \mathcal{L}(x)$ is dimensionless, it follows that the bare QCD coupling constant g_s^{bare} has a mass-dimension of ϵ . Defining $(g_s^{\text{bare}})^2 = 4\pi\alpha_s^{\text{bare}}$, the relation to the dimensionless renormalized coupling $\alpha_s(\mu)$ can be written as [20]

$$\alpha_s^{\text{bare}} = \mu^{2\epsilon} Z_\alpha(\alpha_s(\mu)) \alpha_s(\mu) , \quad (2.15)$$

where μ is an arbitrary mass parameter, called the renormalization scale. In a minimal subtraction scheme, the renormalization factor $Z_\alpha = 1 + \sum_{k=1}^{\infty} \epsilon^{-k} Z_\alpha^{(k)}$ is expanded in inverse powers of ϵ , and the evolution of $\alpha_s(\mu)$ is encoded in the “beta function”

$$\frac{d}{d \ln \mu} \alpha_s(\mu) = \beta(\alpha_s(\mu), \epsilon) . \quad (2.16)$$

We will consistently work in the modified minimal subtraction scheme $\overline{\text{MS}}$, in which all terms multiplying powers of $1/\epsilon - \gamma_E + \ln 4\pi$ are absorbed into the renormalization factors. Since the beta function $\beta(\alpha_s, \epsilon)$ is finite in the limit $\epsilon \rightarrow 0$ (in a renormalizable theory), it can be Taylor expanded around $\epsilon = 0$. It follows [20] that only the first term in this expansion is non-zero and the exact relation reads

$$\begin{aligned} \beta(\alpha_s, \epsilon) &= \beta(\alpha_s) - 2\epsilon \alpha_s , \\ \beta(\alpha_s) &= 2\alpha_s^2 \frac{d}{d\alpha_s} Z_\alpha^{(1)}(\alpha_s) . \end{aligned} \quad (2.17)$$

Throughout this work we will use the following expansion of the beta function in terms of α_s :

$$\beta(\alpha_s) = -2\alpha_s \sum_{k=0}^{\infty} \beta^{(k)} \left(\frac{\alpha_s}{4\pi} \right)^{k+1} , \quad (2.18)$$

with [21]

$$\beta^{(0)} = 11 - \frac{2}{3} n_f , \quad (2.19)$$

$$\begin{aligned}\beta^{(1)} &= 102 - \frac{38}{3} n_f , \\ \beta^{(2)} &= \frac{2857}{2} - \frac{5033}{18} n_f + \frac{325}{54} n_f^2 ,\end{aligned}\tag{2.20}$$

where n_f is the number of flavors that contribute in the loop calculation.

We will also need the wave-function renormalization of the quark fields. In QCD, the (massless or massive) bare and renormalized quark fields are related by $\psi^{\text{bare}} = Z_\psi^{1/2} \psi$ with $Z_\psi = 1 - \alpha_s/(3\pi\epsilon)$. The only quark field in SCET that renormalizes differently is the heavy quark field. Its wave-function renormalization is obviously identical to the heavy quark field in HQET and reads [2] $Z_h = 1 + 2\alpha_s/(3\pi\epsilon)$.

Composite operators Q_i require renormalization beyond that of its field and coupling components, and are renormalized in the same manner. Under renormalization they can mix among each other if they share the same quantum numbers and dimensions. We will only consider operators that are gauge invariant and do not vanish under the application of equation of motions. Therefore one relates

$$Q_i^{\text{bare}} = Z_{ij}(\mu) Q_j(\mu)\tag{2.21}$$

with $Z_{ij} = \delta_{ij} + \sum_{k=1}^{\infty} \epsilon^{-k} Z_{ij}^{(k)}$ in the $\overline{\text{MS}}$ scheme. The μ dependence of an operator Q_i is encoded in the renormalization group equation (RGE). Since the set of all allowed operators $\{Q_1, Q_2, \dots\}$ is a complete basis, one can express the operator $\partial Q_i / \partial \ln \mu$ as a linear combination of Q_1, Q_2, \dots . Defining the anomalous dimension matrix γ through the RGE

$$\frac{d}{d \ln \mu} Q_j = -\gamma_{jk} Q_k ,\tag{2.22}$$

it follows from the fact that the bare operator Q_i^{bare} is independent of μ , that

$$\gamma_{jk} = (Z^{-1})_{ji} \frac{d}{d \ln \mu} Z_{ik} = -2\alpha_s \frac{d}{d\alpha_s} Z_{jk}^{(1)} .\tag{2.23}$$

Here we have used (2.16) and (2.17). In words, *the anomalous dimension is, apart from a minus sign, twice the coefficient of the $1/\epsilon$ term*, when all ultra-violet divergences are regularized dimensionally and all infra-red effects are regularized by other means. For any anomalous dimension $\gamma(\alpha_s)$ we will adopt the expansion

$$\gamma(\alpha) = \sum_{k=0}^{\infty} \gamma^{(k)} \left(\frac{\alpha_s}{4\pi} \right)^{k+1}, \quad (2.24)$$

unless otherwise stated.

Physical amplitudes are given as products of operator matrix elements and Wilson coefficients $C_i(\mu) \langle Q_i(\mu) \rangle$ and are independent of the renormalization scale μ . This implies that the Wilson coefficients must obey the RGE

$$\frac{d}{d \ln \mu} C_j = (\gamma^T)_{jk} C_k, \quad (2.25)$$

where T denotes the transpose of the matrix γ . The above equation will be used below to resum large logarithms to all orders.

2.3 SCET_I

This theory is applicable to processes in which there are only two different momentum modes present, namely hard-collinear and soft ones. An example for such a process is the inclusive decay of a heavy meson such as the B meson. In the rest frame of the B meson the partons carry, with the exception of the massive b quark, momenta that scale like $(\Lambda_{\text{QCD}}, \Lambda_{\text{QCD}}, \Lambda_{\text{QCD}})$, with Λ_{QCD} being the soft QCD scale. The b quark momentum can be split up into the static component $m_b v$ and the dynamic residual momentum k , which also scales like $(\Lambda_{\text{QCD}}, \Lambda_{\text{QCD}}, \Lambda_{\text{QCD}})$. A flavor-changing current turns the b quark into some light but energetic quark. This quark could be a parton of a particular hadron or, more generally, of a hadronic jet of

invariant mass much larger than Λ_{QCD} . We are then faced with the kinematic situation in which a hierarchy of scales emerged: $\Lambda_{\text{QCD}} \ll M \ll E$, where E is the energy of the jet (close to half of the b -quark mass) and M is the jet invariant mass. Specifically, we assume that M is of the “intermediate”¹ order $M \sim \sqrt{E\Lambda_{\text{QCD}}}$. In this kinematic setup the two momentum modes are therefore $(\Lambda_{\text{QCD}}, \Lambda_{\text{QCD}}, \Lambda_{\text{QCD}})$ and $(\Lambda_{\text{QCD}}, E, \sqrt{E\Lambda_{\text{QCD}}})$. When choosing the expansion parameter $\lambda = \Lambda_{\text{QCD}}/E$ we can refer to them as soft and hard-collinear, respectively. (Alternatively, they are also referred to as ultrasoft and collinear when choosing $\lambda = \sqrt{\Lambda_{\text{QCD}}/E}$.)

2.3.1 Power Counting

The full massless QCD fields are separated into hard-collinear and soft momentum modes, e.g. the quark field splits up into the soft quark field q and the hard-collinear quark field $\psi_{hc} = \xi_{hc} + \eta_{hc}$. Analogously, the QCD gluon field A is decomposed, yielding

$$\psi = \xi_{hc} + \eta_{hc} + q, \quad iD^\mu = i\partial^\mu + gA_{hc}^\mu + gA_s^\mu. \quad (2.26)$$

Let us study the effect on the kinetic term in the Lagrangian $\mathcal{L} = \bar{\psi} i \not{D} \psi + \dots$. Since the spinors ξ_{hc} and η_{hc} are constrained by $\not{n}\xi_{hc} = \not{\bar{n}}\eta_{hc} = 0$, we decompose the Dirac matrix γ^μ in light-cone coordinates to $n^\mu \not{n}/2 + \bar{n}^\mu \not{\bar{n}}/2 + \gamma_\perp^\mu$ and expand the Lagrangian.

$$\begin{aligned} \bar{\psi} i \not{D} \psi &= \bar{\xi}_{hc} \frac{\not{n}}{2} i n \cdot D \xi_{hc} + \bar{\eta}_{hc} \frac{\not{\bar{n}}}{2} i \bar{n} \cdot D \eta_{hc} + \bar{\eta}_{hc} i \not{D}_\perp \xi_{hc} + \bar{\xi}_{hc} i \not{D}_\perp \eta_{hc} \\ &\quad + \bar{\xi}_{hc} g \not{A}_{hc} q + \bar{\eta}_{hc} g \not{A}_{hc} q + \bar{q} g \not{A}_{hc} \xi_{hc} + \bar{q} g \not{A}_{hc} \eta_{hc} + \bar{q} (i \not{\partial} + g \not{A}_s) q \end{aligned} \quad (2.27)$$

¹For instance, in inclusive $B \rightarrow X_u$ decays we need to restrict the jet invariant mass to be less than the charm mass for discrimination purposes. Numerically, m_c compares very well with $\sqrt{m_b \Lambda_{\text{QCD}}}$.

Note that we do not allow for interaction terms that are forbidden by kinematics, for example two soft fields cannot couple to a single hard-collinear field. The small component η_{hc} is then integrated out by solving its equation of motion. This yields

$$\eta_{hc} = -\frac{\vec{n}}{2} \frac{1}{i\vec{n} \cdot D} (i\mathcal{D}_\perp \xi_{hc} + g\mathcal{A}_{hc} q) , \quad (2.28)$$

which must be plugged back into (2.27). So far we have merely rewritten the Lagrangian into a more complicated but exact form. In a next step one needs to perform a systematic expansion in λ of this Lagrangian. To do this, it is important to take the scaling of the integration measure in $S = \int d^4x \mathcal{L}$ into account. (So far, we omitted the explicit dependence of the various fields on the position x . We will continue to do so, unless otherwise stated.) For terms involving only soft fields, d^4x scales like λ^{-4} . To see this consider a soft field at position y . Translational invariance relates this field to one at position $x + y$ through an exponential $\exp(i l \cdot x)$, where l is the soft momentum, and $l \cdot x = l_+ \cdot x_- + l_- \cdot x_+ + l_\perp \cdot x_\perp$. Because of the scaling properties of the soft momentum, leading contributions to the action are obtained when x scales like $(\lambda^{-1}, \lambda^{-1}, \lambda^{-1})$. Similarly, for terms involving hard-collinear fields, x scales like $(1, \lambda^{-1}, \lambda^{-1/2})$ and the integration measure $d^4x \sim \lambda^{-2}$.

Inverse covariant derivative operators are also expanded. For brevity, let us introduce the intuitive notation $D_{hc} \equiv \partial - igA_{hc}$ (and $D_s \equiv \partial - igA_s$ will also be used below). When $(i\vec{n} \cdot D)^{-1}$ acts on hard-collinear fields, we must expand

$$\frac{1}{i\vec{n} \cdot D} = \frac{1}{i\vec{n} \cdot D_{hc}} - \frac{1}{i\vec{n} \cdot D_{hc}} g \vec{n} \cdot A_s \frac{1}{i\vec{n} \cdot D_{hc}} + O(\lambda^4) . \quad (2.29)$$

Every term in the effective theory should have a single and homogeneous scaling behaviour. This requirement leads to a subtlety in interaction terms involving soft and hard-collinear fields. In the above notation we have omitted the dependence

on the position and treated all terms as local in that all fields are evaluated at the same position x . According to the above argument, the light-cone components of x in interactions of hard-collinear and soft fields scale like $(1, \lambda^{-1}, \lambda^{-1/2})$, because the vertex carries hard-collinear momentum (since two hard-collinear momenta can not add up to a soft momentum). One must therefore perform a “light-front multipole expansion” [13] of the translation operator with $-i\partial \sim (\lambda, \lambda, \lambda)$

$$\begin{aligned}
\phi_s(x) &= \exp(x \cdot \partial) \phi_s(0) \\
&= \exp(x_+ \cdot \partial_- + x_\perp \cdot \partial_\perp) \exp(x_- \cdot \partial_+) \phi_s(0) \\
&= \phi_s(x_-) + [x_\perp \cdot \partial_\perp] \phi_s(x_-) \\
&\quad + \frac{1}{2} x_+ \cdot [\partial_- \phi_s](x_-) + \frac{1}{2} [x_\perp^\mu x_\perp^\nu \partial_\mu \partial_\nu \phi_s](x_-) + \dots
\end{aligned} \tag{2.30}$$

for any soft field ϕ_s in such interaction terms. This means that all soft fields must be evaluated at a position $x_-^\mu = (\bar{n} \cdot x) n^\mu / 2$ on the light cone, whereas the hard-collinear fields remain at position x . This non-locality is a reflection of the fact that at leading power in λ the total momentum in such interactions is not conserved. However, to put this shocking observation into the right context, we emphasize that translational invariance will be restored order by order in the expansion in λ . At leading power only the “plus component” of the soft momentum is kept when adding it to a hard-collinear momentum: $(\lambda, 1, \lambda^{1/2}) + (\lambda, \lambda, \lambda) = (\lambda, 1, \lambda^{1/2})$. The expanded Lagrangian is then homogeneous in the power counting term by term. This concludes the systematic expansion in powers of λ . We will address the important question of gauge invariance in a separate section below.

Let us turn our attention to the treatment of the b quark in SCET. Heavy quarks are described by the familiar HQET Lagrangian [2]. In the low energy effective theory, the heavy quarks do not couple to hard-collinear fields because

such an interaction would put the quark off-shell. The HQET Lagrangian reads

$$\mathcal{L}_h = \bar{h} i v \cdot D_s h + \frac{1}{2m_b} \left[\bar{h} (iD_s)^2 h + C_{mag}(\mu) \bar{h} \frac{g}{2} \sigma_{\mu\nu} G_s^{\mu\nu} h \right] + O(1/m_b^2) . \quad (2.31)$$

Finally the pure glue (Yang-Mills) Lagrangian $\mathcal{L}_{\text{glue}}$ can be split into soft plus hard-collinear plus interaction terms. The soft and hard-collinear sectors take the same form as in full QCD, including gauge-fixing and ghost terms. The interaction terms are restricted to those that are kinematically allowed, using the same arguments as above.

2.3.2 Wilson lines

The introduction of Wilson lines is a well known concept in HQET. Consider the effect of coupling a gluon with momentum of order $O(\Lambda_{\text{QCD}})$ (soft) to a heavy quark field with momentum $m_b v$. This will lead to a propagator that is off-shell by an amount $(m_b v + k)^2 - m_b^2 \approx 2m_b v \cdot k \sim O(m_b \Lambda_{\text{QCD}})$. If the effective theory describes physics of energies below this scale, such propagators should be integrated out. We can repeat this argument consecutively and find that attaching n gluons with momenta k_i , $i = 1 \dots n$, to a heavy quark line leads to

$$\frac{-g v^{\mu_n} t^{a_n}}{v \cdot (k_1 + \dots + k_n)} \cdot \dots \cdot \frac{-g v^{\mu_2} t^{a_2}}{v \cdot (k_1 + k_2)} \cdot \frac{-g v^{\mu_1} t^{a_1}}{v \cdot k_1} . \quad (2.32)$$

These are precisely the Feynman rules for the object

$$S_v(x) \equiv P \exp \left(i g \int_{-\infty}^0 ds v \cdot A_s(x + sv) \right) , \quad (2.33)$$

which is called a Wilson (or Schwinger) line extending from minus infinity to the interaction point x along the v direction. The path-ordering symbol P denotes that the gluon fields are ordered from left to right in order of decreasing s . In the spirit of effective theories, we integrate the off-shell propagators out by performing

the field redefinition $h(x) \rightarrow S_v(x) h^{(0)}(x)$. The Wilson line S_v has some very useful properties, $S_v^\dagger S_v = S_v S_v^\dagger = 1$ and, most importantly, $S_v^\dagger i v \cdot D_s S_v = i v \cdot \partial$. Performing the field redefinition leads to a free-particle Lagrangian at leading power, $\mathcal{L}_h = \bar{h}^{(0)} i v \cdot \partial h^{(0)} + \dots$, so that the “sterile” field $h^{(0)}$ no longer couples to soft gluons. In practice we will use the Wilson lines S_v only when discussing the renormalization properties of operators that include heavy fields. For explicit loop calculations one can choose to work with either h or $S_v h^{(0)}$, since they lead to the same Feynman rules.

The purpose of this recapitulation is to draw a close analogy to the treatment of hard-collinear gluon attachments, which can be dealt with in the same manner. In full QCD the attachment of a gluon with hard-collinear momentum $E n + \dots$ to a massive quark line carrying momentum $m_b v$ will provide for a Dirac structure

$$\frac{m_b(1 + \not{v}) + E \not{n}}{2m_b E} g A_{hc} \frac{1 + \not{v}}{2} h = \frac{1}{2E} g \bar{n} \cdot A_{hc} \frac{1 + \not{v}}{2} h + \dots, \quad (2.34)$$

where the dots represent power corrections. An infinite succession of such attachments results in the Wilson line W_{hc} [10], which can be written in position space as

$$W_{hc}(x) = P \exp \left(i g \int_{-\infty}^0 ds \bar{n} \cdot A_{hc}(x + s \bar{n}) \right). \quad (2.35)$$

We should point out that the above (somewhat historic) discussion does *not* suggest that the massive b field matches onto the product $(W_{hc} h)$. In fact, it is the combination with a hard-collinear field, $(\bar{\xi}_{hc} W_{hc})$, that appears in explicit matching calculations, e. g. $(\bar{\psi} \Gamma b) \rightarrow (\bar{\xi}_{hc} W_{hc} \Gamma h)$. As discussed below, this combination is also dictated by hard-collinear gauge invariance.

We also need the conjugate operator W_{hc}^\dagger , which has the opposite path ordering and the factor ig replaced by $-ig$. The most important operator properties are

that $W_{hc}^\dagger W_{hc} = W_{hc} W_{hc}^\dagger = 1$ and $W_{hc}^\dagger i\bar{n} \cdot D_{hc} W_{hc} = i\bar{n} \cdot \partial$, following from the fact that $(i\bar{n} \cdot D_{hc} W_{hc}) = 0$ by definition. As a consequence, one obtains the very useful identity [11, 12, 14]

$$\frac{1}{i\bar{n} \cdot D_{hc}} \phi(x) = W_{hc}(x) \frac{1}{i\bar{n} \cdot \partial} W_{hc}^\dagger(x) \phi(x) = -i \int_{-\infty}^0 ds W_{hc}(x) \left[W_{hc}^\dagger \phi \right] (x + s\bar{n}) , \quad (2.36)$$

for any field (or product of fields) $\phi(x)$. This enables us to write the purely hard-collinear quark Lagrangian \mathcal{L}_{hc} (the interaction terms with soft fields will be denoted by \mathcal{L}_{int}) in the following form:

$$\begin{aligned} \mathcal{L}_{hc}(x) = & \bar{\xi}_{hc}(x) \frac{\not{\bar{n}}}{2} i n \cdot D_{hc} \xi_{hc}(x) \\ & -i \int_{-\infty}^0 ds \left[\bar{\xi}_{hc} i \overleftarrow{D}_{hc\perp} W_{hc} \right] (x) \frac{\not{\bar{n}}}{2} \left[W_{hc}^\dagger i \overrightarrow{D}_{hc\perp} \xi_{hc} \right] (x + s\bar{n}) . \end{aligned} \quad (2.37)$$

This Lagrangian sums up an infinite number of leading-order couplings between hard-collinear quarks and hard-collinear gluons. For later purposes, note that $W_{hc} = 1$ in “collinear light-cone gauge” $\bar{n} \cdot A_{hc} = 0$.

One can also introduce the soft Wilson line S_s , analogous to the hard-collinear Wilson line, with $\bar{n} \leftrightarrow n$ interchanged [11, 12]. Again, $S_s = 1$ if we choose the $n \cdot A_s = 0$ gauge. Although S_s is not necessary to construct the Lagrangian for soft fields, it turns out to be very useful in understanding how soft-collinear factorization arises as a property of the effective theory at lowest order. This is similar to the decoupling of HQET fields h from soft fields, which leaves the heavy field $h^{(0)}$ sterile to gluon interactions. It has been shown [11] that the field redefinitions

$$\xi_{hc} = S_s \xi_{hc}^{(0)} , \quad A_{hc}^\mu = S_s A_{hc}^{(0)\mu} S_s^\dagger , \quad c = S_s c^{(0)} S_s^\dagger , \quad (2.38)$$

remove all hard-collinear – soft interactions from the leading-order Lagrangian.

(Above, c denotes the ghost fields.) We will find (and explain in some more detail) an analogous mechanism for the decoupling transformations in SCET_{II} below.

2.3.3 Gauge Transformations

Gluon fields have been split up into two components, hard-collinear and soft. The gauge symmetry of QCD also decomposes into hard-collinear and soft gauge symmetries. It is clear that soft fields do not transform under hard-collinear gauge transformations U_{hc} , since this would change their momentum scaling. Only hard-collinear fields can transform. On the other hand, soft gauge transformations U_s do not alter the kinematic scalings, and therefore all fields transform, including hard-collinear ones. For that matter, soft gluons can be viewed as slowly varying background fields. Hard-collinear gluons transform then covariantly under soft gauge transformations, while they transform inhomogeneously in the hard-collinear sector.

$$\begin{aligned}
\text{hard-coll.:} \quad & A_{hc} \rightarrow U_{hc} A_{hc} U_{hc}^\dagger + \frac{i}{g} U_{hc} [D_s, U_{hc}^\dagger] , & \xi_{hc} &\rightarrow U_{hc} \xi_{hc} , \\
& A_s \rightarrow A_s , & q &\rightarrow q , \\
\text{soft:} \quad & A_{hc} \rightarrow U_s A_{hc} U_s^\dagger , & \xi_{hc} &\rightarrow U_s \xi_{hc} , \\
& A_s \rightarrow U_s A_s U_s^\dagger + \frac{i}{g} U_s [\partial, U_s^\dagger] , & q &\rightarrow U_s q .
\end{aligned} \tag{2.39}$$

Note that the sum $A_{hc} + A_s$ transforms in the usual way under both hard-collinear and soft transformations. We have also introduced the hard-collinear Wilson line $W_{hc}(x)$, which extends from $(-\infty)$ to x , and therefore transforms like $W_{hc}(x) \rightarrow U_{hc}(x) W_{hc}(x) U_{hc}^\dagger(-\infty)$. Let us agree that the gauge transformations $U_{hc}(x)$ become irrelevant for $x \rightarrow -\infty$ and set $U_{hc}(-\infty) = 1$. This will obviously not alter the transformation properties of finite Wilson lines $W_{hc}(0) W_{hc}^\dagger(t\bar{n})$

along the light cone \bar{n} , because the transformations $U_{hc}(-\infty)$ cancel. It will, however, simplify the discussion since now the Wilson lines transform like $W_{hc}(x) \rightarrow U_{hc}(x) W_{hc}(x)$ under hard-collinear gauge transformations. Note that, as a simple but important example, the combinations

$$\mathcal{X}_{hc} = W_{hc}^\dagger \xi_{hc} , \quad \mathcal{A}_{hc}^\mu = \left[W_{hc}^\dagger i D_{hc}^\mu W_{hc} \right] , \quad (2.40)$$

are left invariant. In light-cone gauge $\bar{n} \cdot A_{hc} = 0$, the calligraphic gluon field \mathcal{A}_{hc} is identical to the QCD gluon field, which will make matching calculations particularly simple. We will sometimes refer to the calligraphic fields as “gauge-invariant building blocks”, because it is easy to construct gauge-invariant operators using these fields [14].

The effective Lagrangian before multipole expanding is invariant under the above gauge transformations. However, such a transformation reintroduces terms of different power counting in the Lagrangian. In the end, we wish to construct the theory in such a way that every term in the Lagrangian has a simple (homogeneous) scaling behaviour. This leads to the notion of “homogeneous gauge transformations”, and is discussed in detail in [13]. We have also explored that in interactions with hard-collinear fields, soft fields need to be positioned at x_- rather than x . A new Wilson line extending from x to x_- is then necessary to restore gauge invariance. These Wilson lines need to be expanded in λ , too, which leads to new interaction terms in the subleading Lagrangians. The above arguments will be expanded and discussed in more detail in the case of SCET_{II}.

2.3.4 Heavy-to-Collinear Currents

An important application for SCET is the decay of the heavy b quark to a highly energetic light quark q . Such flavor-changing currents are the result of the weak in-

interactions and appear in the weak effective Hamiltonian description of the Standard Model at energy scales well below the weak scale ~ 100 GeV. The QCD current is $\bar{q} \Gamma b$, where we treat Γ as an arbitrary Dirac structure. At leading power in λ , this current matches onto the SCET current $\bar{\mathcal{X}}_{hc}(x) \Gamma h(x_-)$. As noted before, the dynamical heavy field is treated as a soft particle and is therefore positioned at x_- . The Wilson line in the definition of the gauge-invariant field $\mathcal{X}_{hc} = W_{hc}^\dagger \xi_{hc}$ correctly accounts for an arbitrary power of $\bar{n} \cdot A_{hc}$ gluon insertions. Only the large components $\bar{n} \cdot A_{hc}$ need to be exponentiated since all other components are parametrically smaller and can be expanded. Soft gluon insertions enter at subleading power. Although these subleading currents are known in the literature [12, 22, 23], they are not needed for this work at present (although very important for future continuations of it). There are two categories (labeled as “A” and “B”) which are separately invariant under reparameterization transformations (see section 2.5). The leading current $\bar{\mathcal{X}}_{hc}(x) \Gamma h(x_-)$ belongs to the “A” category and at order $\lambda^{1/2}$ one finds, for example,

$$\begin{aligned} J^{(A1)} &= \bar{\mathcal{X}}_{hc} \Gamma x_\perp \cdot D_s h - \bar{\mathcal{X}}_{hc} i \overleftarrow{\mathcal{D}}_{hc\perp} \frac{1}{i\bar{n} \cdot \overleftarrow{\partial}} \frac{\not{n}}{2} \Gamma h \\ J^{(B1)} &= \bar{\mathcal{X}}_{hc} \Gamma \mathcal{A}_{hc\perp} \frac{\not{n}}{2m_b} h . \end{aligned} \tag{2.41}$$

The calligraphic covariant derivative is defined as $i\mathcal{D}_{hc} = i\partial + \mathcal{A}_{hc}$. All hard-collinear fields are located at position x , and all soft fields at position x_- . “A”- and “B”-type currents are also known at order λ . For the remainder of this section we will consider the most simple case and discuss the matching at leading power only.

The effective fields $\bar{\mathcal{X}}_{hc}$ and h are two-component spinors, in contrast to the four-component spinors \bar{q} and b . Thus, the Dirac basis $\{1, \gamma_5, \gamma^\mu, \gamma^\mu \gamma_5, i\sigma^{\mu\nu}, i\sigma^{\mu\nu} \gamma_5\}$ will be matched onto a smaller basis, which is commonly chosen as $\{1, \gamma_5, \gamma_\perp^\mu\}$. Let

us define the currents

$$J_1 = \bar{\mathcal{X}}_{hc} h , \quad J_5 = \bar{\mathcal{X}}_{hc} \gamma_5 h , \quad J_\perp^\mu = \bar{\mathcal{X}}_{hc} \gamma_\perp^\mu h , \quad (2.42)$$

and the following symmetric and anti-symmetric tensors in the transverse plane

$$g_\perp^{\mu\nu} = g^{\mu\nu} - \frac{n^\mu \bar{n}^\nu + n^\nu \bar{n}^\mu}{2} , \quad \epsilon_\perp^{\mu\nu} = \epsilon^{\mu\nu\alpha\beta} v_\alpha n_\beta , \quad (2.43)$$

for convenience. We use $\epsilon_{0123} = 1$ and $\gamma_5 = i\gamma^0\gamma^1\gamma^2\gamma^3$.

Omitting the dependence on the renormalization scale and denoting the Wilson coefficients by C_i , the matching of heavy-to-light currents onto the above SCET currents reads to all orders in the strong coupling constant and at leading power

$$\begin{aligned} \bar{q} b &\rightarrow C_1 J_1 , \\ \bar{q} \gamma_5 b &\rightarrow C_2 J_5 , \\ \bar{q} \gamma^\mu b &\rightarrow C_3 J_\perp^\mu + (C_4 n^\mu + C_5 v^\mu) J_1 , \\ \bar{q} \gamma^\mu \gamma_5 b &\rightarrow -C_6 i\epsilon_{\mu\nu}^\perp J_\perp^\nu - (C_7 n^\mu + C_8 v^\mu) J_5 , \\ \bar{q} i\sigma^{\mu\nu} b &\rightarrow C_9 (n^\mu g_\perp^{\nu\lambda} - n^\nu g_\perp^{\mu\lambda}) J_\lambda^\perp - C_{10} i\epsilon_\perp^{\mu\nu} J_5 \\ &\quad + C_{11} (v^\mu n^\nu - v^\nu n^\mu) J_1 + C_{12} (v^\mu g_\perp^{\nu\lambda} - v^\nu g_\perp^{\mu\lambda}) J_\lambda^\perp , \\ \bar{q} i\sigma^{\mu\nu} \gamma_5 b &\rightarrow (C_9 + C_{12}) (n^\mu i\epsilon_\perp^{\nu\lambda} - n^\nu i\epsilon_\perp^{\mu\lambda}) J_\lambda^\perp - C_{11} i\epsilon_\perp^{\mu\nu} J_1 \\ &\quad + C_{10} (v^\mu n^\nu - v^\nu n^\mu) J_5 - C_{12} (v^\mu i\epsilon_\perp^{\nu\lambda} - v^\nu i\epsilon_\perp^{\mu\lambda}) J_\lambda^\perp . \end{aligned} \quad (2.44)$$

This follows from the reduction of the Dirac basis. Furthermore, it has been shown [9] that in the naive dimensional regularization scheme of anticommuting γ_5 in $4 - 2\epsilon$ dimensions, there are relations $C_1 = C_2$, $C_3 = C_6$, $C_4 = C_7$, $C_5 = C_8$, $C_{10} = C_{11}$, $C_{12} = 0$, among the coefficient functions that hold true to all orders for massless light quarks. At tree-level, the coefficient functions are

$$C_{1,2,3,4,6,7,9,10,11} = 1 , \quad C_{5,8,12} = 0 . \quad (2.45)$$

One-loop corrections to these Wilson coefficients have been computed and can be found in [9]. Apart from the renormalization scale μ they depend on the large scales $\bar{n} \cdot p$ and m_b . This matching calculation achieves the first step in scale separation, and we will typically need some combination of these Wilson coefficients in later applications (e.g. factorization of the hadronic tensor in inclusive $B \rightarrow X_u l^- \bar{\nu}$ decays).

In this short section we do not present the radiative corrections, and therefore we will also delay the discussion of renormalization-group flow of the coefficient functions to later chapters, i.e. when we need it. Let us just mention without proof that all Wilson coefficient functions C_i share the same anomalous dimension [9], which will be the same (up to a minus sign) as the anomalous dimension of the SCET² current $\bar{\chi}_{hc} \Gamma h$.

2.4 SCET_{II}

The goal is to construct an effective theory in which momentum fluctuations are at most of order the soft QCD scale Λ_{QCD} . The main application for such a theory is the calculation of exclusive Heavy-to-Light decay amplitudes. Introducing the expansion parameter as $\lambda = \Lambda_{\text{QCD}}/E$, the constituents of the B meson have a soft momentum scaling $(\lambda, \lambda, \lambda)$. If the decay product is a light energetic hadron, we assign collinear scaling $(\lambda^2, 1, \lambda)$ to the partons inside this hadron. These are the only momenta that appear on external legs. However, as we have seen in the

²We will see later that the anomalous dimension is independent of the hard-collinear momentum square p^2 . This must be true, because p^2 serves as an infra-red regulator, which does not enter the ultra-violet behaviour encoded in the anomalous dimension. Therefore the anomalous dimension will be the same in both theories SCET_I ($p^2 \sim E\Lambda_{\text{QCD}}$) and SCET_{II} ($p^2 \sim \Lambda_{\text{QCD}}^2$), and we will discuss it in the latter theory.

introductory example in Fig. 2.1, there is an additional long-distance mode (soft-collinear) which scales like $(\lambda^2, \lambda, \lambda^{3/2})$. Such a field communicates with either the soft or the collinear sector but does not appear on external legs, and is therefore referred to as a “messenger”. Whether or not this mode will contribute in the end depends on choices such as infra-red regulators and quark masses. We shall work consistently in the limit of vanishing quark masses for the first family, and therefore include this mode in the effective theory. We will see later that the soft-collinear sector of SCET_{II} provides us with very elegant arguments to discuss important physics such as factorizability and endpoint singularities of decay amplitudes.

Let us deal with the various sectors of SCET_{II} one by one. The effective Lagrangian contains interactions between soft and collinear fields by either the exchange of messenger modes or induced interactions resulting from the exchange of hard-collinear off-shell propagators. The latter are, however, kinematically forbidden in the applications considered in this work [15], because they require exceptional momentum configurations which are typically not generated at leading power in loop graphs. We may therefore neglect such terms. The Lagrangian can be split up as

$$\mathcal{L} = \mathcal{L}_c + \mathcal{L}_s + \mathcal{L}_h + \mathcal{L}_{sc} + \mathcal{L}_{\text{int}} . \quad (2.46)$$

The construction of the collinear, soft, and heavy Lagrangians proceed analogously to our previous discussions [12, 9]:

$$\mathcal{L}_c = \bar{\xi} \frac{\not{n}}{2} i n \cdot D_c \xi - \bar{\xi} i \not{D}_{c\perp} \frac{\not{n}}{2} \frac{1}{i \bar{n} \cdot D_c} i \not{D}_{c\perp} \xi + \mathcal{L}_c^{\text{glue}} , \quad \mathcal{L}_s = \bar{q} i \not{D}_s q + \mathcal{L}_s^{\text{glue}} , \quad (2.47)$$

and the HQET Lagrangian as given in (2.31). Note that, in contrast to the construction of SCET_I, the above Lagrangians are exact to all orders in λ . The gluon Lagrangians in the three sectors retain the same form as in full QCD, but with

the gluon fields restricted to the corresponding subspaces of their soft, collinear, or soft-collinear Fourier modes. The soft-collinear Lagrangian resembles in its form the collinear Lagrangian. This is not surprising, since the light-cone components of a soft-collinear momentum displays the same hierarchy of scales. For completeness (and at the same time reviewing the strategy for \mathcal{L}_c), let us repeat the derivation briefly. Using the projectors $\not{n}\not{n}/4$ and $\not{n}\not{n}/4$, the quark field $q_{sc} = \theta + \sigma$ splits up into small and large components. Analyzing the propagator reveals that $\theta \sim \lambda^2$ is the large component, and $\sigma \sim \lambda^{5/2}$ can be eliminated using the equation of motion

$$\sigma = -\frac{\not{n}}{2} \frac{1}{i\bar{n} \cdot D_{sc}} i\not{D}_{sc\perp} \theta. \quad (2.48)$$

Inserting this result back into the Lagrangian yields the exact result

$$\mathcal{L}_{sc} = \bar{\theta} \frac{\not{n}}{2} i\not{n} \cdot D_{sc} \theta - \bar{\theta} i\not{D}_{sc\perp} \frac{\not{n}}{2} \frac{1}{i\bar{n} \cdot D_{sc}} i\not{D}_{sc\perp} \theta. \quad (2.49)$$

The most important new ingredient of SCET_{II} is the interaction sector between soft-collinear fields with soft or collinear degrees of freedom. The formalism follows along the same lines as the discussion of hard-collinear – soft interactions in SCET_I, but is richer (and more interesting). It has been developed and discussed in detail in [15] and will be outlined in the next section.

In interactions with other fields, the soft-collinear fields (but not the soft and collinear fields) are multipole expanded as

$$\begin{aligned} \phi_{sc}(x) &= \phi_{sc}(x_-) + x_\perp \cdot \partial_\perp \phi_{sc}(x_-) + \dots && \text{in collinear interactions,} \\ \phi_{sc}(x) &= \phi_{sc}(x_+) + x_\perp \cdot \partial_\perp \phi_{sc}(x_+) + \dots && \text{in soft interactions.} \end{aligned} \quad (2.50)$$

As before, the four-vectors $x_- = (\bar{n} \cdot x) n/2$ and $x_+ = (n \cdot x) \bar{n}/2$ are light-cone positions. The first correction terms in (2.50) are of $O(\lambda^{1/2})$, and the omitted terms are of $O(\lambda)$ and higher.

2.4.1 Gauge Transformations and Interaction Terms

Soft-collinear fields can couple to soft or collinear fields without altering their scaling properties. This motivates the treatment of the soft-collinear gluon field as a background field. However, in order to preserve the scaling properties of the fields under gauge transformations one must expand the transformation laws in λ . In close analogy to the discussion in SCET_I, this leads to the following set of “homogeneous” gauge transformations for the quark fields:

$$\begin{aligned}
\text{soft: } q_s(x) &\rightarrow U_s(x) q_s(x), & \text{coll. and soft-coll. fields invariant} \\
\text{collinear: } \xi(x) &\rightarrow U_c(x) \xi(x), & \text{soft and soft-coll. fields invariant} \\
\text{soft-collinear: } q_s(x) &\rightarrow U_{sc}(x_+) q_s(x), & \xi(x) \rightarrow U_{sc}(x_-) \xi(x), \\
& & q_{sc}(x) \rightarrow U_{sc}(x) q_{sc}(x).
\end{aligned} \tag{2.51}$$

The transformation laws for gluons are more complicated, but straightforward [15]. Treating the slowly varying soft-collinear gluons as background fields, we have the following transformation laws under soft and collinear gauge transformations before multipole expansion:

$$A_s^\mu \rightarrow U_s A_s^\mu U_s^\dagger + U_s [iD_{sc}^\mu, U_s^\dagger], \quad A_c^\mu \rightarrow U_c A_c^\mu U_c^\dagger + U_c [iD_{sc}^\mu, U_c^\dagger], \tag{2.52}$$

while the collinear and soft-collinear fields remain invariant under U_s , and soft and soft-collinear fields remain invariant under U_c . Finally, under soft-collinear gauge transformations U_{sc} the fields transform as

$$\begin{aligned}
A_c^\mu &\rightarrow U_{sc} A_c^\mu U_{sc}^\dagger, & \xi &\rightarrow U_{sc} \xi, \\
A_s^\mu &\rightarrow U_{sc} A_s^\mu U_{sc}^\dagger, & q_s &\rightarrow U_{sc} q_s, \\
A_{sc}^\mu &\rightarrow U_{sc} A_{sc}^\mu U_{sc}^\dagger + U_{sc} [i\partial^\mu, U_{sc}^\dagger], & q_{sc} &\rightarrow U_{sc} q_{sc}.
\end{aligned} \tag{2.53}$$

It can be seen from these relations that the combination $(A_s^\mu + A_{sc}^\mu)$ transforms in the usual way under both soft and soft-collinear gauge transformations, while $(A_c^\mu + A_{sc}^\mu)$ transforms in the usual way under both collinear and soft-collinear gauge transformations. In order to preserve a homogeneous power counting, we expand the above rules and keep only the leading-order terms for consistency. This means that the transformation laws are replaced by the homogeneous transformations

$$\begin{aligned}
\text{soft: } \quad n \cdot A_s &\rightarrow U_s n \cdot A_s U_s^\dagger + U_s [in \cdot \partial, U_s^\dagger], & q_s &\rightarrow U_s q_s, \\
A_{s\perp}^\mu &\rightarrow U_s A_{s\perp}^\mu U_s^\dagger + U_s [i\partial_\perp^\mu, U_s^\dagger], \\
\bar{n} \cdot A_s &\rightarrow U_s \bar{n} \cdot A_s U_s^\dagger + U_s [i\bar{n} \cdot D_{sc}(x_+), U_s^\dagger], \\
\text{soft-collinear: } A_s^\mu &\rightarrow U_{sc}(x_+) A_s^\mu U_{sc}^\dagger(x_+), & q_s &\rightarrow U_{sc}(x_+) q_s, \\
& & & (2.54)
\end{aligned}$$

for soft gluon fields and

$$\begin{aligned}
\text{collinear: } \quad \bar{n} \cdot A_c &\rightarrow U_c \bar{n} \cdot A_c U_c^\dagger + U_c [i\bar{n} \cdot \partial, U_c^\dagger], & \xi &\rightarrow U_c \xi, \\
A_{c\perp}^\mu &\rightarrow U_c A_{c\perp}^\mu U_c^\dagger + U_c [i\partial_\perp^\mu, U_c^\dagger], \\
n \cdot A_c &\rightarrow U_c n \cdot A_c U_c^\dagger + U_c [in \cdot D_{sc}(x_-), U_c^\dagger], \\
\text{soft-collinear: } A_c^\mu &\rightarrow U_{sc}(x_-) A_c^\mu U_{sc}^\dagger(x_-), & \xi &\rightarrow U_{sc}(x_-) \xi, \\
& & & (2.55)
\end{aligned}$$

for collinear gluon fields. The soft-collinear gauge sector transforms in the usual form. Let us now return to the interaction Lagrangian. There are no interactions between soft and collinear fields, since such interactions would lead to off-shell momenta of $O(E\Lambda_{\text{QCD}})$. Soft and collinear fields can, however, couple separately to soft-collinear fields. At leading power we have

$$\begin{aligned}
\mathcal{L}_{\text{int}}^{(0)}(x) &= \bar{q}_s(x) \frac{\not{n}}{2} g \bar{n} \cdot A_{sc}(x_+) q_s(x) + \bar{h}(x) \frac{n \cdot v}{2} g \bar{n} \cdot A_{sc}(x_+) h(x) \\
&+ \bar{\xi}(x) \frac{\not{\bar{n}}}{2} g n \cdot A_{sc}(x_-) \xi(x) + \text{pure glue terms}.
\end{aligned} \tag{2.56}$$

Subleading terms have been calculated and can be found in [15].

Momentum conservation implies that soft-collinear fields can only couple to either soft or collinear modes, but not both. More than one soft or collinear particle must be involved in such interactions. The gluon self-couplings can be derived by substituting $A_s^\mu \rightarrow A_s^\mu + \frac{1}{2}n^\mu \bar{n} \cdot A_{sc}(x_+)$ for the gluon field in the soft Yang–Mills Lagrangian and $A_c^\mu \rightarrow A_c^\mu + \frac{1}{2}\bar{n}^\mu n \cdot A_{sc}(x_-)$ for the gluon field in the collinear Yang–Mills Lagrangian, and isolating terms containing the soft-collinear field. The precise form of these interactions will not be relevant to our discussion. Finally, let us note that none of the terms in the SCET Lagrangian (2.46) is renormalized beyond the usual renormalization of the strong coupling and the fields [12, 15].

The multipole expansion of the soft-collinear fields implies that momentum is *not* conserved at these vertices. When a soft (light or heavy) quark with momentum p_s absorbs a soft-collinear gluon with momentum k , the outgoing soft quark carries momentum $p_s + k_-$. Likewise, when a collinear quark with momentum p_c absorbs a soft-collinear gluon with momentum k , the outgoing collinear quark carries momentum $p_c + k_+$.

In order to match the quark and gluon fields of the full theory onto SCET fields obeying the homogeneous gauge transformations one first adopts specific gauges in the soft and collinear sectors, namely soft light-cone gauge $n \cdot A_s = 0$ (SLCG) and collinear light-cone gauge $\bar{n} \cdot A_c = 0$ (CLCG). At leading order in λ , one then introduces the corresponding SCET fields via the substitutions [13, 15]

$$\psi_s|_{\text{SLCG}} \rightarrow R_s S_s^\dagger q_s, \quad b|_{\text{SLCG}} \rightarrow R_s S_s^\dagger h, \quad \psi_c|_{\text{CLCG}} \rightarrow R_c W_c^\dagger \xi. \quad (2.57)$$

The corresponding replacements for gluon fields can be found in [15]. They are a little more complicated, because the homogeneous gauge transformation mixes the

soft and the collinear gluon fields with soft-collinear ones. For example, the two non-zero components of the soft gluon in SLCG are given by

$$\begin{aligned} A_{s\perp}^\mu|_{\text{SLCG}} &\rightarrow R_s S_s^\dagger (iD_{s\perp}^\mu S_s) R_s^\dagger, \\ \bar{n} \cdot A_s|_{\text{SLCG}} &\rightarrow R_s [S_s^\dagger (i\bar{n} \cdot D_{s\perp}^\mu S_s) + S_s^\dagger [\bar{n} \cdot A_{sc}(x_+), S_s]] R_s^\dagger. \end{aligned} \quad (2.58)$$

Similarly for collinear gluons. The quantities

$$\begin{aligned} S_s(x) &= \text{P exp} \left(ig \int_{-\infty}^0 dt n \cdot A_s(x + tn) \right), \\ W_c(x) &= \text{P exp} \left(ig \int_{-\infty}^0 dt \bar{n} \cdot A_c(x + t\bar{n}) \right) \end{aligned} \quad (2.59)$$

are SCET Wilson lines in the soft and collinear sectors [12, 11], which effectively put the SCET fields into light-cone gauge. Small subscripts “s” and “c” are provided to distinguish these Wilson lines from corresponding ones with the soft or collinear gluon fields replaced by soft-collinear ones. The objects R_s and R_c are short gauge strings of soft-collinear fields from x_+ to x (for R_s) and x_- to x (for R_c). They differ from 1 by terms of order $\lambda^{1/2}$ and so must be Taylor expanded. Note that S_s transforms as $S_s(x) \rightarrow U_s(x) S_s(x)$ and $S_s(x) \rightarrow U_{sc}(x_+) S_s(x) U_{sc}^\dagger(x_+)$ under soft and soft-collinear gauge transformations and is invariant under collinear gauge transformations. Likewise, W_c transforms as $W_c(x) \rightarrow U_c(x) W_c(x)$ and $W_c(x) \rightarrow U_{sc}(x_-) W_c(x) U_{sc}^\dagger(x_-)$ under collinear and soft-collinear gauge transformations and is invariant under soft gauge transformations. The short strings only transform under soft-collinear gauge transformations, in such a way that $R_s(x) \rightarrow U_{sc}(x) R_s(x) U_{sc}^\dagger(x_+)$ and $R_c(x) \rightarrow U_{sc}(x) R_c(x) U_{sc}^\dagger(x_-)$. It follows that the expressions on the right-hand side of (2.57) are invariant under soft and collinear gauge transformations and transform as ordinary QCD quark fields under soft-collinear gauge transformations.

Again it is sometimes useful to introduce the calligraphic fields that are gauge-

invariant building blocks

$$\begin{aligned}
W_c^\dagger \xi &= S_{sc}(x_-) \mathcal{X}, & S_s^\dagger q_s &= W_{sc}(x_+) \mathcal{Q}_s, & S_s^\dagger h &= W_{sc}(x_+) \mathcal{H}, \\
W_c^\dagger (iD_{c\perp}^\mu W_c) &= S_{sc}(x_-) \mathcal{A}_{c\perp}^\mu S_{sc}^\dagger(x_-), & S_s^\dagger (iD_{s\perp}^\mu S_s) &= W_{sc}(x_+) \mathcal{A}_{s\perp}^\mu W_{sc}^\dagger(x_+),
\end{aligned} \tag{2.60}$$

where fields without argument live at position x . The quantities W_{sc} and S_{sc} are a new set of Wilson lines defined in analogy with W_c and S_s in (2.59), but, as mentioned above, with the gluon fields replaced by soft-collinear gluon fields in both cases. The calligraphic fields in (2.60) are invariant under soft, collinear, and soft-collinear gauge transformations. This follows from the fact that the new Wilson lines transform as

$$W_{sc}(x_+) \rightarrow U_{sc}(x_+) W_{sc}(x_+), \quad S_{sc}(x_-) \rightarrow U_{sc}(x_-) S_{sc}(x_-) \tag{2.61}$$

under soft-collinear gauge transformations.

2.4.2 Currents

Heavy-to-Collinear Currents

Let us recall from the discussion of Wilson lines that W_{hc} emerged in heavy-to-collinear currents in SCET_I by keeping leading-order attachments of collinear gluons to the heavy quark line. In SCET_{II} we denote this Wilson line by W_c . Note that attachments of soft gluons to the collinear quark line will also lead to off-shell modes, and thus to the appearance of S_s . Naively, one might therefore expect to build up the current $\bar{\xi} S_s^\dagger \Gamma W_c h$, and in a non-abelian theory S_s^\dagger and W_c do not commute. However, adding diagrams involving non-abelian gluon couplings reverses the order of the two Wilson lines [11], as dictated by soft and collinear gauge invariance.

The matching procedure (2.57) reproduces this explicit finding in the following simple way. At tree-level and leading power the QCD current is matched onto the gauge-invariant object (omitting the large HQET phase $e^{-im_b v \cdot x}$)

$$\begin{aligned} \bar{\psi}_c(x) \Gamma b(x) &\rightarrow [\bar{\xi} W_c R_c^\dagger](x) \Gamma [R_s S_s^\dagger h](x) \\ &= [\bar{\xi} W_c](x_+ + x_\perp) \Gamma [S_s^\dagger h](x_- + x_\perp) + O(\lambda). \end{aligned} \quad (2.62)$$

Note that the expression in the first line is not homogeneous in λ . In interactions of soft and collinear fields, the soft fields must be multipole expanded about $x_+ = 0$, while the collinear fields must be multipole expanded about $x_- = 0$. Also, as mentioned above, the quantities R_s and R_c must be expanded and equal 1 to first order. This leads to the result shown in the second line. The terms of $O(\lambda^{1/2})$ in the expansions of R_s and R_c cancel each other [15]. The leading-order SCET current in the final expression is gauge invariant even without the R_s and R_c factors, since soft fields at $x_+ = 0$ and collinear fields at $x_- = 0$ both transform with $U_{sc}(0)$ under soft-collinear gauge transformations.

When radiative corrections are taken into account, the current mixes with analogous operators at different positions on the light cone, and for the case of the heavy-to-collinear currents different Dirac structures can be induced by hard gluon exchange. The correct matching relation reads (setting $x = 0$ for simplicity)

$$\begin{aligned} \bar{\psi}_c(0) \Gamma b(0) &\rightarrow \sum_i \int ds \tilde{C}_i(s, \mu) [\bar{\xi} W_c](s\bar{n}) \Gamma_i [S_s^\dagger h](0) + O(\lambda) \\ &= \sum_i C_i(\bar{n} \cdot P^c, \mu) [\bar{\xi} W_c \Gamma_i S_s^\dagger h](0) + O(\lambda), \end{aligned} \quad (2.63)$$

where translation invariance is used to rewrite the expression in a local form. As in the case of SCET_I, there are only three independent Dirac structures Γ_i allowed. The coefficient functions $C_i(\bar{n} \cdot P^c) = \int ds e^{is\bar{n} \cdot P^c} \tilde{C}_i(s)$ are the Fourier transforms

of the position-space Wilson coefficients \tilde{C}_i and depend on the total collinear momentum operator $P^c = P_{\text{out}}^c - P_{\text{in}}^c$. In fact, by reparameterization invariance (see Section 2.5 below) the dependence of the Wilson coefficient functions on P^c must be through the combination $2v \cdot P_-^c = (v \cdot n)(\bar{n} \cdot P^c)$. Unless otherwise stated, we set $v \cdot n = 1$ for convenience, and work with the above expressions.

Soft-to-Collinear Currents

Arguments along the same line as in the previous section would suggest that the QCD current $\bar{\psi}_c(0) \Gamma \psi_s(0)$ matches simply onto terms of the form $[\bar{\xi} W_c] \Gamma [S_s^\dagger q]$ with the fields evaluated at different positions. This is, however, not quite correct. Note that the soft massless quark field is a full four-component QCD spinor, so that we cannot use the reduced Dirac basis Γ_i . A careful perturbative matching analysis shows that there is a second structure that appears at leading power, involving a perpendicularly polarized collinear gluon [14]. At tree-level, the expression

$$[\bar{\xi} W_c](0) \Gamma [S_s^\dagger q](0) - \int_{-\infty}^0 dt \bar{\xi}(0) \Gamma \left[\frac{\not{n}}{2} \not{D}_{c\perp} W_c \right](0) [S_s^\dagger q](tn) \quad (2.64)$$

sums up an infinite set of leading-order interactions. Despite of the extra perpendicular derivative (which scales like λ), this operator is not subleading because of the large non-localities associated with soft fields (integration in t over a large domain of order λ^{-1}). Radiative corrections mix these currents with similar operators at different positions on the light-cone. Note that because of the factor of \not{n} , the operator vanishes if Γ commutes with \not{n} . The existence of this second operator therefore depends on the particular Dirac structure. For the present work we will only need Dirac structures that are of the form $\Gamma \not{n}$, so that the second term in (2.64) vanishes since $n^2 = 0$. The matching relation of interest therefore reads

$$\begin{aligned}
\bar{\psi}_c(0) \Gamma \frac{\not{n}}{2} \psi_s(0) &\rightarrow \int ds dt \tilde{D}(s, t, \mu) [\bar{\xi} W_c](s\bar{n}) \Gamma \frac{\not{n}}{2} [S_s^\dagger q_s](tn) + O(\lambda) \\
&= D(P_+^s \cdot P_-^c, \mu) [\bar{\xi} W_c \Gamma \frac{\not{n}}{2} S_s^\dagger q_s](0) + O(\lambda).
\end{aligned} \tag{2.65}$$

Again, reparameterization invariance dictates that the Wilson coefficient can only depend on the scalar product $2P_+^s \cdot P_-^c = (n \cdot P^s)(\bar{n} \cdot P^c)$.

Radiative Corrections and Anomalous Dimensions

The momentum-space coefficient functions in (2.63) and (2.65) are renormalized multiplicatively and obey renormalization-group (RG) equations of the Sudakov type [9, 24], i.e. contain an explicit logarithmic renormalization scale dependence,

$$\begin{aligned}
\frac{d}{d \ln \mu} C_i(v \cdot p_{c-}, \mu) &= \gamma_{\xi h}(v \cdot p_{c-}, \mu) C_i(v \cdot p_{c-}, \mu), \\
\frac{d}{d \ln \mu} D(p_{s+} \cdot p_{c-}, \mu) &= \gamma_{\xi q}(p_{s+} \cdot p_{c-}, \mu) D(p_{s+} \cdot p_{c-}, \mu),
\end{aligned} \tag{2.66}$$

where the anomalous dimensions take the form

$$\begin{aligned}
\gamma_{\xi h}(v \cdot p_{c-}, \mu) &= -\frac{1}{2} \Gamma_{\text{cusp}}[\alpha_s(\mu)] \ln \frac{\mu^2}{(2v \cdot p_{c-})^2} + \Gamma_{\xi h}[\alpha_s(\mu)], \\
\gamma_{\xi q}(p_{s+} \cdot p_{c-}, \mu) &= -\Gamma_{\text{cusp}}[\alpha_s(\mu)] \ln \frac{\mu^2}{2p_{s+} \cdot p_{c-}} + \Gamma_{\xi q}[\alpha_s(\mu)].
\end{aligned} \tag{2.67}$$

The coefficients of the logarithmic terms are determined in terms of the universal cusp anomalous dimension $\Gamma_{\text{cusp}} = C_F \alpha_s / \pi + O(\alpha_s^2)$, which plays a central role in the renormalization of Wilson lines with light-like segments [25]. The one-loop expressions for the non-logarithmic terms in the anomalous dimensions can be deduced from the explicit results for the Wilson coefficients derived in [9, 14]. They are

$$\Gamma_{\xi h}(\alpha_s) = -\frac{5}{4} \frac{C_F \alpha_s}{\pi} + O(\alpha_s^2), \quad \Gamma_{\xi q}(\alpha_s) = -\frac{3}{2} \frac{C_F \alpha_s}{\pi} + O(\alpha_s^2). \tag{2.68}$$

It may seem surprising that after hard and hard-collinear scales have been integrated out the operators of the low-energy theory still know about the large

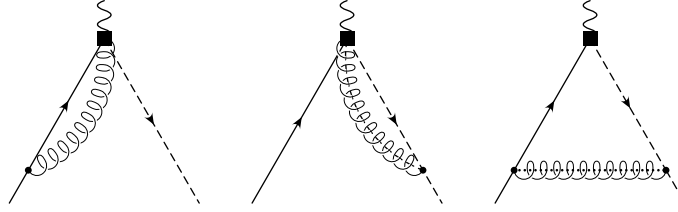


Figure 2.3: SCET graphs contributing to the anomalous dimension of a soft-collinear current. Full lines denote soft fields, dashed lines collinear fields, and dotted lines soft-collinear fields.

scales $v \cdot p_{c-} \sim E$ and $p_{s+} \cdot p_{c-} \sim E\Lambda_{\text{QCD}}$, as is evident from the appearance of the logarithms in (2.67). The reason is that in interactions involving both soft and collinear particles there is a large Lorentz boost $\gamma \sim p_s \cdot p_c / \sqrt{p_s^2 p_c^2} \sim E/\Lambda_{\text{QCD}}$ connecting the rest frames of soft and collinear hadrons, which is fixed by external kinematics and enters the effective theory as a parameter. This is similar to applications of HQET to $b \rightarrow c$ transitions, where the fields depend on the external velocities of the hadrons containing the heavy quarks, and $\gamma = v_b \cdot v_c = O(1)$ is an external parameter that appears in matrix elements and anomalous dimensions of velocity-changing current operators [2, 26]. In the case of SCET, the boost parameter γ can, in some cases, reintroduce a “long-distance type” dependence on the large energy through low-energy operator matrix elements (see for example Section 6).

We will now explain how the results for the anomalous dimensions can be obtained from a calculation of UV poles of SCET loop diagrams [16]. The relevant diagrams needed at one-loop order are shown in Fig. 2.3. They must be supplemented by wave-function renormalization of the quark fields. The gluons connected to the current are part of the Wilson lines W_c and S_s . We regularize IR singularities by keeping the external lines off-shell. The results for the sum of all UV poles must be independent of the IR regulators. For the heavy-to-collinear

current the pole terms obtained from the three diagrams are (here and below we omit the $-i0$ in the arguments of logarithms)

$$\begin{aligned} & \left(\frac{1}{\epsilon^2} - \frac{2}{\epsilon} \ln \frac{-2v \cdot p_s}{\mu} + \frac{1}{\epsilon} \right) + \left(\frac{2}{\epsilon^2} - \frac{2}{\epsilon} \ln \frac{-p_c^2}{\mu^2} + \frac{3}{2\epsilon} \right) \\ & + \left(-\frac{2}{\epsilon^2} + \frac{2}{\epsilon} \ln \frac{(-2v \cdot p_s)(-p_c^2)}{2v \cdot p_{c-} \mu^2} \right) = \frac{1}{\epsilon^2} + \frac{2}{\epsilon} \ln \frac{\mu}{2v \cdot p_{c-}} + \frac{5}{2\epsilon}, \end{aligned} \quad (2.69)$$

while for the soft-to-collinear current we obtain

$$\begin{aligned} & \left(\frac{2}{\epsilon^2} - \frac{2}{\epsilon} \ln \frac{-p_s^2}{\mu^2} + \frac{3}{2\epsilon} \right) + \left(\frac{2}{\epsilon^2} - \frac{2}{\epsilon} \ln \frac{-p_c^2}{\mu^2} + \frac{3}{2\epsilon} \right) \\ & + \left(-\frac{2}{\epsilon^2} + \frac{2}{\epsilon} \ln \frac{(-p_s^2)(-p_c^2)}{2p_{s+} \cdot p_{c-} \mu^2} \right) = \frac{2}{\epsilon^2} + \frac{2}{\epsilon} \ln \frac{\mu^2}{2p_{s+} \cdot p_{c-}} + \frac{3}{\epsilon}. \end{aligned} \quad (2.70)$$

We quote the contributions to the operator renormalization constants Z^{-1} in units of $C_F \alpha_s / 4\pi$ (in the $\overline{\text{MS}}$ subtraction scheme in $4 - 2\epsilon$ dimensions). The three parentheses in the first line of the above equations correspond to the soft, collinear, and soft-collinear contributions, where the first two terms include the corresponding contributions from wave-function renormalization. The $1/\epsilon$ poles of the soft and collinear graphs depend on the IR regulators, but this dependence is precisely canceled by the soft-collinear contribution. By construction, the sum of the soft, collinear, and soft-collinear contributions is IR finite and only contains UV poles, whose coefficients depend on the ratios $v \cdot p_{c-}/\mu$ and $p_{s+} \cdot p_{c-}/\mu^2$. This follows since IR divergences in both the full and the effective theory (which are equivalent at low energy) are regularized by the off-shellness of the external quark lines. The one-loop contributions to the anomalous dimensions $\gamma_{\xi h}$ and $\gamma_{\xi q}$ are given by $-C_F \alpha_s / 2\pi$ times the coefficients of the $1/\epsilon$ poles in the above expressions. They are in agreement with the results (2.67) and (2.68) obtained from the scale dependence of Wilson coefficients.

The calculations presented above make it evident that there is an intricate interplay between the soft, collinear, and soft-collinear diagrams. In dimensional

regularization the dependence of the anomalous dimensions on the hard or hard-collinear scale enters through the loop integral involving the soft-collinear exchange and thus seems to be related to very small momentum scales. However, care must be taken when assigning physical significance to the scales associated with individual diagrams in SCET, because in the soft and collinear diagrams a cancellation of IR and UV divergences takes place. The logarithms appearing in their divergent parts should be interpreted as [cf. (2.70)]

$$\ln \frac{-p_s^2}{\mu^2} + \ln \frac{-p_c^2}{\mu^2} = \ln \frac{Q^2}{\mu^2} + \ln \frac{m_{sc}^2}{\mu^2}, \quad \text{with} \quad m_{sc}^2 = \frac{(-p_s^2)(-p_c^2)}{2p_{s+} \cdot p_{c-}}, \quad (2.71)$$

and thus arise from a cancellation of physics at the hard scale $Q^2 = 2p_{s+} \cdot p_{c-}$ and at the soft-collinear scale m_{sc}^2 . In the sum of all graphs, the soft-collinear contribution precisely cancels the IR piece of the soft and collinear parts, see (2.70). This interpretation is consistent with the fact that the anomalous dimensions measure the change of operator matrix elements under infinitesimal variations of the UV cutoff μ . They are therefore insensitive to the physics at low scales by construction, and the large logarithms in (2.67) are really of short-distance nature.

We would like to close this Section with a (somewhat historic) remark that dates back to the time before soft-collinear fields were introduced to SCET_{II}. After all, for exclusive B decays one identifies the expansion parameter λ with the ratio Λ_{QCD}/E , and therefore the soft-collinear scale m_{sc} is parametrically smaller than Λ_{QCD} . This raises some concerns as to whether the soft-collinear fields have a right to exist. So consider for a few seconds (and not much longer) the soft-collinear sector to be absent. Then the following puzzle arises: We know from the explicit expressions for the Wilson coefficients of the currents that their anomalous dimensions must depend on a scalar product of the collinear momentum with a momentum characterizing the soft quark (i.e., $v \cdot p_{c-}$ or $p_{s+} \cdot p_{c-}$). However, the

SCET Feynman rules imply that the first graph in Fig. 2.3 can only be a function of the soft momentum (i.e., $v \cdot p_s$ or p_s^2), while the second one can only depend on the collinear momentum (i. e. , p_c^2), as is in fact confirmed by the explicit calculation. The apparent “factorization” of soft and collinear degrees of freedom in SCET_{II} (in the hypothetical absence of soft-collinear fields) would thus lead to the conclusion that the anomalous dimensions of the currents are independent of the products $v \cdot p_{c-}$ or $p_{s+} \cdot p_{c-}$, in contradiction with the results for the Wilson coefficients. In fact, factorization would be a generic property of SCET_{II}, since the interaction Lagrangian in (2.56) would no longer exist. This is obviously incorrect; for example it is well known that $B \rightarrow \pi$ transition form factors do not factorize, although they can be described using SCET_{II}.

Although the above argument strongly motivates the use of soft-collinear fields in SCET_{II}, it does not necessitate it. Alternative prescriptions include the introduction of “analytic regulators” [27] where propagators are raised to a non-integer power, and explicit infra-red regulators in the Lagrangian [28]. However, these schemes are not favorable in our opinion because analytic regulators are very complicated and cannot be introduced on the Lagrangian level in a gauge-invariant fashion, and the proposed infra-red regulators in [28] break many important symmetries such as gauge invariance and Lorentz invariance. The soft-collinear sector solves the problem in a much more simple and elegant way.

2.4.3 Four-quark Operators

In many cases in B -decay physics, amplitudes calculated in SCET receive contributions from hadronic matrix elements of four-quark operators, which can be expressed in terms of the leading-order light-cone distribution amplitudes of a light

final-state meson and of the initial state B meson. The relevant SCET operators can be taken as [14, 16]

$$\begin{aligned} Q_{(C)}(s, t) &= [\bar{\xi} W_c](s\bar{n}) \frac{\not{n}}{2} \Gamma_1 T_1 [W_c^\dagger \xi](0) [\bar{q}_s S_s](tn) \frac{\not{n}}{2} \Gamma_2 T_2 [S_s^\dagger h](0) \\ &\equiv \int_0^\infty d\omega e^{-i\omega t} \int_0^{\bar{n} \cdot P} d\sigma e^{i\sigma s} Q_{(C)}(\omega, \sigma), \end{aligned} \quad (2.72)$$

where the color label $C = S$ or O refers to the color singlet-singlet and color octet-octet structures $T_1 \otimes T_2 = \mathbf{1} \otimes \mathbf{1}$ or $T_A \otimes T_A$, respectively. Again, $\bar{n} \cdot P$ is the total momentum carried by all collinear particles, which is fixed by kinematics. (Strictly speaking, this is a momentum operator.) In light-cone gauge, $\omega = n \cdot p_s$ corresponds to the plus component of the momentum of the spectator anti-quark in the B meson, while $\sigma = \bar{n} \cdot p_\xi$ denotes the minus component of the momentum of the quark inside a light final-state meson. It is conventional to introduce a dimensionless variable $u = \sigma / \bar{n} \cdot P \in [0, 1]$ corresponding to the longitudinal momentum fraction carried by the quark.

The momentum-space operators $Q_{(C)}(\omega, \sigma)$ obey the rather complicated RG integro-differential equation

$$\frac{d}{d \ln \mu} Q_{(C)}(\omega, u \bar{n} \cdot P) = - \int_0^\infty d\omega' \int_0^1 du' \gamma_{(C)}(\omega, \omega', u, u', \bar{n} \cdot P, \mu) Q_{(C)}(\omega', u' \bar{n} \cdot P). \quad (2.73)$$

To obtain the anomalous dimensions at leading order we compute the $1/\epsilon$ poles of the diagrams shown in Fig. 2.4 in dimensional regularization and add the contributions from wave-function renormalization. Note that only soft-collinear gluons can be exchanged between the soft and collinear currents. For the color-singlet case $T_1 \otimes T_2 = \mathbf{1} \otimes \mathbf{1}$ we find that the sum of the four diagrams with soft-collinear exchanges (but not each diagram separately) is UV finite. The anomalous dimension is then a combination of the anomalous dimensions for the two non-local currents

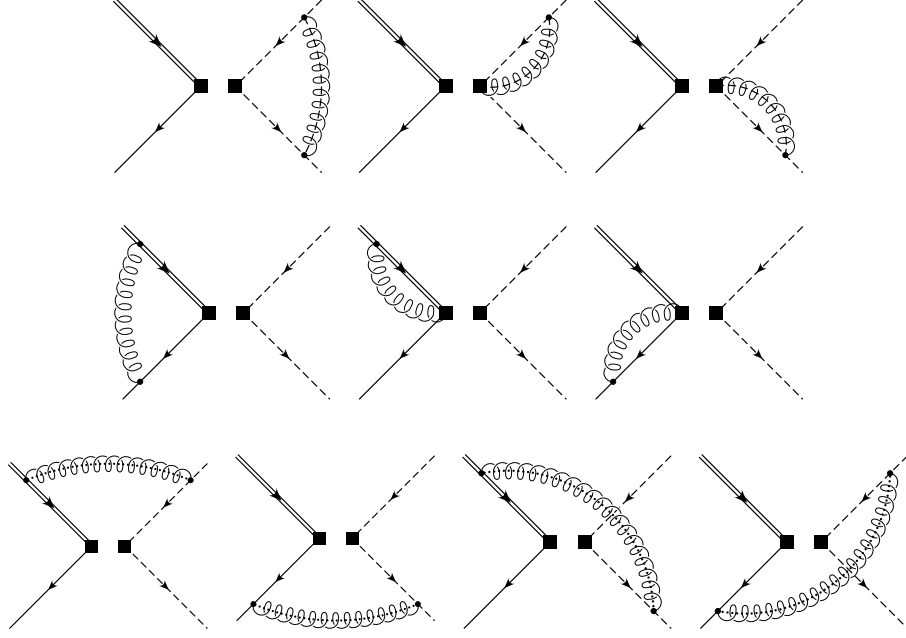


Figure 2.4: SCET graphs contributing to the anomalous dimension of the four-quark operators $Q_{(C)}(\omega, \sigma)$. Full lines denote soft fields, dashed lines collinear fields, and dotted lines soft-collinear fields.

in (2.72). At one-loop order we obtain

$$\gamma_{(S)}(\omega, \omega', u, u', \bar{n} \cdot P, \mu) = \frac{C_F \alpha_s}{\pi} \left[\delta(\omega - \omega') V(u, u') + \delta(u - u') H(\omega, \omega', \mu) \right], \quad (2.74)$$

where (with $\bar{u} \equiv 1 - u$)

$$\begin{aligned} V(u, u') = & - \left[\frac{u}{u'} \left(\frac{1}{u' - u} + c(\Gamma_1) \right) \theta(u'^1 - u) + \frac{\bar{u}}{u'} \left(\frac{1}{u - u'} + c(\Gamma_1) \right) \theta(u - u') \right]_+ \\ & + \frac{1 - c(\Gamma_1)}{2} \delta(u - u') \end{aligned} \quad (2.75)$$

with $c(1) = c(\gamma_5) = 1$, $c(\gamma_\perp^\mu) = 0$ is the Brodsky–Lepage kernel [29] for the evolution of the leading-twist light-cone distribution amplitudes of a light meson, which we have reproduced here using the Feynman rules of SCET. The plus distribution is defined as

$$[f(u, u')]_+ = f(u, u') - \delta(u - u') \int_0^1 dw f(w, u'), \quad (2.76)$$

which coincides with the conventional definition if the distribution acts on functions $g(u)$ but not if it acts on functions $g(u')$. The function

$$H(\omega, \omega', \mu) = \left(\ln \frac{\mu v \cdot n}{\omega} - \frac{5}{4} \right) \delta(\omega - \omega') - \omega \left[\frac{\theta(\omega - \omega')}{\omega(\omega - \omega')} + \frac{\theta(\omega' - \omega)}{\omega'(\omega' - \omega)} \right]_+ \quad (2.77)$$

is the analogous kernel governing the evolution of the leading-order B -meson light-cone distribution amplitude [30]. Here the plus distribution is symmetric in the two arguments and defined as

$$\int_0^\infty d\omega' [f(\omega, \omega')]_+ g(\omega') = \int_0^\infty d\omega' f(\omega, \omega') [g(\omega') - g(\omega)] . \quad (2.78)$$

For the color-octet case $T_1 \otimes T_2 = T_A \otimes T_A$ things are more complicated. In that case the sum of the soft-collinear exchange graphs shown in the last line in Fig. 2.4 does not vanish. However, it provides contributions such that, in the end, the dependence on the IR regulators drops out. Our final result for the anomalous dimension in the octet-octet case is

$$\begin{aligned} \gamma_{(O)}(\omega, \omega', u, u', \bar{n} \cdot P, \mu) &= -\frac{1}{2N} \frac{\alpha_s}{\pi} \left[\delta(\omega - \omega') V(u, u') + \delta(u - u') H(\omega, \omega', \mu) \right] \\ &\quad - \frac{N}{2} \frac{\alpha_s}{\pi} \delta(\omega - \omega') \delta(u - u') \left(\ln \frac{\mu^3}{n \cdot v \omega (\bar{n} \cdot P)^2} - \ln u \bar{u} + \frac{11}{4} \right) . \end{aligned} \quad (2.79)$$

2.4.4 Decoupling transformation

The leading-order interactions between soft-collinear fields and soft or collinear fields in the SCET Lagrangian can be removed by a redefinition of the soft and collinear fields [15]. In analogy with the decoupling of soft gluons in SCET_I [11], we define new fields

$$\begin{aligned} q_s(x) &= W_{sc}(x_+) q_s^{(0)}(x) , & h(x) &= W_{sc}(x_+) h^{(0)}(x) , & \xi(x) &= S_{sc}(x_-) \xi^{(0)}(x) , \\ A_s^\mu(x) &= W_{sc}(x_+) A_s^{(0)\mu}(x) W_{sc}^\dagger(x_+) , & A_c^\mu(x) &= S_{sc}(x_-) A_c^{(0)\mu}(x) S_{sc}^\dagger(x_-) . \end{aligned} \quad (2.80)$$

The quantities W_{sc} and S_{sc} have already been introduced in (2.60), where we studied their gauge transformation properties. The new fields with “(0)” superscripts are invariant under soft-collinear gauge transformations, but there is no longer a soft-collinear background field in their transformation law. Essentially, the leading power effect of the above field redefinition is that the substitutions $A_s^\mu \rightarrow A_s^\mu + \frac{1}{2}n^\mu \bar{n} \cdot A_{sc}(x_+)$ and $A_c^\mu \rightarrow A_c^\mu + \frac{1}{2}\bar{n}^\mu n \cdot A_{sc}(x_-)$ from the multipole expansion are reversed. As a result, when the new fields are introduced in the SCET Lagrangian the terms \mathcal{L}_s , \mathcal{L}_c , and \mathcal{L}_{sc} retain their original form, while the *leading-order interaction Lagrangian* $\mathcal{L}_{\text{int}}^{(0)}$ *vanishes!* Residual interactions between soft-collinear and soft or collinear fields start at $O(\lambda^{1/2})$ [15]. After the field redefinition it is convenient to introduce the gauge-invariant building blocks [14, 15]

$$\begin{aligned} S_s^{(0)\dagger}(x) q_s^{(0)}(x) &= W_{sc}^\dagger(x_+) S_s^\dagger(x) q_s(x) = \mathcal{Q}_s(x), \\ S_s^{(0)\dagger}(x) h^{(0)}(x) &= W_{sc}^\dagger(x_+) S_s^\dagger(x) h(x) = \mathcal{H}(x), \\ W_c^{(0)\dagger}(x) \xi^{(0)}(x) &= S_{sc}^\dagger(x_-) W_c^\dagger(x) \xi(x) = \mathcal{X}(x), \end{aligned} \tag{2.81}$$

which are obviously identical to (2.60) and invariant under all three types of gauge transformations.

The fact that interactions of soft-collinear fields with other fields can be decoupled from the strong-interaction Lagrangian does not necessarily imply that these fields can be ignored at leading order in power counting. The question is whether the decoupling transformation (2.80) leaves external operators such as weak-interaction currents invariant. The analysis of the previous sections indicates that in some cases the soft-collinear exchange graphs contribute to the calculation of the anomalous dimensions. Let us then study what happens when the decoupling transformation is applied to the various types of operators.

Under the transformation (2.80), the heavy-to-collinear and soft-to-collinear

currents in (2.63) and (2.65) transform into (setting $x_\perp = 0$ for simplicity)

$$\begin{aligned} [\bar{\xi} W_c](x_+) \Gamma [S_s^\dagger h](x_-) &\rightarrow \bar{\mathcal{X}}(x_+) S_{sc}^\dagger(0) \Gamma W_{sc}(0) \mathcal{H}(x_-), \\ [\bar{\xi} W_c](x_+) \Gamma [S_s^\dagger q_s](x_-) &\rightarrow \bar{\mathcal{X}}(x_+) S_{sc}^\dagger(0) \Gamma W_{sc}(0) \mathcal{Q}_s(x_-). \end{aligned} \quad (2.82)$$

We observe that the soft-collinear fields *do not* decouple from these currents but rather form a light-like Wilson loop with a cusp at $x = 0$ [16]. The anomalous dimension of the combination $(S_{sc}^\dagger W_{sc})$ is the universal cusp anomalous dimension times a logarithm of the soft-collinear scale, see the first expressions in the second lines in (2.69) and (2.70). After adding the contributions from the soft and collinear sectors, the dependence on the IR regulators drops out. However, the coefficient of the logarithm of $v \cdot p_{c-}$ in the heavy-collinear current and $p_{s+} \cdot p_{c-}$ in the soft-collinear current is unchanged, since both the soft and the collinear part are independent of these large scales. This cancellation also explains why the anomalous dimensions of the heavy-to-collinear and soft-to-collinear currents involve $-\Gamma_{\text{cusp}}$ and $-\frac{1}{2}\Gamma_{\text{cusp}}$, respectively:

$$\begin{aligned} \Gamma_{\text{cusp}} \left[\ln \frac{2p_{s+} \cdot p_{c-} \mu^2}{(-p_s^2)(-p_c^2)} + \ln \frac{-p_s^2}{\mu^2} + \ln \frac{-p_c^2}{\mu^2} \right] &= -\Gamma_{\text{cusp}} \ln \frac{\mu^2}{2p_{s+} \cdot p_{c-}}, \\ \Gamma_{\text{cusp}} \left[\ln \frac{2v \cdot p_{c-} \mu^2}{(-2v \cdot p_s)(-p_c^2)} + \ln \frac{-2v \cdot p_s}{\mu} + \ln \frac{-p_c^2}{\mu^2} \right] &= -\frac{1}{2} \Gamma_{\text{cusp}} \ln \frac{\mu^2}{(2v \cdot p_{c-})^2}. \end{aligned} \quad (2.83)$$

Similar arguments were used by Korchemsky in his analysis of the off-shell Sudakov form factor [31].

The effect of the field redefinition (2.80) on the four-quark operators is different. The color singlet-singlet operator *is invariant*, namely (setting $x = 0$ for simplicity)

$$Q_{(S)}(s, t) \rightarrow \bar{\mathcal{X}}(s\bar{n}) \Gamma_1 \mathcal{X}(0) \bar{\mathcal{Q}}_s(tn) \Gamma_2 \mathcal{H}(0), \quad (2.84)$$

since the additional soft-collinear Wilson lines come in pairs $W_{sc}^\dagger W_{sc} = 1$ and $S_{sc}^\dagger S_{sc} = 1$. The color octet-octet operator is however not invariant, since in that

case the cancellation cannot happen. Instead, one obtains the soft-collinear object [16]

$$\text{Tr}[S_{sc} T_A S_{sc}^\dagger W_{sc} T_B W_{sc}^\dagger](0) . \quad (2.85)$$

The presence of this functional in the octet-octet case explains why soft-collinear modes give a non-zero contribution to the anomalous dimension of the operator $Q_{(O)}$. However, since this operator does not mix into the singlet-singlet operator $Q_{(S)}$, this effect does not propagate into physical decay amplitudes (as hadronic matrix elements of color-octet currents vanish). The decoupling of soft-collinear fields from the color singlet-singlet operator implies that, to all orders in perturbation theory, the anomalous dimension of the four-quark operator $Q_{(S)}$ is the sum of the anomalous dimensions of the two currents $\bar{\mathcal{X}}(s\bar{n})\Gamma_1\mathcal{X}(0)$ and $\bar{Q}_s(tn)\Gamma_2\mathcal{H}(0)$, in accordance with the one-loop result obtained in the previous section. This observation has important implications for applications of SCET to proofs of QCD factorization theorems.

2.5 Reparameterization Invariance

In section 2.4.2 we have briefly touched on reparameterization invariance, on which we expand here. Operators in SCET must be invariant under redefinitions of the light-cone basis vectors n and \bar{n} that leave the scaling properties of fields and momenta unchanged [14, 22, 32]. This property is referred to as reparameterization invariance, and has proved to be a quite powerful tool. For example, it can be used to derive constraints on the Wilson coefficients of SCET operators, often relating the coefficients of some operators to those of others. Reparameterization invariance is a consequence of the invariance of QCD under Lorentz transformations, which is not explicit (but still present) in SCET because of the introduction of the light-cone

vectors n and \bar{n} .

Commonly one distinguishes between three classes of infinitesimal transformations, corresponding to two different transverse boosts and a longitudinal boost:

$$\begin{aligned}
\text{Type I:} \quad & n^\mu \rightarrow n^\mu + \epsilon_\perp^\mu, & \bar{n}^\mu \text{ invariant} & \quad (\text{with } \epsilon_\perp^\mu \sim \lambda) \\
\text{Type II:} \quad & \bar{n}^\mu \rightarrow \bar{n}^\mu + e_\perp^\mu, & n^\mu \text{ invariant} & \quad (\text{with } e_\perp^\mu \sim 1) \\
\text{Type III:} \quad & n^\mu \rightarrow n^\mu / \alpha, & \bar{n}^\mu \rightarrow \alpha \bar{n}^\mu & \quad (\text{with } \alpha \sim 1)
\end{aligned} \tag{2.86}$$

The scaling properties for the parameters are given in parenthesis. As an example, note that the collinear Wilson line W_c is invariant under type I and type III transformations. To derive the transformation property under type II, note that by definition $[\bar{n} \cdot D_c W_c] = 0$. The variation implies that with $\delta \bar{n} \cdot D_c = e_\perp \cdot D_{c\perp}$ one can derive the change δW_c from $\delta [\bar{n} \cdot D_c W_c] = 0$ [32]. It follows that the correct type II transformation behaviour is $W_c \rightarrow W_c - (\bar{n} \cdot D_c)^{-1} e_\perp \cdot D_{c\perp} W_c$. The transformation laws for soft Wilson lines are found using arguments along the same line.

It is then straightforward to show that, for example, the current operators in (2.64) are separately invariant under type I and type II transformations to leading order in λ . In other words, reparameterization invariance links these operators with operators that appear at subleading order in λ . The only non-trivial point in this analysis concerns the transverse collinear derivative $D_{c\perp}^\mu$, which has non-vanishing variations at leading order in λ under both type I and type II transformations,

$$D_{c\perp}^\mu \xrightarrow{\text{type I}} D_{c\perp}^\mu - \frac{\epsilon_\perp^\mu}{2} \bar{n} \cdot D_c + O(\lambda^2), \quad D_{c\perp}^\mu \xrightarrow{\text{type II}} D_{c\perp}^\mu - \frac{n^\mu}{2} e_\perp \cdot D_{c\perp} + O(\lambda^2). \tag{2.87}$$

Note that in both cases the object $\not{n} W^\dagger (i \not{D}_{c\perp} W) = \not{n} \mathcal{A}_{c\perp}$ is left invariant. For type I transformations this follows from $(\bar{n} \cdot D_c W) = 0$, whereas for type II transformations it follows since $\not{n}^2 = 0$. This is an important result, because without

the extra factor of \not{n} , the second operator in (2.64) would not be invariant under a type II reparameterization.

The type III transformations are the most powerful ones and have non-trivial consequences. For example, consider the current operator in (2.65). Type III transformations dictates the dependence of the Wilson coefficient on the plus-component of the soft momentum p_+^s to all orders in perturbation theory. This provides valuable information about the convergence of convolution integrals of hard-scattering kernels (Wilson coefficients) with the B -meson light-cone distribution amplitudes, which will be an important ingredient to factorization proofs. With a slight abuse of notation, the soft-to-collinear current can be written in the following form, in which we used translation invariance to extract the dependence on the large energy E :

$$\bar{\psi}_c(0) \Gamma \psi_s(0) \rightarrow \int dt \tilde{D}(t, E, \mu) [\bar{\xi} W_c](0) \Gamma [S_s^\dagger q_s](tn) + O(\lambda) . \quad (2.88)$$

Performing a variable substitution $t \rightarrow \alpha t$ and a subsequent Type III transformation (which also rescales the energy) one finds that the current operator is invariant only if its Wilson coefficient obeys the homogeneity relation $\tilde{D}_i(t, E, \mu) = \alpha \tilde{D}_i(\alpha t, \alpha E, \mu)$. Taking into account the canonical dimension of the coefficient, it follows that

$$\tilde{D}(t, E, \mu) = \delta(t) d^{(1)}[\alpha_s(\mu)] + \frac{1}{t} d^{(2)}\left[\ln\left(\frac{\mu^2 t}{E}\right), \alpha_s(\mu)\right] . \quad (2.89)$$

where the coefficient functions $d_i^{(j)}$ are dimensionless. Since the dependence of the Wilson coefficients on the renormalization scale μ is logarithmic, we conclude that to all orders of perturbation theory $\tilde{D}(t, E, \mu) \sim 1/t$ modulo logarithms. Therefore the above argument determines the behavior of the momentum-space coefficients on the soft momentum p_+^s to all orders in perturbation theory.

CHAPTER 3

STRUCTURE FUNCTIONS

3.1 The B -meson Light-Cone Distribution Amplitudes

In section 2.4.3 on four-quark operators we learned a valuable lesson that touches the core of QCD-Factorization: Recall that color singlet-singlet operators decouple from the soft-collinear messenger sector, and therefore the collinear and soft sectors do not interact with each other. Exclusive decay amplitudes are then expressible in terms of convolution integrals and matrix elements of operators of the form (2.84). The product $\bar{Q}_s(tn) \Gamma_2 \mathcal{H}(0)$ has a non-vanishing overlap with the B meson, while $\bar{\mathcal{X}}(s\bar{n}) \Gamma_1 \mathcal{X}(0)$ overlaps with the final light meson. The use of gauge-invariant building blocks provides the necessary (finite length) Wilson line to make the bilocal operators gauge invariant, since e.g. $\bar{\mathcal{X}}(s\bar{n}) \Gamma_1 \mathcal{X}(0) = [\bar{\xi} W_c](s\bar{n}) \Gamma_1 [W_c^\dagger \xi](0) = \bar{\xi}(s\bar{n}) [s\bar{n}, 0] \Gamma_1 \xi(0)$. The light-like separation of the fields explains why the corresponding non-perturbative wave functions after projection onto meson states are called "light-cone distribution amplitudes" (LCDAs). For the B meson, two such functions, ϕ_+^B and ϕ_-^B , arise for the two-particle Fock state configurations. They are defined in the HQET trace formalism as [33]

$$\begin{aligned} & \frac{1}{\sqrt{M_B}} \langle 0 | \bar{Q}_s(tn) \Gamma \mathcal{H}(0) | \bar{B}(v) \rangle \\ &= -\frac{iF(\mu)}{2} \int d\omega e^{-i\omega t} \text{tr} \left[\left(\phi_+^B(\omega, \mu) - \frac{\not{n}}{2} \left[\phi_-^B(\omega, \mu) - \phi_+^B(\omega, \mu) \right] \right) \Gamma \frac{1 + \not{v}}{2} \gamma_5 \right], \end{aligned} \quad (3.1)$$

where $F(\mu)$ denotes the asymptotic value of $\sqrt{M_B} f_B$ in the heavy-quark limit. (M_B is the B -meson mass and f_B its decay constant.) The variable ω can be interpreted as the plus component of the spectator momentum. Often times it suffices to only consider these two-particle LCDAs, since currents with an extra soft

gluon are power suppressed. However, they become also important if the quantity of interest is itself power suppressed, which is the case for e.g. $B \rightarrow \text{light meson}$ form factors at large recoil. It will then be necessary to also define wave functions containing an additional soft gluon or a derivative. The latter can, however, be eliminated using the equations of motion. Let us define the three-particle LCDAs of the B meson in analogy with (3.1) as [34]

$$\langle 0 | \bar{Q}_s(t\bar{n}) \mathcal{A}_{s\perp}^\mu(s\bar{n}) \Gamma \mathcal{H}(0) | B \rangle = - \frac{iF(\mu)\sqrt{M_B}}{2} \text{tr} \left[\Gamma \frac{1 + \not{v}}{2} \gamma_5 \gamma_\perp^\mu \left(\frac{1}{2} \tilde{A}_1(t, s) + \frac{\not{v}}{2} \tilde{A}_2(t, s) \right) \right]. \quad (3.2)$$

Since $n \cdot \mathcal{A}_s = 0$, the full light-cone decomposition of the gluon field \mathcal{A}_s reads $\mathcal{A}_s = \mathcal{A}_{s,\perp} + \not{v} v \cdot \mathcal{A}_s$ and there are in principle two more wave functions one can define, namely

$$\langle 0 | \bar{Q}_s(t\bar{n}) v \cdot \mathcal{A}_s(s\bar{n}) \Gamma \mathcal{H}(0) | B \rangle = - \frac{iF(\mu)\sqrt{M_B}}{2} \text{tr} \left[\Gamma \frac{1 + \not{v}}{2} \gamma_5 \left(\tilde{A}_3(t, s) + \frac{\not{v}}{2} \tilde{A}_4(t, s) \right) \right]. \quad (3.3)$$

The three-particle LCDAs $A_1(\omega_1, \omega_2), \dots, A_4(\omega_1, \omega_2)$ are defined as the Fourier transforms of $A_1(t, s), \dots, A_4(t, s)$, in close analogy to (3.1).

Equation of Motion constraints. The above LCDAs are related through the equation of motions. In particular, the equation of motion for the light quark field $i\not{D} q_s = 0$, which in terms of collinear fields implies $i\not{\partial} Q_s(x) = -\mathcal{A}_s(x) Q_s(x)$, allows us to express ϕ_-^B entirely in terms of the leading LCDA ϕ_+^B and the three-particle wave function A_1 . It is straightforward to use (3.1) with $\Gamma = \gamma^\mu$ and act with a partial derivative with respect to the position z of the light quark field. Since $\not{\partial} = (\not{v}/2) n \cdot \partial + (\not{v}/2) \bar{n} \cdot \partial + \not{\partial}_\perp$ is the partial derivative in all directions, it is crucial to keep z slightly off the light cone, and set it to the final value $z = tn$ only

after the derivative has been performed. When z is not light-like, the Wilson line $[z, 0] = P \exp[i \int_0^z dz \cdot A_s(z)]$ is no longer given in terms of the product $S_s(z)S_s^\dagger(0)$, but rather as the product of path-ordered exponentials

$$[z, 0] = S_s(z) P \exp \left[i \int_0^1 d\alpha z \cdot \mathcal{A}_s(\alpha z) \right] S_s^\dagger(0) . \quad (3.4)$$

Expanding the Wilson line and taking a partial derivative will then lead to the combination¹ $\mathcal{A}_s(z) - \int_0^1 d\alpha \mathcal{A}_s(\alpha z)$ on the left-hand side of (3.1), while the wave functions on the right-hand side carry additional dependence on $z^2 \neq 0$, which needs to be taken into account when performing the derivative. The result is [34]

$$\begin{aligned} & \omega \phi_-^B(\omega) + \int_0^\omega d\omega' [\phi_+^B(\omega') - \phi_-^B(\omega')] \\ = & - \int_0^\infty d\omega_1 d\omega_2 \delta(\omega - \omega_1 - \omega_2) A_1(\omega_1, \omega_2) \\ & + \int_0^1 d\alpha \int_0^\infty d\omega_1 d\omega_2 \delta(\omega - \omega_1 - \alpha\omega_2) A_1(\omega_1, \omega_2) . \end{aligned} \quad (3.5)$$

Finally we state the explicit expression that eliminates $\phi_-^B(\omega)$ by solving the above equation. Taking a derivative with respect to ω leads to the desired result

$$\begin{aligned} \phi_-^B(\omega) = & - \int_0^\omega d\omega' \frac{\phi_+^B(\omega')}{\omega'} + \int_{\omega_1+\omega_2 \leq \omega} d\omega_1 d\omega_2 \frac{\omega_2}{\omega_1(\omega_1 + \omega_2)^2} A_1(\omega_1, \omega_2) \\ & + \int_0^\omega d\omega_1 \int_{\omega-\omega_1}^\infty d\omega_2 \frac{\omega - \omega_1}{\omega \omega_1 \omega_2} A_1(\omega_1, \omega_2) . \end{aligned} \quad (3.6)$$

The remaining LCDAs A_2, \dots, A_4 are not relevant to the present work.

As mentioned earlier, many applications require only one of the above LCDAs at leading power, $\phi_+^B(\omega, \mu)$. Physically, the sensitivity to this universal, non-perturbative function arises in processes which involve hard interactions with the soft spectator quark in the B -meson, for example in $B \rightarrow \gamma l^- \bar{\nu}$, $B \rightarrow K^* \gamma$, etc.

¹This combination coincides with a gluon field in Fock-Schwinger gauge $\mathcal{A}_{\text{FSG}}(z) = \int_0^1 d\alpha \alpha G^{\mu\nu}(\alpha z) n_\mu \gamma_\nu$.

A generic factorizable decay amplitude may be written as

$$\mathcal{A} = \int_0^\infty \frac{d\omega}{\omega} T(E\omega, \mu) \phi_+^B(\omega, \mu), \quad (3.7)$$

where it is assumed that the μ dependence cancels between the hard-scattering kernel T and the LCDA. In writing the amplitude in this way, a first step of scale separation was achieved, since the kernel depends on the physics associated with large energy scales, i.e. does not contain large logarithms for $\mu \sim \sqrt{E\Lambda_{\text{QCD}}}$, whereas the LCDA is a universal, non-perturbative function which “lives” on low scales $\mu \sim \Lambda_{\text{QCD}}$. Since there is no one scale μ at which neither of the two quantities contain large logarithms it is crucial to resum those large (Sudakov) logarithms to gain full control over the separation of physics at different scales. We thus have to derive and solve the renormalization-group evolution for the LCDA or, equivalently, the hard-scattering kernel [24, 30].

3.1.1 Renormalization-Group Evolution

Different operators that share the same quantum numbers can mix under renormalization. It is therefore appropriate to write the relation between bare operator $O_+^{\text{bare}}(\omega) = \int dt e^{i\omega t} \bar{Q}_s(tn) \Gamma \mathcal{H}(0)$ and renormalized one as

$$O_+^{\text{ren}}(\omega, \mu) = \int d\omega' Z_+(\omega, \omega', \mu) O_+^{\text{bare}}(\omega'). \quad (3.8)$$

In the case at hand the operator is, up to a Dirac trace, the product of $F(\mu)$ and the LCDA $\phi_+^B(\omega, \mu)$. The renormalization-group equation is an integro-differential equation in which the anomalous dimension is convoluted with the LCDA [30]:

$$\frac{d}{d \ln \mu} \phi_+^B(\omega, \mu) = - \int_0^\infty d\omega' \gamma_+(\omega, \omega', \mu) \phi_+^B(\omega', \mu). \quad (3.9)$$

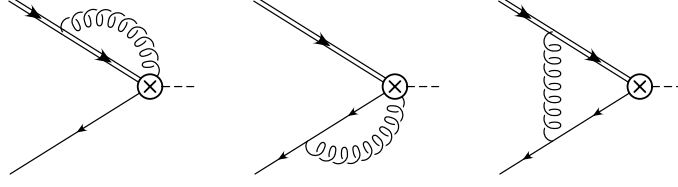


Figure 3.1: One-loop diagrams for the calculation of the anomalous dimension of the B -meson light-cone distribution amplitude.

The anomalous dimension γ_+ is related to the renormalization factor Z_+ through

$$\gamma_+(\omega, \omega', \mu) = - \int d\tilde{\omega} \frac{dZ_+(\omega, \tilde{\omega}, \mu)}{d \ln \mu} Z_+^{-1}(\tilde{\omega}, \omega', \mu) - \gamma_F(\alpha_s) \delta(\omega - \omega'). \quad (3.10)$$

Here γ_F is the universal anomalous dimension of local heavy-light currents in HQET, which determines the scale dependence of $F(\mu)$. We may separate the on- and off-diagonal terms of γ_+ and express it as

$$\gamma_+(\omega, \omega', \mu) = \left[\Gamma_{\text{cusp}}(\alpha_s) \ln \frac{\mu}{\omega} + \gamma(\alpha_s) \right] \delta(\omega - \omega') + \omega \Gamma(\omega, \omega', \alpha_s) \quad (3.11)$$

to all orders in perturbation theory. The cusp anomalous dimension $\Gamma_{\text{cusp}}(\alpha_s)$ appears as the coefficient of the $\ln \mu$ term and has a geometric origin [25]: Since an effective heavy-quark field $h(0)$ can be expressed as the product of a free field $h^{(0)}(0)$ and a Wilson line $S_v(0)$ extending from $(-\infty)$ to 0 along the v -direction, the matrix element in (3.1) contains $S_s(z) S_s^\dagger(0) S_v(0)$ which can be combined to form a single Wilson line with a cusp at the origin, as shown in Fig. 3.2(a). (Recall that soft Wilson lines S_s extend along the n -direction.) The appearance of the single $\ln \mu$ term distinguishes the anomalous dimension of the B -meson LCDA from the familiar Brodsky-Lepage kernel [29]. On the one-loop level the $\ln \mu$ term appears in the calculation of the first diagram in Fig. 3.1, where the gluon from the Wilson line $S_s(z) S_s^\dagger(0)$ connects to the heavy-quark Wilson line $S_v(0)$.

By evaluating the diagrams in Fig. 3.1, we find the one-loop expressions [30]

(denoted by the superscript $^{(1)}$) to be $\Gamma_{\text{cusp}}^{(1)} = 4$, $\gamma^{(1)} = -2$, and

$$\Gamma^{(1)}(\omega, \omega') = -\Gamma_{\text{cusp}}^{(1)} \left[\frac{\theta(\omega' - \omega)}{\omega'(\omega' - \omega)} + \frac{\theta(\omega - \omega')}{\omega(\omega - \omega')} \right]_+ , \quad (3.12)$$

where we have used that $\gamma_F^{(1)} = -3$ is the one-loop coefficient of the anomalous dimension of heavy-to-light currents. The subscript $+$ denotes the standard “plus distribution” which is defined as

$$\int d\omega' [\dots]_+ f(\omega') = \int d\omega' [\dots] (f(\omega') - f(\omega)) \quad (3.13)$$

for any (test-) function $f(\omega')$. This ensures that $\int d\omega' \Gamma(\omega, \omega') = 0$.

The first key toward solving the RG equation (3.9) concerns the off-diagonal term $\omega \Gamma(\omega, \omega', \mu)$ in the anomalous dimension (3.11). We observe that

$$\int_0^\infty d\omega' \omega \Gamma(\omega, \omega', \alpha_s) (\omega')^a = \omega^a \mathcal{F}(a, \alpha_s) \quad (3.14)$$

on dimensional grounds. The dimensionless function \mathcal{F} can only depend on the (in general complex) exponent a . We can use a power-law ansatz

$$f(\omega, \mu, \mu_0, a(\mu)) = \left(\frac{\omega}{\mu_0} \right)^{a(\mu)} e^{U(a(\mu), \mu)} \quad (3.15)$$

with an arbitrary mass parameter μ_0 . The function f solves the RG equation (3.9), if the exponent $a(\mu)$ and the normalization $U(a(\mu), \mu)$ obey the differential equations

$$\begin{aligned} \frac{d}{d \ln \mu} a(\mu) &= \Gamma_{\text{cusp}}(\alpha_s) , \\ \frac{d U(a(\mu), \mu)}{d \ln \mu} &= -\gamma(\alpha_s) - \mathcal{F}(a(\mu), \alpha_s) - \ln \frac{\mu}{\mu_0} \Gamma_{\text{cusp}}(\alpha_s) . \end{aligned} \quad (3.16)$$

The first equation can be immediately integrated and yields $a(\mu) = \eta + g(\mu, \mu_0)$ with initial value $\eta = a(\mu_0)$ and

$$g(\mu, \mu_0) = \int_{\alpha_s(\mu_0)}^{\alpha_s(\mu)} \frac{d\alpha}{\beta(\alpha)} \Gamma_{\text{cusp}}(\alpha) . \quad (3.17)$$

With this solution at hand, the second equation integrates to

$$U(a(\mu), \mu) = - \int_{\alpha_s(\mu_0)}^{\alpha_s(\mu)} \frac{d\alpha}{\beta(\alpha)} \left[\gamma(\alpha) + g_\mu(\alpha) + \mathcal{F}(\eta + g_0(\alpha), \alpha) \right], \quad (3.18)$$

where $g_\mu(\alpha) = g(\mu, \mu_\alpha)$, $g_0(\alpha) = g(\mu_\alpha, \mu_0)$, and μ_α is defined such that $\alpha_s(\mu_\alpha) = \alpha$.

Note that $g(\mu_0, \mu_0) = 0$ and $U(\eta, \mu_0) = 0$ in this construction.

The second key to the solution concerns the initial condition $\phi_+^B(\omega, \mu_0)$. Defining the Fourier transform $\varphi_0(t)$ of the LCDA at scale μ_0 with respect to $\ln(\omega/\mu_0)$ allows us to express the ω dependence in the desired power-law form

$$\phi_+^B(\omega, \mu_0) = \frac{1}{2\pi} \int_{-\infty}^{\infty} dt \varphi_0(t) \left(\frac{\omega}{\mu_0} \right)^{it}. \quad (3.19)$$

We therefore obtain an exact analytic expression for the solution of the RG equation (3.9) as the single integral [30]

$$\phi_+^B(\omega, \mu) = \frac{1}{2\pi} \int_{-\infty}^{\infty} dt \varphi_0(t) f(\omega, \mu, \mu_0, \eta = it). \quad (3.20)$$

3.1.2 Asymptotic behaviour

The solution (3.20) enables us to extract the asymptotic behaviour of the LCDA $\phi_+^B(\omega, \mu)$ as $\omega \rightarrow 0$ and $\omega \rightarrow \infty$ by deforming the integration contour in the complex t plane. We hence need to study the analytic structure of the integrand $\varphi_0(t) f(\omega, \mu, \mu_0, it) \sim \omega^{it+g(\mu, \mu_0)}$. If ω is very small we can deform the contour into the lower half plane, and then the position of the nearest pole to the real axis determines the ω dependence of $\phi_+^B(\omega, \mu)$. Similarly the nearest pole in the upper half plane dominates for very large ω .

Let us study the analytic structure of $f(\omega, \mu, \mu_0, it)$ at leading order in RG-improved perturbation theory. Using the one-loop expressions (3.12) and the definition (3.14) we find

$$\mathcal{F}^{(1)}(a) = \Gamma_{\text{cusp}}^{(1)} [\Psi(1+a) + \Psi(1-a) + 2\gamma_E] . \quad (3.21)$$

Ψ and γ_E denote the logarithmic derivative of the Euler-Gamma function and the Euler-constant, respectively. Plugging this result into eq. (3.18) with $\eta = it$ one obtains (using the short-hand notation $g \equiv g(\mu, \mu_0)$)

$$e^{U(it+g,\mu)} \propto \frac{\Gamma(1+it) \Gamma(1-it-g)}{\Gamma(1-it) \Gamma(1+it+g)} . \quad (3.22)$$

The function $f(\omega, \mu, \mu_0, it)$ has poles along the imaginary axis, and the closest to the real axis are located at $t = i$ and $t = -i(1-g)$. Using the one-loop expression (3.17) we observe that the function g vanishes at $\mu = \mu_0$ by definition and grows monotonously as μ increases. Therefore the position of the pole in the lower complex plane approaches the real axis under renormalization evolution, as illustrated in Fig. 3.2(b). These poles “compete” with the singularities arising from $\varphi_0(t)$ for the nearest position to the real axis. Let us assume that, for a given model of $\phi_+^B(\omega, \mu_0)$, the LCDA grows like ω^δ for small ω and falls off like $\omega^{-\xi}$ for large ω . The corresponding poles of the function $\varphi_0(t)$ are then located at $t = -i\delta$ and $t = i\xi$. We therefore obtain the asymptotic behaviour of the renormalized

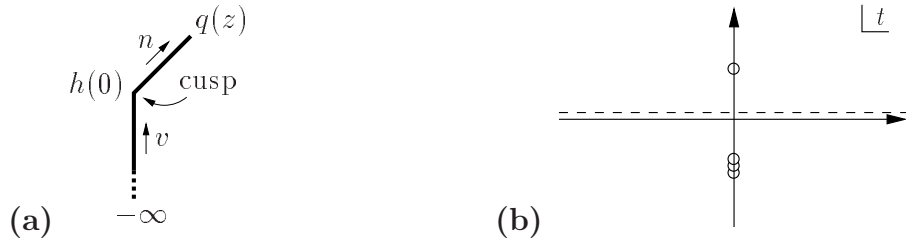


Figure 3.2: **(a)** Left: The cusp in the Wilson line $S_s(z)S_s^\dagger(0)S_v(0)$. **(b)** Right: Poles of the function $f(\dots, it)$ in the complex t plane. The upper pole remains stationary under renormalization flow, whereas the position of the lower pole moves toward the real axis for increasing μ .

LCDA as

$$\phi_+^B(\omega, \mu) \sim \begin{cases} \omega^{\min(1, \delta+g)}; & \text{for } \omega \rightarrow 0, \\ \omega^{-\min(1, \xi)+g}; & \text{for } \omega \rightarrow \infty. \end{cases} \quad (3.23)$$

The two immediate observations are that, regardless of how small the value of δ is, evolution effects will drive the small ω behaviour toward linear growth, and that the renormalized LCDA at a scale $\mu > \mu_0$ will fall off slower than $1/\omega$ irrespective of how fast it vanishes at $\mu = \mu_0$.

The emergence of a radiative tail after (even infinitesimally small) evolution seems, at first sight, a very strange property of the LCDA, because it implies that the normalization integral of $\phi_+^B(\omega, \mu)$ is UV divergent. This can be understood as the corresponding *local* operator $\bar{Q}(0) \Gamma \mathcal{H}(0)$ requires an additional subtraction when renormalized [33]. However, this is not an obstacle for practical applications, since only $\phi_+^B(\omega, \mu)/\omega$ modulo logarithms appears. An integral over this function remains UV finite as long as $g(\mu, \mu_0) < 1$, at which point the pole at $t = -i(1-g)$ reaches the real axis and the formalism presented above breaks down.

It is evident from (3.23) that evolution effects mix different moments of the LCDA. For example, the first inverse moment of $\phi_+^B(\omega, \mu)$ defines a parameter

$$\frac{1}{\lambda_B(\mu)} = \int_0^\infty \frac{d\omega}{\omega} \phi_+^B(\omega, \mu), \quad (3.24)$$

which is connected to a fractional inverse moment of order $1-g(\mu, \mu')$ at a different scale μ' . This makes it impossible to calculate the scale dependence of $\lambda_B(\mu)$ in perturbation theory without knowledge of functional form of the LCDA.

3.2 The Shape Function

The shape function is a non-perturbative structure function that encodes the Fermi motion of the heavy quark inside the B meson. While the LCDA discussed in the

last section has a rough interpretation as a probability distribution for the plus component of the spectator-quark momentum (the evolution effects do not quite fit into this interpretation), the shape function describes the plus component of the residual momentum of the heavy quark. It enters the calculation of inclusive $B \rightarrow \text{light particles}$ decays such as $\bar{B} \rightarrow X_u l^- \bar{\nu}$ and $\bar{B} \rightarrow X_s \gamma$, and is defined as the forward matrix element of the bilocal heavy-to-heavy current

$$\frac{\langle \bar{B}(v) | \bar{h} \Gamma \delta(\omega - i n \cdot D) h | \bar{B}(v) \rangle}{2M_B} = S(\omega) \frac{1}{2} \text{tr} \left(\Gamma \frac{1 + \not{v}}{2} \right). \quad (3.25)$$

The soft function $S(\omega)$ coincides with the shape function $f(k_+)$ introduced in [35]. Only one function arises in the HQET trace formalism, because v is the only vector available by external kinematics. The shape function $S(\omega)$ has support for $\omega \in]-\infty, \bar{\Lambda}]$, which can be understood as follows:

The B -meson momentum can be decomposed into $P_B = m_b v + k$, where m_b is the b -quark mass, and k is the dynamical “residual” momentum. For the sake of the argument, the variable ω can be thought of as the plus component $n \cdot k$. Let us work in the rest frame and choose the coordinate system such that the three-momentum \vec{k} points in the $+z$ direction. One may then parameterize $k^\mu = \omega v^\mu + |\vec{k}| n^\mu$, so that $\omega = n \cdot k$ holds. The calculation of

$$M_B^2 = P_B^2 = (m_b + \omega)^2 + 2|\vec{k}|(m_b + \omega) \quad (3.26)$$

leads to the endpoints of the allowed ω interval for the cases $|\vec{k}| = 0$ and $|\vec{k}| \rightarrow \infty$, which can be read off as $\omega = (M_B - m_b)$ and $\omega \rightarrow -m_b$, respectively. In the heavy-quark limit $m_b \rightarrow \infty$, one therefore finds the support interval mentioned above, where $(M_B - m_b) \xrightarrow{m_b \rightarrow \infty} \bar{\Lambda}$ is used. The quantity $\bar{\Lambda} \sim O(\Lambda_{\text{QCD}})$ is an HQET parameter and depends on the particular definition of the heavy-quark mass.

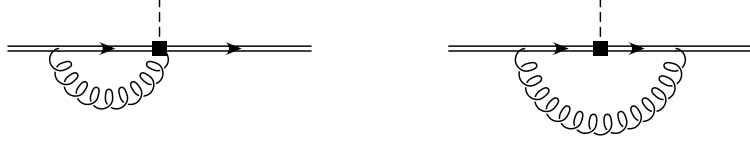


Figure 3.3: Radiative corrections to the shape function. The bilocal HQET operator is denoted by the black square. A mirror copy of the first graph is not shown.

3.2.1 Renormalization-Group Evolution

Renormalized shape function

According to (3.25), the shape function is defined in terms of a hadronic matrix element in HQET and thus cannot be calculated perturbatively. However, the renormalization properties of this function can be studied using perturbation theory. To this end, we evaluate the matrix element (3.25) in HQET using external heavy-quark states with residual momentum k . For the time being, $v \cdot k$ is kept non-zero to regularize infra-red singularities. The relevant one-loop graphs are depicted in Fig. 3.3. Adding the tree contribution, we obtain for the matrix element of the bare shape-function operator $O(\omega) = \bar{h} \Gamma \delta(\omega - in \cdot D) h$ (expressed in terms of renormalized fields) [36]

$$\begin{aligned}
 S_{\text{bare}}(\omega) &= Z_h \delta(\omega - n \cdot k) - \frac{4C_F g_s^2}{(4\pi)^{2-\epsilon}} \Gamma(1 + \epsilon) \\
 &\times \left\{ \frac{1}{\epsilon} \int_0^\infty dl l^{-1-2\epsilon} \left[\delta(\omega - n \cdot k) - \delta(\omega - n \cdot k + l) \right] \left(1 + \frac{\delta}{l} \right)^{-\epsilon} \right. \\
 &\quad \left. + \theta(n \cdot k - \omega) (n \cdot k - \omega)^{-\epsilon} (n \cdot k - \omega + \delta)^{-1-\epsilon} \right\}, \quad (3.27)
 \end{aligned}$$

where $\delta = -2v \cdot k$, and

$$Z_h = 1 + \frac{4C_F g_s^2}{(4\pi)^{2-\epsilon}} \Gamma(2\epsilon) \Gamma(1 - \epsilon) \delta^{-2\epsilon} \quad (3.28)$$

is the off-shell wave function renormalization constant of a heavy quark in HQET. The next step is to extract the ultra-violet poles from this result, which determine the anomalous dimension of the shape function. The renormalized shape function is related to the bare shape function through

$$\begin{aligned} S_{\text{ren}}(\omega) &= \int_{-\infty}^{\bar{\Lambda}} d\omega' Z_S(\omega, \omega') S_{\text{bare}}(\omega'), \quad \text{with} \\ Z_S(\omega, \omega') &= \delta(\omega - \omega') + \frac{C_F \alpha_s}{4\pi} z_S(\omega, \omega') + \dots \end{aligned} \quad (3.29)$$

The result for Z_S following from (3.27) must be interpreted as a distribution on test functions $F(\omega')$ with support on the interval $-\infty < \omega' \leq \bar{\Lambda}$. We find

$$\begin{aligned} z_S(\omega, \omega') &= \left(\frac{2}{\epsilon^2} + \frac{4}{\epsilon} \ln \frac{\mu}{\bar{\Lambda} - \omega} - \frac{2}{\epsilon} \right) \delta(\omega - \omega') - \frac{4}{\epsilon} \left(\frac{\theta(\omega' - \omega)}{\omega' - \omega} \right)_+ \\ &= \left(\frac{2}{\epsilon^2} - \frac{2}{\epsilon} \right) \delta(\omega - \omega') - \frac{4}{\epsilon} \left(\frac{1}{\omega' - \omega} \right)_*^{[\mu]}. \end{aligned} \quad (3.30)$$

Evidently, the renormalization factor Z_S depends on the parameter $\bar{\Lambda}$ setting the upper limit on the integration over ω' in (3.29), which combines with the plus distribution (see (3.13)) to form a star distribution in the variable $(\omega' - \omega)$. The star distributions are generalized plus distributions defined as [36, 37]

$$\begin{aligned} \int_{\leq 0}^z dx F(x) \left(\frac{1}{x} \right)_*^{[u]} &= \int_0^z dx \frac{F(x) - F(0)}{x} + F(0) \ln \frac{z}{u}, \\ \int_{\leq 0}^z dx F(x) \left(\frac{\ln(x/u)}{x} \right)_*^{[u]} &= \int_0^z dx \frac{F(x) - F(0)}{x} \ln \frac{x}{u} + \frac{F(0)}{2} \ln^2 \frac{z}{u}, \end{aligned} \quad (3.31)$$

where $F(x)$ is a smooth test function. For later purposes, we note the useful rescaling identities

$$\begin{aligned} \lambda \left(\frac{1}{\lambda x} \right)_*^{[u]} &= \left(\frac{1}{x} \right)_*^{[u/\lambda]} = \left(\frac{1}{x} \right)_*^{[u]} + \delta(x) \ln \lambda, \\ \lambda \left(\frac{\ln(\lambda x/u)}{\lambda x} \right)_*^{[u]} &= \left(\frac{\ln(\lambda x/u)}{x} \right)_*^{[u/\lambda]} = \left(\frac{\ln(x/u)}{x} \right)_*^{[u]} + \left(\frac{1}{x} \right)_*^{[u]} \ln \lambda + \frac{\delta(x)}{2} \ln^2 \lambda. \end{aligned} \quad (3.32)$$

We can now determine the renormalized shape function from (3.29). The result must once again be interpreted as a distribution, this time on test functions $F(\omega)$ integrated over a *finite* interval $-\Lambda_{\text{had}} \leq \omega \leq \bar{\Lambda}$. (In practice, the value of Λ_{had} is set by kinematics or by virtue of some experimental cut.) The result is

$$S_{\text{parton}}(\omega) = \delta(\omega - n \cdot k) \left\{ 1 - \frac{C_F \alpha_s}{\pi} \left[\frac{\pi^2}{24} + L_2 \left(\frac{-\delta}{\Lambda_{\text{had}} + n \cdot k} \right) \right] \right\} \quad (3.33)$$

$$- \frac{C_F \alpha_s}{\pi} \left\{ \left[\frac{\theta(n \cdot k - \omega)}{n \cdot k - \omega} \left(\ln \frac{n \cdot k - \omega}{\mu} + \ln \frac{n \cdot k - \omega + \delta}{\mu} \right) \right]_+ \right.$$

$$\left. + \delta(n \cdot k - \omega) \ln^2 \frac{\Lambda_{\text{had}} + n \cdot k}{\mu} + \frac{\theta(n \cdot k - \omega)}{n \cdot k - \omega + \delta} + \delta(n \cdot k - \omega) \ln \frac{\delta}{\mu} \right\}.$$

While it was useful to keep the heavy quark off-shell in the calculation of the ultra-violet renormalization factor, the limit $\delta = -2v \cdot k \rightarrow 0$ can be taken in the result for the renormalized shape functions without leading to infra-red singularities.

This gives

$$S_{\text{parton}}(\omega) = \delta(\omega - n \cdot k) \left(1 - \frac{C_F \alpha_s}{\pi} \frac{\pi^2}{24} \right) \quad (3.34)$$

$$- \frac{C_F \alpha_s}{\pi} \left[2 \left(\frac{1}{n \cdot k - \omega} \ln \frac{n \cdot k - \omega}{\mu} \right)_*^{[\mu]} + \left(\frac{1}{n \cdot k - \omega} \right)_*^{[\mu]} \right],$$

where the star distributions must now be understood as distributions in the variable $(n \cdot k - \omega)$. We stress that these results for the renormalized shape function are obtained in the parton model and can in no way provide a realistic prediction for the functional form of $S(\omega)$. Only the dependence on the ultra-violet renormalization scale μ can be trusted.

Evolution of the shape function

The next goal is to solve the integro-differential evolution equation

$$\frac{d}{d \ln \mu} S(\omega, \mu) = - \int d\omega' \gamma_S(\omega, \omega', \mu) S(\omega', \mu). \quad (3.35)$$

In the upcoming calculation of the differential decay rate in inclusive $\bar{B} \rightarrow X_u l^- \bar{\nu}$ decays we will require the shape function at an intermediate scale $\mu_i \sim \sqrt{m_b \Lambda_{\text{QCD}}}$. If the shape function was known at some lower scale μ_0 , it would be necessary to evolve it according to (3.35).

At one-loop order, the anomalous dimension for the shape function is twice the coefficient of the $1/\epsilon$ pole in the renormalization factor Z_S . From (3.30), we obtain

$$\gamma_S(\omega, \omega', \mu) = \frac{C_F \alpha_s}{\pi} \left[\left(2 \ln \frac{\mu}{\bar{\Lambda} - \omega} - 1 \right) \delta(\omega - \omega') - 2 \left(\frac{\theta(\omega' - \omega)}{\omega' - \omega} \right)_+ \right]. \quad (3.36)$$

The evolution equation (3.35) can be solved analytically using the aforementioned general method presented in the previous section for the case of the B -meson LCDA [30]. It is convenient to change variables from ω to $\hat{\omega} = \bar{\Lambda} - \omega \in [0, \infty[$ and define $\hat{S}(\hat{\omega}) \equiv S(\bar{\Lambda} - \hat{\omega})$. The renormalization-group equation then reads

$$\frac{d}{d \ln \mu} \hat{S}(\hat{\omega}, \mu) = - \int_0^\infty d\hat{\omega}' \hat{\gamma}_S(\hat{\omega}, \hat{\omega}', \mu) \hat{S}(\hat{\omega}', \mu), \quad (3.37)$$

where the anomalous dimension can be written in the general form

$$\hat{\gamma}_S(\hat{\omega}, \hat{\omega}', \mu) = 2 \left[\Gamma_{\text{cusp}}(\alpha_s) \ln \frac{\mu}{\hat{\omega}} + \gamma(\alpha_s) \right] \delta(\hat{\omega} - \hat{\omega}') + 2\mathcal{G}(\hat{\omega}, \hat{\omega}', \alpha_s). \quad (3.38)$$

This is obviously analogous to the RGE (3.9) governing the LCDA. The logarithmic term containing the cusp anomalous dimension can again be interpreted geometrically. Since the heavy-quark field $h(x)$ in HQET can be represented as a Wilson line along the v direction, the field $\mathcal{H}(x)$ entering the SCET formalism contains the product of a light-like Wilson line (along n) and a time-like Wilson line (along v), which form a cusp at point x . The shape function contains two such cusps, each of which produces a contribution to the anomalous dimension proportional to $\Gamma_{\text{cusp}} \ln \mu$ [25]. The one-loop coefficients of the remaining terms in (3.38) are

$$\gamma_0 = -2C_F, \quad \mathcal{G}_0(\hat{\omega}, \hat{\omega}') = -\Gamma_0 \left(\frac{\theta(\hat{\omega} - \hat{\omega}')}{\hat{\omega} - \hat{\omega}'} \right)_+. \quad (3.39)$$

The general solution of (3.37) can be obtained (in close analogy to our previous discussion) using the fact that on dimensional grounds

$$\int_0^\infty d\hat{\omega}' \mathcal{G}(\hat{\omega}, \hat{\omega}', \alpha_s) (\hat{\omega}')^a \equiv \hat{\omega}^a \mathcal{F}(a, \alpha_s), \quad (3.40)$$

where the function \mathcal{F} only depends on the exponent a and the coupling constant. We set $\mathcal{F}(0, \alpha_s) = 0$ by definition, thereby determining the split between the terms with γ and \mathcal{G} in (3.38). The integral on the left-hand side is convergent as long as $\text{Re } a > -1$. At one-loop order we find from (3.39)

$$\mathcal{F}(a, \alpha_s) = \Gamma_0 \frac{\alpha_s}{4\pi} \left[\psi(1+a) + \gamma_E \right] + \dots, \quad (3.41)$$

where $\psi(z)$ is the logarithmic derivative of the Euler Γ function. Relation (3.40) implies that the ansatz

$$f(\hat{\omega}, \mu, \mu_0, \tau) = \left(\frac{\hat{\omega}}{\mu_0} \right)^{\tau + 2g(\mu, \mu_0)} \exp U_S(\tau, \mu, \mu_0) \quad (3.42)$$

with

$$\begin{aligned} g(\mu, \mu_0) &= \int_{\alpha_s(\mu_0)}^{\alpha_s(\mu)} d\alpha \frac{\Gamma_{\text{cusp}}(\alpha)}{\beta(\alpha)}, \\ U_S(\tau, \mu, \mu_0) &= -2 \int_{\alpha_s(\mu_0)}^{\alpha_s(\mu)} \frac{d\alpha}{\beta(\alpha)} \left[g(\mu, \mu_\alpha) + \gamma(\alpha) + \mathcal{F}(\tau + 2g(\mu_\alpha, \mu_0), \alpha) \right], \end{aligned} \quad (3.43)$$

provides a solution to the evolution equation (3.37) with initial condition

$f(\hat{\omega}, \mu_0, \mu_0, \tau) = (\hat{\omega}/\mu_0)^\tau$ at some scale μ_0 . Here μ_α is defined such that $\alpha_s(\mu_\alpha) = \alpha$, and τ can be an arbitrary complex parameter. Note that $g(\mu, \mu_0) > 0$ if $\mu > \mu_0$.

We now assume that the shape function $\hat{S}(\hat{\omega}, \mu_0)$ is given at the low scale μ_0 and define its Fourier transform with respect to $\ln(\hat{\omega}/\mu_0)$ through

$$\hat{S}(\hat{\omega}, \mu_0) = \frac{1}{2\pi} \int_{-\infty}^{\infty} dt \mathcal{S}_0(t) \left(\frac{\hat{\omega}}{\mu_0} \right)^{it}. \quad (3.44)$$

The exact result for the shape function at a different scale μ is then given by

$$\hat{S}(\hat{\omega}, \mu) = \frac{1}{2\pi} \int_{-\infty}^{\infty} dt \mathcal{S}_0(t) f(\hat{\omega}, \mu, \mu_0, it). \quad (3.45)$$

With the help of this formula, it is straightforward to derive explicit expressions for the evolution of the shape function from the hadronic scale μ_0 up to the intermediate scale μ_i at any order in renormalization-group improved perturbation theory. Setting $r_2 = \alpha_s(\mu_0)/\alpha_s(\mu_i) > 1$, we obtain for the evolution function at leading order

$$f(\hat{\omega}, \mu_i, \mu_0, it) = e^{V_S(\mu_i, \mu_0)} \left(\frac{\hat{\omega}}{\mu_0} \right)^{it + \frac{\Gamma_0}{\beta_0} \ln r_2} \frac{\Gamma(1 + it)}{\Gamma(1 + it + \frac{\Gamma_0}{\beta_0} \ln r_2)}, \quad (3.46)$$

where

$$\begin{aligned} V_S(\mu_i, \mu_0) = & \frac{\Gamma_0}{2\beta_0^2} \left[-\frac{4\pi}{\alpha_s(\mu_0)} (r_2 - 1 - \ln r_2) + \frac{\beta_1}{2\beta_0} \ln^2 r_2 \right. \\ & \left. + \left(\frac{\Gamma_1}{\Gamma_0} - \frac{\beta_1}{\beta_0} \right) \left(1 - \frac{1}{r_2} - \ln r_2 \right) \right] \\ & - \frac{\Gamma_0}{\beta_0} \gamma_E \ln r_2 - \frac{\gamma_0}{\beta_0} \ln r_2 + O\left[(r_2 - 1) \alpha_s(\mu)\right]. \end{aligned} \quad (3.47)$$

This result is valid as long as $(\Gamma_0/\beta_0) \ln r_2 < 1$, which is the case for all reasonable parameter values. Missing for a resummation at next-to-leading order are the $O(\alpha_s)$ contributions to V_S , which vanish for $\mu \rightarrow \mu_0$. For all practical purposes, given the intrinsic uncertainties in our knowledge of the shape function, it will be sufficient to use the equations given above. As mentioned earlier, we typically have $\mu_i \sim m_c$, and so the running between μ_i and μ_0 should be performed in a theory with $n_f = 3$ light quark flavors. The relevant expansion coefficients are then $\Gamma_0 = \frac{16}{3}$, $\Gamma_1 = \frac{304}{3} - \frac{16}{3}\pi^2$, $\gamma_0 = -\frac{8}{3}$, and $\beta_0 = 9$, $\beta_1 = 64$.

The leading-order result presented above can be simplified further. When (3.46) is inserted into (3.45), the integration over t can be performed analytically. Setting

$\eta = (\Gamma_0/\beta_0) \ln r_2 > 0$, the relevant integral is

$$I = \frac{1}{2\pi} \int_{-\infty}^{\infty} dt \mathcal{S}_0(t) \left(\frac{\hat{\omega}}{\mu_0} \right)^{it} \frac{\Gamma(1+it)}{\Gamma(1+it+\eta)}, \quad (3.48)$$

where

$$\mathcal{S}_0(t) = \int_0^{\infty} \frac{d\hat{\omega}'}{\hat{\omega}'} \hat{S}(\hat{\omega}', \mu_0) \left(\frac{\hat{\omega}'}{\mu_0} \right)^{-it} \quad (3.49)$$

is the Fourier transform of the shape function as defined in (3.44). The integrand of the t -integral has poles on the positive imaginary axis located at $t = in$ with $n \geq 1$ an integer. For $\hat{\omega} < \hat{\omega}'$ the integration contour can be closed in the lower half-plane avoiding all poles, hence yielding zero. For $\hat{\omega} > \hat{\omega}'$ we use the theorem of residues to obtain

$$I = \int_0^{\hat{\omega}} d\hat{\omega}' R(\hat{\omega}, \hat{\omega}') \hat{S}(\hat{\omega}', \mu_0), \quad (3.50)$$

where

$$R(\hat{\omega}, \hat{\omega}') = \frac{1}{\hat{\omega}} \sum_{j=0}^{\infty} \left(-\frac{\hat{\omega}'}{\hat{\omega}} \right)^j \frac{1}{\Gamma(j+1) \Gamma(\eta-j)} = \frac{1}{\Gamma(\eta)} \frac{1}{\hat{\omega}^\eta (\hat{\omega} - \hat{\omega}')^{1-\eta}}. \quad (3.51)$$

Note that $R(\hat{\omega}, \hat{\omega}') \rightarrow \delta(\hat{\omega} - \hat{\omega}')$ in the limit $\eta \rightarrow 0$, corresponding to $\mu_i \rightarrow \mu_0$, as it should be.

Our final result for the shape function at the intermediate hard-collinear scale, valid at leading order in renormalization-group improved perturbation theory, can now be written in the simple form [36, 38, 39] (valid for $\mu_i > \mu_0$, so that $\eta > 0$)

$$\hat{S}(\hat{\omega}, \mu_i) = e^{V_S(\mu_i, \mu_0)} \frac{1}{\Gamma(\eta)} \int_0^{\hat{\omega}} d\hat{\omega}' \frac{\hat{S}(\hat{\omega}', \mu_0)}{\mu_0^\eta (\hat{\omega} - \hat{\omega}')^{1-\eta}}, \quad (3.52)$$

with V_S as given in (3.47).

From the above equation one can derive scaling relations for the asymptotic behavior of the shape function for $\hat{\omega} \rightarrow 0$ and $\hat{\omega} \rightarrow \infty$ (corresponding to $\omega \rightarrow \bar{\Lambda}$ and $\omega \rightarrow -\infty$). If the function $\hat{S}(\hat{\omega}, \mu_0)$ at the low scale μ_0 vanishes proportional

to $\hat{\omega}^\zeta$ near the endpoint, the shape function at a higher scale $\mu_i > \mu$ vanishes faster, proportional to $\hat{\omega}^{\zeta+\eta}$. Similarly, if $\hat{S}(\hat{\omega}, \mu_0)$ falls off like $\hat{\omega}^{-\xi}$ for $\hat{\omega} \rightarrow \infty$, the shape function renormalized at a higher scale vanishes like $\hat{\omega}^{-\min(1,\xi)+\eta}$. Irrespective of the initial behavior of the shape function, evolution effects generate a radiative tail that falls off slower than $1/\hat{\omega}$. This fact implies that the normalization integral of $\hat{S}(\hat{\omega}, \mu)$ as well as all positive moments are ultra-violet divergent. The field-theoretic reason is that the bilocal shape-function operator contains ultra-violet singularities as $z_- \rightarrow 0$, which are not subtracted in the renormalization of the shape function. The situation is analogous to the case of the B -meson light-cone distribution amplitude discussed in [30, 33], see Section 3.1.2. These divergences are never an obstacle in practice. Convolution integrals with the shape function are always cut off at some finite value of $\hat{\omega}$ by virtue of phase-space or some experimental cut.

3.2.2 Properties of the shape function

Information about the shape function can be extracted from a study of its moments using a local operator product expansion. Naively, one would define the moments $M_N = \int_{-\infty}^{\bar{\Lambda}} d\omega \omega^N S(\omega)$. Prior to our work in [36], the general understanding was that, at tree level, $M_0 = 1$ is fixed by the normalization of the shape function, $M_1 = 0$ by virtue of the HQET equation of motion $iv \cdot D h = 0$ (which implicitly uses the pole-mass definition of m_b), and $M_2 = -\lambda_1/3$ is given by the matrix element of the kinetic-energy operator. However, it was not clear how to systematically include radiative corrections to these relations. Apart from the obvious dependence on HQET parameters such as $\bar{\Lambda}$ and λ_1 , the moments M_N must also depend on the renormalization scale μ . However, as was studied in the last Sec-

tion, quantum corrections result in the appearance of a radiative tail, rendering all moments with $N \geq 0$ ultra-violet divergent. Since in any physical process the integration over the shape function is restricted to finite intervals, it suffices to define the moments with an ultra-violet cutoff, such that

$$M_N(\Lambda_{\text{UV}}, \mu) = \int_{-\Lambda_{\text{UV}}}^{\bar{\Lambda}} d\omega \omega^N S(\omega, \mu). \quad (3.53)$$

In the following Subsections we will expand the finite quantities $M_N(\Lambda_{\text{UV}}, \mu)$ in a local HQET operator product expansion, assuming that Λ_{UV} is large compared to Λ_{QCD} . The only relevant operators up to dimension 5 are of the form $\bar{h}(in \cdot D)^m h$ with $m = 0, 1, 2$, whose matrix elements are given as $1, 0, -\lambda_1/3$, respectively [35, 40, 41, 42].

Moments in the pole scheme

We can write an expansion of the form

$$M_N(\Lambda_{\text{UV}}, \mu) = \Lambda_{\text{UV}}^N \left\{ K_0^{(N)}(\Lambda_{\text{UV}}, \mu) + K_2^{(N)}(\Lambda_{\text{UV}}, \mu) \cdot \frac{(-\lambda_1)}{3\Lambda_{\text{UV}}^2} + O\left[\left(\frac{\Lambda_{\text{QCD}}}{\Lambda_{\text{UV}}}\right)^3\right] \right\}, \quad (3.54)$$

where the coefficients $K_i^{(N)}$ can be determined from a perturbative matching calculation using on-shell external b -quark states with residual momentum k . By evaluating the moments of the renormalized shape function in (3.34), one finds at one-loop order [36]

$$M_N^{\text{parton}}(\Lambda_{\text{UV}}, \mu) = (n \cdot k)^N \left\{ 1 - \frac{C_F \alpha_s}{\pi} \left(\ln^2 \frac{\Lambda_{\text{UV}} + n \cdot k}{\mu} + \ln \frac{\Lambda_{\text{UV}} + n \cdot k}{\mu} + \frac{\pi^2}{24} \right) - \frac{C_F \alpha_s}{\pi} \sum_{j=1}^N \frac{1}{j} \left(1 + 2 \ln \frac{\Lambda_{\text{UV}} + n \cdot k}{\mu} - \sum_{l=j}^N \frac{2}{l} \right) \left[\left(-\frac{\Lambda_{\text{UV}}}{n \cdot k} \right)^j - 1 \right] \right\}. \quad (3.55)$$

We then expand this result in powers of $n \cdot k / \Lambda_{\text{UV}}$. Keeping the first three terms in the expansion yields

$$\begin{aligned}
M_0^{\text{parton}}(\Lambda_{\text{UV}}, \mu) &= 1 - \frac{C_F \alpha_s}{\pi} \left(\ln^2 \frac{\Lambda_{\text{UV}}}{\mu} + \ln \frac{\Lambda_{\text{UV}}}{\mu} + \frac{\pi^2}{24} \right) \\
&\quad - \frac{C_F \alpha_s}{\pi} \left[\frac{n \cdot k}{\Lambda_{\text{UV}}} \left(2 \ln \frac{\Lambda_{\text{UV}}}{\mu} + 1 \right) + \frac{(n \cdot k)^2}{\Lambda_{\text{UV}}^2} \left(-\ln \frac{\Lambda_{\text{UV}}}{\mu} + \frac{1}{2} \right) + \dots \right], \\
M_1^{\text{parton}}(\Lambda_{\text{UV}}, \mu) &= n \cdot k \left[1 - \frac{C_F \alpha_s}{\pi} \left(\ln^2 \frac{\Lambda_{\text{UV}}}{\mu} - \ln \frac{\Lambda_{\text{UV}}}{\mu} + \frac{\pi^2}{24} - 1 \right) \right] \\
&\quad - \frac{C_F \alpha_s}{\pi} \left[\Lambda_{\text{UV}} \left(-2 \ln \frac{\Lambda_{\text{UV}}}{\mu} + 1 \right) + \frac{(n \cdot k)^2}{\Lambda_{\text{UV}}} 2 \ln \frac{\Lambda_{\text{UV}}}{\mu} + \dots \right], \\
M_2^{\text{parton}}(\Lambda_{\text{UV}}, \mu) &= (n \cdot k)^2 \left[1 - \frac{C_F \alpha_s}{\pi} \left(\ln^2 \frac{\Lambda_{\text{UV}}}{\mu} - 2 \ln \frac{\Lambda_{\text{UV}}}{\mu} + \frac{\pi^2}{24} - \frac{1}{2} \right) \right] \\
&\quad - \frac{C_F \alpha_s}{\pi} \left[\Lambda_{\text{UV}}^2 \ln \frac{\Lambda_{\text{UV}}}{\mu} + n \cdot k \Lambda_{\text{UV}} \left(-2 \ln \frac{\Lambda_{\text{UV}}}{\mu} + 3 \right) + \dots \right].
\end{aligned} \tag{3.56}$$

On the other hand, we need to calculate the one-loop expressions for the local operators $\bar{h}(in \cdot D)^m h$. The relevant diagrams are the same as in Fig. 3.3, where now the black square represents the local operators. The result is non-trivial when keeping $v \cdot k$ non-zero to regularize infra-red singularities. However, for the matching calculation we need the limit $v \cdot k \rightarrow 0$, which can be taken without problems in the sum of all diagrams (but not for each individual diagram). In that case, the one-loop corrections vanish and the matrix elements reduce simply to their tree-level values. It follows that in (3.56) we must identify $(n \cdot k)^n \rightarrow \langle \bar{h}(in \cdot D)^n h \rangle$. Substituting the results for the HQET matrix elements given earlier, we obtain for the Wilson coefficients of the first three moments

$$\begin{aligned}
K_0^{(0)} &= 1 - \frac{C_F \alpha_s}{\pi} \left(\ln^2 \frac{\Lambda_{\text{UV}}}{\mu} + \ln \frac{\Lambda_{\text{UV}}}{\mu} + \frac{\pi^2}{24} \right), & K_2^{(0)} &= \frac{C_F \alpha_s}{\pi} \left(\ln \frac{\Lambda_{\text{UV}}}{\mu} - \frac{1}{2} \right), \\
K_0^{(1)} &= \frac{C_F \alpha_s}{\pi} \left(2 \ln \frac{\Lambda_{\text{UV}}}{\mu} - 1 \right), & K_2^{(1)} &= -2 \frac{C_F \alpha_s}{\pi} \ln \frac{\Lambda_{\text{UV}}}{\mu}, \\
K_0^{(2)} &= -\frac{C_F \alpha_s}{\pi} \ln \frac{\Lambda_{\text{UV}}}{\mu}, & K_2^{(2)} &= 1 - \frac{C_F \alpha_s}{\pi} \left(\ln^2 \frac{\Lambda_{\text{UV}}}{\mu} - 2 \ln \frac{\Lambda_{\text{UV}}}{\mu} + \frac{\pi^2}{24} - \frac{1}{2} \right).
\end{aligned} \tag{3.57}$$

We observe that this result reduces to the naive moment relations mentioned above in the tree-level approximation. The perturbative quantum corrections can be

trusted as long as the ratio Λ_{UV}/μ is of $O(1)$.

The shape-function scheme

We have stressed before that the value of the moments depend on the definition of the heavy-quark mass. So far, our calculations have assumed the definition of the heavy-quark mass as a pole mass, m_b^{pole} , which is implied by the HQET equation of motion $iv \cdot D h = 0$. Results such as (3.57) are valid in this particular scheme. A more general choice is to allow for a residual mass term δm in HQET, such that $iv \cdot D h = \delta m h$ with $\delta m = O(\Lambda_{\text{QCD}})$ [43]. It is well known that the pole mass is an ill-defined concept, which suffers from infra-red renormalon ambiguities [44, 45]. The parameter $\bar{\Lambda}_{\text{pole}} = M_B - m_b^{\text{pole}}$, which determines the support of the shape function in the pole-mass scheme, inherits the same ambiguities. It is therefore advantageous to eliminate the pole mass in favor of some short-distance mass. For the analysis of inclusive B -meson decays, a proper choice is to use a so-called low-scale subtracted heavy-quark mass $m_b(\mu_f)$ [46], which is obtained from the pole mass by removing a long-distance contribution proportional to a subtraction scale μ_f , writing $m_b^{\text{pole}} = m_b(\mu_f) + \mu_f g\left(\alpha_s(\mu), \frac{\mu_f}{\mu}\right) \equiv m_b(\mu_f) + \delta m$. As long as $m_b(\mu_f)$ is defined in a physical way, the resulting perturbative expressions after elimination of the pole mass are well-behaved and not plagued by renormalon ambiguities. Replacing the pole mass by the physical mass shifts the values of $n \cdot k$ and ω by an amount δm , since $n \cdot (m_b^{\text{pole}} v + k) = m_b(\mu_f) + (n \cdot k + \delta m)$, and because the covariant derivative in the definition of the shape function in (3.25) must be replaced by $in \cdot D - \delta m$ [43]. At the same time, $\bar{\Lambda}_{\text{pole}} = \bar{\Lambda}(\mu_f) - \delta m$, where $\bar{\Lambda}(\mu_f) = M_B - m_b(\mu_f)$ is a physical parameter. Note that this leaves the parameter $\hat{\omega} = \bar{\Lambda} - \omega$ and hence the shape function $\hat{S}(\hat{\omega}, \mu)$ invariant! This follows

since $\bar{\Lambda}_{\text{pole}} - \omega_{\text{pole}} = \bar{\Lambda}(\mu_f) - (\omega_{\text{pole}} + \delta m)$, where ω_{pole} denotes the value in the pole-mass scheme used so far. We now *choose* δm such that the first moment M_1 vanishes, thereby defining a low-scale subtracted heavy-quark mass to all orders in perturbation theory (with $\mu_f = \Lambda_{\text{UV}}$), called the “shape-function mass” m_b^{SF} [36]. The shape-function mass can be related to any other short-distance mass using perturbation theory. To this end, one uses the fact that (3.56) implies a relation to the pole mass

$$m_b^{\text{pole}} = m_b^{\text{SF}}(\mu_f, \mu) + \mu_f \frac{C_F \alpha_s(\mu)}{\pi} \left[\left(1 - 2 \ln \frac{\mu_f}{\mu} \right) + \frac{2}{3} \frac{(-\lambda_1)}{\mu_f^2} \ln \frac{\mu_f}{\mu} + \dots \right]. \quad (3.58)$$

Given the above expression, it is easy to relate also to the potential-subtracted mass introduced in [47] and to the kinetic mass defined in [48, 49].

$$m_b^{\text{SF}}(\mu_f, \mu_f) = m_b^{\text{PS}}(\mu_f) = m_b^{\text{kin}}(\mu_f) + \mu_f \frac{C_F \alpha_s(\mu_f)}{3\pi} \quad (3.59)$$

After the introduction of the shape-function mass, the coefficients $K_n^{(1)}$ in (3.57) vanish by definition. At one-loop order, the remaining coefficients of the zeroth and second moment remain unchanged since $\delta m = O(\alpha_s)$. Proceeding in an analogous way, we can use the second moment to define a physical kinetic-energy parameter, commonly called μ_π^2 . This quantity can be used to replace the HQET parameter λ_1 , which like the pole mass suffers from infra-red renormalon ambiguities [50]. At one-loop order, we obtain [36]

$$\begin{aligned} \frac{\mu_\pi^2(\Lambda_{\text{UV}}, \mu)}{3} &\equiv \frac{M_2^{\text{phys}}(\Lambda_{\text{UV}}, \mu)}{M_0^{\text{phys}}(\Lambda_{\text{UV}}, \mu)} \\ &= -\frac{C_F \alpha_s(\mu)}{\pi} \Lambda_{\text{UV}}^2 \ln \frac{\Lambda_{\text{UV}}}{\mu} + \frac{(-\lambda_1)}{3} \left[1 + \frac{C_F \alpha_s(\mu)}{\pi} \left(3 \ln \frac{\Lambda_{\text{UV}}}{\mu} + \frac{1}{2} \right) \right] + \dots \end{aligned} \quad (3.60)$$

This definition is similar to the running parameter μ_π^2 defined in the kinetic scheme

[48, 49]. At one-loop order, the two parameters are related by

$$\mu_\pi^2(\mu_f, \mu_f) = -\mu_f^2 \frac{C_F \alpha_s(\mu_f)}{\pi} + [\mu_\pi^2(\mu_f)]_{\text{kin}} \left[1 + \frac{C_F \alpha_s(\mu_f)}{2\pi} \right]. \quad (3.61)$$

Given a value for the kinetic energy in the shape-function scheme for some choice of scales, we can solve (3.58) and (3.60) to obtain values for m_b^{SF} and μ_π^2 at any scale, using the fact that m_b^{pole} and λ_1 are scale independent.

3.2.3 Moments of the scheme-independent function $\hat{S}(\hat{\omega}, \mu)$

The variable $\hat{\omega} = \bar{\Lambda} - \omega$ and with it the function $\hat{S}(\hat{\omega}, \mu) = S(\omega)$ are independent under redefinition of the heavy-quark mass. It will be useful to rewrite the moment relations derived above in terms of these quantities, defining a new set of moments

$$\hat{M}_N(\mu_f, \mu) = \int_0^{\mu_f + \bar{\Lambda}(\mu_f, \mu)} d\hat{\omega} \hat{\omega}^N \hat{S}(\hat{\omega}, \mu). \quad (3.62)$$

This yields

$$\begin{aligned} \hat{M}_0(\mu_f, \mu) &= 1 - \frac{C_F \alpha_s(\mu)}{\pi} \left(\ln^2 \frac{\mu_f}{\mu} + \ln \frac{\mu_f}{\mu} + \frac{\pi^2}{24} \right) \\ &\quad + \frac{C_F \alpha_s(\mu)}{\pi} \left(\ln \frac{\mu_f}{\mu} - \frac{1}{2} \right) \frac{\mu_\pi^2(\mu_f, \mu)}{3\mu_f^2} + \dots, \\ \frac{\hat{M}_1(\mu_f, \mu)}{\hat{M}_0(\mu_f, \mu)} &= \bar{\Lambda}(\mu_f, \mu), \quad \frac{\hat{M}_2(\mu_f, \mu)}{\hat{M}_0(\mu_f, \mu)} = \frac{\mu_\pi^2(\mu_f, \mu)}{3} + \bar{\Lambda}(\mu_f, \mu)^2, \end{aligned} \quad (3.63)$$

where the parameters $\bar{\Lambda}(\mu_f, \mu) = M_B - m_b^{\text{SF}}(\mu_f, \mu)$ and $\mu_\pi^2(\mu_f, \mu)$ should be considered as known physical quantities. The moments with $N \geq 1$ give simply a restatement of the shape-function scheme definition. Another interesting aspect is that the expression for $\hat{M}_0(\mu_f, \mu)$ can be used to extract the precise form of the asymptotic tail of the shape function, since μ_f is considered to be much larger than Λ_{QCD} in our calculation.

Asymptotic behavior of the shape function

Taking the derivative of the zeroth moment \hat{M}_0 in (3.62) with respect to μ_f , one obtains

$$\hat{S}(\hat{\omega}, \mu) \Big|_{\hat{\omega}=\mu_f+\bar{\Lambda}(\mu_f, \mu)} = \left(1 - \frac{dm_b^{\text{SF}}(\mu_f, \mu)}{d\mu_f}\right)^{-1} \frac{d}{d\mu_f} \hat{M}_0(\mu_f, \mu). \quad (3.64)$$

From (3.63) we find at one-loop order

$$\begin{aligned} \hat{S}(\hat{\omega}, \mu) = & -\frac{C_F \alpha_s(\mu)}{\pi} \frac{1}{\hat{\omega} - \bar{\Lambda}} \left[\left(2 \ln \frac{\hat{\omega} - \bar{\Lambda}}{\mu} + 1\right) \right. \\ & \left. + \frac{2}{3} \frac{\mu_\pi^2}{(\hat{\omega} - \bar{\Lambda})^2} \left(\ln \frac{\hat{\omega} - \bar{\Lambda}}{\mu} - 1\right) + \dots \right]. \end{aligned} \quad (3.65)$$

The precise definitions of $\bar{\Lambda}$ and μ_π^2 are not specified at this order. (Note that the shape function cannot depend on the value of the cutoff μ_f .) Relation (3.65) is a model-independent result as long as $\hat{\omega} \gg \Lambda_{\text{QCD}}$. We stress the remarkable fact that this radiative tail of the shape function is *negative*, in contrast with the naive expectation based on a probabilistic interpretation of the shape function as a momentum distribution function. The point is that the definition of the renormalized shape function requires scheme-dependent ultra-violet subtractions. From (3.65) it follows that the shape function must have a zero, which for sufficiently large μ is located at a value $\hat{\omega}_0 \approx \bar{\Lambda} + \mu/\sqrt{e}$.

CHAPTER 4

INCLUSIVE SEMILEPTONIC DECAYS

Due to experimental cuts in the measurement of the inclusive $B \rightarrow X_u l^- \bar{\nu}$ decays one is generally faced with a situation in which the hadronic final state X_u is constraint to have large energy $E_H \sim M_B$, but only moderate invariant mass $s_H = m_X^2 \sim \Lambda_{\text{QCD}} M_B$. This kinematic region, called the “shape-function region”, is the dominant phase space in which the final state cannot contain charmed hadrons. The calculation of the inclusive differential decay rate uses the optical theorem and assumes quark-hadron duality. This assumption is justified when integrating over large portions of the phase space, corresponding to the summation over many final hadronic states. To calculate the total decay rate, i.e. including all of phase space, all kinematic quantities are integrated over a domain of order M_B , and one can perform an operator product expansion (OPE) to systematically compute power corrections. However, as mentioned above, when it is necessary to calculate the differential decay rate in the shape-function region, the calculation becomes more difficult because of the presence of three separated mass scales: the hard scale M_B , the hard-collinear scale $\sqrt{\Lambda_{\text{QCD}} M_B}$, and the soft scale Λ_{QCD} . To properly disentangle the physics associated with these scales requires a sophisticated effective field-theory machinery.

A systematic treatment consists of matching QCD onto SCET_I in a first step, in which hard quantum fluctuations are integrated out. The degrees of freedom in SCET_I are referred to as soft and hard-collinear to indicate that the invariant final state momenta have fluctuations of order the intermediate scale $\sqrt{\Lambda_{\text{QCD}} M_B}$, much larger than Λ_{QCD} . It is therefore possible to treat them perturbatively. The expansion parameter of SCET_I is hence defined as $\lambda = \Lambda_{\text{QCD}}/E_H$.

In a second step, SCET_I is matched onto HQET, and hard-collinear modes are integrated out. The resulting expressions for inclusive differential decay rates have the factorized form $d\Gamma \sim H J \otimes S$ [51]. The function H contains the hard corrections, the jet function J , which describes the properties of the final-state hadronic jet, contains the hard-collinear effects, and the shape function S accounts for the internal soft dynamics in the B meson [35, 52]. The \otimes symbol implies a convolution over a light-cone momentum variable ω associated with the residual momentum of the b quark inside the B meson.

4.1 Factorization theorem

Using the optical theorem, the hadronic physics relevant to the inclusive semileptonic decay $\bar{B} \rightarrow X_u l^- \bar{\nu}$ can be related to a hadronic tensor $W^{\mu\nu}$ defined via the discontinuity of the forward B -meson matrix element of a correlator of two flavor-changing weak currents $J^\mu = \bar{u}\gamma^\mu(1 - \gamma_5)b$ [53, 54, 55]. We define

$$W^{\mu\nu} = \frac{1}{\pi} \text{Im} \frac{\langle \bar{B}(v) | T^{\mu\nu} | \bar{B}(v) \rangle}{2M_B}, \quad T^{\mu\nu} = i \int d^4x e^{iq \cdot x} \text{T} \{ J^{\dagger\mu}(0), J^\nu(x) \}. \quad (4.1)$$

Here v is the B -meson velocity and q the momentum carried by the lepton pair. After the field redefinition $b(x) = e^{-im_b v \cdot x} b'(x)$, which is always the first step in the construction of an effective heavy field, the phase factor in (4.1) becomes $e^{i(q-m_b v) \cdot x} \equiv e^{-ip \cdot x}$, where $p = m_b v - q$ corresponds to the momentum of the jet of light partons into which the b -quark decays. We will assume that these partons can be described by hard-collinear fields. This is justified in the shape-function region, in which case the current correlator can be expanded in non-local light-cone operators [35, 40, 52].

The hadronic tensor in (4.1) factorizes at leading power [36], as can be shown in the following way: The jet momentum (and likewise the momentum of the

hadronic final state) scales like $p^\mu \sim E(\lambda, 1, \sqrt{\lambda})$. (For the jet momentum, $p_\perp = 0$ by choice of the coordinate system.) The jet invariant mass, $p^2 \sim E\Lambda_{\text{QCD}}$, defines a hybrid, intermediate short-distance scale. The appropriate effective field theory for integrating out the short-distance fluctuations associated with the hard scale p_- is SCET_I , see Section 2.3 but with hard-collinear and soft degrees of freedom instead of collinear and ultrasoft ones. Below a matching scale $\mu_h \sim m_b$, the semileptonic current can be expanded as

$$\bar{u}(x)\gamma^\mu(1-\gamma_5)b'(x) = \sum_{i=1}^3 \int ds \tilde{C}_i(s) \bar{\mathcal{X}}_{hc}(x+s\bar{n}) \Gamma_i^\mu \mathcal{H}(x_-) + \dots, \quad (4.2)$$

where the dots denote higher-order terms in the SCET expansion, which can be neglected at leading power in Λ_{QCD}/m_b . The hard-collinear light-quark field $\mathcal{X}_{hc}(x) = S_s^\dagger(x_-) W_{hc}^\dagger(x) \xi_{hc}(x)$ and the soft heavy-quark field $\mathcal{H}(x_-) = S_s^\dagger(x_-) h(x_-)$ are SCET building blocks that are invariant under a set of homogeneous soft and hard-collinear gauge transformations [13, 14, 15]. These are the ingredients of SCET_I after the field redefinitions (2.38) and (2.40). Because of the reduced Dirac basis between collinear spinors in (4.2), we may choose any three independent Dirac structures that do not vanish between the spinors. A convenient choice is

$$\Gamma_1^\mu = \gamma^\mu(1-\gamma_5), \quad \Gamma_2^\mu = v^\mu(1+\gamma_5), \quad \Gamma_3^\mu = \frac{n^\mu}{n \cdot v} (1+\gamma_5). \quad (4.3)$$

The current correlator in (4.1) then becomes

$$T^{\mu\nu} = i \int d^4x e^{-ip \cdot x} \sum_{i,j=1}^3 \int ds dt \tilde{C}_j^*(t) \tilde{C}_i(s) \times \\ \text{Tr} \{ \bar{\mathcal{H}}(0) \bar{\Gamma}_j^\mu \mathcal{X}_{hc}(t\bar{n}), \bar{\mathcal{X}}_{hc}(x+s\bar{n}) \Gamma_i^\nu \mathcal{H}(x_-) \} + \dots. \quad (4.4)$$

In a second step, the hard-collinear fluctuations associated with the light-quark jet can be integrated out by matching SCET onto HQET at an intermediate scale $\mu_i \sim \sqrt{m_b \Lambda_{\text{QCD}}}$. At leading order the SCET Lagrangian (when written in terms of

the gauge-invariant fields such as \mathcal{X}_{hc}) does not contain interactions between hard-collinear and soft fields, due to the decoupling transformation (2.38). Since the external B -meson states only contain soft constituents, we can take the vacuum matrix element over the hard-collinear fields, defining a jet function

$$\langle \Omega | T \{ \mathcal{X}_{hc,k}(t\bar{n}), \bar{\mathcal{X}}_{hc,l}(x + s\bar{n}) \} | \Omega \rangle \equiv \delta_{kl} \tilde{\mathcal{J}}(x + (s-t)\bar{n}) + \dots, \quad (4.5)$$

where k, l are color indices, and we have used translational invariance to determine the dependence on the coordinate vectors. Shifting the integration variable from x to $z = x + (s-t)\bar{n}$, with $z_- = x_-$, and introducing the Fourier-transformed Wilson coefficient functions $C_i(\bar{n} \cdot p) = \int ds e^{is\bar{n} \cdot p} \tilde{C}_i(s)$, we then obtain

$$T^{\mu\nu} = i \sum_{i,j=1}^3 C_j^*(\bar{n} \cdot p) C_i(\bar{n} \cdot p) \int d^4 z e^{-ip \cdot z} \bar{\mathcal{H}}(0) \bar{\Gamma}_j^\mu \tilde{\mathcal{J}}(z) \Gamma_i^\nu \mathcal{H}(z_-) + \dots \quad (4.6)$$

In the next step, we rewrite the bilocal heavy-quark operator as [35]

$$\begin{aligned} \bar{\mathcal{H}}(0) \Gamma \mathcal{H}(z_-) &= (\bar{h} S_s)(0) \Gamma e^{z_- \cdot \partial_+} (S_s^\dagger h)(0) = \bar{h}(0) \Gamma e^{z_- \cdot D_+} h(0) \\ &= \int d\omega e^{-\frac{i}{2}\omega \bar{n} \cdot z} \bar{h}(0) \Gamma \delta(\omega - in \cdot D) h(0), \end{aligned} \quad (4.7)$$

where Γ may be an arbitrary Dirac structure, and we have used the property $in \cdot D S_s = S_s in \cdot \partial$ of the soft Wilson line S_s . When this expression is used in (4.6), the resulting formula for the correlator involves the Fourier transform of the jet function,

$$\int d^4 z e^{-ip \cdot z} \tilde{\mathcal{J}}(z) = \not{p}_- \mathcal{J}(p^2), \quad (4.8)$$

however with p^μ replaced by the combination $p_\omega^\mu \equiv p^\mu + \frac{1}{2}\omega \bar{n}^\mu$. Intuitively, this happens as only the plus component of the soft residual momentum of the b quark adds to the hard-collinear momentum p . Using that $p_{\omega-} = p_-$, we now obtain

$$T^{\mu\nu} = i \sum_{i,j=1}^3 H_{ij}(\bar{n} \cdot p) \int d\omega \mathcal{J}(p_\omega^2) \bar{h} \bar{\Gamma}_i^\mu \not{p}_- \Gamma_j^\nu \delta(\omega - in \cdot D) h + \dots, \quad (4.9)$$

where $H_{ij}(\bar{n} \cdot p) = C_j^*(\bar{n} \cdot p) C_i(\bar{n} \cdot p)$ are called the hard functions.

We need the discontinuity of the jet function, $J(p^2) = \frac{1}{\pi} \text{Im} [i\mathcal{J}(p^2)]$, in order to compute the hadronic tensor. The B -meson matrix element of the soft operator is evaluated using the HQET trace formalism, which allows us to write [2]

$$\frac{\langle \bar{B}(v) | \bar{h} \Gamma \delta(\omega - i n \cdot D) h | \bar{B}(v) \rangle}{2M_B} = S(\omega) \frac{1}{2} \text{tr} \left(\Gamma \frac{1 + \not{v}}{2} \right) + \dots \quad (4.10)$$

at leading power in the heavy-quark expansion. Clearly, the soft function $S(\omega)$ is the shape function, which was studied in Section 3.2. This gives the factorization formula

$$W^{\mu\nu} = \sum_{i,j=1}^3 H_{ij}(\bar{n} \cdot p) \text{tr} \left(\bar{\Gamma}_i^\mu \frac{\not{p}_-}{2} \Gamma_j^\nu \frac{1 + \not{v}}{2} \right) \int d\omega J(p_\omega^2) S(\omega) + \dots \quad (4.11)$$

In the final expressions (4.9) and (4.11) the dependence on the three scales $\bar{n} \cdot p \sim m_b$, $p_\omega^2 \sim m_b \Lambda_{\text{QCD}}$ and $\omega \sim \Lambda_{\text{QCD}}$ has been factorized into the hard, jet, and shape functions, respectively. The factorization formula (4.11) was derived at tree level in [35, 52], and was conjectured to hold to all orders in perturbation theory in [51]. The derivation presented above [36] is equivalent to an all-order proof of this formula first presented in [11] (see also [8]). The limits of integration in the convolution integral are determined by the facts that the jet function has support for $p_\omega^2 \geq 0$, and the shape function has support for $-\infty < \omega \leq \bar{\Lambda}$. The argument p_ω^2 of the jet function can be rewritten in the “partonic variable” $\bar{n} \cdot p$ and the “hadronic variable” $n \cdot P_H \sim O(\Lambda_{\text{QCD}})$:

$$p_\omega^2 = p^2 + \bar{n} \cdot p \omega = \bar{n} \cdot p (n \cdot P_H - (\bar{\Lambda} - \omega)) \equiv \bar{n} \cdot p (n \cdot P_H - \hat{\omega}), \quad (4.12)$$

where $P_H = M_B v - q = p + \bar{\Lambda} v$ is the 4-momentum of the hadronic final state, and the variable $\hat{\omega} = \bar{\Lambda} - \omega \geq 0$. Finally, $n \cdot P_H = E_H - |\vec{P}_H| = s_H/2E_H + O(\Lambda_{\text{QCD}}^2/m_b)$ is related to the hadronic invariant mass and energy of the final state. The usefulness

of this variable has also been emphasized in [38, 56]. We shall see below that expressing the convolution integral in terms of the new variable $\hat{\omega}$ eliminates any spurious dependence of the decay spectra on the b -quark pole mass.

Using the fact that the Wilson coefficients C_i are real and hence H_{ij} is symmetric in its indices, we find

$$\begin{aligned} \sum_{i,j=1}^3 H_{ij} \text{tr} \left(\bar{\Gamma}_i^\mu \frac{\not{p}_-}{2} \Gamma_j^\nu \frac{1+\not{p}}{2} \right) &= 2H_{11} (p_-^\mu v^\nu + p_-^\nu v^\mu - g^{\mu\nu} v \cdot p_- - i\epsilon^{\mu\nu\alpha\beta} p_{-\alpha} v_\beta) \\ &+ 2H_{22} v \cdot p_- v^\mu v^\nu + 2(H_{12} + H_{23}) (p_-^\mu v^\nu + p_-^\nu v^\mu) + 2(2H_{13} + H_{33}) \frac{p_-^\mu p_-^\nu}{v \cdot p_-}, \end{aligned} \quad (4.13)$$

which may be compared with the general Lorentz decomposition of the hadronic tensor given in [37]:

$$\begin{aligned} W^{\mu\nu} &= W_1 (p^\mu v^\nu + p^\nu v^\mu - g^{\mu\nu} v \cdot p - i\epsilon^{\mu\nu\alpha\beta} p_\alpha v_\beta) - W_2 g^{\mu\nu} \\ &+ W_3 v^\mu v^\nu + W_4 (p^\mu v^\nu + p^\nu v^\mu) + W_5 p^\mu p^\nu \end{aligned} \quad (4.14)$$

We see that the structure function W_2 is not generated at leading order in the SCET expansion. Since only the Wilson coefficient C_1 is non-zero at tree-level, the structure function W_1 receives leading-power contributions at tree level, whereas W_4 and W_5 receive leading-power contributions at $O(\alpha_s(m_b))$. The function W_3 receives leading-power contributions only at $O(\alpha_s^2(m_b))$, which is beyond the accuracy of a next-to-leading order calculation.

4.2 Matching calculations

We derive expressions for the perturbative functions $H_{ij}(\bar{n} \cdot p)$ and $J(p_\omega^2)$, that enter the factorization formula in (4.11) at next-to-leading order in α_s . To this end, we match expressions for the hadronic tensor obtained in full QCD, SCET, and HQET, using for simplicity on-shell external b -quark states.

4.2.1 Hard functions

Perturbative expressions for the hadronic functions W_i in the decomposition (4.14) have been obtained in [37] by evaluating one-loop Feynman graphs for the current correlator $T^{\mu\nu}$ using on-shell external quark states with residual momentum k (satisfying $v \cdot k = 0$) in full QCD. The leading terms in the region of hard-collinear jet momenta are

$$\begin{aligned}
\frac{1}{2} W_1 &= \delta(p_k^2) \left[1 - \frac{C_F \alpha_s}{4\pi} \left(8 \ln^2 y - 10 \ln y + \frac{2 \ln y}{1-y} + 4L_2(1-y) + \frac{4\pi^2}{3} + 5 \right) \right] \\
&\quad + \frac{C_F \alpha_s}{4\pi} \left[-4 \left(\frac{\ln(p_k^2/m_b^2)}{p_k^2} \right)_*^{[m_b^2]} + (8 \ln y - 7) \left(\frac{1}{p_k^2} \right)_*^{[m_b^2]} \right] + \dots, \\
\frac{1}{2} W_4 &= \delta(p_k^2) \frac{C_F \alpha_s}{4\pi} \frac{2}{1-y} \left(\frac{y \ln y}{1-y} + 1 \right) + \dots, \\
\frac{m_b}{4} W_5 &= \delta(p_k^2) \frac{C_F \alpha_s}{4\pi} \frac{2}{1-y} \left(\frac{1-2y}{1-y} \ln y - 1 \right) + \dots,
\end{aligned} \tag{4.15}$$

whereas W_2 and W_3 do not receive leading-power contributions at this order. Here $\alpha_s \equiv \alpha_s(\mu)$, $y = \bar{n} \cdot p/m_b$, and $p_k^2 = p^2 + \bar{n} \cdot p n \cdot k$. The star distributions are generalized plus distributions, which also play an important role in the renormalization of the shape function. They have been introduced in (3.31) and obey the rescaling identities (3.32). In order to find the hard functions H_{ij} , we need the discontinuity of the current correlator (4.4) between on-shell heavy-quark states in SCET, keeping i, j fixed. The corresponding tree diagram yields

$$D^{(0)} = K \delta(p_k^2), \quad \text{with} \quad K = \bar{u}_b(v) \bar{\Gamma}_j^\mu \not{p}_- \Gamma_i^\nu u_b(v), \tag{4.16}$$

where $u_b(v)$ are on-shell HQET spinors normalized to unity, and the quantity K corresponds to the Dirac trace in (4.11). The interpretation of this result in terms of hard, jet, and soft functions is that, at tree level, $J^{(0)}(p_\omega^2) = \delta(p_\omega^2)$ and $S_{\text{parton}}^{(0)}(\omega) = \delta(\omega - n \cdot k)$ in the free-quark decay picture. It follows that the

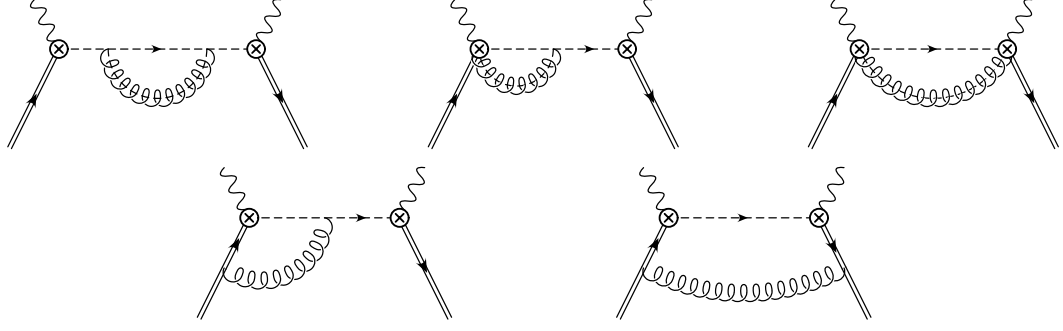


Figure 4.1: One-loop diagrams contributing to the current correlator in SCET. The effective current operators are denoted by crossed circles, and hard-collinear propagators are drawn as dashed lines. Mirror graphs obtained by exchanging the two currents are not shown.

convolution integral $\int d\omega J(p_\omega^2) S(\omega)$ in (4.11) produces $\delta(p_k^2)$, and comparison with (4.15) shows that $H_{11}^{(0)} = 1$, while all other hard functions vanish at tree level.

At one-loop order we need to evaluate the SCET diagrams shown in Fig. 4.1. The first three graphs contain hard-collinear gluon exchanges, while the last two diagrams contain soft exchanges. For the sum of all hard-collinear exchange graphs, we find [36]

$$D_{hc}^{(1)} = K \frac{C_F \alpha_s}{4\pi} \left[\left(\frac{4}{\epsilon^2} + \frac{3}{\epsilon} + 7 - \pi^2 \right) \delta(p_k^2) \right. \quad (4.17)$$

$$\left. + 4 \left(\frac{\ln(p_k^2/\mu^2)}{p_k^2} \right)_*^{[\mu^2]} - \left(\frac{4}{\epsilon} + 3 \right) \left(\frac{1}{p_k^2} \right)_*^{[\mu^2]} \right]. \quad (4.18)$$

The sum of the soft contributions is given by

$$D_s^{(1)} = K \frac{C_F \alpha_s}{4\pi} \left[\left(-\frac{2}{\epsilon^2} - \frac{4}{\epsilon} L + \frac{2}{\epsilon} - 4L^2 + 4L - \frac{\pi^2}{6} \right) \delta(p_k^2) \right. \\ \left. - 8 \left(\frac{\ln(p_k^2/\mu^2)}{p_k^2} \right)_*^{[\mu^2]} + \left(\frac{4}{\epsilon} + 8L - 4 \right) \left(\frac{1}{p_k^2} \right)_*^{[\mu^2]} \right], \quad (4.19)$$

where $L = \ln(\bar{n} \cdot p/\mu)$. The $1/\epsilon$ poles in the sum of the hard-collinear and soft contributions are subtracted by a multiplicative renormalization factor Z_J^2 applied

to the bare current correlator in (4.4), where

$$Z_J = 1 + \frac{C_F \alpha_s}{4\pi} \left(-\frac{1}{\epsilon^2} + \frac{2}{\epsilon} L - \frac{5}{2\epsilon} \right) \quad (4.20)$$

is the (momentum-space) current renormalization constant in SCET [9]. Since the wave-function renormalization factor of on-shell heavy quarks is equal to 1, the sum of (4.17) and (4.19) after subtraction of the pole terms is matched with the results in (4.15), so that the hard functions equal

$$\begin{aligned} H_{11}(\bar{n} \cdot p) &= 1 + \frac{C_F \alpha_s}{4\pi} \left(-4L^2 + 10L - 4 \ln y - \frac{2 \ln y}{1-y} - 4L_2(1-y) - \frac{\pi^2}{6} - 12 \right), \\ H_{12}(\bar{n} \cdot p) &= \frac{C_F \alpha_s}{4\pi} \frac{2}{1-y} \left(\frac{y \ln y}{1-y} + 1 \right), \\ H_{13}(\bar{n} \cdot p) &= \frac{C_F \alpha_s}{4\pi} \frac{y}{1-y} \left(\frac{1-2y}{1-y} \ln y - 1 \right). \end{aligned} \quad (4.21)$$

4.2.2 Jet function

The SCET loop graphs in Fig. 4.1 determine the one-loop contributions to the product of the jet function and the shape function in (4.11). We may write this product symbolically as $J^{(1)} \otimes S^{(0)} + J^{(0)} \otimes S^{(1)}$, where the \otimes symbol means a convolution in ω . Although the realistic shape function is a hadronic quantity, we may use its partonic version to determine the perturbative jet function. Its one-loop contribution $J^{(1)}$ must therefore be extracted from the results (4.17) and (4.19). To this end, we need the renormalized shape function at one-loop order in the parton model, which has been done in Section 3.2.1. It follows that the renormalized jet function is given by the distribution [36]

$$J(p_\omega^2) = \delta(p_\omega^2) + \frac{C_F \alpha_s}{4\pi} \left[(7 - \pi^2) \delta(p_\omega^2) + 4 \left(\frac{\ln(p_\omega^2/\mu^2)}{p_\omega^2} \right)_*^{[\mu^2]} - 3 \left(\frac{1}{p_\omega^2} \right)_*^{[\mu^2]} \right]. \quad (4.22)$$

It will often be useful to separate the dependence on $\bar{n} \cdot p$ and $n \cdot P_H$ in this result

by means of the substitution $p_\omega^2 = y \hat{p}_\omega^2$, where $\hat{p}_\omega^2 = m_b(n \cdot P_H - \hat{\omega})$ according to (4.12). Using the identities (3.32), we find

$$y J(p_\omega^2) \equiv \hat{J}(\hat{p}_\omega^2, y) = \delta(\hat{p}_\omega^2) + \frac{C_F \alpha_s}{4\pi} \left[(2 \ln^2 y - 3 \ln y + 7 - \pi^2) \delta(\hat{p}_\omega^2) + 4 \left(\frac{\ln(\hat{p}_\omega^2/\mu^2)}{\hat{p}_\omega^2} \right)^{[\mu^2]}_* + (4 \ln y - 3) \left(\frac{1}{\hat{p}_\omega^2} \right)^{[\mu^2]}_* \right]. \quad (4.23)$$

4.3 Sudakov resummation

Equations (4.21) and (4.22) determine the short-distance objects H_{ij} and J in the factorization formula (4.11) at one-loop order in perturbation theory. However, there is no common choice of the renormalization scale μ that would eliminate all large logarithms from these results. Likewise, the shape function, being a hadronic matrix element, is naturally renormalized at some low scale, whereas the short-distance objects contain physics at higher scales. The problem of large logarithms arising from the presence of disparate mass scales can be dealt with using renormalization-group equations. Proceeding in three steps, our strategy will be as follows:

1. We match QCD onto SCET and extract matching conditions for the hard functions H_{ij} at a high scale $\mu_h \sim m_b$. At that scale, no large logarithms appear and so the hard functions can be reliably computed using perturbation theory. We then evolve them down to an intermediate hard-collinear scale $\mu_i \sim \sqrt{m_b \Lambda_{\text{QCD}}}$ by solving the renormalization-group equation

$$\frac{d}{d \ln \mu} H_{ij}(\bar{n} \cdot p, \mu) = 2\gamma_J(\bar{n} \cdot p, \mu) H_{ij}(\bar{n} \cdot p, \mu), \quad (4.24)$$

where $\gamma_J = \gamma_{\xi h}$ is the anomalous dimension of the semileptonic heavy-to-collinear current in SCET, see the first line in (2.67).

2. Starting from a model for the shape function $S(\omega, \mu_0)$ at some low scale $\mu_0 = \text{few} \times \Lambda_{\text{QCD}}$ large enough to trust perturbation theory. Such a model could be provided by a QCD-inspired approach such as QCD sum rules or lattice QCD, or it could be tuned to experimental data. We then solve the integro-differential evolution equation (3.35) to obtain the shape function at the intermediate scale μ_i .
3. Lastly we combine the results for the hard functions and for the shape function with the jet function J in (4.22) at the scale μ_i , where J is free of large logarithms and so has a reliable perturbative expansion. The dependence on the matching scales μ_h and μ_i cancels in the final result (to the order at which we are working).

We begin with the evolution of the hard functions. The anomalous dimension γ_J for the SCET current is twice the coefficient of the $1/\epsilon$ pole in the renormalization factor Z_J in (4.20). More generally [9, 24],

$$\gamma_J(\bar{n} \cdot p, \mu) = -\Gamma_{\text{cusp}}(\alpha_s) \ln \frac{\mu}{\bar{n} \cdot p} + \gamma'(\alpha_s) = \frac{C_F \alpha_s}{\pi} \left(-\ln \frac{\mu}{\bar{n} \cdot p} - \frac{5}{4} \right) + \dots, \quad (4.25)$$

where $\Gamma_{\text{cusp}} = C_F \alpha_s / \pi + \dots$ is the universal cusp anomalous dimension governing the ultra-violet singularities of Wilson lines with light-like segments [25]. The exact solution to the evolution equation (4.24) can be written as [36]

$$H_{ij}(\bar{n} \cdot p, \mu_i) = H_{ij}(\bar{n} \cdot p, \mu_h) \exp U_H(\bar{n} \cdot p, \mu_h, \mu_i), \quad (4.26)$$

where

$$U_H(\bar{n} \cdot p, \mu_h, \mu_i) = 2 \int_{\alpha_s(\mu_h)}^{\alpha_s(\mu_i)} \frac{d\alpha}{\beta(\alpha)} \left[\Gamma_{\text{cusp}}(\alpha) \left(\ln \frac{\bar{n} \cdot p}{\mu_h} - \int_{\alpha_s(\mu_h)}^{\alpha} \frac{d\alpha'}{\beta(\alpha')} \right) + \gamma'(\alpha) \right]. \quad (4.27)$$

Setting $r_1 = \alpha_s(\mu_i)/\alpha_s(\mu_h) > 1$, and expanding the evolution function to $O(\alpha_s)$,

we obtain

$$e^{U_H(\bar{n} \cdot p, \mu_h, \mu_i)} = e^{V_H(\mu_h, \mu_i)} \left(\frac{\bar{n} \cdot p}{\mu_h} \right)^{-\frac{\Gamma_0}{\beta_0} \ln r_1} \times \left[1 - \frac{\alpha_s(\mu_h)}{4\pi} \frac{\Gamma_0}{\beta_0} \left(\frac{\Gamma_1}{\Gamma_0} - \frac{\beta_1}{\beta_0} \right) (r_1 - 1) \ln \frac{\bar{n} \cdot p}{\mu_h} \right], \quad (4.28)$$

where

$$V_H(\mu_h, \mu_i) = \frac{\Gamma_0}{2\beta_0^2} \left[\frac{4\pi}{\alpha_s(\mu_h)} \left(1 - \frac{1}{r_1} - \ln r_1 \right) + \frac{\beta_1}{2\beta_0} \ln^2 r_1 - \left(\frac{\Gamma_1}{\Gamma_0} - \frac{\beta_1}{\beta_0} \right) (r_1 - 1 - \ln r_1) \right] - \frac{\gamma'_0}{\beta_0} \ln r_1 + O\left[(r_1 - 1) \alpha_s(\mu_h)\right]. \quad (4.29)$$

(As a reminder, the QCD β -function is given in (2.18), and we expanded all anomalous dimensions as in (2.24).) The terms proportional to $1/\alpha_s(\mu_h)$ resum the leading, double logarithmic terms to all orders in perturbation theory. The remaining $O(1)$ terms in V_H contribute at leading, single-logarithmic order. At next-to-leading order, the corrections proportional to the coupling $\alpha_s(\mu_h)$ are included. In our case, the only piece missing for a complete resummation at next-to-leading order is the $O(\alpha_s)$ contribution to V_H ,

$$\frac{\alpha(\mu_h)}{4\pi} \left\{ \begin{aligned} & (\ln r_1) \left[\frac{r_1 \beta_1}{2\beta_0^4} (\beta_0 \Gamma_1 - \beta_1 \Gamma_0) + \frac{\Gamma_0}{2\beta_0^4} (\beta_1^2 - \beta_0 \beta_2) \right] \\ & + \frac{(r_1 - 1)^2}{4\beta_0^4} \left[\Gamma_0 (\beta_0 \beta_2 - \beta_1^2) + \beta_0 (\beta_1 \Gamma_1 - \beta_0 \Gamma_2) \right] \\ & + \frac{(r_1 - 1)}{2\beta_0^3} \left[(\beta_2 \Gamma_0 - \beta_1 \Gamma_1) + 2\beta_0 (\beta_1 \gamma'_0 - \beta_0 \gamma'_1) \right] \end{aligned} \right\}, \quad (4.30)$$

which is independent of the kinematic variable $\bar{n} \cdot p$ and vanishes for $\mu_i \rightarrow \mu_h$. To compute these terms would require to calculate the cusp anomalous dimension to three loops (knowledge of Γ_2) and the anomalous dimension γ' to two loops (γ'_1). While the former has recently been computed in [57], the latter is still missing

up to date. This implies a universal, process-independent small uncertainty in the normalization of inclusive B -decay spectra in the shape-function region. We stress, however, that this uncertainty cancels in all ratios of decay distributions, even between $\bar{B} \rightarrow X_u l^- \bar{\nu}$ and $\bar{B} \rightarrow X_s \gamma$ spectra.

It is appropriate to perform the running between μ_h and μ_i in a theory with $n_f = 4$ light quark flavors, since the intermediate scale μ_i will be of order m_c in our applications below. The relevant expansion coefficients are, as far as they are known,

$$\begin{aligned} \Gamma_0 &= \frac{16}{3}, \quad \Gamma_1 = \frac{2576}{27} - \frac{16}{3}\pi^2, \quad \Gamma_2 = \frac{96488}{81} - \frac{5152}{27}\pi^2 + \frac{176}{15}\pi^4 - \frac{160}{9}\zeta_3, \\ \beta_0 &= \frac{25}{3}, \quad \beta_1 = \frac{154}{3}, \quad \beta_2 = \frac{21943}{54}, \\ \gamma'_0 &= -\frac{20}{3}. \end{aligned} \tag{4.31}$$

4.4 Differential decay rates and spectra

As mentioned earlier, the hadronic tensor is most naturally expressed in terms of the variables $n \cdot P_H$ and $\bar{n} \cdot p$ in the shape-function region. It is thus useful to derive expressions for the decay rates in terms of these variables. Our theoretical results are valid as long as $n \cdot P_H$ can be considered as being of order a hadronic scale (say, a few $\times \Lambda_{\text{QCD}}$), whereas $\bar{n} \cdot p$ is integrated over a domain of order $m_b \gg \Lambda_{\text{QCD}}$. It is this integration which provides a sampling over sufficiently many hadronic final states needed to ensure quark–hadron duality [58]. The distribution in $\bar{n} \cdot p$ will be described in terms of a “partonic” scaling variable $y = \bar{n} \cdot p/m_b$, while the distribution in the orthogonal light-cone component is described in terms of the dimensionfull *hadronic* variable $P_+ \equiv n \cdot P_H = E_H - |\vec{P}_H|$. At leading order in Λ_{QCD}/m_b , we obtain from [37] the triple differential decay rate

$$\frac{d^3\Gamma}{d\bar{x} dy dP_+} = 12m_b \Gamma_{\text{tree}} y(y - \bar{x}) \left[(1 + \bar{x} - y) \frac{W_1}{2} + \bar{x} \left(\frac{W_4}{2} + \frac{m_b W_5}{4} \right) \right] + \dots, \quad (4.32)$$

where $\bar{x} = 1 - x$, and $x = 2E_l/m_b$ is a scaling variable proportional to the energy of the charged lepton measured in the B -meson rest frame. The quantity $\Gamma_{\text{tree}} = G_F^2 |V_{ub}|^2 (m_b^{\text{pole}})^5 / (192\pi^3)$ denotes the leading power, tree-level expression for the total $\bar{B} \rightarrow X_u l^- \bar{\nu}$ decay rate. The hadronic function W_i are written in the factorized form, which are found to be [36]

$$\begin{aligned} \frac{W_1}{2} &= \left\{ 1 + \frac{C_F \alpha_s(m_b)}{4\pi} \left[-4 \ln^2 y + (6 - c) \ln y - \frac{2 \ln y}{1 - y} - 4L_2(1 - y) \right. \right. \\ &\quad \left. \left. - \frac{\pi^2}{6} - 12 \right] \right\} y^{-1-a} e^{V_H(m_b, \mu_i)} \int_0^{n \cdot P_H} d\hat{\omega} \hat{J}(\hat{p}_\omega^2, y, \mu_i) \hat{S}(\hat{\omega}, \mu_i) + \dots, \\ \frac{W_4}{2} + \frac{m_b W_5}{4} &= \frac{C_F \alpha_s(m_b)}{4\pi} \frac{2 \ln y}{1 - y} y^{-1-a} e^{V_H(m_b, \mu_i)} \\ &\quad \times \int_0^{n \cdot P_H} d\hat{\omega} \hat{J}(\hat{p}_\omega^2, y, \mu_i) \hat{S}(\hat{\omega}, \mu_i) + \dots, \end{aligned} \quad (4.33)$$

where the dots represent power corrections in Λ_{QCD}/m_b . The result for the rescaled jet function $\hat{J}(\hat{p}_\omega^2, y, \mu_i)$ is the expression in (4.23). Furthermore we need the Sudakov exponent V_H in (4.29). This function is independent of the kinematic variables y and \hat{p}_ω^2 . In addition, we need

$$\begin{aligned} a &= \frac{\Gamma_0}{\beta_0} \ln r_1 = \frac{16}{25} \ln \frac{\alpha_s(\mu_i)}{\alpha_s(m_b)}, \\ c &= \frac{4}{\beta_0} \left(\frac{\Gamma_1}{\Gamma_0} - \frac{\beta_1}{\beta_0} \right) (r_1 - 1) = \left(\frac{10556}{1875} - \frac{12\pi^2}{25} \right) \left(\frac{\alpha_s(\mu_i)}{\alpha_s(m_b)} - 1 \right). \end{aligned} \quad (4.34)$$

For simplicity, we have identified the high-energy matching scale μ_h with the heavy-quark mass m_b . In the variables \bar{x} , y , and P_+ , the phase space is remarkably simple:

$$0 \leq P_+ \leq M_B - 2E_l = m_b \bar{x} + \bar{\Lambda}, \quad \frac{P_+ - \bar{\Lambda}}{m_b} \leq \bar{x} \leq y \leq 1. \quad (4.35)$$

If E_l is integrated over a domain of order $m_b \gg \Lambda_{\text{QCD}}$, i. e. \bar{x} is integrated over a domain of order unity, one can replace the second condition by $0 \leq \bar{x} \leq y \leq 1$ at

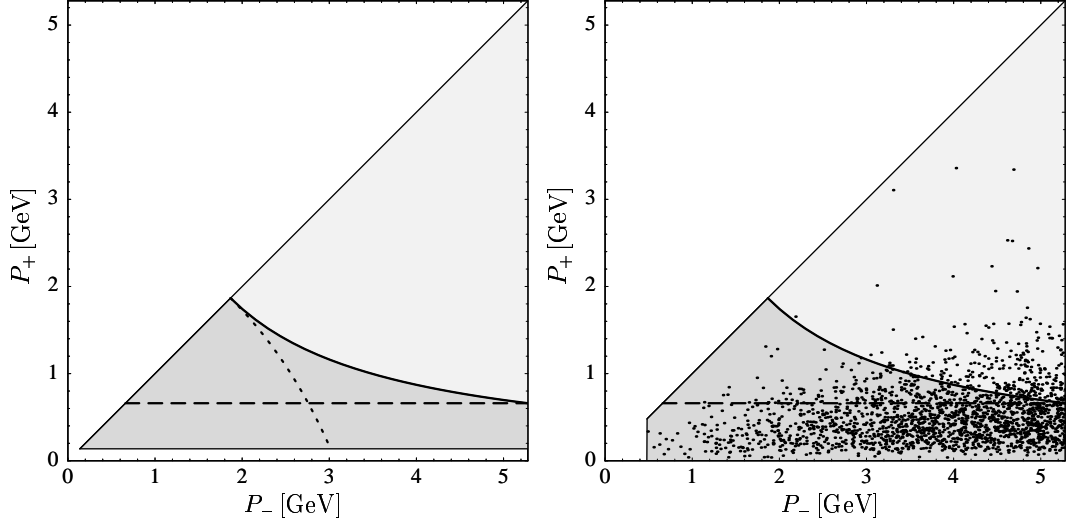


Figure 4.2: Hadronic phase space for the light-cone variables P_- and P_+ (left), and theory phase space for $m_b = 4.8 \text{ GeV}$ (right). The scatter points indicate the distribution of events as predicted by the model of [37]. In each plot the solid line separates the regions where $s_H < M_D^2$ (dark gray) and $s_H > M_D^2$ (light gray), whereas the dashed line corresponds to $P_+ = M_D^2/M_B$. The dotted line in the first plot shows the contour where $q^2 = (M_B - M_D)^2$.

leading power in Λ_{QCD}/m_b . If, on the other hand, the lepton energy is restricted to be close to its kinematic limit, $E_l \approx M_B/2$, then $\bar{x} = O(\Lambda_{\text{QCD}}/m_b)$, and at leading order the rate (4.32) can be simplified to

$$\frac{d^3\Gamma}{dE_l dy dP_+} = 24\Gamma_{\text{tree}} y^2 (1-y) \frac{W_1}{2} + \dots, \quad (4.36)$$

with $0 \leq y \leq 1$ and $0 \leq P_+ \leq M_B - 2E_l$.

In general, the hadronic tensor can be described in terms of the quantities $P_{\pm} = E_H \mp |\vec{P}_H|$, whose true phase-space is $M_{\pi} \leq P_+ \leq P_- \leq M_B$, corresponding to a triangular region in the (P_-, P_+) plane. The variable P_- is related to our parton variables by $P_- = \bar{n} \cdot p + \bar{\Lambda} = m_b y + \bar{\Lambda}$. In our theoretical description based on quark-hadron duality P_+ starts from 0, while the small region with $P_- < \bar{\Lambda}$ is left unpopulated. This is illustrated in Fig. 4.2. Contours of constant hadronic or

leptonic invariant mass in the (P_-, P_+) plane are easy to visualize, since

$$s_H = P_H^2 = P_+ P_-, \quad q^2 = (M_B - P_+)(M_B - P_-) \quad (4.37)$$

are given by very simple expressions. The solid and dotted lines in the left-hand plot in Fig. 4.2 show the contours where $s_H = M_D^2$ and $q^2 = (M_B - M_D)^2$, respectively, which can be used to separate $\bar{B} \rightarrow X_u l^- \bar{\nu}$ events from semileptonic decays with charm hadrons in the final state. The dashed horizontal line shows the maximum allowed value of P_+ when a cut $E_l \geq (M_B^2 - M_D^2)/(2M_B)$ is applied to the charged-lepton energy, which implies $P_+ \leq M_D^2/M_B$. We will see later that this cut, which is obviously another way of eliminating the charm background, allows for a systematic treatment of the theoretical prediction, and is therefore of great interest. In the right-hand plot, we indicate the density of events in theory phase space obtained using the model of [37].¹ It is apparent that the vast majority of events is located in the shape-function region of small P_+ and large P_- .

In the remainder of this section, we present analytic results to the order of accuracy we have worked so far, for a variety of spectra in $\bar{B} \rightarrow X_u l^- \bar{\nu}$ decays. They are obtained by integrating over the scaling variable y before integrating over the hadronic variable P_+ , changing variables from P_+ to $\hat{p}_\omega^2 = m_b(P_+ - \hat{\omega})$. The integral over the shape-function variable $\hat{\omega}$ is left until the end, so that our formulae are model independent. We will always present fractional decay rates normalized to the total inclusive rate

$$\Gamma(\bar{B} \rightarrow X_u l^- \bar{\nu}) \equiv \Gamma_{\text{tot}} = \Gamma_{\text{tree}} \left[1 + \frac{C_F \alpha_s(m_b)}{4\pi} \left(\frac{25}{2} - 2\pi^2 \right) \right] + \dots, \quad (4.38)$$

¹While not rigorously implementing shape-function effects beyond tree level, the model of [37] has the advantage that it interpolates between the shape-function region and the remainder of phase space, where a local operator product expansion can be employed. On the contrary, our more rigorous discussion here is limited to the region of hard-collinear jet momenta. However, the scatter plot shown in the figure provides a reasonably realistic impression of the population in phase space.

where the dots represent higher-order perturbative corrections as well as power corrections of order $(\Lambda_{\text{QCD}}/m_b)^2$ and higher. This procedure offers the advantage of eliminating the strong sensitivity to the heavy-quark (pole) mass. The integrals over the parton variable y encountered in our analysis can be reduced to a set of master integrals defined as

$$\begin{aligned}
I_1(b, z) &= \int_0^z dy y^b = \frac{z^{1+b}}{1+b}, \\
I_2(b, z) &= \int_0^z dy y^b \ln y = \frac{z^{1+b}}{1+b} \left(\ln z - \frac{1}{1+b} \right), \\
I_3(b, z) &= \int_0^z dy y^b \ln^2 y = \frac{z^{1+b}}{1+b} \left(\ln^2 z - \frac{2 \ln z}{1+b} + \frac{2}{(1+b)^2} \right), \\
I_4(b, z) &= \int_0^z dy y^b \frac{\ln y}{1-y} = \sum_{j=0}^{\infty} \frac{z^{1+b+j}}{1+b+j} \left(\ln z - \frac{1}{1+b+j} \right), \\
I_5(b, z) &= \int_0^z dy y^b L_2(1-y) = \frac{z^{1+b}}{1+b} L_2(1-z) - \frac{I_4(1+b, z)}{1+b},
\end{aligned} \tag{4.39}$$

where $b > -1$ and $z \leq 1$ are arbitrary real numbers.

4.4.1 Charged-lepton energy spectrum

Near the charged-lepton energy endpoint, where we can assume that $M_B - 2E_l$ is of order a hadronic scale, the underlying event falls into the shape-function region of large $\bar{n} \cdot p$ and small $n \cdot P_H$. Starting from the triple differential rate in (4.36), we obtain for the normalized energy spectrum [36]

$$\begin{aligned}
\frac{1}{\Gamma_{\text{tot}}} \frac{d\Gamma}{dE_l} &= \frac{4T(a)}{m_b} e^{V_H(m_b, \mu_i)} \int_0^{M_B - 2E_l} d\hat{\omega} \hat{S}(\hat{\omega}, \mu_i) \left\{ 1 + \frac{C_F \alpha_s(m_b)}{4\pi} H(a) \right. \\
&\quad + \frac{C_F \alpha_s(\mu_i)}{4\pi} \left[2 \ln^2 \frac{m_b(M_B - 2E_l - \hat{\omega})}{\mu_i^2} \right. \\
&\quad + \left(4f_2(a) - 3 \right) \ln \frac{m_b(M_B - 2E_l - \hat{\omega})}{\mu_i^2} \\
&\quad \left. \left. + \left(7 - \pi^2 - 3f_2(a) + 2f_3(a) \right) \right] \right\}.
\end{aligned} \tag{4.40}$$

Here

$$\begin{aligned}
T(a) &= 6 \left[I_1(1-a, 1) - I_1(2-a, 1) \right], \\
f_n(a) &= \frac{I_n(1-a, 1) - I_n(2-a, 1)}{I_1(1-a, 1) - I_1(2-a, 1)}, \\
H(a) &= \frac{11\pi^2}{6} - \frac{49}{2} + (6-c)f_2(a) - 4f_3(a) - 2f_4(a) - 4f_5(a).
\end{aligned} \tag{4.41}$$

At leading power in Λ_{QCD}/m_b the heavy-quark mass in the denominator of the prefactor on the right-hand side of (4.40) can be replaced by $m_b + \omega = M_B - \hat{\omega}$, which removes any sensitivity to the definition of m_b . This replacement can indeed be justified by studying power corrections to the shape function [59, 60].

All our results for decay rates will have a similar structure, but the definitions of the functions T , f_n , and H will be different in each case. The tree-level result can be recovered by setting $V_H = 0$ and $a = 0$, in which case $T(0) = 1$, and the spectrum is simply given in terms of an integral over the shape function [35]. Using the above result, it is straightforward to calculate the fraction $F_E = \Gamma(E_l \geq E_0)/\Gamma_{\text{tot}}$ of all $\bar{B} \rightarrow X_u l^- \bar{\nu}$ events with charged-lepton energy above a threshold E_0 . Defining $\Delta_E = M_B - 2E_0$, we find

$$\begin{aligned}
F_E(\Delta_E) &= T(a) e^{V_H(m_b, \mu_i)} \int_0^{\Delta_E} d\hat{\omega} \frac{2(\Delta_E - \hat{\omega})}{M_B - \hat{\omega}} \hat{S}(\hat{\omega}, \mu_i) \left\{ 1 + \frac{C_F \alpha_s(m_b)}{4\pi} H(a) \right. \\
&\quad + \frac{C_F \alpha_s(\mu_i)}{4\pi} \left[2 \ln^2 \frac{m_b(\Delta_E - \hat{\omega})}{\mu_i^2} + \left(4f_2(a) - 7 \right) \ln \frac{m_b(\Delta_E - \hat{\omega})}{\mu_i^2} \right. \\
&\quad \left. \left. + \left(14 - \pi^2 - 7f_2(a) + 2f_3(a) \right) \right] \right\}.
\end{aligned} \tag{4.42}$$

Note that the fraction $F_E(\Delta_E)$ is given in terms of a weighted integral over the shape function, with a weight factor of order Λ_{QCD}/m_b that vanishes at the upper end of integration. As a result, only a small fraction of events is contained in the lepton endpoint region.

4.4.2 Hadronic P_+ spectrum

Applying a lower cut on the charged-lepton energy restricts the variable P_+ to be less than Δ_E . However, a cut on P_+ does *not* restrict the lepton energy to be in the endpoint region. Still, the fraction of events with $P_+ \leq \Delta_E$ samples the same hadronic phase space as the lepton-endpoint cut, but it contains significantly more events. Such a cut therefore offers an excellent opportunity to determine the CKM matrix element $|V_{ub}|$.

To determine the fraction of events that survive, we integrate over \bar{x} and y in the range $0 \leq \bar{x} \leq y \leq 1$ before integrating over P_+ . The result is

$$\begin{aligned}
 F_P(\Delta_P) = & T(a) e^{V_H(m_b, \mu_i)} \int_0^{\Delta_P} d\hat{\omega} \hat{S}(\hat{\omega}, \mu_i) \left\{ 1 + \frac{C_F \alpha_s(m_b)}{4\pi} H(a) \right. \\
 & + \frac{C_F \alpha_s(\mu_i)}{4\pi} \left[2 \ln^2 \frac{m_b(\Delta_P - \hat{\omega})}{\mu_i^2} + (4f_2(a) - 3) \ln \frac{m_b(\Delta_P - \hat{\omega})}{\mu_i^2} \right. \\
 & \left. \left. + (7 - \pi^2 - 3f_2(a) + 2f_3(a)) \right] \right\}, \quad (4.43)
 \end{aligned}$$

where now

$$\begin{aligned}
 T(a) &= 6I_1(2 - a, 1) - 4I_1(3 - a, 1), \\
 H(a) &= \frac{11\pi^2}{6} - \frac{49}{2} + (6 - c)f_2(a) - 4f_3(a) - 2[f_4(a) - \Delta f_4(a)] - 4f_5(a), \quad (4.44)
 \end{aligned}$$

and

$$\begin{aligned}
 f_n(a) &= \frac{3I_n(2 - a, 1) - 2I_n(3 - a, 1)}{3I_1(2 - a, 1) - 2I_1(3 - a, 1)}, \\
 \Delta f_4(a) &= \frac{I_4(3 - a, 1)}{3I_1(2 - a, 1) - 2I_1(3 - a, 1)}. \quad (4.45)
 \end{aligned}$$

The contribution Δf_4 arises from the terms contained in the structure functions W_4 and W_5 in (4.33). A comparison of the result for $F_P(\Delta_P)$ in (4.43) with the expression for $F_E(\Delta_E)$ in (4.42) yields that the cut on hadronic P_+ contains a much larger fraction of all $\bar{B} \rightarrow X_u l^- \bar{\nu}$ events. As a matter of fact, $F_P(\Delta_P)$ is

directly given in terms of an integral over the shape function, without a weight function of order Λ_{QCD}/m_b . (At tree level, $F_P(\Delta_P) = \int_0^{\Delta_P} d\hat{\omega} \hat{S}(\hat{\omega})$.) Since the shape function peaks around $\hat{\omega} \approx \bar{\Lambda} \approx 0.5$ GeV, we expect a high efficiency for values of Δ_P in the vicinity of the “optimal cut” $\Delta_P = M_D^2/M_B$, which eliminates the charm background.

4.4.3 Hadronic invariant mass spectrum

A cut on the hadronic invariant mass in the final state constitutes the ideal separator between $\bar{B} \rightarrow X_u l^- \bar{\nu}$ and $\bar{B} \rightarrow X_c l^- \bar{\nu}$ events, since any final state containing a charm hadron has invariant mass above M_D . Let us discuss the cut $\sqrt{s_H} \leq M_D$ by examining the phase-space picture of Fig. 4.2. The available phase space for a cut on $P_+ \leq M_D^2/M_B$ is fully contained. In addition there is a triangle-shaped region of larger P_+ , which culminates in a cusp where $P_+ = P_- = M_D$. Near the cusp, both light-cone momentum components are of the same order, and hence this portion of phase space should not be treated using our theoretical description based on the collinear expansion. A priori, it is not evident that we can compute the fractional rate $F_M(s_0) = \Gamma(s_H \leq s_0)/\Gamma_{\text{tot}}$ in a controlled heavy-quark expansion.

To see what happens, it is instructive to first ignore radiative corrections. At tree level, it is straightforward to obtain

$$F_M(s_0) = \int_0^{\Delta_s} d\hat{\omega} \hat{S}(\hat{\omega}) + \int_{\Delta_s}^{\sqrt{s_0}} d\hat{\omega} \hat{S}(\hat{\omega}) \left(\frac{\Delta_s}{\hat{\omega}} \right)^3 \left(2 - \frac{\Delta_s}{\hat{\omega}} \right), \quad (4.46)$$

where $\Delta_s = s_0/M_B$. The calculation of this event fraction requires knowledge of the shape function over a wider range in $\hat{\omega}$ than in the case of the event fraction with a cut on P_+ . The first integral is the same as for $F_P(\Delta_s)$ in (4.43) and corresponds to the region in phase space where $P_+ \leq s_0/M_B$. The second integral corresponds

to the phase space above the dashed line in Fig. 4.2. The region near the cusp corresponds to the upper integration region in the second integral. Note that, due to the rapid fall-off of the integrand, the tip of the triangle region only gives a power-suppressed contribution to the decay rate. When radiative corrections are included, the result for the integrated hadronic invariant mass spectrum becomes rather complicated. In general, we may split up the contributions into

$$F_M(s_0) = F_M^{\text{box}}(s_0) + F_M^{\text{triangle}}(s_0), \quad \text{with} \quad F_M^{\text{box}}(s_0) = F_P(\Delta_s), \quad (4.47)$$

The box contribution is given by the expression for the rate fraction $F_P(\Delta_P)$ in (4.43) evaluated with $\Delta_P = \Delta_s = s_0/M_B$. For the remaining contribution from the triangular region, we obtain [36].

$$\begin{aligned} F_M^{\text{triangle}}(s_0) = & e^{V_H(m_b, \mu_i)} \int_{\Delta_s}^{\sqrt{s_0}} d\hat{\omega} \hat{S}(\hat{\omega}, \mu_i) \left[G_1(\Delta_s/\hat{\omega}) + \frac{C_F \alpha_s(\mu_i)}{4\pi} G_2(\Delta_s, \hat{\omega}) \right] \\ & + e^{V_H(m_b, \mu_i)} \int_0^{\Delta_s} d\hat{\omega} \hat{S}(\hat{\omega}, \mu_i) \frac{C_F \alpha_s(\mu_i)}{4\pi} G_3(\Delta_s, \hat{\omega}), \end{aligned} \quad (4.48)$$

where

$$\begin{aligned} G_1(z) = T(a, z) \left\{ 1 + \frac{C_F \alpha_s(m_b)}{4\pi} H(a, z) \right. \\ \left. + \frac{C_F \alpha_s(\mu_i)}{4\pi} [7 - \pi^2 - 3f_2(a, z) + 2f_3(a, z)] \right\} \end{aligned} \quad (4.49)$$

contains the same functions T , H and f_n as defined in (4.44) and (4.45), but with all master integrals replaced by $I_n(b, 1) \rightarrow I_n(b, z)$. In addition, we need

$$\begin{aligned} G_2(\Delta_s, \hat{\omega}) = & \int_0^{\mu_i^2/m_b} \frac{dP}{P} \left\{ \ln \frac{m_b P}{\mu_i^2} \left[k_1 \left(\frac{\Delta_s}{P + \hat{\omega}} \right) - k_1 \left(\frac{\Delta_s}{\hat{\omega}} \right) \right] \right. \\ & \left. + \left[k_2 \left(\frac{\Delta_s}{P + \hat{\omega}} \right) - k_2 \left(\frac{\Delta_s}{\hat{\omega}} \right) \right] \right\} \\ & + \int_{\mu_i^2/m_b}^{\sqrt{s_0} - \hat{\omega}} \frac{dP}{P} \left[\ln \frac{m_b P}{\mu_i^2} k_1 \left(\frac{\Delta_s}{P + \hat{\omega}} \right) + k_2 \left(\frac{\Delta_s}{P + \hat{\omega}} \right) \right], \quad (4.50) \\ G_3(\Delta_s, \hat{\omega}) = & \int_{\Delta_s}^{\sqrt{s_0}} \frac{dP}{P - \hat{\omega}} \left[\ln \frac{m_b(P - \hat{\omega})}{\mu_i^2} k_1 \left(\frac{\Delta_s}{P} \right) + k_2 \left(\frac{\Delta_s}{P} \right) \right], \end{aligned}$$

where

$$\begin{aligned} k_1(z) &= 4 \left[6I_1(2-a, z) - 4I_1(3-a, z) \right] = 4T(a, z), \\ k_2(z) &= 4 \left[6I_2(2-a, z) - 4I_2(3-a, z) \right] - 3 \left[6I_1(2-a, z) - 4I_1(3-a, z) \right], \end{aligned} \quad (4.51)$$

with the constant a given in (4.34). For orientation, a typical numerical value is $a \approx 0.335$ for $\mu_i = 1.5$ GeV.

As mentioned above, the phase-space region near the cusp where $\hat{\omega} \sim \sqrt{s_0}$ or $P \sim \sqrt{s_0}$ gives a power-suppressed contribution to the decay rate. More precisely, we find that the contribution is given by

$$F_M(s_0) \ni e^{V_H(m_b, \mu_i)} \frac{C_F \alpha_s(\mu_i)}{\pi} \frac{6}{(3-a)^2} \left(\frac{\Delta_s}{\sqrt{s_0}} \right)^{3-a} \left(\frac{7}{4} + \frac{3}{3-a} \right) + \dots, \quad (4.52)$$

where the dots represent higher-order power corrections. For $s_0 \sim m_b \Lambda_{\text{QCD}}$, the above result thus scales like $(\Lambda_{\text{QCD}}/m_b)^{(3-a)/2}$, whereas $F_M(s_0)$ is of $O(1)$. For consistency, we should therefore omit the term in (4.52), which can be done by replacing all occurrences of $\sqrt{s_0}$ in upper integration limits in (4.48) and (4.50) with ∞ , which we will use this prescription in our numerical analysis in Section 4.6.

4.4.4 Combined cuts on hadronic and leptonic invariant mass

Bauer et al. have proposed to reduce the sensitivity to shape-function effects in the extraction of $|V_{ub}|$ by combining a cut on hadronic invariant mass with a cut $q^2 \geq q_0^2$ on the invariant mass squared of the lepton pair [61]. The first plot in Fig. 4.3 shows that this eliminates a large portion of the events with large P_- . We indicate the remaining phase space for several choices of cuts, for example $(s_0, q_0^2) = (M_D^2, 0)$ (solid line), $(M_D^2, 6 \text{ GeV}^2)$ (dashed line), and $((1.7 \text{ GeV})^2, 8 \text{ GeV}^2)$ (dotted line).

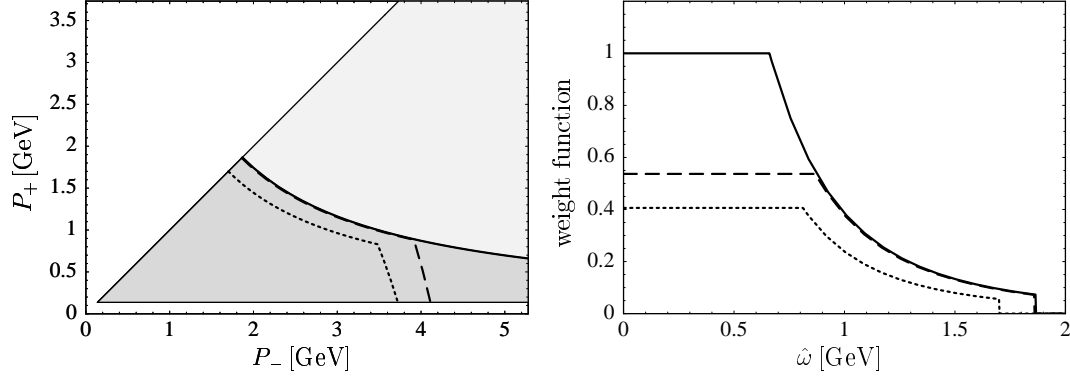


Figure 4.3: Phase-space constraints (left) and weight functions (right) for combined cuts on the hadronic and leptonic invariant mass: $(s_0, q_0^2) = (M_D^2, 0)$ (solid), $(M_D^2, 6 \text{ GeV}^2)$ (dashed), and $((1.7 \text{ GeV})^2, 8 \text{ GeV}^2)$ (dotted).

For the corresponding event fraction at tree level, we obtain

$$F_{\text{comb}}(s_H \leq s_0, q^2 \geq q_0^2) = y_0^3 (2 - y_0) \int_0^{\Delta_s/y_0} d\hat{\omega} \hat{S}(\hat{\omega}) + \int_{\Delta_s/y_0}^{\sqrt{s_0}} d\hat{\omega} \hat{S}(\hat{\omega}) \left(\frac{\Delta_s}{\hat{\omega}} \right)^3 \left(2 - \frac{\Delta_s}{\hat{\omega}} \right), \quad (4.53)$$

where $y_0 = 1 - q_0^2/(m_b M_B)$, and $\Delta_s = s_0/M_B$ as above. For a fixed hadronic-mass cut s_0 , the effect of the additional cut on q^2 is to broaden the support of the first integral, while at the same time reducing its weight due to the prefactor. To illustrate this point, we show in the second plot in Fig. 4.3 the weight functions under the integral with the shape function for the three different choices of (s_0, q_0^2) mentioned above. The sensitivity to the precise form of the shape function is reduced because the weight functions become progressively more shallow as the value of q_0^2 is raised. However, this reduction comes at the price of a significant reduction of the rate, raising questions about the validity of the assumption of quark-hadron duality. We will see in Section 4.6 that the *relative* uncertainty due to shape-function effects is not strongly (although somewhat) reduced when imposing an additional cut on q^2 .

4.5 Model-independent relations between spectra

As we have seen in the previous section, all spectra and event fractions are expressed in terms of weighted integrals of perturbative functions over the (universal, i.e. process independent) shape function. Therefore they all require the knowledge of the function form of the shape function, which cannot be calculated using analytic techniques. One way would be to adopt a specific model or extract the shape function from experiment. Alternatively, it is possible to derive model-independent relations between different decay distributions in which the shape function has been eliminated [35]. The most promising strategy is to relate event fractions in semileptonic $\bar{B} \rightarrow X_u l^- \bar{\nu}$ decays to a weighted integral over the $\bar{B} \rightarrow X_s \gamma$ photon spectrum, which at present provides the most direct access to the shape function. While it is straightforward to derive such relations at tree level, radiative corrections introduce non-trivial complications [62, 63, 64, 65]. Since our formalism [36] has yet to be applied to the $\bar{B} \rightarrow X_s \gamma$ photon spectrum, we will instead derive a relation between the charged-lepton energy spectrum and a weighted integral over the P_+ spectrum, which is in many respects very similar to the photon spectrum. We wish to construct a *perturbative* weight function $w(\Delta, P_+)$ such that at leading power in Λ_{QCD}/m_b

$$\int_{E_0}^{M_B/2} dE_l \frac{d\Gamma}{dE_l} = \int_0^\Delta dP_+ w(\Delta, P_+) \frac{d\Gamma}{dP_+}, \quad \Delta = M_B - 2E_0. \quad (4.54)$$

This relation is independent of the shape function and hence insensitive to hadronic physics. The construction of the weight function is straightforward order by order in perturbation theory. Using the results of the previous section, we find

$$w(\Delta, P_+) = \frac{2(\Delta - P_+)}{M_B - P_+} \frac{3(4 - a)}{(6 - a)(2 - a)} \left\{ 1 + \frac{C_F \alpha_s(m_b)}{4\pi} h_1(a) \right\}$$

$$+ \frac{C_F \alpha_s(\mu_i)}{4\pi} \left[h_2(a) \ln \frac{m_b(\Delta - P_+)}{\mu_i^2} + h_3(a) \right] \Big\}, \quad (4.55)$$

where

$$\begin{aligned} h_1(a) &= 2 - 2 \frac{3952 - 5416a + 2988a^2 - 838a^3 + 120a^4 - 7a^5}{(6-a)(4-a)^2(3-a)(2-a)^2} \\ &\quad + c \frac{20 - 8a + a^2}{(6-a)(4-a)(2-a)}, \\ h_2(a) &= -4 \frac{20 - 8a + a^2}{(6-a)(4-a)(2-a)}, \\ h_3(a) &= \frac{5056 - 6744a + 3556a^2 - 942a^3 + 127a^4 - 7a^5}{(6-a)(4-a)^2(3-a)(2-a)^2}. \end{aligned} \quad (4.56)$$

The lesson we learned from this prototype relation (4.54) should be applied in the future to the $\bar{B} \rightarrow X_s \gamma$ photon spectrum. Using similar methods, it will be possible to construct a shape-function independent relation of the form

$$F_P(\Delta) = \frac{1}{\Gamma_s} \int_{\frac{M_B - \Delta}{2}}^{\frac{M_B}{2}} dE_\gamma \frac{d\Gamma_s}{dE_\gamma} w_s(\Delta, E_\gamma), \quad (4.57)$$

where at tree level the weight function is simply $w_s(\Delta, E_\gamma) = 1$. It is also possible (although far more complicated) to relate the $\bar{B} \rightarrow X_s \gamma$ photon spectrum to the hadronic invariant mass spectrum $F_M(s_0)$ in (4.47). However, because of the larger integration domain over the shape function, such a relation would require input of the photon spectrum beyond the region where it is currently experimentally accessible.

The alert reader might wonder about the appearance of the renormalization scale μ_i in the weight function, since $w(\Delta, P_+)$ is formally independent of the scale μ_i (because there is nothing to cancel a potential μ_i dependence in (4.54)). Expanding the resummed result for the weight function to first order in α_s , we obtain the simple expression

$$w(\Delta, P_+) \Big|_{1\text{-loop}} = \frac{2(\Delta - P_+)}{M_B - P_+} \left[1 + \frac{C_F \alpha_s}{4\pi} \left(-\frac{5}{3} \ln \frac{\Delta - P_+}{m_b} - \frac{17}{36} \right) \right], \quad (4.58)$$

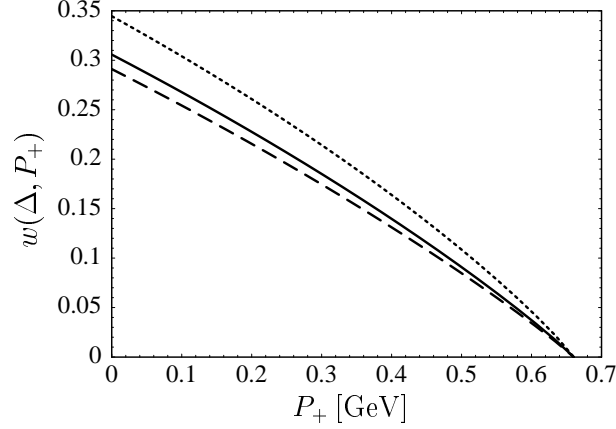


Figure 4.4: Weight function $w(\Delta, P_+)$ entering the rate relation (4.54) for $\Delta = M_D^2/M_B$ and three different choices of the intermediate scale, namely $\mu_i = 1.5$ GeV (solid), 2.0 GeV (dashed), and 1.0 GeV (dotted). The weight function is formally independent of μ_i .

in which the dependence on μ_i has canceled. However, since this formula contains a large logarithm and the scale to be used in α_s is undetermined, it should not be used for phenomenological applications. A visualization of the resummed weight function in (4.55) for different choices of μ_i is given in Fig. 4.4. As is apparent, the function is pretty uneventful, since apart from the rational prefactor, the P_+ dependence is given through a single logarithm.

4.6 Numerical results

We are now ready to study the implications of our analysis for phenomenology. We start by deriving the numerical values for the shape-function mass and kinetic energy including errors. We then present a model for the shape function which satisfies all theoretical constraints, as derived in Chapter 3. Finally, we present numerical results for the various decay rates and spectra investigated in Section 4.4. We use the two-loop running coupling constant in the $\overline{\text{MS}}$ scheme, normalized

such that $\alpha_s(M_Z) = 0.119$. Our standard choice of the intermediate matching scale is $\mu_i = 1.5 \text{ GeV}$. This corresponds to setting $\mu_i^2 = m_b \Lambda_{\text{had}}$ with a typical hadronic scale $\Lambda_{\text{had}} \approx 0.5 \text{ GeV}$. The values of the strong coupling evaluated at these scales are $\alpha_s(m_b) \simeq 0.222$ and $\alpha_s(\mu_i) \simeq 0.375$. The corresponding values of the perturbative parameters a and c defined in (4.34) are $a \simeq 0.335$ and $c \simeq 0.614$. Finally, the leading-order Sudakov factor in (4.33) takes the value $e^{V_H(m_b, \mu_i)} \simeq 1.21$.

4.6.1 Shape-function mass and kinetic energy

A value for the shape-function mass can be obtained by combining the relations (3.58) or (3.59) with existing predictions for the b -quark mass in the relevant renormalization schemes. The potential-subtracted mass at the scale $\mu_f = 2 \text{ GeV}$ has been determined from moments of the $b\bar{b}$ cross section and the mass of the $\Upsilon(1S)$ state [66]. Using the first relation in (3.59), we find [36] $m_b^{\text{SF}}(2 \text{ GeV}, 2 \text{ GeV}) = m_b^{\text{PS}}(2 \text{ GeV}) = (4.59 \pm 0.08) \text{ GeV}$. From a similar analysis the kinetic mass has been determined at the scale $\mu_f = 2 \text{ GeV}$ to be $m_b^{\text{kin}}(1 \text{ GeV}) = (4.57 \pm 0.06) \text{ GeV}$ [49]. From the second relation in (3.59) it then follows that $m_b^{\text{SF}}(1 \text{ GeV}, 1 \text{ GeV}) = (4.65 \pm 0.06) \text{ GeV}$. Computing the scale dependence of the shape-function mass (using the fact that the pole mass is RG invariant), we obtain at the intermediate scale the values $m_b^{\text{SF}}(\mu_i, \mu_i) = (4.61 \pm 0.08) \text{ GeV}$ and $m_b^{\text{SF}}(\mu_i, \mu_i) = (4.65 \pm 0.06) \text{ GeV}$, respectively. Alternatively, we may use relation (3.58) in conjunction with an experimental determination of the b -quark pole mass from moments of inclusive $\bar{B} \rightarrow X_c l^- \bar{\nu}$ and $\bar{B} \rightarrow X_s \gamma$ decay spectra. Using the average value $\bar{\Lambda}_{\text{pole}} = (0.375 \pm 0.065) \text{ GeV}$ obtained from [67, 68, 69, 70], we find $m_b^{\text{SF}}(\mu_i, \mu_i) = (4.67 \pm 0.07) \text{ GeV}$. It is quite remarkable that these different determinations of the shape-function mass, which use rather different physics input, give highly consistent results. Combining them,

we quote our default value for the shape-function mass at the intermediate scale $\mu_i = 1.5 \text{ GeV}$ as

$$m_b^{\text{SF}}(\mu_i, \mu_i) = (4.65 \pm 0.07) \text{ GeV}. \quad (4.59)$$

The corresponding $\bar{\Lambda}$ parameter is $\bar{\Lambda}(\mu_i, \mu_i) = (0.63 \pm 0.07) \text{ GeV}$.

A value of the kinetic-energy parameter in the shape-function scheme can be obtained from (3.60) or (3.61). Using the first relation and the experimental value $-\lambda_1 = (0.25 \pm 0.06) \text{ GeV}^2$ [68, 69, 70] yields $\mu_\pi^2(\mu_i, \mu_i) = (0.271 \pm 0.064) \text{ GeV}^2$. Alternatively, we may use the result for the kinetic-energy parameter obtained in the kinetic scheme, $[\mu_\pi^2(1 \text{ GeV})]_{\text{kin}} = (0.45 \pm 0.10) \text{ GeV}^2$ [49], to get from (3.61) the value $\mu_\pi^2(\mu_i, \mu_i) = (0.254 \pm 0.107) \text{ GeV}^2$. Again, the two determinations are in very good agreement with each other. Combining them, we obtain

$$\mu_\pi^2(\mu_i, \mu_i) = (0.27 \pm 0.07) \text{ GeV}^2. \quad (4.60)$$

4.6.2 Model shape functions

In our analysis of decay rates below, we will adopt a model for the shape function $\hat{S}(\hat{\omega}, \mu_i)$ at the intermediate scale. For the purpose of illustration, we use a two-component ansatz for the shape function that is a generalization of the model employed in [37, 41]. The form we propose is [36]

$$\hat{S}(\hat{\omega}, \mu) = \frac{N}{\Lambda} \left(\frac{\hat{\omega}}{\Lambda} \right)^{b-1} \exp \left(-b \frac{\hat{\omega}}{\Lambda} \right) - \frac{C_F \alpha_s(\mu)}{\pi} \frac{\theta(\hat{\omega} - \Lambda - \mu/\sqrt{e})}{\hat{\omega} - \Lambda} \left(2 \ln \frac{\hat{\omega} - \Lambda}{\mu} + 1 \right), \quad (4.61)$$

where Λ and b are model parameters, and Λ differs from the pole-scheme parameter $\bar{\Lambda}_{\text{pole}}$ by an amount of $O(\alpha_s(\mu))$. In the limit $\alpha_s(\mu) \rightarrow 0$ this function reduces to the familiar model used in [37, 41]. The radiative tail ensures the correct leading asymptotic behavior of the shape function as displayed in (3.65). This in turn gives

the correct power-like dependence of shape-function moments on the integration cutoff. In our model, this tail is glued onto a “primordial”, exponential function such that the combined result is continuous. The normalization factor N is given by

$$N = \left[1 - \frac{C_F \alpha_s(\mu)}{\pi} \left(\frac{\pi^2}{24} - \frac{1}{4} \right) \right] \frac{b^b}{\Gamma(b)}, \quad (4.62)$$

which is determined such that the integral over the shape function from $\hat{\omega} = 0$ to $\mu_f + \bar{\Lambda}(\mu_f, \mu)$ coincides with the first expression in (3.63) up to second-order corrections. By evaluating the first moment of the model shape function, we find that the model parameter Λ is related to the HQET parameter $\bar{\Lambda}$ in the pole scheme and the shape-function scheme as

$$\Lambda = \bar{\Lambda}_{\text{pole}} + \frac{C_F \alpha_s(\mu)}{\pi} \frac{2\mu}{\sqrt{e}}, \quad \Lambda = \bar{\Lambda}(\mu_i, \mu_i) + \mu_i \left(\frac{2}{\sqrt{e}} - 1 \right) \frac{C_F \alpha_s(\mu_i)}{\pi}. \quad (4.63)$$

Finally, the model parameter b can be adjusted to reproduce a given value for the second moment of the shape function.

Table 4.1 collects the parameters of the model shape functions at the intermediate scale $\mu_i = 1.5 \text{ GeV}$ corresponding to different values of $\bar{\Lambda}(\mu_i, \mu_i)$ and $\mu_\pi^2(\mu_i, \mu_i)$. The left-hand (right-hand) plot in Fig. 4.5 shows three models for the shape function obtained by varying the parameters $\bar{\Lambda}$ and μ_π^2 in a correlated (anti-correlated) way. In both cases, the solid, dashed, and dotted curves refer to different values of $\bar{\Lambda}$, as indicated in the table. In Fig. 4.6 we illustrate the renormalization-group evolution of the shape function as studied in Chapter 3. The sharply peaked solid line shows our model function evaluated with $\Lambda = 0.495 \text{ GeV}$ and $b = 3.0$, which we use as an ansatz for the function $\hat{S}(\hat{\omega}, \mu_0)$ at the low scale $\mu_0 = 1 \text{ GeV}$. (For comparison, the dotted gray curve shows the default choice for the shape function adopted in [37, 41], which exhibits a very similar shape except for the missing

Table 4.1: Parameters and moments of the model shape functions at the intermediate scale μ_i . The running quantities m_b^{SF} , $\bar{\Lambda}$, and μ_π^2 are defined in the shape-function scheme and evaluated at $\mu_f = \mu = \mu_i = 1.5 \text{ GeV}$.

| Model | Lines | $m_b^{\text{SF}} [\text{GeV}]$ | $\bar{\Lambda} [\text{GeV}]$ | $\mu_\pi^2 [\text{GeV}^2]$ | $\Lambda [\text{GeV}]$ | b |
|-------|--------|--------------------------------|------------------------------|----------------------------|------------------------|------|
| S1 | Dotted | 4.72 | 0.56 | 0.20 | 0.611 | 2.84 |
| S2 | | | | 0.27 | 0.617 | 2.32 |
| S3 | | | | 0.34 | 0.626 | 1.92 |
| S4 | Solid | 4.65 | 0.63 | 0.20 | 0.680 | 3.57 |
| S5 | | | | 0.27 | 0.685 | 2.93 |
| S6 | | | | 0.34 | 0.692 | 2.45 |
| S7 | Dashed | 4.58 | 0.70 | 0.20 | 0.751 | 4.40 |
| S8 | | | | 0.27 | 0.753 | 3.61 |
| S9 | | | | 0.34 | 0.759 | 3.03 |

radiative tail.) The broad solid curve gives the shape function at the intermediate scale $\mu_i = 1.5 \text{ GeV}$ as obtained from the evolution equation (3.52). The barely visible dashed-dotted curve shows our default model for the function $\hat{S}(\hat{\omega}, \mu_i)$, which coincides with the solid line in the left-hand plot. The beautiful agreement of the two curves gives us confidence in the consistency of our models adopted for the shape function at the intermediate scale.

4.6.3 Predictions for decay spectra and event fractions

We are now ready to present our results for the decay spectra and partially integrated event fractions in $\bar{B} \rightarrow X_u l^- \bar{\nu}$ decays. In order to illustrate the sensitivity

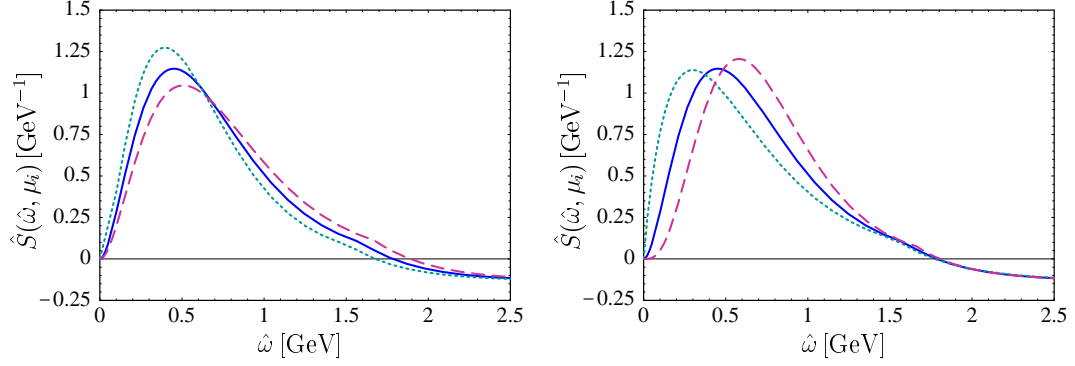


Figure 4.5: Various models for the shape function at the intermediate scale $\mu_i = 1.5 \text{ GeV}$, corresponding to different parameter settings in Table 4.1. Left: Functions S1, S5, S9 with “correlated” parameter variations. Right: Functions S3, S5, S7 with “anti-correlated” parameter variations.

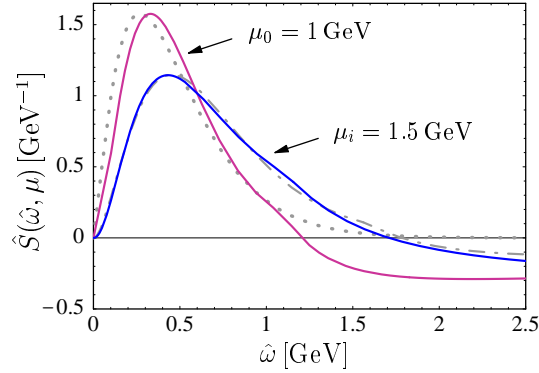


Figure 4.6: Renormalization-group evolution of a model shape function from a low scale μ_0 (sharply peaked solid curve) to the intermediate scale μ_i (broad solid curve). See the text for an explanation of the other curves.

to shape-function effects we use all nine shape functions S1 through S9 in Table 4.1, thus varying the parameters $\bar{\Lambda}(\mu_i, \mu_i)$ and $\mu_\pi^2(\mu_i, \mu_i)$ independently. This is quite conservative because we neglect any possible correlation between them. For each physical quantity we draw three bands corresponding to the three different values of $\bar{\Lambda}$. The width of each band reflects the sensitivity to the variation of μ_π^2 .

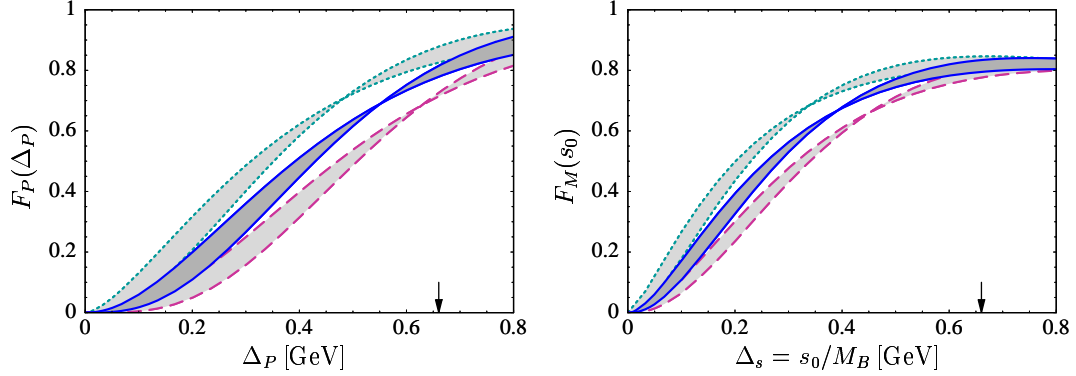


Figure 4.7: Fraction of $\bar{B} \rightarrow X_u l^- \bar{\nu}$ events with hadronic light-cone momentum $P_+ \leq \Delta_P$ (left), and fraction of events with hadronic invariant mass $s_H \leq s_0$ (right). In each plot, the three bands correspond to the values $\bar{\Lambda} = 0.63$ GeV (solid curves), 0.70 GeV (dashed curves), and 0.56 GeV (dotted curves). Their width reflects the sensitivity to the value of μ_π^2 varied in the range between 0.20 and 0.34 GeV². The arrow indicates the point at which the charm background starts.

The following predictions for spectra and rate fractions refer to the leading term in the heavy-quark expansion. We note that our calculations would break down if the cuts on kinematic variables were taken to be too strict, because then the spectra would become dominated by hadronic resonance effects. Parametrically, this happens when the quantities Δ_P , Δ_s , or Δ_E become of order $\Lambda_{\text{QCD}}^2/M_B \sim 50$ MeV. On the other hand, taking too large values of Δ_P , Δ_s , or Δ_E such that they are not of $O(\Lambda_{\text{QCD}})$ anymore invalidates the collinear expansion.

In Fig. 4.7 we show predictions for the fractions of all $\bar{B} \rightarrow X_u l^- \bar{\nu}$ events with hadronic light-cone momentum $P_+ \leq \Delta_P$, and with hadronic invariant mass squared $s_H \leq s_0$. Recall that, for $\Delta_P = \Delta_s = s_0/M_B$, the hadronic invariant mass fraction F_M differs from the fraction F_P by the contribution of the events in the triangular region above the dashed line in Fig. 4.2. Comparing the two plots, we observe that this additional contribution is predicted to be very small.

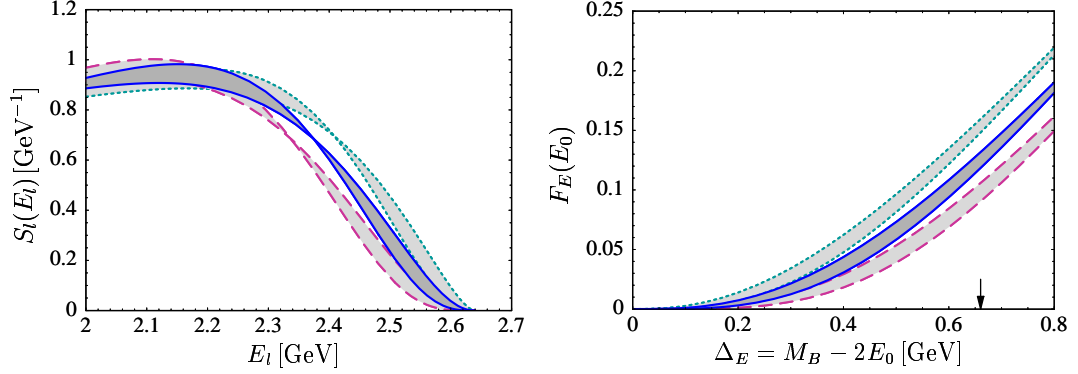


Figure 4.8: Charged-lepton energy spectrum in the region near the kinematic endpoint (left), and fraction of events with charged-lepton energy $E_l \geq E_0$ (right). The meaning of the bands and the arrow is the same as in Fig. 4.7.

(Note that for large values of Δ_s we even find a negative contribution to the rate from the triangle region for some choices of the shape function. This feature is unphysical and should be fixed by the inclusion of power corrections to our leading-order predictions.) The arrows on the horizontal axes indicate the points $\Delta_{P,s} = M_D^2/M_B$, beyond which final states containing charm hadrons are kinematically allowed. With this choice of the cut, both rate fractions capture about 80% of all events. While it is well known that a hadronic invariant mass cut $\sqrt{s_H} \leq M_D$ provides a very efficient discrimination against charm background [71, 72, 73], here we observe that the same is true for a cut on the P_+ variable.

Our results for the lepton energy spectrum $S_l(E_l) = (1/\Gamma_{\text{tot}}) (d\Gamma/dE_l)$, and for the event fraction with a cut $E_l \geq E_0$, are displayed in Fig. 4.8. The right-hand plot shows that with $\Delta_E = M_D^2/M_B$ only about 10–15% of all events are retained, and the theoretical calculation is very sensitive to shape-function effects. Such a cut is therefore much less efficient than the cuts on s_H or P_+ . As a result, an extraction of $|V_{ub}|$ from the charged-lepton endpoint region is theoretically disfavored.

The shape-function sensitivity is rather small for values of Δ_P and Δ_s near the charm threshold. This is to some extent a consequence of our improved knowledge of the shape-function parameters. On the other hand we observe an interesting “focus mechanism” in that the three bands in the P_+ and the hadronic invariant mass (but *not* for the charged lepton energy) event fractions start to converge near the charm threshold. This is due to a subtle interplay between the jet function and the shape function, which is explained in more detail in [36]. The important observation is that the leading logarithm in the jet function has the opposite sign as found in a straightforward partonic calculation. The convergence is somewhat surprising since the model shape functions at the intermediate scale μ_i are rather different for values around $\hat{\omega} \sim \Lambda_{\text{QCD}}$ (see Fig. 4.5), and the argument that they share the same norm is not applicable yet. One way of thinking about this mechanism is to notice that the broadening of the shape function under renormalization-group evolution from a low scale up to the intermediate scale (Fig. 4.6) is a perturbative effect, which should not lead to an increased shape-function sensitivity. Because the convolution of the shape function with the jet and hard functions is independent of the scale μ_i , the broadening of the shape function must be compensated by perturbative logarithms in the jet function.

This focus effect did not take place in earlier studies such as [37, 71, 72, 73, 74], where parton-model spectra were convoluted with a primordial shape function. As mentioned earlier, in the parton model the leading Sudakov logarithm comes with the opposite (negative) sign, hence causing an anti-focus effect of the radiative corrections. This also explains why our prediction for the hadronic invariant mass fraction F_M exhibits a smaller shape-function sensitivity than what has been found in most previous analyses.

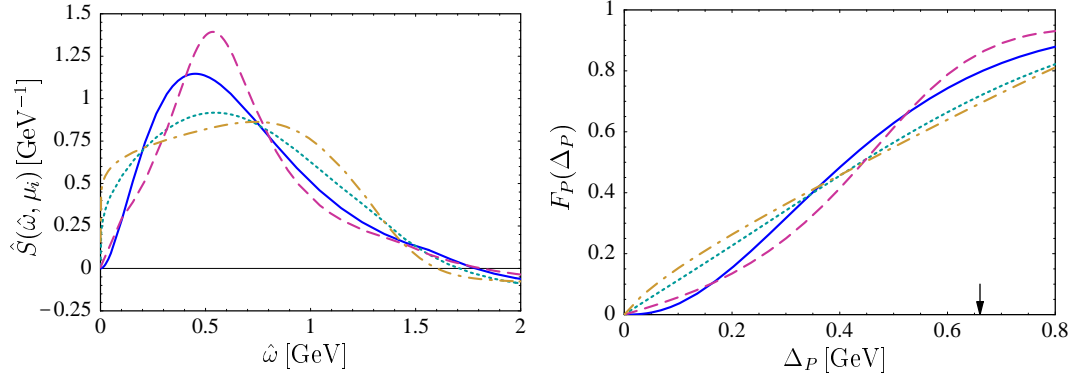


Figure 4.9: Left: Four examples of shape functions with identical normalization and first two moments, corresponding to $\bar{\Lambda}(\mu_i, \mu_i) = 0.63 \text{ GeV}$ and $\mu_\pi^2(\mu_i, \mu_i) = 0.27 \text{ GeV}^2$, but different functional form. Right: Corresponding results for the event fraction $F_P(\Delta_P)$.

We shall stress again that the knowledge of the first few moments does not determine the functional form of the shape function. In order to demonstrate this, we have constructed several functions of different functional forms, but with identical norm, first, and second moment. To correctly account for the asymptotic behaviour $\hat{\omega} \gg \Lambda_{\text{QCD}}$, we have added the second term in (4.61) to each of the functions. They are shown on the left-hand side of Fig. 4.9. All of them are thus allowed by the required moment analysis and could be considered as variations of the shape function. Some of the curves are admittedly extreme, given the fact that the $b \rightarrow s\gamma$ photon spectrum is identical to the shape function at tree level. Any information about the shape function can be used to eliminate some of these curves. At present, however, we stress that using the model shape functions S1 through S9 sample even the variation of the functional form, as the event fraction predictions on the right-hand side of Fig. 4.9 fall within the bands studied earlier.

We summarize our phenomenological results in Table 4.2, in which we compare the shape-function sensitivity (which is the only uncertainty considered here) of

Table 4.2: Comparison of different theoretical methods using inclusive B -decay rates to extract the CKM matrix element $|V_{ub}|$. The error on the efficiency represents the sensitivity to the shape function only. All results refer to the leading term in the heavy-quark expansion.

| Method | Cut | Efficiency |
|---|--|---------------------------|
| Hadronic invariant mass | $s_H \leq M_D^2$ | $(81.4^{+3.2}_{-3.7})\%$ |
| | $s_H \leq (1.7 \text{ GeV})^2$ | $(78.2^{+4.9}_{-5.2})\%$ |
| | $s_H \leq (1.55 \text{ GeV})^2$ | $(72.7^{+6.4}_{-6.3})\%$ |
| Hadronic P_+ | $P_+ \leq \frac{M_D^2}{M_B} = 0.66 \text{ GeV}$ | $(79.6^{+8.2}_{-8.2})\%$ |
| | $P_+ \leq 0.55 \text{ GeV}$ | $(69.0^{+9.7}_{-12.1})\%$ |
| Charged-lepton energy | $E_l \geq \frac{M_B^2 - M_D^2}{2M_B} = 2.31 \text{ GeV}$ | $(12.5^{+3.4}_{-3.5})\%$ |
| | $E_l \geq 2.2 \text{ GeV}$ | $(22.2^{+3.2}_{-3.6})\%$ |
| Combined (s_H, q^2) cuts [tree level only] | $s_H \leq M_D^2, \quad q^2 \geq 0$ | $(74.6^{+5.1}_{-5.1})\%$ |
| | $s_H \leq M_D^2, \quad q^2 \geq 6 \text{ GeV}^2$ | $(45.7^{+1.8}_{-2.0})\%$ |
| | $s_H \leq (1.7 \text{ GeV})^2, \quad q^2 \geq 8 \text{ GeV}^2$ | $(33.4^{+1.6}_{-1.8})\%$ |

different kinematic cuts. The first two blocks of entry address the high-efficiency methods of cutting on the hadronic invariant mass s_H and the variable P_+ . The efficiency for the optimal cut $s_H \leq M_D^2$ is remarkably precise; however, due to detector resolution effects it is necessary to relax that cut somewhat. We state

results for upper limits on the invariant mass of 1.7 GeV and 1.55 GeV, for which the relative uncertainty increases somewhat. Cutting on P_+ introduces a relative uncertainty of order 10%, which is still acceptable. Again, experimental constraints might force us to move away from the optimal cut. However, it might be possible to stay closer to the optimal cut due to the apparent “buffer zone”. (We will discuss the charm background in much more detail below.)

The only low-efficiency method we discuss is a cut on the charged-lepton energy. Unlike the previous two methods, such a measurement does not require the reconstruction of the neutrino in the decay $\bar{B} \rightarrow X_u l^- \bar{\nu}$, and is therefore favored by experiment. However, due to the low efficiency one has to worry also about other theoretical uncertainties like weak annihilation effects [75], which are expected to contribute less than 3% to the total rate and can therefore be safely neglected in high-efficiency methods like the s_H and P_+ cuts. Our prediction for the lepton energy event fractions are significantly larger than have been reported in the past, and suggest that the extracted value of $|V_{ub}|$ needs to be corrected to lower values.

For completeness, we also give results for some combined cuts on hadronic and leptonic invariant mass, which have been briefly discussed in Section 4.4.4. Contrary to the other cases, these numbers refer to the tree-level approximation and so should be taken with caution. For reference, we quote again the (tree-level) result for the pure hadronic invariant mass cut, which differs significantly from the corresponding result including radiative corrections. While the additional cut on leptonic q^2 reduces the shape-function sensitivity, it comes along with a strong reduction of the efficiency. For instance, the combined cut $\sqrt{s_H} \leq 1.7 \text{ GeV}$ and $q^2 \geq 8 \text{ GeV}^2$ employed in a recent analysis of the Belle Collaboration [76] has an efficiency of about 33% (at tree level and leading order in Λ_{QCD}/m_b), which is much

smaller than the efficiency of the pure hadronic invariant mass cut $\sqrt{s_H} \leq 1.7 \text{ GeV}$. However, the sensitivity to shape-function effects is only slightly better in the case of the combined cut.

4.7 Charm background

One of the main advantages of the P_+ spectrum over the hadronic-mass spectrum is a better control of the charm background. In order to study this in more detail, we investigate the OPE prediction for the normalized $\hat{p}_+ = n \cdot p/m_b$ spectrum in $\bar{B} \rightarrow X_c l^- \bar{\nu}$ decays,

$$\frac{1}{\Gamma_c} \frac{d\Gamma_c}{d\hat{p}_+} = \frac{2(\varrho - \hat{p}_+^2)^2}{f(\varrho) \hat{p}_+^5} \left[\hat{p}_+^3 (3 - 2\hat{p}_+) + \varrho \hat{p}_+ (3 - 8\hat{p}_+ + 3\hat{p}_+^2) - \varrho^2 (2 - 3\hat{p}_+) \right], \quad (4.64)$$

where $\varrho \leq \hat{p}_+ \leq \sqrt{\varrho}$ with $\varrho = (m_c/m_b)^2$, and

$$f(\varrho) = 1 - 8\varrho + 8\varrho^3 - \varrho^4 - 12\varrho^2 \ln \varrho. \quad (4.65)$$

We only include tree-level contributions from dimension-3 operators [77].

In this approximation, inclusive charm events are located along a single line $p_+ p_- = m_c^2$, or in terms of the hadronic variables $(P_+ - \bar{\Lambda})(P_- - \bar{\Lambda}) = (M_D - \bar{\Lambda})^2$, in Fig. 4.2. This line starts at the tip of the triangle $P_+ = P_- = M_D$ and extends to the right while always staying above the solid line $s_H = M_D^2$. Because $\mathcal{O}(\alpha_s)$ corrections redistribute these events into the light-gray segment above that line, the integral over the spectrum in (4.64) serves as an upper bound on the inclusive charm background. In the same approximation, the hadronic mass distribution is given by

$$\frac{1}{\Gamma_c} \frac{d\Gamma_c}{d\hat{s}} = \frac{2}{f(\varrho) \varepsilon} \sqrt{z^2 - 4\varrho} \left[z(3 - 2z) - \varrho(4 - 3z) \right], \quad \text{with } z = \frac{\hat{s} - \varepsilon^2 - \varrho}{\varepsilon}. \quad (4.66)$$

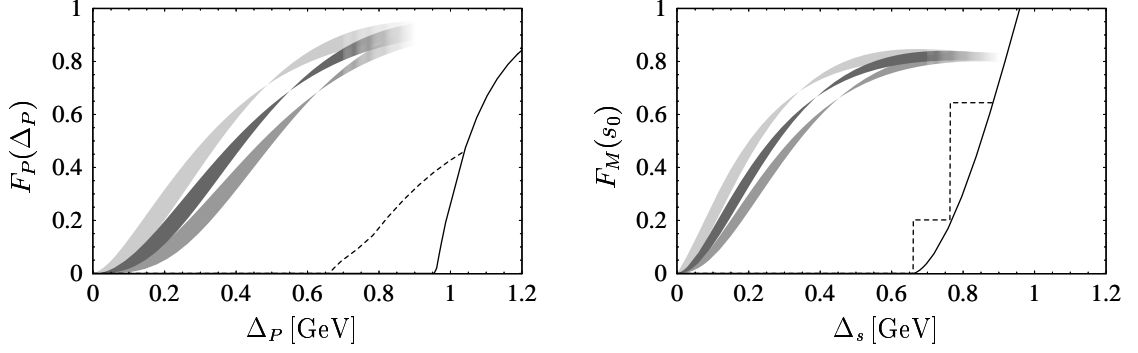


Figure 4.10: Fraction of $\bar{B} \rightarrow X_u l^- \nu$ events with $P_+ \leq \Delta_P$ (left) and $s_H \leq s_0$ (right). The bands are identical to the ones in Fig. 4.7. The curves represent the background from inclusive $\bar{B} \rightarrow X_c l^- \bar{\nu}$ (solid) and exclusive $\bar{B} \rightarrow D^{(*)} l^- \bar{\nu}$ decays (dashed), normalized to the total inclusive semileptonic charm rate.

Here, $\hat{s} = s_H/m_b^2$, $\varepsilon = \bar{\Lambda}/m_b$, and phase space is such that $(\sqrt{\varrho} + \varepsilon)^2 \leq \hat{s} \leq (\varrho + \varepsilon)(1 + \varepsilon)$.

The results for the event fractions F_P and F_M are summarized in Fig. 4.10. The bands show the inclusive $\bar{B} \rightarrow X_u l^- \bar{\nu}$ event fractions for different shape-function models as discussed above, while the solid lines give predictions for the inclusive $\bar{B} \rightarrow X_c l^- \bar{\nu}$ background spectra as obtained from equations. (4.64) and (4.66). The latter are normalized to their total decay rate Γ_c , which is about 60 times larger than Γ_u . In the case of the fraction F_M , the inclusive charm background starts right at the threshold $\Delta_s = (m_c + \bar{\Lambda})^2/M_B \simeq M_D^2/M_B$. In the case of the F_P event fraction, on the contrary, the inclusive charm background starts at a value $\Delta_P = m_c^2/m_b + \bar{\Lambda} \approx 0.96 \text{ GeV}$, which is significantly larger than the value $\Delta_P = M_D^2/M_B \approx 0.66 \text{ GeV}$ above which final states containing charm mesons are kinematically allowed. This is a consequence of the fact that there is a gap between the charm threshold $s_H = M_D^2$ and the start of the inclusive $b \rightarrow c$ events. In reality this gap is filled by exclusive modes containing the hadronic final states

D , D^* , or $D\pi$, $D\pi\pi$. The exclusive contributions to the hadronic P_+ spectrum from $\bar{B} \rightarrow D^{(*)}l^-\bar{\nu}$ decays are

$$\begin{aligned} \frac{d\Gamma_D}{dP_+} &= \frac{G_F^2 |V_{cb}|^2 M_B^5}{48\pi^3} \frac{(1+r)^2 r^3}{P_+} (w^2 - 1)^2 |\mathcal{F}_D(w)|^2, \\ \frac{d\Gamma_{D^*}}{dP_+} &= \frac{G_F^2 |V_{cb}|^2 M_B^5}{48\pi^3} \frac{(1-r_*)^2 r_*^3}{P_+} (w^2 - 1)(w + 1)^2 \\ &\quad \times \left(1 + \frac{4w}{w+1} \frac{1 - 2wr_* + r_*^2}{(1-r_*)^2} \right) |\mathcal{F}_{D^*}(w)|^2, \end{aligned} \quad (4.67)$$

where $M_{D^{(*)}}^2/M_B \leq P_+ \leq M_{D^{(*)}}$ and $r_{(*)} = M_{D^{(*)}}/M_B$. The recoil variable $w = v \cdot v'$ is given by $M_{D^{(*)}}^2 + P_+^2 = 2w M_{D^{(*)}} P_+$. The corresponding contributions to the hadronic mass spectrum are given by

$$\frac{d\Gamma_{D^{(*)}}}{ds_H} = \Gamma_{D^{(*)}} \cdot \delta(s_H - M_{D^{(*)}}^2). \quad (4.68)$$

The exclusive contributions to the event fractions are given by the dashed lines in Fig. 4.10. To obtain these curves we have used an ansatz for the form factors $\mathcal{F}_{D^{(*)}}(w)$ that is consistent with experimental data on the recoil spectra and branching fractions. The fact that these exclusive modes are very well understood should help to model the background. The smooth onset of the $D^{(*)}$ background is a direct consequence of the fact that the ideal P_+ cut touches the charm region at only a single point in phase space (see Fig. 4.2). On the contrary, the region of phase space when applying the s_H cut borders the background along the curve separating the light- and dark-shaded regions, which leads to a step increment in the event fraction F_M . As a consequence, one needs to move away from the ideal cut $s_H = M_D^2$ because of smearing effects due to experimental resolution. It is our hope that it will be possible to stay closer to the ideal cut when performing a P_+ analysis. In this case, both the P_+ and s_H discrimination methods lead to comparable efficiencies and shape-function uncertainties, as emphasized earlier in the discussion after Table 4.2.

4.8 Theoretical accuracy of a $|V_{ub}|$ measurement

As a final remark to this long Chapter, let us comment on the applicability of the theoretical framework developed in this work. According to Fig. 4.2 most of the $\bar{B} \rightarrow X_u l^- \bar{\nu}$ events are located in the shape-function region of large P_- and small to moderate P_+ , in which a systematic heavy-quark expansion using SCET power counting is valid. It allows us to calculate inclusive decay rates integrated over domains $\Delta P_- \sim M_B$ and $\Delta P_+ \ll M_B$, where typically $\Delta P_+ \sim \Lambda_{\text{QCD}}$. (In the examples above, $\Delta P_+ = \Delta_E$, Δ_P , or Δ_s , respectively.) While the corresponding predictions for decay spectra and event fractions are sufficient to analyze experimental data over most of the phase space relevant to measurements of the CKM matrix element $|V_{ub}|$, it would be of interest to extend the validity of the theoretical description outside the shape-function region. Let us in the following paragraph comment on such a prospect.

In the case where $\Delta P_- \sim \Delta P_+ \sim M_B$ are both large, the decay spectra can be computed using a local operator product expansion. The resulting prediction for the normalized $\bar{B} \rightarrow X_u l^- \bar{\nu}$ spectrum in the variable $\hat{p}_+ = p_+/m_b = (P_+ - \bar{\Lambda})/m_b$ reads [77]

$$\begin{aligned} \frac{1}{\Gamma_u} \frac{d\Gamma_u}{d\hat{p}_+} &= \left(1 - \frac{463}{36} \frac{\alpha_s}{3\pi}\right) \delta(\hat{p}_+) \\ &+ \frac{\alpha_s}{3\pi} \left[-4 \left(\frac{\ln \hat{p}_+}{\hat{p}_+} \right)_* - \frac{26}{3} \left(\frac{1}{\hat{p}_+} \right)_* + h(\hat{p}_+) \right] \\ &- \left(\frac{17\lambda_1}{18m_b^2} + \frac{3\lambda_2}{2m_b^2} \right) \delta'(\hat{p}_+) - \frac{\lambda_1}{6m_b^2} \delta''(\hat{p}_+), \end{aligned} \quad (4.69)$$

where $0 \leq \hat{p}_+ \leq 1$, and

$$\begin{aligned} h(p) &= \frac{158}{9} + \frac{407p}{18} - \frac{367p^2}{6} + \frac{118p^3}{3} - \frac{100p^4}{9} + \frac{11p^5}{6} - \frac{7p^6}{18} \\ &- \left(\frac{4}{3} - \frac{46p}{3} - 6p^2 + \frac{16p^3}{3} \right) \ln p - 4p^2(3-2p) \ln^2 p. \end{aligned} \quad (4.70)$$

We include the contributions from dimension-3 operators at $O(\alpha_s)$ and those from dimension-5 operators (whose matrix elements are proportional to the heavy-quark effective theory parameters $\lambda_{1,2}$) at tree level, using [55, 37]. If the \hat{p}_+ spectrum is integrated without a weight function, the tree-level power corrections from dimension-5 operators vanish. This is in accordance with the fact that subleading shape functions have zero norm at tree level [59].

An interesting question is whether it will be possible to match the Factorization approach for the shape-function region $\Delta P_+ \sim \Lambda_{\text{QCD}}$ and the OPE approach for $\Delta P_+ \sim M_B$ in some intermediate region of ΔP_+ values that are numerically (but not parametrically) large compared with Λ_{QCD} . If the two predictions were to agree in an overlap region, this could be used to construct a theoretical description of inclusive $\bar{B} \rightarrow X_u l^- \bar{\nu}$ decay distributions that is valid over the entire phase space. While this is an exciting prospect, we note that performing a systematic operator product expansion in the overlap region is far from trivial. For a hierarchy of scales $\Lambda_{\text{QCD}} \ll \Delta_P \ll m_b$ we obtain with $\bar{\Delta} = \Delta_P - \bar{\Lambda}$

$$F_P(\Delta_P) = 1 - \frac{\alpha_s}{3\pi} \left[\left(2 \ln^2 \frac{m_b}{\bar{\Delta}} - \frac{26}{3} \ln \frac{m_b}{\bar{\Delta}} + \frac{463}{36} \right) - \frac{\bar{\Delta}}{m_b} \left(\frac{4}{3} \ln \frac{m_b}{\bar{\Delta}} + \frac{170}{9} \right) \right] + \dots \quad (4.71)$$

For $\Delta_P \sim 1 \text{ GeV}$, the power correction in the second term leads to an enhancement of the fraction F_P by 5–10%. This is of similar magnitude as tree-level estimates of (zero-norm) subleading shape-function effects on the E_l and s_H spectra [60, 78].

The leading-order term in Eq. (4.71) can also be obtained from Eq. (4.43) by taking the limit $\Delta_P \gg \Lambda_{\text{QCD}}$. Interestingly, such an analysis uncovers that in this kinematic range there is an enhanced class of power corrections of the form $(\Lambda_{\text{QCD}}/\bar{\Delta})^n$ with $n \geq 2$, which arise first at $O(\alpha_s)$ (see also [79]). The leading corrections to the expression above are given by

$$\delta F_P(\Delta_P) = -\frac{\alpha_s}{3\pi} \left(2 \ln \frac{m_b}{\bar{\Delta}} - \frac{7}{3} \right) \frac{\mu_\pi^2}{3\bar{\Delta}^2}. \quad (4.72)$$

It follows that for sufficiently large $\bar{\Delta}$ the event fraction can be expressed as a double expansion in $\bar{\Delta}/m_b$ and $\Lambda_{\text{QCD}}/\bar{\Delta}$. Because of the hierarchy of scales $\Delta P_+^2 \ll \Delta P_+ M_B \ll M_B^2$, again a two-step procedure is in order. (An example of such an approach can be found in [80].) Such a multi-scale OPE is non-trivial and left for future work. For now we merely note the estimate that subleading power contributions to the event fraction F_P result to about 10%.

We are now ready to give an in-depth look at the prospect of determining $|V_{ub}|$ from a P_+ measurement. A list of relevant theoretical uncertainties to the fraction of events with the optimal cut $P_+ \leq M_D^2/M_B$ is [77]

$$F_P = (79.6 \pm 10.8 \pm 6.2 \pm 8.0)\%, \quad (4.73)$$

where the errors represent the sensitivity to the shape function (as stated in Table 4.2), an estimate of $\mathcal{O}(\alpha_s^2)$ contributions, and power corrections, respectively. The uncertainty due to our ignorance of the shape function is obtained in part by varying the parameters $\bar{\Lambda} = M_B - m_b$ (4.59) and μ_π^2 (4.60) in the shape-function scheme, determining its first two moments ($\delta F_P = {}^{+8.2}_{-8.1}\%$). Furthermore we vary the functional form of S , as depicted in Fig. 4.9 ($\delta F_P = {}^{+6.3}_{-7.8}\%$).

Higher-order perturbative effects are estimated by studying the dependence on the matching scales μ_i and μ_h , varied in the ranges $1.25 \text{ GeV} \leq \mu_i \leq 1.75 \text{ GeV}$ ($\delta F_P = {}^{+4.7}_{-4.9}\%$) and $m_b/\sqrt{2} \leq \mu_h \leq \sqrt{2} m_b$ ($\delta F_P = {}^{+4.1}_{-3.9}\%$).

Every single error stated here can be reduced in the future within the systematic framework presented in [36, 77]. A proper treatment of subleading power corrections in the shape-function region is now feasible. In addition, the leading shape-function uncertainty can be eliminated using model-independent relations

such as (4.57). Finally the perturbative uncertainty can be reduced by computing the $\mathcal{O}(\alpha_s^2)$ corrections to equation (4.43).

The CKM-matrix element $|V_{ub}|$ can be extracted by comparing a measurement of the partial rate $\Gamma_u(P_+ \leq \Delta_P)$ with a theoretical prediction for the product of the event fraction F_P and the total inclusive $\bar{B} \rightarrow X_u l^- \bar{\nu}$ rate. The resulting theoretical uncertainty on $|V_{ub}|$ up to date is

$$\frac{\delta|V_{ub}|}{|V_{ub}|} = (\pm 7 \pm 4 \pm 5 \pm 4)\%, \quad (4.74)$$

where the last error comes from the uncertainty in the total rate (4.38) as can be found in [81, 82]. Because of the large efficiency of the P_+ cut, weak annihilation effects [75] have an influence on $|V_{ub}|$ of less than 2% and can be safely neglected.

QCD-Factorization has provided us with a powerful method to systematically improve the calculation of event distributions in the shape-function region. The hadronic P_+ spectrum is the preferred application of this framework, and the possibility of a high-precision determination of $|V_{ub}|$ through a measurement of the partial decay rate $\Gamma_u(P_+ \leq \Delta_P)$ is an exciting prospect.

CHAPTER 5

EXCLUSIVE RADIATIVE DECAYS

The radiative, semileptonic decay $B \rightarrow \gamma l \nu$ provides a clean environment for the study of soft-collinear interactions [83]. This process is particularly simple in that no hadrons appear in the final state. Yet, there is sensitivity to the light-cone structure of the B meson, probed by the coupling of the high-energy photon to the soft spectator quark inside the heavy meson. Therefore this decay mode serves as an opportunity to learn QCD factorization and Sudakov resummation for exclusive decays in a realistic environment [24]. Our main goal is to establish the QCD factorization formula [84]

$$\mathcal{A}(B^- \rightarrow \gamma l^- \bar{\nu}_l) \propto M_B f_B Q_u \int_0^\infty dl_+ \frac{\phi_+^B(l_+, \mu)}{l_+} T(l_+, E_\gamma, m_b, \mu) \quad (5.1)$$

to all orders in perturbation theory and at leading power in Λ_{QCD}/m_b . Here $Q_u = \frac{2}{3}$ is the electric charge of the up-quark (in units of e), and $T = 1 + O(\alpha_s)$ is a perturbative hard-scattering kernel. The decay constant f_B and the LCDA ϕ_+^B have been introduced in Section 3.1. The physics underlying the factorization formula is that a high-energy photon coupling to the soft constituents of the B -meson produces quantum fluctuations far off their mass shell, which can be integrated out in a low-energy effective theory. As usual we choose the photon direction to be the z -direction, so that the photon momentum is $E_\gamma n$. The two transverse polarization states of the photon can be expressed in terms of the basis vectors $\varepsilon_\mp^\mu = \frac{1}{\sqrt{2}}(0, 1, \mp i, 0)$, which correspond to left- and right-circular polarization, respectively.

The new complication, as compared to the factorization of the *inclusive* case of the last Chapter, is that the final theory is SCET_{II}. Radiative decays are partic-

ularly simple in that the only external “collinear” particle is the electromagnetic photon, which carries a purely light-like momentum. Therefore the only hadronic constituents present are the HQET fields describing quarks and gluons of the B meson. While it is possible to match QCD directly onto this theory, a two-step matching procedure through the intermediate theory SCET_I has the advantage of integrating out off-shell propagators of order E_γ^2 and $E_\gamma\Lambda_{\text{QCD}}$ in separate steps. This suggests a second stage of “perturbative” factorization [14, 85, 86], which we will establish below. It says that the hard-scattering kernel itself can be factorized as

$$T(l_+, E_\gamma, m_b, \mu) = H\left(\frac{2E_\gamma}{\mu}, \frac{2E_\gamma}{m_b}\right) \cdot J\left(\frac{2E_\gamma l_+}{\mu^2}\right). \quad (5.2)$$

Factorization holds as long as the photon is energetic in the B -meson rest frame, meaning that E_γ is of the order of the b -quark mass. In order to prove the factorization formula (5.1) one needs to show that [4]:

1. The decay amplitude can be expanded in powers of transverse momenta (i.e. in powers of $\Lambda_{\text{QCD}}/E_\gamma$) and, at leading order, can be expressed in terms of a convolution with the B -meson LCDA as shown in (5.1).
2. After subtraction of infra-red contributions corresponding to the B -meson decay constant and LCDA, the leading contributions to the amplitude come from hard internal lines, i.e., the hard-scattering kernel T is free of infra-red singularities to all orders in perturbation theory.
3. The convolution integral of the hard-scattering kernel with the LCDA is convergent.
4. Non-valence Fock states do not give rise to leading contributions.

In the next Section we will address all of the above points.

5.1 Proof of factorization

In the full theory, the hadronic part of the decay amplitude for $B \rightarrow \gamma l \nu$ is given by the time-ordered product of a weak, flavor-changing current $(\bar{u}b)_{V-A}$ and the electro-magnetic currents $(\bar{u}\mathcal{A}^{(\text{em})}u)$, $(\bar{b}\mathcal{A}^{(\text{em})}b)$. However, attachments of the energetic photon field to the massive b -quark line leads to power suppression [14], and so at leading power in SCET, the time-ordered product is matched onto trilocal operators of the form

$$\begin{aligned} & \sum_{q=u,b} ie Q_q \int d^4x T \left\{ [\bar{u}\gamma^\mu(1-\gamma_5)b](0), [\bar{q}\mathcal{A}^{(\text{em})}q](x) \right\} \\ \rightarrow & \sum_i \int ds dt \tilde{C}_i(t, s, v \cdot q, m_b, \mu) \bar{Q}_s(tn) \mathcal{A}_{c\perp}^{(\text{em})}(s\bar{n}) \frac{\not{n}}{2} \Gamma_i \mathcal{H}(0). \end{aligned} \quad (5.3)$$

The Wilson coefficients \tilde{C}_i receive contributions only from Feynman diagrams where the photon is emitted from the spectator quark line. The fields $\mathcal{A}^{(\text{em})}$ and Q_s are located at the appropriate light cones, which reflects the SCET scaling properties of the photon and spectator-quark momenta. $\mathcal{A}_{c\perp}^{(\text{em})}$ is the electromagnetic analog of the gauge-invariant collinear gluon field defined in (2.60). To first order in e we have

$$\mathcal{A}_{c\perp}^{(\text{em})}(0) = \bar{n}_\alpha \gamma_\mu^\perp \int_{-\infty}^0 dw e F^{\alpha\mu}(w\bar{n}). \quad (5.4)$$

The Feynman rule for this object is simply $e \not{\varepsilon}^*$, where ε is the photon polarization vector. Finally, from the fact that the leptonic weak current $\bar{\nu}\gamma_\mu(1-\gamma_5)l$ is conserved (in the limit where the lepton mass is neglected) it follows that the relevant Dirac structures Γ_i in (5.3) can be taken as $\Gamma_1 = \gamma^\mu(1-\gamma_5)$ and $\Gamma_2 = n^\mu(1+\gamma_5)$.

We can use the trace formalism in HQET and the definition of the B -meson LCDA (3.1). Performing the relevant traces, we find that at leading power in Λ_{QCD}/m_b the decay amplitude vanishes if the photon has right-circular polariza-

tion, while for a photon with left-circular polarization it is given by

$$\begin{aligned} \mathcal{A}(B^- \rightarrow \gamma_L l^- \bar{\nu}_l) &= \frac{iG_F}{\sqrt{2}} V_{ub} e \bar{u}_l(p_l) \not{\epsilon}_-^* (1 - \gamma_5) v_\nu(p_\nu) \\ &\times \sqrt{M_B} F(\mu) \int d\omega C_1(\omega, \bar{n} \cdot q, v \cdot q, m_b, \mu) \phi_+^B(\omega, \mu) + \dots, \end{aligned} \quad (5.5)$$

where the dots represent power-suppressed contributions. Only the SCET operator with Dirac structure $\Gamma_1 = \gamma^\mu(1 - \gamma_5)$ contributes to the decay amplitude. C_1 denotes the Fourier transform of \tilde{C}_1 , and we will continue the discussion in momentum space. The HQET parameter $F(\mu)$ is related to the physical B -meson decay constant through $f_B \sqrt{M_B} = K_F(m_b, \mu) F(\mu) [1 + O(\Lambda_{\text{QCD}}/m_b)]$, where at next-to-leading order in the $\overline{\text{MS}}$ scheme [87]

$$K_F(m_b, \mu) = 1 + \frac{C_F \alpha_s(\mu)}{4\pi} \left(3 \ln \frac{m_b}{\mu} - 2 \right). \quad (5.6)$$

Combining these results, it follows that the terms shown in the second line of (5.5) equal those on the right-hand side of the factorization formula (5.1) if we identify the hard-scattering kernel as

$$\frac{Q_u}{l_+} T(l_+, E_\gamma, m_b, \mu) = K_F^{-1}(m_b, \mu) C_1(l_+, 2E_\gamma, E_\gamma, m_b, \mu). \quad (5.7)$$

We thus completed the first of the four steps to prove factorization.

We proceed to prove the convergence of the convolution integral in (5.1). The key ingredient here is to note that the invariance of SCET operators under reparameterization of the light-cone basis vectors n and \bar{n} can be used to deduce the dependence of Wilson coefficient functions on the separation t between the component fields of non-local operators. This has been discussed in some detail in Section 2.5. In our case, invariance of the operators in (5.3) under the type III rescaling transformation $n^\mu \rightarrow n^\mu/\alpha$ and $\bar{n}^\mu \rightarrow \alpha \bar{n}^\mu$ (with fixed v) implies that

$$\tilde{C}_i(t, \bar{n} \cdot q, v \cdot q, m_b, \mu) = \tilde{C}_i(\alpha t, \alpha \bar{n} \cdot q, v \cdot q, m_b, \mu) \quad (5.8)$$

to all orders in perturbation theory. In other words, the variables t and $\bar{n} \cdot q$ can only appear in the combination $\bar{n} \cdot q/t$, but not individually. The coefficient functions can be factorized further by noting that $v \cdot q$ and m_b enter only through hard or hard-collinear interactions with the heavy quark. The corresponding modes can be integrated out in a first matching step onto SCET_I and lead to a functions $\tilde{H}_i(v \cdot q, m_b, \mu)$, which depend on the Dirac structure of the weak current containing the heavy quark. The non-localities of the component fields in (5.3) result from the coupling of hard-collinear fields to the soft spectator quark in the B meson. These effects live on scales of order $m_b \Lambda_{\text{QCD}}$ and can be integrated out in a second step by matching onto SCET_{II}, leading to the function $\tilde{J}(t, \bar{n} \cdot q, \mu)$. Therefore

$$\tilde{C}_i(t, \bar{n} \cdot q, v \cdot q, m_b, \mu) = \tilde{H}_i\left(\frac{2v \cdot q}{\mu}, x_\gamma\right) \cdot \tilde{J}\left(\frac{\bar{n} \cdot q}{\mu^2 t}\right), \quad (5.9)$$

where $x_\gamma \equiv 2v \cdot q/m_b = 2E_\gamma/m_b$ is a scaling variable of order 1. The corresponding result for the hard-scattering kernel obtained after Fourier transformation has the form shown in (5.2) if we identify

$$\begin{aligned} H\left(\frac{2v \cdot q}{\mu}, x_\gamma\right) &= K_F^{-1}(m_b, \mu) \tilde{H}_1\left(\frac{2v \cdot q}{\mu}, x_\gamma\right), \\ \frac{Q_u}{l_+} J\left(\frac{\bar{n} \cdot q l_+}{\mu^2}\right) &= \int dt e^{-il_+ t} \tilde{J}\left(\frac{\bar{n} \cdot q}{\mu^2 t}\right), \end{aligned} \quad (5.10)$$

where $\bar{n} \cdot q l_+ = 2E_\gamma l_+$. Since the dependence of the coefficient functions on the renormalization scale is logarithmic, it follows that to all orders in perturbation theory the Wilson coefficients in (5.9) scale like $\tilde{C}_i \sim 1$ modulo logarithms. (Correspondingly, the kernel scales like $T \sim 1$ modulo logarithms.) The convergence of the convolution integral in (5.5) in the infra-red region $t \rightarrow \infty$, corresponding to the region $l_+ \rightarrow 0$ in the factorization formula (5.1), then follows to all orders in perturbation theory as long as the integral converges at tree level. Because the B meson has a spatial size of order $1/\Lambda_{\text{QCD}}$ due to confinement, the bilocal matrix

element must vanish faster than $1/t$ for $t \gg 1/\Lambda_{\text{QCD}}$, and so the integral over t is convergent. The absence of endpoint divergences in convolution integrals is connected to the question of whether the infra-red degrees of freedom have correctly been identified in the effective theory [86]. If we had found endpoint singularities as $l_+ \rightarrow 0$, we would have to include other, long-distance modes in the construction of the effective theory (such as soft-collinear modes), thus invalidating factorization.

Finally, let us demonstrate that more complicated projections onto the B meson involving higher Fock states or transverse parton momenta only enter at subleading order in power counting. This can be seen from the rules for constructing SCET operators out of gauge-invariant building blocks (2.60), as explained in [14]. Projections sensitive to transverse momentum components contain extra derivatives and so are power suppressed. Projections corresponding to non-valence Fock states contain insertions of the soft gluon field \mathcal{A}_s . Since \mathcal{A}_s scales like Λ_{QCD} , such insertions lead to power suppression unless this field is integrated over a domain of extension $1/\Lambda_{\text{QCD}}$. Reparameterization invariance dictates that such an insertion must be accompanied by a factor of n in the numerator, or by a factor of \bar{n} in the denominator. The only possibility to insert a factor of n in the numerator is through the combination $\int du \not{n} \mathcal{A}_{s\perp}(un)$, which vanishes since the operator already contains a factor of \not{n} , and $n^2 = 0$. For a factor of \bar{n} in the denominator, we might insert e. g. $\bar{n}/(u \bar{n} \cdot q)$, which scales like Λ_{QCD}/m_b . One might object that an insertion of $v \cdot n$ invalidates the above argument. However, such a factor cannot appear as interactions with the heavy quark can be integrated out before the final matching onto SCET_{II} . This also ensures that the factor \not{n} must appear to the left of Γ_i . We have thus completed the proof of the factorization formula (5.1) to all orders in perturbation theory, and at leading power in Λ_{QCD}/m_b .

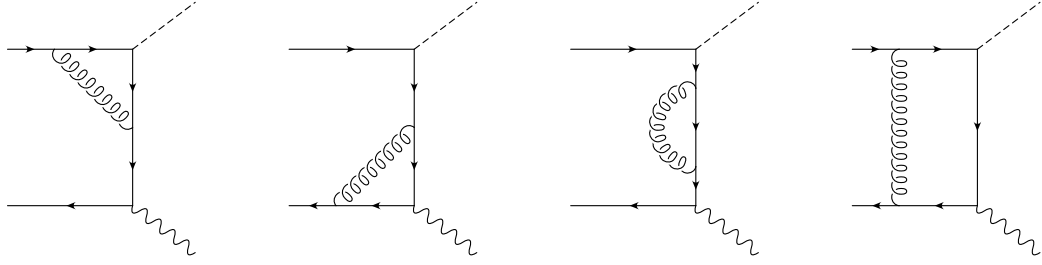


Figure 5.1: One-loop diagrams in the full theory contributing at leading power to the $B \rightarrow \gamma l \nu$ decay amplitude.

5.2 Calculation of the hard-scattering kernel

We derive the Wilson coefficients \tilde{C}_i in (5.3) by performing a matching calculation using on-shell external quark states. To this end, we assign incoming momenta $m_b v$ to the heavy quark and l with $l^2 = 0$ to the soft light quark. By construction, the Wilson coefficients are independent of the nature of the external states. Soft gluon emission from the external quark lines cancel in the matching. However, emissions from the internal quark propagator in the full theory lead to the build-up of the finite-length Wilson line $S_s(tn)S_s^\dagger(0)$. To one-loop precision, the coefficient functions can be written in the form [24]

$$C_i = \frac{Q_u}{l_+} \left[\delta_{i1} + \frac{C_F \alpha_s(\mu)}{4\pi} c_i + \dots \right]. \quad (5.11)$$

To obtain the NLO corrections c_i we evaluate the one-loop contributions to the decay amplitude in the full theory and in SCET. The relevant diagrams in full QCD are shown in Fig. 5.1. In addition there is a contribution from the wave-function renormalization for the heavy quark. Using anti-commuting γ_5 (and, as usual, working in $4 - 2\epsilon$ dimensions), the diagrams evaluate to the following bare expressions:

$$A_1^{\text{QCD}} = \left(\frac{m_b}{\mu} \right)^{-2\epsilon} \left[-\frac{1}{2\epsilon} - \ln^2 \frac{2E_\gamma l_+}{m_b^2} - 2(1 - 2 \log x_\gamma) \ln \frac{2E_\gamma l_+}{m_b^2} \right]$$

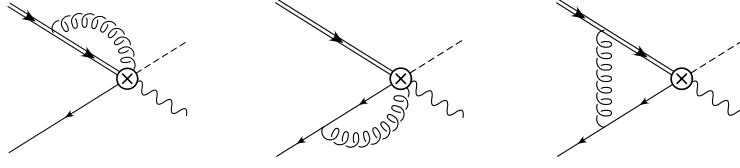


Figure 5.2: One-loop diagrams in the effective theory whose contribution to the amplitude needs to be subtracted in the calculation of the Wilson coefficients.

$$\begin{aligned}
 & -4 \ln^2 x_\gamma + \frac{2-3x_\gamma}{1-x_\gamma} \ln x_\gamma - 2L_2(1-x_\gamma) - 2 - \pi^2 \Big] \\
 & + \left(\frac{2E_\gamma l_+}{\mu^2} \right)^{-\epsilon} \left(-\frac{2}{\epsilon} - 5 \right) + \left(\frac{-2v \cdot l}{\mu} \right)^{-2\epsilon} \left[-\frac{1}{\epsilon^2} + \ln^2 \left(\frac{-2v \cdot l}{l_+} \right) + \frac{7\pi^2}{12} \right], \\
 A_2^{\text{QCD}} &= \left(\frac{m_b}{\mu} \right)^{-2\epsilon} \frac{x_\gamma \ln x_\gamma}{1-x_\gamma}.
 \end{aligned} \tag{5.12}$$

The expression A_1^{QCD} receives contributions from the weak current vertex correction and wave-function renormalization for the heavy quark (first bracket), the electro-magnetic vertex correction and self-energy insertion (second term), and the box diagram (last term, which depends on $v \cdot l$ in addition to l_+ [24, 83]).

On the low-energy theory side we evaluate the one-loop order contributions, which can be written as $C_{1\text{-loop}} \otimes \langle O_{\text{SCET}} \rangle_{\text{tree}} + C_{\text{tree}} \otimes \langle O_{\text{SCET}} \rangle_{1\text{-loop}}$. The relevant diagrams are shown in Fig. 5.2 and evaluate to

$$\begin{aligned}
 A_1^{\text{SCET}} &= \left(\frac{l_+}{\mu} \right)^{-2\epsilon} \left(-\frac{1}{\epsilon^2} - \frac{3\pi^2}{4} \right) \\
 &+ \left(\frac{-2v \cdot l}{\mu} \right)^{-2\epsilon} \left[-\frac{1}{\epsilon^2} + \ln^2 \left(\frac{-2v \cdot l}{l_+} \right) + \frac{7\pi^2}{12} \right], \\
 A_2^{\text{SCET}} &= 0.
 \end{aligned} \tag{5.13}$$

The first term in the expression for A_1^{SCET} corresponds to the first two diagrams in the figure, while the second term is obtained from the last graph. Note that this is precisely the same contribution as obtained from the box diagram in the full theory. The difference of the expressions given in (5.12) and (5.13) determines

the NLO contributions to the Wilson coefficient functions. Subtracting the pole terms in the $\overline{\text{MS}}$ scheme, we find

$$\begin{aligned}
c_1 &= -2 \ln^2 \frac{m_b}{\mu} + (5 - 4 \ln x_\gamma) \ln \frac{m_b}{\mu} + \ln^2 \frac{2E_\gamma l_+}{\mu^2} - 2 \ln^2 x_\gamma \\
&\quad + \frac{2 - 3x_\gamma}{1 - x_\gamma} \ln x_\gamma - 2L_2(1 - x_\gamma) - 7 - \frac{\pi^2}{4}, \\
c_2 &= \frac{x_\gamma \ln x_\gamma}{1 - x_\gamma}.
\end{aligned} \tag{5.14}$$

These results for the Wilson coefficients agree with the expressions for the hard-scattering kernel given in [84] and [85], apart from the contribution of the HQET decay constant $F(\mu)$. (The authors of [84] and [85] assumed an unconventional m_b -dependent definition of the B -meson LCDA.) After simplification we find the hard-scattering kernel at next-to-leading order [24]

$$\begin{aligned}
T(l_+, E_\gamma, m_b, \mu) &= 1 + \frac{C_F \alpha_s(\mu)}{4\pi} \left[-2 \ln^2 \frac{2E_\gamma}{\mu} + 2 \ln \frac{2E_\gamma}{\mu} + \ln^2 \frac{2E_\gamma l_+}{\mu^2} \right. \\
&\quad \left. - \frac{x_\gamma \ln x_\gamma}{1 - x_\gamma} - 2L_2(1 - x_\gamma) - 5 - \frac{\pi^2}{4} \right]. \tag{5.15}
\end{aligned}$$

The renormalization-scale dependence is, despite appearance, entirely given in the form $2 \ln^2(\mu/l_+) - 2 \ln(\mu/l_+) + \mu$ -independent terms, which can therefore be canceled against the μ dependence of the LCDA $\phi_+^B(l_+, \mu)$ under the convolution integral in (5.1). The remaining large logarithms $\ln(E_\gamma/l_+)$ need to be resummed to all orders in perturbation theory. This can be done by stating the result in the above form, factorizing the kernel into a hard function H (which contains $\ln(2E_\gamma/\mu)$) and a jet function J (which contains $\ln(2E_\gamma l_+/\mu^2)$), and solving their RGEs.

5.3 Resummation of large logarithms

The hard-scattering kernel T can be systematically factorized when performing the matching calculation in two separate steps $\text{QCD} \rightarrow \text{SCET}_I \rightarrow \text{SCET}_{II}$ [14, 85, 86].

The hard function $H(2E_\gamma/\mu, x_\gamma)$ arises when integrating out off-shell fluctuations of order m_b , while fluctuations around the intermediate scale $m_b\Lambda_{\text{QCD}}$ lead to the jet function. Since the scale $m_b\Lambda_{\text{QCD}}$ arises only from a scalar product of a soft momentum with a collinear momentum, one can simply set $l = 0$ in our previous matching calculation, which ensures that only the hard fluctuations are integrated out [24]. After the function H has been identified in this way, the jet function is constructed using that $J = T/H$. Specifically, for $l = 0$ the second and third diagrams in Fig. 5.1 involve scaleless integrals that vanish in dimensional regularization, while the box graph can readily be shown to vanish at leading power. The remaining contribution from the weak vertex correction and wave-function renormalization for the heavy quark yields

$$A_1^{\text{QCD}}\Big|_{l=0} = \left(\frac{m_b}{\mu}\right)^{-2\epsilon} \left[-\frac{1}{\epsilon^2} - \frac{5}{2\epsilon} + \frac{2\ln x_\gamma}{\epsilon} - 2\ln^2 x_\gamma + \frac{2-3x_\gamma}{1-x_\gamma} \ln x_\gamma - 2L_2(1-x_\gamma) - 6 - \frac{\pi^2}{12} \right], \quad (5.16)$$

while the expression for $A_2^{\text{QCD}}\Big|_{l=0}$ is the same as that for A_2^{QCD} given in (5.12). After $\overline{\text{MS}}$ subtractions the above result determines the hard function \tilde{H}_1 defined in (5.8). Using the first relation in (5.10), it then follows that

$$H\left(\frac{2E_\gamma}{\mu}, x_\gamma\right) = 1 + \frac{C_F \alpha_s(\mu)}{4\pi} \left[-2\ln^2 \frac{2E_\gamma}{\mu} + 2\ln \frac{2E_\gamma}{\mu} - \frac{x_\gamma \ln x_\gamma}{1-x_\gamma} - 2L_2(1-x_\gamma) - 4 - \frac{\pi^2}{12} \right]. \quad (5.17)$$

The knowledge of the hard-scattering kernel (5.15) and the above result for the hard function yields the jet function, which is thus given by

$$J\left(\frac{2E_\gamma l_+}{\mu^2}\right) = 1 + \frac{C_F \alpha_s(\mu)}{4\pi} \left(\ln^2 \frac{2E_\gamma l_+}{\mu^2} - 1 - \frac{\pi^2}{6} \right). \quad (5.18)$$

In order to proceed we need RG equations obeyed by the various coefficient functions. The fact that the decay amplitude in (5.1) is scale independent links

the scale dependence of the hard-scattering kernel to the evolution of the LCDA $\phi_+^B(\omega, \mu)$ [33]. By analyzing the renormalization properties of this function, as we have done in Section 3.1.1, it follows that the hard-scattering kernel satisfies the integro-differential equation (for $l_+ > 0$) [30]¹

$$\frac{d}{d \ln \mu} T(l_+, \mu) = \left[\Gamma_{\text{cusp}}(\alpha_s) \ln \frac{\mu}{l_+} + \gamma(\alpha_s) \right] T(l_+, \mu) + \int_0^\infty d\omega l_+ \Gamma(\omega, l_+, \alpha_s) T(\omega, \mu), \quad (5.19)$$

where Γ_{cusp} is the universal cusp anomalous dimension familiar from the theory of the renormalization of Wilson loops [25] and $\Gamma(\omega, \omega', \alpha_s)$ is given in equation (3.12). From the functional forms of the hard and jet functions given above, it follows that the hard component and the jet function obey the RG equations

$$\frac{d}{d \ln \mu} H(\mu) = \left[-\Gamma_{\text{cusp}}(\alpha_s) \ln \frac{\mu}{2E_\gamma} + \gamma(\alpha_s) - \gamma'(\alpha_s) \right] H(\mu), \quad (5.20)$$

$$\begin{aligned} \frac{d}{d \ln \mu} J(l_+, \mu) &= \left[\Gamma_{\text{cusp}}(\alpha_s) \ln \frac{\mu^2}{2E_\gamma l_+} + \gamma'(\alpha_s) \right] J(l_+, \mu) \\ &+ \int_0^\infty d\omega l_+ \Gamma(\omega, l_+, \alpha_s) J(\omega, \mu). \end{aligned} \quad (5.21)$$

The anomalous dimensions γ and γ' do not have a simple geometric interpretation and must be determined by explicit calculation, unlike is the case for the cusp anomalous dimension [51]. From (5.17) and (5.18) we find

$$\gamma(\alpha_s) = -2C_F \frac{\alpha_s}{4\pi} + O(\alpha_s^2), \quad \gamma'(\alpha_s) = O(\alpha_s^2). \quad (5.22)$$

We now discuss the general solution of the evolution equations (5.19) and (5.20). Exact solutions can be written down analogously to the discussion in Section 3.1.1. We define the dimensionless function

$$\mathcal{F}(a, \alpha_s) = \int d\omega \omega' \Gamma(\omega, \omega', \alpha_s) \left(\frac{\omega}{\omega'} \right)^{-a}. \quad (5.23)$$

¹For simplicity of notation, we omit the arguments E_γ , m_b , and x_γ for the remainder of this section. Also, unless otherwise indicated, $\alpha_s \equiv \alpha_s(\mu)$.

This is the same function as previously defined in (3.14), and for convenience we restate the one-loop order result (3.21) as

$$\mathcal{F}^{(1)}(a, \alpha_s) = \Gamma_{\text{cusp}}^{(1)}(\alpha_s) \left[\psi(1+a) + \psi(1-a) + 2\gamma_E \right], \quad (5.24)$$

where $\psi(z)$ is the logarithmic derivative of the Euler Γ -function. We start by solving the first equation in (5.20) with the initial condition for $H(\mu_h)$ evaluated at a high scale $\mu_h \sim m_b$, for which it does not contain large logarithms. We then evolve the function $H(\mu)$ down to an intermediate scale $\mu_i \sim \sqrt{m_b \Lambda_{\text{QCD}}}$ and multiply it by the result $J(l_+, \mu_i)$ for the jet function, which at the intermediate scale is free of large logarithms and can be written in the general form $J(l_+, \mu_i) \equiv \mathcal{J}[\alpha_s(\mu_i), \ln(2E_\gamma l_+/\mu_i^2)]$. This determines the kernel $T(l_+, \mu_i)$ at the intermediate scale. Finally, we solve (5.19) and compute the evolution down to a low-energy scale $\mu \sim \text{few} \times \Lambda_{\text{QCD}}$. The exact solution is given by

$$T(l_+, \mu) = H(\mu_h) \mathcal{J}[\alpha_s(\mu_i), \nabla_\eta] \exp U(l_+, \mu, \mu_i, \mu_h, \eta) \Big|_{\eta=0}, \quad (5.25)$$

where the notation $\mathcal{J}[\alpha_s(\mu_i), \nabla_\eta]$ means that one must replace each logarithm of the ratio $2E_\gamma l_+/\mu_i^2$ by a derivative with respect to an auxiliary parameter η . The evolution function U is given by [24]

$$\begin{aligned} U(l_+, \mu, \mu_i, \mu_h, \eta) = & \int_{\alpha_s(\mu_h)}^{\alpha_s(\mu_i)} d\alpha \frac{\Gamma_{\text{cusp}}(\alpha)}{\beta(\alpha)} \left[\ln \frac{2E_\gamma}{\mu_h} - \int_{\alpha_s(\mu_h)}^{\alpha} \frac{d\alpha'}{\beta(\alpha')} \right] - \int_{\alpha_s(\mu_h)}^{\alpha_s(\mu_i)} d\alpha \frac{\gamma'(\alpha)}{\beta(\alpha)} \\ & - \int_{\alpha_s(\mu_i)}^{\alpha_s(\mu)} d\alpha \frac{\Gamma_{\text{cusp}}(\alpha)}{\beta(\alpha)} \left[\ln \frac{l_+}{\mu} + \int_{\alpha}^{\alpha_s(\mu)} \frac{d\alpha'}{\beta(\alpha')} \right] + \int_{\alpha_s(\mu_h)}^{\alpha_s(\mu)} d\alpha \frac{\gamma(\alpha)}{\beta(\alpha)} \\ & + \eta \ln \frac{2E_\gamma l_+}{\mu_i^2} + \int_{\alpha_s(\mu_i)}^{\alpha_s(\mu)} \frac{d\alpha}{\beta(\alpha)} \mathcal{F} \left(-\eta + \int_{\alpha_s(\mu_i)}^{\alpha} d\alpha' \frac{\Gamma_{\text{cusp}}(\alpha')}{\beta(\alpha')}, \alpha \right). \end{aligned} \quad (5.26)$$

Given this exact result, it is straightforward to derive approximate expressions for the kernel at given orders in RG-improved perturbation theory, by using perturbative expansions of the anomalous dimensions and β -function to the required order. Unfortunately, controlling terms of $O(\alpha_s)$ in the evolution function U would require knowledge of all anomalous dimensions at two-loop order, which at present is lacking. (It also requires the cusp anomalous dimension to three loops, which has been computed only recently [57].) We will, however, control the dependence on the variables l_+ and E_γ to $O(\alpha_s)$. As usual, we write

$$\beta(\alpha_s) = -2\alpha_s \sum_{n=0}^{\infty} \beta_n \left(\frac{\alpha_s}{4\pi}\right)^{n+1}, \quad \Gamma_{\text{cusp}}(\alpha_s) = \sum_{n=0}^{\infty} \Gamma_n \left(\frac{\alpha_s}{4\pi}\right)^{n+1}, \quad (5.27)$$

and similarly for the anomalous dimensions γ and γ' . The relevant expansion coefficients are listed in (4.31) and (4.31), and we also find $\gamma_0 = -2C_F$, $\gamma'_0 = 0$. Defining the ratios $r_1 = \alpha_s(\mu_i)/\alpha_s(\mu_h)$ and $r_2 = \alpha_s(\mu)/\alpha_s(\mu_i)$, we obtain our final result [24]

$$\begin{aligned} T(l_+, \mu) &= e^{U_0(\mu, \mu_i, \mu_h)} \left(\frac{l_+}{\mu}\right)^{c \ln r_2} \left(\frac{2E_\gamma}{\mu_h}\right)^{-c \ln r_1} \\ &\times \left\{ 1 + \frac{C_F \alpha_s(\mu_h)}{4\pi} \left[-2 \ln^2 \frac{2E_\gamma}{\mu_h} + 2 \ln \frac{2E_\gamma}{\mu_h} - \frac{x_\gamma \ln x_\gamma}{1-x_\gamma} - 2L_2(1-x_\gamma) - 4 - \frac{\pi^2}{12} \right] \right. \\ &\quad + \frac{C_F \alpha_s(\mu_i)}{4\pi} \left[\left(\ln \frac{2E_\gamma l_+}{\mu_i^2} - \psi(1+c \ln r_2) - \psi(1-c \ln r_2) - 2\gamma_E \right)^2 \right. \\ &\quad \left. \left. - \psi'(1+c \ln r_2) + \psi'(1-c \ln r_2) - 1 - \frac{\pi^2}{6} \right] \right. \\ &\quad \left. + \frac{\Gamma_0}{2\beta_0} \left(\frac{\Gamma_1}{\Gamma_0} - \frac{\beta_1}{\beta_0} \right) \left[\frac{\alpha_s(\mu) - \alpha_s(\mu_i)}{4\pi} \ln \frac{l_+}{\mu} - \frac{\alpha_s(\mu_i) - \alpha_s(\mu_h)}{4\pi} \ln \frac{2E_\gamma}{\mu_h} \right] \right\}, \end{aligned} \quad (5.28)$$

where $c = \Gamma_0/2\beta_0$, and

$$\begin{aligned} U_0(\mu, \mu_i, \mu_h) &= \frac{\Gamma_0}{4\beta_0^2} \left\{ (1 - \ln r_1) \frac{4\pi}{\alpha_s(\mu_h)} + (1 + \ln r_2) \frac{4\pi}{\alpha_s(\mu)} - \frac{8\pi}{\alpha_s(\mu_i)} \right. \\ &\quad \left. + \frac{\beta_1}{2\beta_0} (\ln^2 r_1 + \ln^2 r_2) + \left(\frac{\Gamma_1}{\Gamma_0} - \frac{\beta_1}{\beta_0} \right) \left(\ln \frac{r_1}{r_2} + 2 - r_1 - \frac{1}{r_2} \right) \right\} \end{aligned}$$

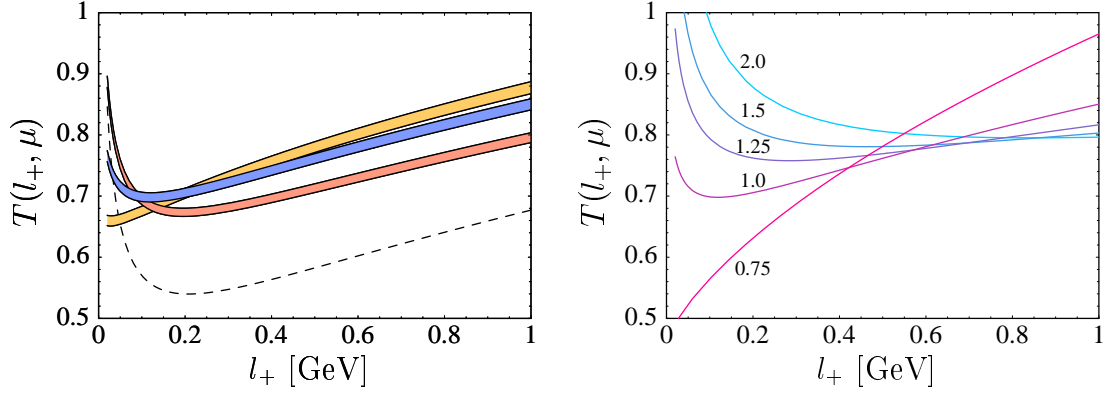


Figure 5.3: RG-improved predictions for the hard-scattering kernel at maximum photon energy. *Left:* Results at $\mu = 1$ GeV. The bands refer to different values of the intermediate matching scale: $\mu_i^2 = \Lambda_h m_b$ (center), $2\Lambda_h m_b$ (top), $0.5\Lambda_h m_b$ (bottom). Their width reflects the sensitivity to the high-energy matching scale μ_h^2 , varied between $2m_b^2$ and $0.5m_b^2$. The dashed line shows the result obtained at one-loop order. *Right:* Dependence of the kernel on the renormalization scale μ , varied between 0.75 GeV and 2.0 GeV as indicated on the curves.

$$-\frac{\gamma_0}{2\beta_0} \ln(r_1 r_2) - \ln \frac{\Gamma(1 + c \ln r_2)}{\Gamma(1 - c \ln r_2)} - 2\gamma_E c \ln r_2 + O(\alpha_s) \quad (5.29)$$

corresponds to the function U evaluated with $\eta = 0$, $l_+ = \mu$, and $2E_\gamma = \mu_h$.

Finally, let us study the effects from Sudakov resummation numerically. In the left-hand plot in Fig. 5.3 we compare the resummed hard-scattering kernel (5.28) with the expanded $O(\alpha_s)$ approximation (5.15). The effect is maximized by setting the photon energy to its highest possible value of $E_\gamma = m_b/2$. (Numerically, we work with the pole mass $m_b = 4.8$ GeV.) The renormalization scale μ is chosen to 1 GeV, which is a reasonable scale for the B -meson LCDA. The matching scales μ_h and μ_i are varied around their “natural” choices $\mu_h = 2E_\gamma$ and $\mu_i = \sqrt{2E_\gamma \Lambda_h}$, where $\Lambda_h = 0.5$ GeV serves as a typical hadronic scale, are taken as default values. We use the two-loop running coupling normalized at $\alpha_s(m_b) = 0.22$ and set $n_f = 4$ for the number of light quark flavors. (For simplicity, we do not match onto a

three-flavor theory even for low renormalization scales.) We find that resummation effects decrease the magnitude of the radiative corrections, i.e., the resummed kernel is closer to the tree-level value ($T = 1$) than the one-loop result. The fact that after Sudakov resummation the radiative corrections are moderate in magnitude persists even for asymptotically large b -quark masses. For instance, setting $m_b = 50 \text{ GeV}$ we find after resummation $T(l_+, \mu) = 0.74$ at $l_+ = \mu = 1 \text{ GeV}$. (Fixed-order perturbation theory breaks down for such large values of the quark mass. From (5.15) we would obtain $T(l_+, \mu) = 0.08$ with these parameter values.) The figure also exhibits that our results are stable under variation of the two matching scales. Varying μ_i^2 and μ_h^2 by factors of 2 changes the result for the kernel by less than 10%. This suggests that the unknown NNLO corrections to the function U_0 in (5.29) are perhaps not very important.

The scale dependence of the resummed expression for the kernel is illustrated in the right-hand plot in Fig. 5.3, which shows the functional dependence of $T(l_+, \mu)$ for maximal photon energy and several values of μ . The matching scales are set to their default values $\mu_h = m_b = 4.8 \text{ GeV}$ and $\mu_i = \sqrt{\Lambda_h m_b} \simeq 1.55 \text{ GeV}$. We observe a significant scale dependence of the kernel, especially as one lowers μ below the intermediate scale μ_i . In other words, the second stage of running (for $\mu < \mu_i$) is numerically significant.

CHAPTER 6

EXCLUSIVE SEMILEPTONIC DECAYS

6.1 Heavy-to-light form factors at large recoil

Transitions of the B meson into light pseudoscalar or vector mesons are parameterized in terms of scalar functions, called form factors, that depend only on the Lorentz invariant quantity q^2 , where $q = p_B - p_M$ is the momentum transfer from the B -meson onto the light final meson M . They are defined by the following Lorentz decompositions of bilinear quark current matrix elements:

$$\langle P(p_P) | \bar{q} \gamma^\mu b | \bar{B}(p_B) \rangle = f_+(q^2) \left[p_B^\mu + p_P^\mu - \frac{M_B^2 - m_P^2}{q^2} q^\mu \right] + f_0(q^2) \frac{M_B^2 - m_P^2}{q^2} q^\mu, \quad (6.1)$$

$$\langle P(p_P) | \bar{q} \sigma^{\mu\nu} q_\nu b | \bar{B}(p_B) \rangle = \frac{if_T(q^2)}{M_B + m_P} [q^2(p_B^\mu + p_P^\mu) - (M_B^2 - m_P^2) q^\mu], \quad (6.2)$$

where m_P the mass of the pseudoscalar meson. The relevant form factors for B decays into vector mesons with polarization vector ε and mass m_V are defined as

$$\langle V(p_V, \varepsilon^*) | \bar{q} \gamma^\mu b | \bar{B}(p_B) \rangle = \frac{2iV(q^2)}{M_B + m_V} \epsilon^{\mu\nu\rho\sigma} \varepsilon_\nu^* p_{V\rho} p_{B\sigma}, \quad (6.3)$$

$$\langle V(p_V, \varepsilon^*) | \bar{q} \gamma^\mu \gamma_5 b | \bar{B}(p_B) \rangle = 2m_V A_0(q^2) \frac{\varepsilon^* \cdot q}{q^2} q^\mu + \quad (6.4)$$

$$(M_B + m_V) A_1(q^2) \left[\varepsilon^{*\mu} - \frac{\varepsilon^* \cdot q}{q^2} q^\mu \right] - A_2(q^2) \frac{\varepsilon^* \cdot q}{M_B + m_V} \left[p_B^\mu + p_V^\mu - \frac{M_B^2 - m_V^2}{q^2} q^\mu \right],$$

$$\langle V(p_V, \varepsilon^*) | \bar{q} \sigma^{\mu\nu} q_\nu b | \bar{B}(p_B) \rangle = 2T_1(q^2) \epsilon^{\mu\nu\rho\sigma} \varepsilon_\nu^* p_{B\rho} p_{V\sigma}, \quad (6.5)$$

$$\begin{aligned} \langle V(p_V, \varepsilon^*) | \bar{q} \sigma^{\mu\nu} \gamma_5 q_\nu b | \bar{B}(p_B) \rangle &= (-i) T_2(q^2) [(M_B^2 - m_V^2) \varepsilon^{*\mu} - (\varepsilon^* \cdot q) (p_B^\mu + p_V^\mu)] \\ &+ (-i) T_3(q^2) (\varepsilon^* \cdot q) \left[q^\mu - \frac{q^2}{M_B^2 - m_V^2} (p_B^\mu + p_V^\mu) \right]. \end{aligned} \quad (6.6)$$

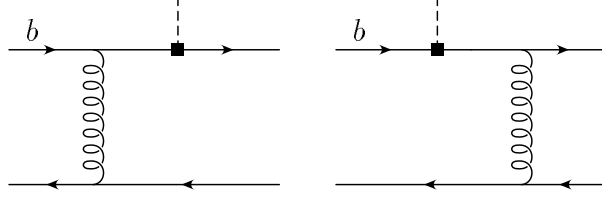


Figure 6.1: Gluon exchange contributions to heavy-to-light form factors. The flavor-changing current is denoted by a dashed line. The lines to the left belong to the B meson, and those to the right belong to the light meson M .

In many applications form factors are needed near zero momentum transfer ($q^2 \approx 0$), corresponding to a kinematic situation in which a flavor-changing weak current turns a heavy B meson at rest into a highly energetic light meson. Such heavy-to-light transitions at high recoil are suppressed in QCD by inverse powers of the heavy-quark mass m_b . (This is contrary to the case of heavy-to-heavy transitions such as $B \rightarrow D$, which are unsuppressed in the heavy-quark limit [2].) The challenge in understanding the physics of these processes is to describe properly the transformation of the soft constituents of the B meson into the fast moving, collinear constituents of the energetic light meson in the final state. At lowest order in perturbation theory this transformation can be achieved by the exchange of a gluon, as depicted in Fig. 6.1. Naive power counting suggests that the nature of the gluons is hard-collinear, as they turn the soft spectator quark into a collinear constituent of the final meson of energy

$$E = \frac{M_B^2 + m_M^2 - q^2}{2M_B} \gg \Lambda_{\text{QCD}} \quad (6.7)$$

in the B -meson rest frame. The meson momentum can be written as $p_M^\mu = En^\mu + O(m_M^2/4E)$, which is nearly light-like. We assume that the partons inside the light meson carry a significant fraction of its total energy, and that the light constituents of the B meson carry soft momenta of order Λ_{QCD} . This justifies to describe the

process using SCET. It would then appear that the form factor is governed by a sufficiently hard gluon exchange, which can be dealt with using perturbative methods for hard exclusive QCD processes [29, 88]. The situation is, as we shall see below, not quite that simple [12, 14, 27, 86, 89, 90, 91]. Leading contributions to the form factors also arise when the exchanged gluon is of long-distance nature, leading to the “soft overlap” (also called Feynman mechanism). As an example, a straightforward calculation of the two diagrams in Fig. 6.1 yields

$$A = -g^2 \left(\Gamma \frac{m_b(1 + \not{v}) - x_2 E \not{n}}{4m_b E^2 x_2^2 n \cdot l} \gamma_\mu + \gamma_\mu \frac{E \not{n} - \not{l}}{4E^2 x_2 (n \cdot l)^2} \Gamma \right) t_a * \gamma^\mu t_a + \dots, \quad (6.8)$$

where $v^\mu = (1, 0, 0, 0)$ is the B -meson velocity, Γ denotes the Dirac structure of the flavor-changing current, the $*$ product means that the two factors must be sandwiched between quark spinors, and the dots represent power-suppressed terms. Here we assigned an incoming momentum l to the light spectator anti-quark, and the outgoing parton momenta p_1 and p_2 collinear to the light-meson momentum are parameterized as

$$p_1^\mu = x_1 E n^\mu + p_\perp^\mu + \dots, \quad p_2^\mu = x_2 E n^\mu - p_\perp^\mu + \dots, \quad (6.9)$$

with the fractions x_1, x_2 , subject to the constraint $x_1 + x_2 = 1$. Assuming that l is soft and x_i of order unity one finds that the amplitude (6.8) scales like $1/(E^2 \Lambda_{\text{QCD}})$. However, assuming linear distributions for $x_2 \rightarrow 0$ and $n \cdot l \rightarrow 0$ in the endpoints of the meson LCDAs, it is evident from (6.8) that the corresponding convolution integrals for a hadronic amplitude diverge at these endpoints [92, 93]. In other words, the above analysis breaks down for such momentum configurations because the gluon exchange is no longer of short-distance nature. Naively, form factors would then be dominated by this soft overlap, since it is not suppressed by a perturbative coupling constant α_s . However, it has sometimes been argued that

the summation of large Sudakov logarithms associated with the soft gluon exchange mechanism may lead to a strong suppression of the soft overlap term, essentially reinstating the perturbative nature of the form factors (see, e.g., [94, 95, 96]). The assumption of a short-distance nature of heavy-to-light form factors at large recoil is the basis of the pQCD approach to exclusive hadronic B decays [97], which is often considered a competitor to QCD factorization. Leaving aside some conceptual problems associated with this treatment [98], the issue of Sudakov logarithms is an intricate one, because contributions to the form factors can arise from several different energy scales. Besides the hard scale $E \sim M_B$ and the hadronic scale Λ_{QCD} , interactions between soft and collinear partons involve the intermediate hard-collinear scale of order $\sqrt{E\Lambda_{\text{QCD}}}$. To settle the question of Sudakov suppression of the soft overlap contribution is one of the main motivations for our work [89].

6.2 Spin-symmetry and factorization

The discussion of heavy-to-light form factors in the heavy-quark limit $E \gg \Lambda_{\text{QCD}}$ can be summarized by the factorization formula [90]

$$f_i^{B \rightarrow M}(E) = C_i(E, \mu_I) \zeta_M(\mu_I, E) + T_i(E, \sqrt{E\Lambda_{\text{QCD}}}, \mu) \otimes \phi_B(\mu) \otimes \phi_M(\mu) + \dots, \quad (6.10)$$

where the dots represent terms that are of subleading order in Λ_{QCD}/E . C_i and T_i are calculable short-distance coefficient functions, ϕ_B and ϕ_M denote the leading-order LCDAs of the B meson and the light meson M , and the \otimes products imply convolutions over light-cone momentum fractions. The functions ζ_M denote universal form factors that only depend on the nature of the light final-state meson but not on the Lorentz structure of the currents whose matrix elements define the

various form factors. The first term in the factorization formula therefore implies spin-symmetry relations between different form factors, which were first derived in [18] by considering the large-energy limit of QCD. The second term in (6.10), which arises from hard-collinear gluon exchange, breaks these symmetry relations [90].

The arguments E and $\sqrt{E\Lambda_{\text{QCD}}}$ in the short-distance coefficients C_i and T_i are representative for any of the hard or hard-collinear scales in the problem, respectively. The form of the factorization formula shown in (6.10) assumes that the factorization scale μ_I in the first term is chosen to lie between the hard scale E and the hard-collinear scale $\sqrt{E\Lambda_{\text{QCD}}}$, whereas the scale μ in the second term is chosen to lie below the hard-collinear scale. The Wilson coefficients C_i receive contributions at tree level, whereas the hard-scattering kernels T_i start at first order in $\alpha_s(\sqrt{E\Lambda_{\text{QCD}}})$. Naively, one would conclude that the spin-symmetry preserving term provides the leading contribution to the form factors in the heavy-quark limit. Only then the notion of an approximate spin symmetry would be justified. However, the situation is more complicated because as written in (6.10) the universal functions $\zeta_M(\mu_I, E)$ still depend on the short-distance scale $\sqrt{E\Lambda_{\text{QCD}}}$; in fact, their E -dependence remains unspecified. We will see how this dependence on the large energy enters the amplitudes when our technology of scale separation is applied. The matching of a QCD form factor onto matrix elements in SCET is done in two steps: $\text{QCD} \rightarrow \text{SCET}_I \rightarrow \text{SCET}_{II}$. In close analogy to the previous applications discussed in this thesis, hard fluctuations with virtualities on the scale $E \sim M_B$ are integrated out in a first step, while in the second step hard-collinear modes with virtualities of order $\sqrt{E\Lambda_{\text{QCD}}}$ are removed. Both steps of this matching are understood for the hard-scattering term in the factorization formula, for which the

kernels T_i can be factorized as [86]

$$T_i(E, \sqrt{E\Lambda_{\text{QCD}}}, \mu) = \sum_j H_{ij}(E, \mu) \otimes J_j(\sqrt{E\Lambda_{\text{QCD}}}, \mu). \quad (6.11)$$

Below we will focus on the universal functions $\zeta_M(E, \mu_I)$ entering the first term in (6.10). (The notation μ_I serves as a reminder that the factorization scale for this term is defined in the intermediate effective theory SCET_I .) In [86, 91] these functions are defined in terms of matrix elements in the intermediate effective theory SCET_I , which leaves open the possibility that they could be dominated by short-distance physics. Here we show [89] that the functions ζ_M renormalized at a hard-collinear scale $\mu_{hc} \sim \sqrt{E\Lambda_{\text{QCD}}}$ can be factorized further according to

$$\zeta_M(\mu_{hc}, E) = \sum_k D_k^{(M)}(\sqrt{E\Lambda_{\text{QCD}}}, \mu_{hc}, \mu) \otimes \xi_k^{(M)}(\mu, E), \quad (6.12)$$

where the functions $\xi_k^{(M)}$ are defined in terms of hadronic matrix elements of SCET_{II} operators. By solving the RG equation for these operators we show that the universal form factors ζ_M do not receive a significant perturbative suppression, neither by a power of $\alpha_s(\sqrt{E\Lambda_{\text{QCD}}})$ nor by resummed Sudakov logarithms. This statement holds true even in the limit where M_B is taken to be much larger than the physical B -meson mass. Perhaps somewhat surprisingly, we find that there exists a leading contribution to the soft functions ζ_M , for which the hard-collinear scale $\sqrt{E\Lambda_{\text{QCD}}}$ is without physical significance. Switching from SCET_I to SCET_{II} , one describes the same physics using a different set of degrees of freedom. This observation leads us to the most important conclusion of this work, namely that *the long-distance, soft overlap contribution to heavy-to-light form factors exists*. However, we point out that even at low hadronic scales $\mu \sim \Lambda_{\text{QCD}}$ the functions $\xi_k^{(M)}$ contain a dependence on the large recoil energy E which is of long-distance nature and cannot be factorized using RG techniques. As a result, it is impossible

to determine the asymptotic behavior of the QCD form factors $f_i^{B \rightarrow M}$ as $E \rightarrow \infty$ using short-distance methods.

In order to prove the factorization formula (6.10) one needs to show that all contributions to the form factors that do not obey spin-symmetry relations can be written in terms of convolution integrals involving the leading-order LCDAs of the B meson and the light meson. Specifically, this means showing that (i) no higher Fock states (or higher-twist two-particle distribution amplitudes) contribute at leading power, and (ii) the convolution integrals are convergent to all orders in perturbation theory. Point (i) can be dealt with using the power-counting rules of SCET along with reparameterization invariance [86, 91]. Here we use our formalism to complete step (ii) of the factorization proof. (The convergence of the convolution integral over the B -meson LCDA can also be shown using arguments along the lines of the discussion around equation (5.8).)

6.3 Matching calculations

In the matching of the intermediate effective theory SCET_I onto the final low-energy effective theory SCET_{II} , hard-collinear modes with virtuality of order $\sqrt{E\Lambda_{\text{QCD}}}$ are integrated out, and their effects are included in short-distance coefficient functions. Our primary goal in this section is to construct a basis of operators relevant to the matching of the universal functions ζ_M in (6.10) onto the low-energy theory (at leading power in $\lambda = \Lambda_{\text{QCD}}/E$), and to calculate their Wilson coefficients at lowest order in perturbation theory. As always, matching calculations can be done using on-shell external quark and gluon states rather than the physical meson states, whose matrix elements define the form factors. The results for the Wilson coefficients are insensitive to infra-red physics.

6.3.1 Spin-symmetric contributions

Heavy-to-light form factors are defined in terms of $B \rightarrow M$ matrix elements of flavor-changing currents $\bar{q} \Gamma b$. The spin-symmetric contributions to the form factors are characterized by the fact that in the intermediate effective theory (i.e., after hard fluctuations with virtuality $\mu \sim E \sim M_B$ are integrated out) they contain the Dirac structure Γ sandwiched between the two projection operators $\frac{1}{4} \not{n} \not{\gamma}$ and $\frac{1}{2}(1 + \not{v})$. This implies that Γ can be decomposed into a linear combination of only three independent Dirac structures, which leads to symmetry relations between various form factors [18]. As was shown in the equations (2.42) and (2.44), the relevant operators in SCET_I can be written as time-ordered products of the effective Lagrangian with effective current operators $J_M^{(0)}(x) = [\bar{\xi}_{hc} W_{hc}](x) \Gamma_M h(x_-)$ defined by the matching relation

$$\bar{q} \Gamma b = \sum_M K_M^\Gamma(m_b, E, \mu) J_M^{(0)} + \dots, \quad (6.13)$$

where the dots denote power-suppressed terms. Here $\Gamma_M = 1, \gamma_5, \gamma_{\perp\nu}$ is one of the three Dirac basis matrices that remain after the projections onto the two-component spinors $\bar{\xi}_{hc}$ and h . The variable E entering the coefficients K_M^Γ is the total energy carried by collinear particles (more precisely, $2E = \bar{n} \cdot p_c^{\text{tot}}$), which in our case coincides with the energy of the final-state meson M . Since the Lagrangian is a Lorentz scalar, it follows that for $B \rightarrow M$ transitions each of the three possibilities corresponds to a particular choice of the final-state meson (hence the label “ M ” on Γ_M), namely $\Gamma_M = 1$ for $M = P$ a pseudoscalar meson, $\Gamma_M = \gamma_5$ for $M = V_{\parallel}$ a longitudinally polarized vector meson, and $\Gamma_M = \gamma_{\perp\nu}$ for $M = V_{\perp}$ a transversely polarized vector meson. The coefficients K_M^Γ for the various currents that are relevant in the discussion of heavy-to-light form factors are summarized in Table 6.1, where we use the definitions (2.43) for the transverse tensors $g_{\perp}^{\mu\nu}$ and

Table 6.1: Coefficients K_M^Γ arising in the leading-order matching of flavor-changing currents from QCD onto SCET_I. The coefficients C_i are defined in equation (2.44) and given beyond tree-level in [9]. We denote $\hat{q} = q/M_B$ and $\hat{E} = E/M_B$, where $q = p_B - p_M$.

| Current | $M = P$ | $M = V_\parallel$ | $M = V_\perp$ |
|---|---------------------------------------|---------------------------------------|---|
| $\bar{q} \Gamma b$ | $(\Gamma_M = 1)$ | $(\Gamma_M = \gamma_5)$ | $(\Gamma_M = \gamma_{\perp\nu})$ |
| $\bar{q} \gamma^\mu b$ | $(n^\mu C_4 + v^\mu C_5)$ | — | $g_\perp^{\mu\nu} C_3$ |
| $\bar{q} \gamma^\mu \gamma_5 b$ | — | $-(n^\mu C_7 + v^\mu C_8)$ | $-i\epsilon_\perp^{\mu\nu} C_6$ |
| $\bar{q} i\sigma^{\mu\nu} \hat{q}_\nu b$ | $[v^\mu - (1 - \hat{E})n^\mu] C_{11}$ | — | $-g_\perp^{\mu\nu} [C_9 + (1 - \hat{E})C_{12}]$ |
| $\bar{q} i\sigma^{\mu\nu} \gamma_5 \hat{q}_\nu b$ | — | $[v^\mu - (1 - \hat{E})n^\mu] C_{10}$ | $-i\epsilon_\perp^{\mu\nu} (C_9 + \hat{E}C_{12})$ |

$\epsilon_\perp^{\mu\nu}$. Once a definition for the heavy-to-light form factors is adopted, it is an easy exercise to read off from the table which of the coefficient functions C_i contribute to a given form factor. This determines the functions $C_i(E, \mu_1)$ in (6.10). (In general, these functions are linear combinations of the C_i in Table 6.1.)

Next, we match the time-ordered product $i \int d^4x \text{T} \{ J_M^{(0)}(0), \mathcal{L}_{\text{SCET}_I}(x) \}$ onto operators in SCET_{II}, focusing first on operators which include soft and collinear fields only. The insertion of a subleading interaction from the SCET_I Lagrangian is required to transform the soft B -meson spectator anti-quark into a hard-collinear final-state parton. In the resulting SCET_{II} interaction terms the soft and collinear fields must be multipole expanded, since their momenta have different scaling properties with the expansion parameter λ [12], see Section 2.3.1. Soft fields are expanded about $x_+ = 0$ while collinear ones are expanded about $x_- = 0$. In general, collinear fields can live on different x_+ positions while soft fields can live on different x_- positions. The relevant operators can be written as matrix elements of color singlet-singlet four-quark operators multiplied by position-dependent Wilson

coefficients, i.e. [14, 16]

$$\begin{aligned} \int ds dt \tilde{D}_k(s, t, E, \mu) & [(\bar{\xi} W_c)(x_+ + x_\perp) \dots (W_c^\dagger \xi)(x_+ + x_\perp + s\bar{n})] \\ & \times [(\bar{q}_s S_s)(x_- + x_\perp + tn) \dots (S_s^\dagger h)(x_- + x_\perp)], \end{aligned} \quad (6.14)$$

where the dots represent different Dirac structures. There is no need to include color octet-octet operators, since they have vanishing projections onto physical hadron states and do not mix into the color singlet-singlet operators under renormalization. The Fourier transforms of the coefficient functions defined as

$$D_k(\omega, u_2, E, \mu) = \int ds e^{2iEu_2s} \int dt e^{-i\omega t} \tilde{D}_k(s, t, E, \mu) \quad (6.15)$$

coincide with the momentum-space Wilson coefficient functions, which we will calculate below. (In the matching calculation, ω is identified with the component $n \cdot l$ of the incoming spectator momentum, and u_2 is identified with the longitudinal momentum fraction x_2 carried by the collinear anti-quark in the final-state meson.) When we rewrite the operators above in terms of the gauge-invariant building blocks defined in (2.60), all factors of the soft-collinear Wilson lines $S_{sc}(0)$ and $W_{sc}(0)$ cancel out, as explained after equation (2.84), since the collinear fields are evaluated at $x_- = 0$ and the soft fields at $x_+ = 0$. Hence, we can rewrite the operators in the form (setting $x = 0$ for simplicity)

$$\int ds dt \tilde{D}_k(s, t, E, \mu) [\tilde{\mathcal{X}}(0) \dots \mathcal{X}(s\bar{n})] [\bar{\mathcal{Q}}_s(tn) \dots \mathcal{H}(0)]. \quad (6.16)$$

At leading order in λ , operators can also contain insertions of transverse derivatives or gauge fields between the collinear or soft quark fields. Since $\partial_\perp^\mu \sim \lambda$ and $\mathcal{A}_{c\perp}^\mu \sim \mathcal{A}_{s\perp}^\mu \sim \lambda$, such transverse insertions must be accompanied by a factor of $\not{n}/in \cdot \partial_s \sim \lambda^{-1}$. The inverse derivative operator acts on a light soft field and implies an integration over the position of that field on the n light-cone, the effect

of which can be absorbed into the Wilson coefficient functions. The appearance of \not{n} in the numerator is enforced by reparameterization invariance, as derived in equation (2.87). It then follows that in our case only single insertions of transverse objects are allowed [14, 24]. Finally, the multipole expansion of the soft fields ensures that the component $\bar{n} \cdot p_s$ of soft momenta does not enter Feynman diagrams at leading power. Likewise, at leading power there are no operators that contain $in \cdot \partial_c \sim \lambda^2$ (acting on collinear fields) or $n \cdot \mathcal{A}_c \sim \lambda^2$, since these are always suppressed with respect to the corresponding transverse quantities. The new structures containing gluon fields are of the form

$$\begin{aligned} & \int dr ds dt \tilde{D}_k(r, s, t, E, \mu) [\bar{\mathcal{X}}(0) \dots \mathcal{A}_{c\perp}^\mu(r\bar{n}) \dots \mathcal{X}(s\bar{n})] [\bar{\mathcal{Q}}_s(tn) \dots \mathcal{H}(0)], \\ & \int ds dt du \tilde{D}_k(s, t, u, E, \mu) [\bar{\mathcal{X}}(0) \dots \mathcal{X}(s\bar{n})] [\bar{\mathcal{Q}}_s(tn) \dots \mathcal{A}_{s\perp}^\mu(un) \dots \mathcal{H}(0)], \end{aligned} \quad (6.17)$$

and we define the corresponding Fourier-transformed coefficient functions in analogy to (6.15) as $D_k(u_2, u_3, \omega, E, \mu)$ and $D_k(\omega_1, \omega_2, u_2, E, \mu)$. In matching calculations, u_3 is identified with the longitudinal momentum fraction x_3 carried by a final-state collinear gluon, while ω_1 and ω_2 are associated with the components $n \cdot l_q$ and $n \cdot l_g$ of the incoming soft anti-quark and gluon momenta.

We are now in a position to construct a basis of four-quark operators relevant to the discussion of the universal functions ζ_M in (6.10) [89]. These operators must transform like the current $J_M^{(0)}$ under Lorentz transformations. Also, the soft and collinear parts of the four-quark operators must have non-zero projections onto the B meson and the final-state meson M . We set the transverse momenta of the mesons to zero, in which case there is no need to include operators with transverse derivatives acting on the products of all soft or collinear fields.

Case $M = P$: The resulting operators must transform as a scalar ($\Gamma_M = 1$). A basis of such operators is

$$\begin{aligned}
O_1^{(P)} &= g^2 [\bar{\mathcal{X}}(0) \frac{\vec{\not{n}}}{2} \gamma_5 \mathcal{X}(s\bar{n})] [\bar{\mathcal{Q}}_s(tn) \frac{\vec{\not{n}}\not{n}}{4} \gamma_5 \mathcal{H}(0)], \\
O_2^{(P)} &= g^2 [\bar{\mathcal{X}}(0) \frac{\vec{\not{n}}}{2} \gamma_5 i\vec{\not{\partial}}_\perp \mathcal{X}(s\bar{n})] [\bar{\mathcal{Q}}_s(tn) \frac{\not{n}}{2} \gamma_5 \mathcal{H}(0)], \\
O_3^{(P)} &= g^2 [\bar{\mathcal{X}}(0) \frac{\vec{\not{n}}}{2} \gamma_5 \mathcal{A}_{c\perp}(r\bar{n}) \mathcal{X}(s\bar{n})] [\bar{\mathcal{Q}}_s(tn) \frac{\not{n}}{2} \gamma_5 \mathcal{H}(0)], \\
O_4^{(P)} &= g^2 [\bar{\mathcal{X}}(0) \frac{\vec{\not{n}}}{2} \gamma_5 \mathcal{X}(s\bar{n})] [\bar{\mathcal{Q}}_s(tn) \mathcal{A}_{s\perp}(un) \frac{\not{n}}{2} \gamma_5 \mathcal{H}(0)].
\end{aligned} \tag{6.18}$$

The soft and collinear currents both transform like a pseudoscalar.

Case $M = V_\parallel$: The resulting operators must transform as a pseudo-scalar ($\Gamma_M = \gamma_5$). A basis of such operators is obtained by omitting the γ_5 between the two collinear spinor fields in (6.18), so that the collinear currents transform like a scalar. The Wilson coefficients for the cases $M = P$ and $M = V_\parallel$ coincide up to an overall sign due to parity invariance.

Case $M = V_\perp$: The resulting operators must transform as a transverse vector ($\Gamma_M = \gamma_{\perp\nu}$). A basis of such operators is

$$\begin{aligned}
O_1^{(V_\perp)} &= g^2 [\bar{\mathcal{X}}(0) \frac{\vec{\not{n}}}{2} \gamma_{\perp\nu} \gamma_5 \mathcal{X}(s\bar{n})] [\bar{\mathcal{Q}}_s(tn) \frac{\vec{\not{n}}\not{n}}{4} \gamma_5 \mathcal{H}(0)], \\
O_2^{(V_\perp)} &= g^2 [\bar{\mathcal{X}}(0) \frac{\vec{\not{n}}}{2} (i\epsilon_{\nu\alpha}^\perp - g_{\nu\alpha}^\perp \gamma_5) i\partial_\perp^\alpha \mathcal{X}(s\bar{n})] [\bar{\mathcal{Q}}_s(tn) \frac{\not{n}}{2} \gamma_5 \mathcal{H}(0)], \\
O_3^{(V_\perp)} &= g^2 [\bar{\mathcal{X}}(0) \frac{\vec{\not{n}}}{2} (i\epsilon_{\nu\alpha}^\perp - g_{\nu\alpha}^\perp \gamma_5) \mathcal{A}_{c\perp}^\alpha(r\bar{n}) \mathcal{X}(s\bar{n})] [\bar{\mathcal{Q}}_s(tn) \frac{\not{n}}{2} \gamma_5 \mathcal{H}(0)], \\
O_4^{(V_\perp)} &= g^2 [\bar{\mathcal{X}}(0) \frac{\vec{\not{n}}}{2} \gamma_{\perp\nu} \gamma_5 \mathcal{X}(s\bar{n})] [\bar{\mathcal{Q}}_s(tn) \mathcal{A}_{s\perp}(un) \frac{\not{n}}{2} \gamma_5 \mathcal{H}(0)].
\end{aligned} \tag{6.19}$$

The soft currents transform like a pseudoscalar, while the collinear currents transform like a transverse axial-vector. (The relative sign between the two terms in $O_{2,3}^{(V_\perp)}$ can be determined by considering left and right-handed spinors $\bar{\mathcal{X}}$ and using relation (6.22) below.)

It is not necessary to include operators with a derivative on the soft spectator anti-quark. All such operators would contain $\bar{Q}_s (-i \overleftarrow{\not{\partial}}_\perp) \not{n}$, which can be related to a linear combination of the operators $O_1^{(M)}$ and $O_4^{(M)}$ using the equation of motion for the light-quark field.

Wilson coefficients of four-quark operators

We now calculate the momentum-space Wilson coefficients of the operators $O_i^{(M)}$ at tree level [89]. The relevant graphs must contain a hard-collinear gluon exchange, which turns the soft B -meson spectator anti-quark into a collinear parton that can be absorbed by the final-state hadron. These hard-collinear gluons are integrated out when SCET_I is matched onto SCET_{II}. However, at $O(\alpha_s)$ we can obtain the Wilson coefficients in SCET_{II} by directly matching QCD amplitudes onto the low-energy theory, without going through an intermediate effective theory.

As we have seen, at leading power the universal form factors ζ_M receive contributions from ordinary four-quark operators as well as from four-quark operators containing an additional collinear or soft gluon field. We start with a discussion of the matching calculation for the operators $O_{1,2}^{(M)}$, whose coefficients can be obtained by analyzing the diagrams shown in Fig. 6.1 in the kinematic region where the outgoing quarks are collinear and the incoming quarks are soft. The resulting expression for the amplitude in the full theory has already been given in (6.8). Note that, by assumption, $n \cdot l \sim \Lambda_{\text{QCD}}$ and $x_2 \sim 1$, so that the result is well defined and it is consistent to neglect subleading terms in the gluon propagators.

We wish to express the result for the QCD amplitude as a combination of SCET_{II} matrix elements multiplied by coefficient functions. To this end, we must first eliminate the superficially leading term in (6.8) using the equations of motion.

Assigning momenta to the two outgoing collinear lines as shown in (6.9), it follows that

$$\gamma_\mu E \not{\Gamma} \Gamma * \gamma^\mu = \frac{\not{p}_\perp}{x_1} \gamma_\mu \Gamma * \gamma^\mu - 2\Gamma * \frac{\not{p}_\perp}{x_2} + \dots, \quad (6.20)$$

where the dots denote power-suppressed terms. In the next step we use a Fierz transformation to recast the amplitude into a form that is convenient for our analysis. Taking into account that between collinear spinors the Dirac basis contains only three independent matrices, we find for general matrices M and N

$$\begin{aligned} 2(\bar{u}_\xi M u_h) (\bar{v}_q N v_\xi) &= (\bar{u}_\xi \frac{\not{\bar{p}}}{2} v_\xi) (\bar{v}_q N \frac{\not{p}}{2} M u_h) + (\bar{u}_\xi \frac{\not{\bar{p}}}{2} \gamma_5 v_\xi) (\bar{v}_q N \gamma_5 \frac{\not{p}}{2} M u_h) \\ &\quad + (\bar{u}_\xi \frac{\not{\bar{p}}}{2} \gamma_{\perp\alpha} v_\xi) (\bar{v}_q N \gamma_\perp^\alpha \frac{\not{p}}{2} M u_h). \end{aligned} \quad (6.21)$$

To simplify the Dirac algebra we use the identities

$$\gamma_\perp^\mu \gamma_5 \not{p} = i\epsilon_\perp^{\mu\nu} \gamma_{\perp\nu} \not{p}, \quad \gamma_\perp^\mu \gamma_\perp^\nu \not{p} = (g_\perp^{\mu\nu} - i\epsilon_\perp^{\mu\nu} \gamma_5) \not{p}. \quad (6.22)$$

Finally, we include a minus sign from fermion exchange under the Fierz transformation and project the collinear and soft “currents” in the resulting expressions onto color-singlet states.

Once in this form, the different contributions to the amplitude can be readily identified with matrix elements of the operators $O_{1,2}^{(M)}$. For $M = P, V_\parallel$ we obtain

$$D_1^{(P)} = -D_1^{(V_\parallel)} = -\frac{C_F}{N} \frac{1+u_2}{4E^2 u_2^2 \omega}, \quad D_2^{(P)} = -D_2^{(V_\parallel)} = -\frac{C_F}{N} \frac{1}{4E^2 u_1 u_2^2 \omega^2}, \quad (6.23)$$

while for $M = V_\perp$ we find

$$D_1^{(V_\perp)} = \frac{C_F}{N} \frac{1}{4E^2 u_2^2 \omega}, \quad D_2^{(V_\perp)} = \frac{C_F}{N} \frac{1}{4E^2 u_2^2 \omega^2}. \quad (6.24)$$

Wilson coefficients of four-quark operators with an extra gluon

The matching calculation for the operators $O_{3,4}^{(M)}$ proceeds along the same lines. However, in this case it is necessary to study diagrams with four external quarks

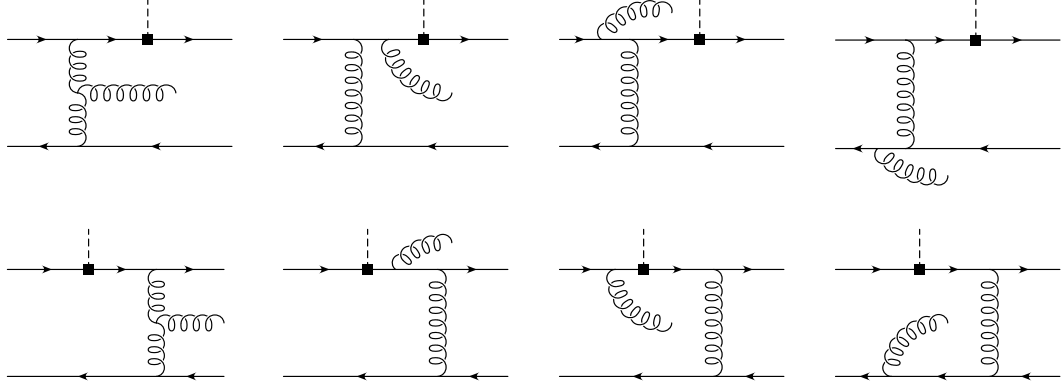


Figure 6.2: Diagrams relevant to the matching calculation for operators containing an extra collinear gluon.

and an external gluon, which we treat as a background field. Let us first discuss the case with three collinear particles in the final state. The relevant QCD graphs are shown in Fig. 6.2. Physically, they correspond to non-valence Fock states of the light final-state meson, but this interpretation is irrelevant for the matching calculation, which can be done with free quark and gluon states.

By assumption, each of the three collinear particles carries large momentum components along the n direction. We denote the corresponding longitudinal momentum fractions by x_1 (quark), x_2 (anti-quark) and x_3 (gluon), where $x_1 + x_2 + x_3 = 1$. The calculation of the diagrams in Fig. 6.2 exhibits that at leading power the amplitude depends only on the light-cone components $n \cdot l$ and $\bar{n} \cdot p_i = 2Ex_i$ of the external momenta, and that only transverse components of the external gluons fields must be kept. These observations are in accordance with the structure of the operator $O_3^{(M)}$. One must add to the diagrams shown in the figure a contribution arising from the application of the equation of motion for the collinear quark fields that led to (6.20). One way of obtaining it is to include diagrams with gluon emission from the external collinear quark lines in the matching calculation.

Performing the Fierz transformation and projecting onto the color singlet-singlet operators $O_3^{(M)}$, we obtain the coefficient functions

$$\begin{aligned} D_3^{(P)} = -D_3^{(V_{\parallel})} &= \frac{1}{8E^2(u_2 + u_3)^2\omega^2} \left[\frac{u_3}{u_2} - 1 + \frac{2}{N^2} - \frac{2C_F}{N} \frac{(u_2 + u_3)^2}{u_2(u_1 + u_3)} \right], \\ D_3^{(V_{\perp})} &= -\frac{1}{8E^2(u_2 + u_3)^2\omega^2} \left[\frac{u_3}{u_2} - 1 + \frac{2}{N^2} + \frac{1}{N^2} \frac{(u_2 + u_3)^2}{u_2(u_1 + u_2)} \right]. \end{aligned} \quad (6.25)$$

Next, we calculate the contributions from diagrams with three external soft particles, which physically correspond to three-particle Fock states of the B meson. Again there are eight diagrams, analogous to those in Fig. 6.2. The initial soft gluon is attached to either an off-shell intermediate line or a collinear line. The diagrams with external gluons must again be supplemented by a contribution resulting from the application of the equation of motion $\bar{v}_q \not{l} = O(g)$ used in the analysis of the four-quark amplitude in (6.8). After Fierz transformation and projection onto the color singlet-singlet operators $O_4^{(M)}$, we find the coefficient functions

$$\begin{aligned} D_4^{(P)} = -D_4^{(V_{\parallel})} &= \frac{1}{8E^2u_2^2(\omega_1 + \omega_2)^2} \left[\left(1 - \frac{2C_F}{N} u_2 \right) \frac{\omega_2}{\omega_1} + \frac{1}{N^2} \right], \\ D_4^{(V_{\perp})} &= -\frac{1}{8E^2u_2^2(\omega_1 + \omega_2)^2} \left[\left(1 + \frac{1}{N^2} \frac{u_2}{u_1} \right) \frac{\omega_2}{\omega_1} + \frac{1}{N^2} \frac{1}{u_1} \right]. \end{aligned} \quad (6.26)$$

The variables ω_1 and ω_2 correspond to the light-cone components $n \cdot l_q$ and $n \cdot l_g$ of the incoming momenta of the soft anti-quark and gluon, respectively.

Endpoint singularities

The Wilson coefficients of the SCET_{II} four-quark operators become singular in the limit where some of the momentum components of the external particles tend to zero. When the $B \rightarrow M$ matrix elements of the operators $O_k^{(M)}$ are evaluated, these singularities give rise to endpoint divergences of the resulting convolution integrals with LCDAs. For instance, the matrix elements of the operators $O_1^{(M)}$ and $O_4^{(M)}$ involve the leading twist-2 projection onto the light meson M . The

corresponding LCDAs ϕ_M are expected to vanish linearly as $u_2 \rightarrow 0$, whereas the corresponding coefficients contain terms that grow like $1/u_2^2$, giving rise to logarithmically divergent convolution integrals. Similarly, the operators $O_2^{(M)}$ and $O_3^{(M)}$ involve the leading-order projection onto the B -meson LCDA $\phi_B^{(+)}$, which is expected to vanish linearly as $\omega \rightarrow 0$ [30]. Once again, logarithmic singularities arise because the corresponding coefficients contain terms that grow like $1/\omega^2$.

While the logarithmic divergences in the convolution integrals could be avoided by introducing some infra-red regulators, they indicate that leading-order contributions to the amplitudes arise from momentum regions that cannot be described correctly in terms of collinear or soft fields. In Section 6.4, we will explain that in SCET_{II} these configurations are accounted for by matrix elements of operators containing the soft-collinear messenger fields.

6.3.2 Spin-symmetry breaking contributions

The two-particle amplitude in (6.8) also includes contributions for which the Dirac structure is different from $\not{h} \Gamma h$. These give rise to symmetry-breaking contributions to the form factors. We shall not derive a complete basis of all possible symmetry-breaking operators (there are many) but rather list the ones that enter at first order in α_s . Since the spin-symmetry violating terms can be factorized in the form of the second term in (6.10), they are associated with a short-distance coupling constant $\alpha_s(\sqrt{E\Lambda_{\text{QCD}}})$. It is therefore appropriate in this case to include the coupling constant in the Wilson coefficient functions.

Let Γ denote the Dirac structure of the flavor-changing currents $\bar{q} \Gamma b$, whose matrix elements define the form factors. To first order in α_s , the spin-symmetry breaking terms can then be obtained from the matrix elements of two operators

given by

$$\begin{aligned}
Q_1 &= [\bar{\mathcal{X}}(0) \frac{\not{n}}{2} \begin{pmatrix} 1 \\ \gamma_5 \\ \gamma_{\perp\alpha} \end{pmatrix} \mathcal{X}(s\bar{n})] [\bar{\mathcal{Q}}_s(tn) \frac{\not{n}}{2} \gamma_\mu \begin{pmatrix} 1 \\ -\gamma_5 \\ -\gamma_\perp^\alpha \end{pmatrix} \Gamma \gamma^\mu \not{n} \mathcal{H}(0)], \\
Q_2 &= [\bar{\mathcal{X}}(0) \frac{\not{n}}{2} \begin{pmatrix} 1 \\ \gamma_5 \\ 0 \end{pmatrix} \mathcal{X}(s\bar{n})] [\bar{\mathcal{Q}}_s(tn) \frac{\not{n}\not{n}}{4} \begin{pmatrix} 1 \\ -\gamma_5 \\ 0 \end{pmatrix} \Gamma \mathcal{H}(0)],
\end{aligned} \tag{6.27}$$

where each line contributes for a different final-state meson M . The corresponding Wilson coefficients are

$$\hat{T}_1 = -\frac{C_F}{N} \frac{\pi\alpha_s}{2M_B E u_2 \omega}, \quad \hat{T}_2 = \frac{C_F}{N} \frac{\pi\alpha_s}{E^2 u_2 \omega}. \tag{6.28}$$

Linear combinations of \hat{T}_1 and \hat{T}_2 determine (up to prefactors) the hard-scattering kernels T_i in (6.10). The matrix elements of the operators $Q_{1,2}$ can be expressed in terms of the leading-order LCDAs of the B meson and the light meson M . Only the B -meson LCDA called $\phi_B^{(+)}$ contributes [33] because of the factor \not{n} next to $\bar{\mathcal{Q}}_s$. This property holds true to all orders in perturbation theory [86]. The resulting convolution integrals are convergent. Evaluating these matrix elements we reproduce the spin-symmetry breaking terms obtained in [90].

6.4 Physics of endpoint singularities – a toy model

Our strategy in the previous sections has been to perform matching calculations by expanding QCD amplitudes in powers of Λ_{QCD}/E , assuming that collinear and soft external momenta have the scaling assigned to them in SCET. We have then matched the results onto SCET_{II} operators containing soft and collinear fields and read off the corresponding Wilson coefficient functions in momentum

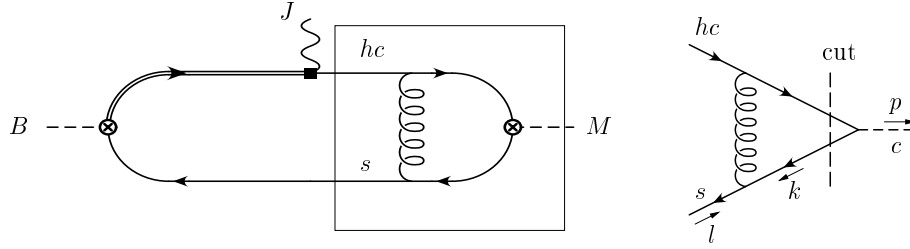


Figure 6.3: Triangle subgraph whose spectral function can be used to study endpoint singularities on the collinear side.

space. A problematic aspect of this procedure has been the observation that, if the matrix elements of the effective-theory operators are expressed in terms of meson LCDAs, then the resulting convolution integrals do not converge. Endpoint singularities arise, which correspond to exceptional momentum configurations in which some of the partons inside the external hadrons carry very small momentum. The question naturally arises how one should interpret these singularities, and whether the results we found for the short-distance coefficient functions are in fact correct.

The fact that endpoint configurations are not kinematically suppressed points to the relevance of new momentum modes. In the limit $x_2 \rightarrow 0$, the scaling associated with the collinear anti-quark in the final state of Fig. 6.1 changes from $(\lambda^2, 1, \lambda)$ to $(\lambda^2, \lambda, \dots)$. Likewise, in the limit $n \cdot l \rightarrow 0$, the scaling associated with the soft spectator anti-quark in the initial state changes from $(\lambda, \lambda, \lambda)$ to $(\lambda^2, \lambda, \dots)$. The soft-collinear messenger fields in the SCET_{II} Lagrangian have precisely the scaling properties corresponding to these exceptional configurations. (Since the modes in an effective theory are always on-shell, the transverse components of soft-collinear momenta scale like $\lambda^{3/2}$. We will see below that this is not really relevant.)

The purpose of this section is to analyze the interplay of the various modes present in SCET_{II} and to see how soft-collinear messengers are connected with the phenomenon of endpoint singularities. We will do this with the help of a toy example. Consider the triangle subgraph enclosed by the box in the diagram shown on the left-hand side in Fig. 6.3, which is one of the two gluon-exchange graphs relevant to the $B \rightarrow M$ form factors (see Fig. 6.1). To understand the physics of endpoint singularities we focus on the side of the light meson M (an analogous discussion could be given for the B -meson side). We study the discontinuity of the triangle diagram in the external collinear momentum p^2 . The resulting spectral density $\varrho(p^2)$ models the continuum of light final-state hadrons that can be produced on the collinear side. We will not bother to project out a particular light meson from this spectral density. For simplicity, we will also ignore any numerator structure in the triangle subgraph and instead study the corresponding scalar triangle, as discussed in [15, 89].

Let us define the discontinuity

$$\frac{1}{2\pi i} \left[I(p^2 + i0) - I(p^2 - i0) \right] \equiv D \cdot \theta(p^2) \quad (6.29)$$

of the scalar triangle integral

$$I = i\pi^{-d/2} \mu^{4-d} \int d^d k \frac{2l_+ \cdot p_-}{(k^2 + i0) [(k+l)^2 + i0] [(k+p)^2 + i0]} \quad (6.30)$$

in $d = 4 - 2\epsilon$ space-time dimensions, where p is the outgoing collinear momentum and l the incoming soft momentum. It will be convenient to define the invariants $L^2 \equiv -l^2 - i0$ and $Q^2 \equiv -(l-p)^2 = 2l_+ \cdot p_- + \dots$, which scale like $L^2 \sim \lambda^2$ and $Q^2 \sim \lambda$. (In physical units, $L^2 \sim \Lambda_{\text{QCD}}^2$ and $Q^2 \sim E\Lambda_{\text{QCD}}$ with $E \gg \Lambda_{\text{QCD}}$.) We will assume that these quantities are non-zero. From [15], we can obtain explicit results for the discontinuity D and for the various regions of loop momentum k

that give a non-vanishing contribution. We find that

$$D = \ln \frac{Q^2}{L^2} + O(\epsilon, \lambda), \quad (6.31)$$

and that the momentum configurations that contribute to this result are those where the loop momentum is either collinear, meaning that $k \sim (\lambda^2, 1, \lambda)$, or soft-collinear, meaning that $k \sim (\lambda^2, \lambda, \lambda^{3/2})$. The contributions from these two regions are

$$\begin{aligned} D_C &= \frac{\Gamma(-\epsilon)}{\Gamma(1-2\epsilon)} \left(\frac{\mu^2}{p^2} \right)^\epsilon = -\frac{1}{\epsilon} + \gamma_E - \ln \frac{\mu^2}{p^2} + O(\epsilon), \\ D_{SC} &= \Gamma(\epsilon) \left(\frac{\mu^2 Q^2}{p^2 L^2} \right)^\epsilon = \frac{1}{\epsilon} - \gamma_E + \ln \frac{\mu^2 Q^2}{p^2 L^2} + O(\epsilon), \end{aligned} \quad (6.32)$$

which add up to the correct answer.

It is instructive to rewrite these results in a more transparent form. To this end we use Cutkosky rules to evaluate the discontinuities of the diagrams directly and perform all phase-space integrations except the integral over the light-cone component $\bar{n} \cdot k$ of the loop momentum, which we parameterize as $\bar{n} \cdot k \equiv -x_2 \bar{n} \cdot p$. As in previous sections, x_2 denotes the fraction of longitudinal momentum carried by the anti-quark in the final-state. The exact result for the discontinuity of the scalar triangle is ($\bar{x}_2 \equiv 1 - x_2$)

$$\begin{aligned} D &= \frac{1}{\Gamma(1-\epsilon)} \left(\frac{\mu^2}{p^2} \right)^\epsilon \int_0^1 dx_2 \frac{(x_2 \bar{x}_2)^{-\epsilon}}{x_2 + L^2/Q^2} + O(\lambda) \\ &= \int_0^1 dx_2 \frac{1}{x_2 + L^2/Q^2} + O(\epsilon, \lambda) = \int_{L^2/Q^2}^1 \frac{dx_2}{x_2} + O(\epsilon, \lambda). \end{aligned} \quad (6.33)$$

The collinear and soft-collinear contributions separately are divergent even though they correspond to tree diagrams (after the two propagators have been cut). We obtain

$$\begin{aligned} D_C &= \frac{1}{\Gamma(1-\epsilon)} \left(\frac{\mu^2}{p^2} \right)^\epsilon \int_0^1 \frac{dx_2}{x_2} (x_2 \bar{x}_2)^{-\epsilon}, \\ D_{SC} &= \frac{1}{\Gamma(1-\epsilon)} \left(\frac{\mu^2}{p^2} \right)^\epsilon \int_0^\infty dx_2 \frac{x_2^{-\epsilon}}{x_2 + L^2/Q^2}. \end{aligned} \quad (6.34)$$

The collinear contribution is infra-red singular for $x_2 \rightarrow 0$, which is an example of an endpoint singularity. In the present case, the singularity is regularized dimensionally by keeping ϵ non-zero. The soft-collinear contribution is infra-red finite but ultra-violet divergent, since x_2 runs up to ∞ . Again, this divergence is regularized dimensionally. Evaluating the remaining integrals one recovers the exact results in (6.32).

Several comments are in order:

i) The result for the spectral density in the full theory is finite. The endpoint singularity is regularized by keeping subleading terms in the hard-collinear propagator $1/[-(k+l)^2] \simeq 1/(x_2 Q^2 + L^2)$. When the subleading terms are dropped based on naive power counting (as we did in the analysis of the previous sections) the full-theory result reduces to the contribution obtained from the collinear region. An endpoint singularity arises in this case, which however can be regularized dimensionally. In order for this to happen in the realistic case of external meson states, it would be necessary to perform the projections onto the meson LCDAs in $d \neq 4$ dimensions. The factor $(x_2 \bar{x}_2)^{-\epsilon}$ in (6.34) would then correspond to a modification of the LCDAs, which renders the convolution integrals finite.

ii) The collinear approximation fails for values $x_2 = O(\lambda)$. For such small momentum fractions the exact full-theory result is reproduced by the contribution obtained from the soft-collinear region. In fact, the collinear and soft-collinear contributions in (6.34) coincide with the first terms in the Taylor expansion of the full-theory result in (6.33) in the limits where $x_2 = O(1) \gg L^2/Q^2$ and $x_2 = O(\lambda) \ll 1$. The fact that x_2 runs up to ∞ in the soft-collinear contribution is not a problem. In dimensional regularization the integral receives significant contributions only from the region where $x_2 \sim L^2/Q^2 = O(\lambda)$. To see this, one

can introduce a cutoff δ to separate the collinear and soft-collinear contributions, chosen such that $1 \gg \delta \gg \lambda$. This cutoff is introduced as an infra-red regulator in the collinear integral ($\int_0^1 \rightarrow \int_\delta^1$) and as an ultra-violet regulator in the soft-collinear integral ($\int_0^\infty \rightarrow \int_0^\delta$). The integrals can then be evaluated setting $\epsilon \rightarrow 0$. This yields $D_C = -\ln \delta$ and $D_{SC} = \ln \delta + \ln \frac{Q^2}{L^2} + O(\lambda/\delta)$. The sum of the two contributions once again reproduces the exact result.

iii) Next, note that the soft-collinear contribution *precisely* reproduces the endpoint behavior of the full-theory amplitude. It is irrelevant in this context that the soft-collinear virtuality $k_{sc}^2 \sim E^2 \lambda^3$ is parametrically smaller than the QCD scale Λ_{QCD}^2 . What matters is that the plus and minus components of the soft-collinear momentum, $k_{sc} \sim (\lambda^2, \lambda, \dots)$, are of the same order as the corresponding components of a collinear momentum in the endpoint region, where $\bar{n} \cdot p \sim \lambda$ rather than being $O(1)$.

iv) Finally, we see that the endpoint divergences we encountered in the Section 6.3.1 were not regularized because we dropped the dimensional regulator when performing the projections onto meson LCDAs. This, however, does not affect the results for the Wilson coefficients of the SCET_{II} operators, which remain valid. In the toy model, the collinear contribution is represented in the effective theory as the discontinuity of the integral (corresponding to the first diagram on the right-hand side in Fig. 6.4)

$$\begin{aligned} I_C &= i\pi^{-d/2} \mu^{4-d} \int d^d k \frac{2l_+ \cdot p_-}{(k^2 + i0)(2k_- \cdot l_+) [(k+p)^2 + i0]} \\ &= i\pi^{-d/2} \mu^{4-d} \int d^d k \frac{(-1)}{x_2} \frac{1}{(k^2 + i0) [(k+p)^2 + i0]}, \end{aligned} \quad (6.35)$$

which shows that the Wilson coefficient resulting from integrating out the hard-collinear propagator is simply $-1/u_2$.

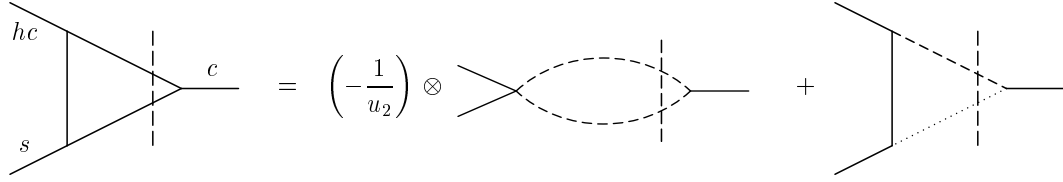


Figure 6.4: Collinear and soft-collinear contributions to the scalar triangle graph in SCET_{II} . Dashed (dotted) lines represent collinear (soft-collinear) propagators.

To summarize this discussion, we stress that to reproduce the behavior of the full amplitude it is necessary to include in the effective theory contributions involving collinear fields and those involving soft-collinear messengers, as indicated in Fig. 6.4. The latter ones represent the exact behavior of the amplitude in the endpoint region. Whether or not endpoint configurations contribute at leading order in power counting is equivalent to the question of whether or not operators involving soft-collinear fields can arise at leading power. This shows the power of our formalism. Operators containing soft-collinear fields can be used to parameterize in a systematic way the long-distance physics associated with endpoint configurations in the external mesons states. This will be discussed in more detail in the next section. It also follows that the scaling properties of operators containing soft-collinear fields can be used to make model-independent statements about the convergence of convolution integrals that arise in QCD factorization theorems such as (6.10). We will exploit this connection in Section 6.7.

6.5 Soft-collinear messengers and the soft overlap

In Section 6.3 we have derived four-quark operators built out of collinear and soft fields, which contribute at leading order to the universal soft functions ζ_M in (6.10).

Power counting shows that the products of these operators with their Wilson coefficients scale like λ^4 . (Here one uses that $dr \sim ds \sim 1$ and $dt \sim du \sim \lambda^{-1}$.) Taking into account the counting of the external hadron states, $|B\rangle \sim \lambda^{-3/2}$ and $\langle M| \sim \lambda^{-1}$, it follows that the corresponding contributions to the universal form factors scale like $\lambda^{3/2}$. In other words, heavy-to-light form factors are quantities that vanish at leading order in the large-energy expansion. The fact that the resulting convolution integrals were infra-red singular suggested that there should be other contributions of the same order in power counting, which cannot be described in terms of collinear or soft fields.

An important observation made in the previous section was that the endpoint behavior of QCD amplitudes is described in the low-energy theory in terms of diagrams involving soft-collinear messenger fields. For instance, in the last graph in Fig. 6.4 the soft spectator anti-quark inside the B meson turns into a soft-collinear anti-quark by the emission of a soft gluon. The soft-collinear anti-quark is then absorbed by the final-state meson. In a similar way, endpoint singularities on the B -meson side would correspond to a situation where the initial state contains a soft-collinear spectator anti-quark, which absorbs a collinear gluon and turns into a collinear anti-quark. The SCET_{II} Lagrangian contains the corresponding interaction terms only at subleading order in λ . However, because the universal form factors ζ_M themselves are power-suppressed quantities, these subleading interactions will nevertheless give rise to leading-power contributions.

We will need the first two non-vanishing orders in the interactions that couple a soft-collinear quark to a soft or collinear quark. The results are most transparent when expressed in terms of the gauge-invariant building blocks introduced in (2.60). They are [15]

$$\mathcal{L}_{\bar{q}\theta}^{(1/2)} = \bar{\mathcal{Q}}_s \mathcal{A}_{s\perp} W_{sc}^\dagger \theta, \quad \mathcal{L}_{\bar{\theta}\xi}^{(1/2)} = \bar{\sigma} S_{sc} \mathcal{A}_{c\perp} \mathcal{X}, \quad (6.36)$$

and

$$\begin{aligned} \mathcal{L}_{\bar{q}\theta}^{(1)} &= \bar{\mathcal{Q}}_s \mathcal{A}_{s\perp} W_{sc}^\dagger (x_\perp \cdot D_{sc} \theta + \sigma) + \bar{\mathcal{Q}}_s \frac{\not{n}}{2} \bar{n} \cdot \mathcal{A}_s W_{sc}^\dagger \sigma, \\ \mathcal{L}_{\bar{\theta}\xi}^{(1)} &= \bar{\sigma} x_\perp \cdot \overleftarrow{D}_{sc} S_{sc} \mathcal{A}_{c\perp} \mathcal{X} - \bar{\theta} S_{sc} \mathcal{A}_{c\perp} \frac{\not{n}}{2} \frac{1}{i\bar{n} \cdot \partial} (i\not{\partial}_\perp + \mathcal{A}_{c\perp}) \mathcal{X} + \bar{\theta} S_{sc} \frac{\not{n}}{2} n \cdot \mathcal{A}_c \mathcal{X}, \end{aligned} \quad (6.37)$$

where

$$\sigma = -\frac{\not{n}}{2} \frac{1}{i\bar{n} \cdot D_{sc}} i\not{D}_{sc\perp} \theta \quad (6.38)$$

contains the “small components” of the soft-collinear quark field, which are integrated out in the construction of the effective Lagrangian. The longitudinal components of the calligraphic gluon fields are defined in [15]. (Note also that $n \cdot \mathcal{A}_s = 0$ and $\bar{n} \cdot \mathcal{A}_c = 0$.) The soft-collinear fields enter these results in combinations such as $W_{sc}^\dagger \theta$ or $S_{sc}^\dagger \theta$, which are gauge invariant. Soft and collinear fields live at position x , while soft-collinear fields are evaluated at position x_+ for $\mathcal{L}_{\bar{q}\theta}$ and x_- for $\mathcal{L}_{\bar{\theta}\xi}$. The measure d^4x associated with these interactions scales like λ^{-4} . The superscript on the Lagrangians indicates at which order in power counting ($\lambda^{1/2}$ or λ) the corresponding terms contribute to the action.

Next, we need the representation of the flavor-changing SCET_I current $J_M^{(0)}$ in (6.13) in terms of operators in the low-energy theory SCET_{II}. As shown in [16], at leading power, and at the matching scale $\mu = \mu_{hc}$, the relation reads

$$J_M^{(0)}(x) \rightarrow \mathcal{J}_M^{(0)}(x) = \bar{\mathcal{X}}(x_+ + x_\perp) \Gamma_M(S_{sc}^\dagger W_{sc})(0) \mathcal{H}(x_- + x_\perp) \quad (6.39)$$

with a Wilson coefficient equal to unity. The anomalous dimensions of the currents are the same in the two theories. The product $(S_{sc}^\dagger W_{sc})(0)$ arises since soft-collinear messenger fields cannot be decoupled from the current operator $\mathcal{J}_M^{(0)}$ in SCET_{II}, contrary to the case of the color singlet-singlet four-quark operators discussed in Section 6.3.

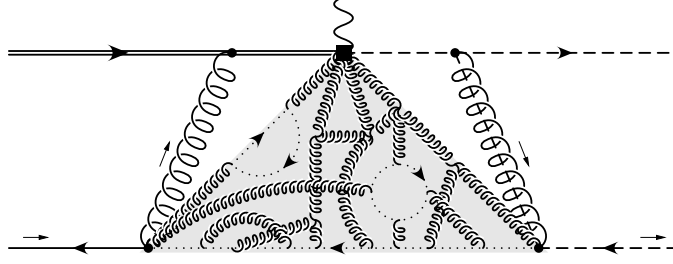


Figure 6.5: An artist's view of the soft-collinear messenger contribution to the form factors. The shaded region contains soft-collinear interactions. The arrows indicate the flow of the components $n \cdot p_s$ (left) and $\bar{n} \cdot p_c$ (right) of soft and collinear momenta, which do not enter the soft-collinear block.

Using these results, we can write down a tri-local operator whose matrix element provides a long-distance contribution to the universal form factors. It is

$$O_5^{(M)} = i^2 \int d^4x d^4y \text{T} \left\{ \mathcal{L}_{\bar{q}\theta}^{(1/2)}(x) \mathcal{L}_{\theta\xi}^{(1)}(y) \mathcal{J}_M^{(0)}(0) + \mathcal{L}_{\bar{q}\theta}^{(1)}(x) \mathcal{L}_{\theta\xi}^{(1/2)}(y) \mathcal{J}_M^{(0)}(0) \right\}. \quad (6.40)$$

Even after the decoupling transformation (2.60) this operator contains arbitrarily complicated soft-collinear exchanges, as illustrated in the cartoon in Fig. 6.5.

Note that the superficially leading term in the time-ordered product cancels [15]. This can be understood as follows:

After the decoupling transformation the strong-interaction part of the SCET_{II} Lagrangian no longer contains unsuppressed interactions between soft-collinear messengers and soft or collinear fields. In order to preserve a transparent power counting it is then convenient to define hadron states in the effective theory as eigenstates of one of the two leading-order Lagrangians \mathcal{L}_s and \mathcal{L}_c . For instance, we define a “SCET pion” to be a bound state of only collinear fields, and a “SCET B meson” to be a bound state of only soft fields. The SCET pion state coincides with the true pion, because the collinear Lagrangian is equivalent to the QCD

Lagrangian [12].¹ The SCET B meson coincides with the asymptotic heavy-meson state as defined in heavy-quark effective theory. It is important in this context that time-ordered products of soft-collinear fields with only collinear or only soft fields vanish to all orders as a consequence of analyticity [15]. Hence, soft-collinear modes do not affect the spectrum of hadronic eigenstates of the collinear or soft Lagrangians.

Once the SCET_{II} hadron states are defined in this way, each term in the time-ordered product (6.40) can be factorized into a part containing all soft and collinear fields times a vacuum correlation function of the soft-collinear fields. These vacuum correlators must be invariant under rotations in the transverse plane. It follows that the correlator arising from the superficially leading term in the time-ordered product vanishes, since

$$\langle \Omega | T \{ (\bar{\sigma} S_{sc})_i(y_-) (S_{sc}^\dagger W_{sc})_{jk}(0) (W_{sc}^\dagger \theta)_l(x_+) \} | \Omega \rangle \quad (6.41)$$

contains a single transverse derivative (see (6.38)).

The leading terms in the time-ordered product in (6.40) scale like λ^4 , since $\mathcal{J}_M^{(0)} \sim \lambda^{5/2}$. They thus contribute at the same order in power counting to the universal functions ζ_M as the four-quark operators discussed in Section 6.3. When $O_5^{(M)}$ is added to the list of four-quark operators a complete description of the soft-overlap contribution is obtained. The Wilson coefficient of this new operator follows from the fact that there is no non-trivial matching coefficient in (6.39), that the current operators have the same anomalous dimensions in SCET_I and SCET_{II}, and that the SCET_{II} Lagrangian is not renormalized. Hence, to all

¹The endpoint region of the pion wave function is not described in terms of a Fock component containing a soft-collinear parton, but rather in terms of a time-ordered product of the SCET pion state with an insertion of the Lagrangian $\mathcal{L}_{\bar{\theta}\xi}$. This insertion is non-zero only in processes where also soft partons are involved.

orders in perturbation theory

$$D_5^{(M)}(\mu_{hc}, \mu) = \frac{C_i(\mu)}{C_i(\mu_{hc})} \equiv D_5(\mu_{hc}, \mu), \quad (6.42)$$

which is in fact a universal function, independent of the labels “ i ” and “ M ”. As before, μ_{hc} denotes the hard-collinear matching scale, at which the transition $\text{SCET}_I \rightarrow \text{SCET}_{II}$ is made. The appearance of $C_i(\mu_{hc})$ in the denominator of this relation is due to the fact that this coefficient was factored out in the definition of $D_k^{(M)}$, see (6.10) and (6.12).

If we define by $\xi_k^{(M)}$ the $B \rightarrow M$ hadronic matrix elements of the operators $O_k^{(M)}$, then the sum $\zeta_M = \sum_k D_k^{(M)} \xi_k^{(M)}$ describes the entire soft overlap contribution. Each term in this sum gives a contribution of order $\lambda^{3/2}$ to the form factors, in accordance with the scaling law obtained a long time ago in the context of QCD sum rules [99]. We have thus completed the derivation of the new factorization formula (6.12). Whereas the Wilson coefficients $D_k^{(M)}$ depend on the renormalization scale μ as well as on the hard-collinear scale $\mu_{hc} \sim \sqrt{E\Lambda_{\text{QCD}}}$, the characteristic scale of the hadronic matrix elements $\xi_k^{(M)}$ is the QCD scale Λ_{QCD} , not the hard-collinear scale. While this is obvious for the matrix elements of the operator $O_5^{(M)}$, it also holds true for the remaining matrix elements, for which the sensitivity to long-distance physics is signaled by the presence of endpoint singularities. It remains to discuss how our results are affected by single and double logarithmic corrections arising in higher orders of perturbation theory.

6.6 Operator mixing and Sudakov logarithms

Because the operators $O_k^{(M)}$ share the same global quantum numbers they can mix under renormalization. This mixing is governed by a 5×5 matrix of anomalous

dimension kernels, which are in general complicated functions of the light-cone variables u_i and ω_i . The anomalous dimension matrix governing this mixing has the structure

$$\gamma = \left(\begin{array}{cccc|c} \gamma_{11} & 0 & 0 & \gamma_{14} & 0 \\ 0 & \gamma_{22} & \gamma_{23} & 0 & 0 \\ 0 & \gamma_{32} & \gamma_{33} & 0 & 0 \\ \gamma_{41} & 0 & 0 & \gamma_{44} & 0 \\ \hline \gamma_{51} & \gamma_{52} & \gamma_{53} & \gamma_{54} & \gamma_{55} \end{array} \right). \quad (6.43)$$

Because the operators $O_{1\dots 4}^{(M)}$ consist of products of soft and collinear currents (after decoupling of soft-collinear messengers), the entries in the upper left 4×4 sub-matrix can all be written as sums of soft and collinear anomalous dimensions for the corresponding current operators. We have taken into account that the operators $O_2^{(M)}$ and $O_3^{(M)}$ mix under renormalization (this mixing is determined by the mixing of twist-3 two-particle and three-particle LCDAs for light mesons), as do the operators $O_1^{(M)}$ and $O_4^{(M)}$ (this mixing has not yet been worked out but is allowed on general grounds). The operator $O_5^{(M)}$ consisting of a triple time-ordered product requires the “local” operators as counter-terms; however, those operators do not mix back into $O_5^{(M)}$.

Because of the structure of the anomalous dimension matrix it follows that the coefficient γ_{55} is one of the eigenvalues, which governs the scale dependence of the Wilson coefficient D_5 in (6.42). This coefficient coincides with the well-known anomalous dimension of the current operators $J_M^{(0)}$ and $\mathcal{J}_M^{(0)}$ computed in Section 2.4.2. The corresponding “operator eigenvector” can be written as a linear combination (in the convolution sense)

$$\mathcal{O}_5^{(M)} = O_5^{(M)} + \sum_{k=1}^4 d_k^{(M)} \otimes O_k^{(M)}, \quad (6.44)$$

where the coefficients $d_k^{(M)}$ are independent of the high-energy matching scale μ_{hc} . The other four eigenvectors are linear combinations of the operators $O_k^{(M)}$ with $k \neq 5$. This observation has an important consequence: The decomposition of the form factors in terms of matrix elements of these eigenvectors implies that there exists a contribution from $\mathcal{O}_5^{(M)}$. The remaining contributions can be written as endpoint-finite convolution integrals that involve both two- and three-particle LCDAs of the initial and final mesons. Leaving such factorizable terms aside, it follows that the combination of operators contributing to the universal form factors must, up to an overall factor, coincide with the eigenvector $\mathcal{O}_5^{(M)}$, and hence

$$d_k^{(M)} = \frac{D_k^{(M)}}{D_5} \quad (6.45)$$

to all orders in perturbation theory. With a slight abuse of notation, let us now denote by ζ_M the $B \rightarrow M$ hadronic matrix element of the eigenvector $\mathcal{O}_5^{(M)}$ in SCET_{II}. Combining (6.10) and (6.42), we then find that the spin-symmetric universal form-factor term can be rewritten as

$$C_i(E, \mu_I) \zeta_M(\mu_I, E) \Big|_{\text{SCET}_I} = C_i(E, \mu) \zeta_M(\mu, E) \Big|_{\text{SCET}_{II}}. \quad (6.46)$$

This relation is not as dull as it seems; rather, it contains the remarkable message that for the soft overlap contribution to heavy-to-light form factors the intermediate hard-collinear scale is without *any* physical significance. Switching from SCET_I to SCET_{II} we merely describe the same physics using a different set of degrees of freedom. In other words, there is no use of going through an intermediate effective theory. The RG evolution of the soft functions ζ_M remains the same all the way from the high-energy scale $E \sim M_B$ down to hadronic scales $\mu \sim \Lambda_{\text{QCD}}$. The physics of the soft overlap term is thus rather different from the physics of the spin-symmetry breaking corrections in the factorization formula (6.10), for which

the hard-collinear scale is of physical significance. Any spin-symmetry breaking contribution involves at least one hard-collinear gluon exchange, and the amplitude factorizes below the scale μ_{hc} .

The result (6.46) allows us to systematically resum the short-distance logarithms arising in the evolution from high energies down to hadronic scales. The RG equation obeyed by the Wilson coefficient functions is [9, 16]

$$\frac{d}{d \ln \mu} C_i(E, \mu) = \left(\Gamma_{\text{cusp}}[\alpha_s(\mu)] \ln \frac{2E}{\mu} + \gamma[\alpha_s(\mu)] \right) C_i(E, \mu), \quad (6.47)$$

where the coefficient of the logarithmic term is determined by the cusp anomalous dimension [25]. Its solution is

$$C_i(E, \mu) = C_i(E, \mu_h) \exp U(\mu_h, \mu, E), \quad (6.48)$$

where $\mu_h \sim 2E$ is the high-energy matching scale for the transition from QCD to SCET, at which the values of the Wilson coefficients can be reliably computed using fixed-order perturbation theory. The RG evolution function can be written as

$$U(\mu_h, \mu, E) = \int_{\alpha_s(\mu_h)}^{\alpha_s(\mu)} d\alpha \frac{\Gamma_{\text{cusp}}(\alpha)}{\beta(\alpha)} \left[\ln \frac{2E\gamma}{\mu_h} - \int_{\alpha_s(\mu_h)}^{\alpha} \frac{d\alpha'}{\beta(\alpha')} \right] + \int_{\alpha_s(\mu_h)}^{\alpha_s(\mu)} d\alpha \frac{\gamma(\alpha)}{\beta(\alpha)}, \quad (6.49)$$

where $\beta(\alpha_s) = d\alpha_s/d \ln \mu$. The dependence on the high-energy matching scale μ_h cancels against that of the Wilson coefficients $C_i(E, \mu_h)$ in (6.48). Note that after exponentiation the evolution function contains an energy and scale-dependent factor $\exp U(\mu_h, \mu, E) \propto E^{a(\mu)}$, where

$$a(\mu) = \int^{\alpha_s(\mu)} d\alpha \frac{\Gamma_{\text{cusp}}(\alpha)}{\beta(\alpha)}. \quad (6.50)$$

In order for this scale dependence to be canceled, the low-energy hadronic matrix element must carry an energy dependence of the form $(\Lambda_{\text{QCD}}/E)^{a(\mu)}$.

Evaluating the hadronic matrix elements at a low scale means that all *short-distance* dependence on the large energy E is extracted and resummed in the coefficient functions. However, in the present case the matrix elements still contain a long-distance dependence on the large scale E , which cannot be factorized [16]. The reason is that the large energy enters the effective theory as an external variable imprinted by the particular kinematics of soft-to-collinear transitions. Because of the large Lorentz boost $\gamma = E/m_M$ connecting the rest frames of the B meson and the light meson M , the low-energy effective theory knows about the large scale E even though hard quantum fluctuations have been integrated out. This is similar to applications of heavy-quark effective theory to $b \rightarrow c$ transitions, where the fields depend on the external velocities of the hadrons containing the heavy quarks, and $\gamma = v_b \cdot v_c$ is an external parameter that appears in the matrix elements of velocity-changing current operators [26, 2]. In the present case, it is perhaps reasonable to assume that the primordial energy dependence of the hadronic matrix elements at some low hadronic scale might be moderate, so that the dominant E dependence is of short-distance nature and can be extracted into the Wilson coefficient functions. However, there will always be some energy dependence left in the matrix elements; even if we assume that it is absent for some value of μ , it will unavoidably be reintroduced when we change the scale. As a result, it is impossible to determine the asymptotic behavior of the QCD form factors $f_i^{B \rightarrow M}(q^2)$ using short-distance methods.²

Let us now proceed to study the numerical importance of short-distance Sudakov logarithms. Given the exact results in (6.48) and (6.49), it is straightforward

²The same phenomenon is known to occur in the case of the Sudakov form factor, for which the coefficient of the double logarithm is sensitive to infra-red physics [31, 100].

to derive approximate expressions for the resummed Wilson coefficients at a given order in RG-improved perturbation theory by using perturbative expansions of the anomalous dimensions and β -function. Unfortunately, controlling terms of $O(\alpha_s)$ in the evolution function U would require knowledge of the cusp anomalous dimension to three-loop order (and knowledge of γ to two-loop order), which at present is lacking. We can, however, control the dependence on the recoil energy E to $O(\alpha_s)$. Following [24], we define the ratio $r = \alpha_s(\mu)/\alpha_s(\mu_h)$ and obtain

$$e^{U(\mu_h, \mu, E)} = e^{U_0(\mu_h, \mu)} \left(\frac{2E}{\mu_h} \right)^{-\frac{\Gamma_0}{2\beta_0} \ln r} \left[1 - \frac{\alpha_s(\mu_h)}{4\pi} \frac{\Gamma_0}{2\beta_0} \left(\frac{\Gamma_1}{\Gamma_0} - \frac{\beta_1}{\beta_0} \right) (r-1) \ln \frac{2E}{\mu_h} \right], \quad (6.51)$$

where

$$U_0(\mu_h, \mu) = \frac{\Gamma_0}{4\beta_0^2} \left[\frac{4\pi}{\alpha_s(\mu_h)} \left(1 - \frac{1}{r} - \ln r \right) + \frac{\beta_1}{2\beta_0} \ln^2 r - \left(\frac{\Gamma_1}{\Gamma_0} - \frac{\beta_1}{\beta_0} \right) (r-1 - \ln r) \right] - \frac{\gamma_0}{2\beta_0} \ln r + O(\alpha_s). \quad (6.52)$$

The only piece missing for a complete resummation at next-to-next-to-leading order is the $O(\alpha_s)$ contribution to U_0 , which is independent of E . The relevant expansion coefficients are $\Gamma_0 = \frac{16}{3}$, $\Gamma_1 = \frac{1072}{9} - \frac{16}{3}\pi^2 - \frac{160}{27}n_f$, $\gamma_0 = -\frac{20}{3}$, and $\beta_0 = 11 - \frac{2}{3}n_f$, $\beta_1 = 102 - \frac{38}{3}n_f$. We set $n_f = 4$ in our numerical work.

In Fig. 6.6 we show the dependence of the Wilson coefficients $C_i(E, \mu)$ on the large energy E . We choose $\mu_h = 2E$ for the high-energy matching scale and use the tree-level initial conditions $C_i(E, \mu_h) = 1$, which is consistent at next-to-leading order. We fix μ at a low hadronic scale in order to maximize the effect of Sudakov logarithms. The maximum recoil energy in $B \rightarrow \pi$ transitions is such that $2E_{\max} \simeq 5.3 \text{ GeV}$. Obviously, for such values the perturbative resummation effects are very moderate. In the energy range $1 \text{ GeV} < 2E < M_B$ the Wilson coefficients differ from unity by no more than about 20%. The extrapolation to

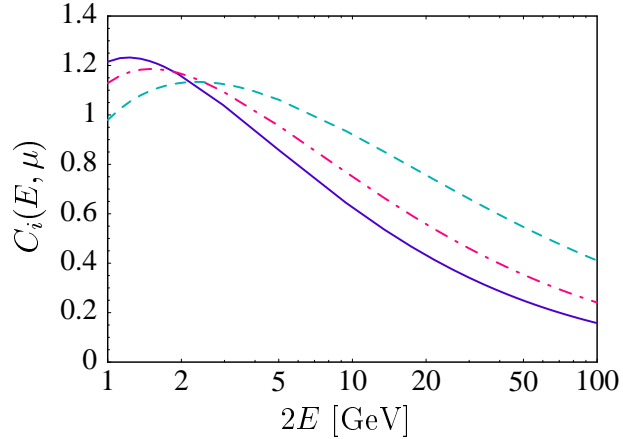


Figure 6.6: Energy dependence of the Wilson coefficients $C_i(E, \mu)$ at next-to-leading order in RG-improved perturbation theory. The three curves correspond to $\alpha_s(\mu) = 1$ (solid), $\alpha_s(\mu) = 0.75$ (dashed-dotted), and $\alpha_s(\mu) = 0.5$ (dashed), which are representative of typical hadronic scales.

larger energy values shows that Sudakov suppression remains a moderate effect even for very large recoil energy.

6.7 Factorization of spin-symmetry breaking effects

Using the close connection between messenger exchange and endpoint singularities discussed in Section 6.4, the formalism of soft-collinear fields can be used to demonstrate the convergence of convolution integrals in QCD factorization theorems. If messenger exchange is unsuppressed, the convolution integrals diverge at the endpoints, spoiling factorization. By the same reasoning, convolution integrals are finite if soft-collinear messenger contributions are absent at leading power.

Let us apply this method to show, to all orders in perturbation theory, that the convolution integrals entering the spin-symmetry breaking term in the factorization formula (6.10) are free of endpoint singularities. As mentioned in the Introduction,

this is an essential ingredient still missing from the proof of this formula. With our technology the proof is rather simple and consists of only the following two steps:

1. Soft-collinear messenger fields can be decoupled from the four-quark operators mediating spin-symmetry breaking effects, which are of the type shown in (6.27). The reason is that in the color singlet-singlet case the operators are invariant under the field redefinition (2.60) [16]. It follows that their matrix elements factorize into separate matrix elements of soft and collinear currents, which can be written in terms of the leading-order LCDAs of the external mesons. If the messengers did not decouple, they would introduce unsuppressed interactions between the soft and collinear parts of the four-quark operators, thereby spoiling factorization.

2. Time-ordered products containing interactions of soft-collinear messengers with soft or collinear fields do not contribute to the spin-symmetry violating term in (6.10). This follows from SCET power counting. The insertions of the Lagrangians $\mathcal{L}_{\bar{q}\theta}$ and $\mathcal{L}_{\bar{\theta}\xi}$ in (6.40) cost a factor $\lambda^{3/2}$, meaning that they can only come together with a leading-order current operator of the type $\bar{\mathcal{X}} \dots \mathcal{H} \sim \lambda^{5/2}$. (Note that there are no $O(\lambda^{1/2})$ corrections to the current that could make the vacuum correlator (6.41) involving $\mathcal{L}_{\bar{q}\theta}^{(1/2)}$ and $\mathcal{L}_{\bar{\theta}\xi}^{(1/2)}$ non-zero [16].) However, such a current will always be of the form (6.39) because of the projection properties of the heavy-quark and collinear-quark spinors. It thus respects the spin-symmetry relations.

These two observations imply that at leading order in Λ_{QCD}/E soft-collinear exchanges do not contribute to the spin-symmetry breaking term in the factorization formula, and hence the corresponding convolution integrals are convergent.

CHAPTER 7

CONCLUSION

QCD-Factorization theorems are statements about leading power properties of amplitudes *to all orders in the strong coupling constant*. The use of effective field theories enables one to prove such theorems rigorously, and thus take a significant step further from past fixed-order proofs. In this thesis we demonstrated this technique on some decay modes that are particularly clean in the sense of simplicity of QCD-factorization formulae. The first part of this work was devoted to a detailed introduction to Soft-Collinear Effective Theory (SCET), which describes the infra-red physics of strong interactions between light, but highly energetic partons with soft heavy or light degrees of freedom. The crucial advantage of this theory is that it allows for a systematic expansion in inverse powers of the heavy-quark mass already at the Lagrangian level, therefore allowing for all-order proofs. Furthermore, SCET enables us to perform perturbative calculations for systems in which local operator expansions break down due to long-distance effects. This is a significant improvement of our ability to compute the strong-interaction effects of weak decays of heavy mesons. Furthermore we investigated two non-perturbative structure functions: the B -meson light-cone distribution function, which enters the calculation of exclusive decay amplitudes in the high-recoil region, and the shape function, which encodes the Fermi-motion of the heavy quark inside the B -meson for the calculation of inclusive decay modes. In particular, we have derived important relations that link the (finite-interval) moments of the shape function to the values of local HQET operators.

To gain full control over the separation of physics of different energy scales, it is necessary to perform a resummation of large logarithms. We have demon-

strated this technique for inclusive $B \rightarrow X_u l^- \bar{\nu}$ and exclusive $B^- \rightarrow \gamma l^- \bar{\nu}$ and $\bar{B} \rightarrow M l^- \bar{\nu}$ (where M is a light pseudoscalar or vector meson), using a sophisticated multi-step matching procedure and solving renormalization-group equations (RGEs). In the inclusive decay mode we matched $\text{QCD} \rightarrow \text{SCET}_I \rightarrow \text{HQET}$. The intermediate theory SCET_I contains soft and hard-collinear degrees of freedom, the latter being momentum modes with large energy E and moderate invariant momentum square of order $E\Lambda_{\text{QCD}}$. In a second step, these modes are removed, resulting in a description within heavy-quark effective theory (HQET). The triple differential decay rate was then expressed at leading power in Λ_{QCD}/E and at next-to-leading order in renormalization-group improved perturbation theory in terms of Wilson coefficient functions H and J , convoluted with the matrix element of a single HQET operator, the shape function S . This formulation is valid in the shape-function region of phase space, where the X_u system is energetic and light, as anticipated. Model-independent results have been derived for various event fractions and spectra, including a cut on the charged-lepton energy, the hadronic variable $P_+ = E_H - |\vec{P}_H|$, and the hadronic invariant mass. Finally we have computed numerical predictions using models for the shape function that are consistent with all known constraints. As a result, event fractions needed for the extraction of the CKM matrix element $|V_{ub}|$ are found to be much larger than previously anticipated. This in turn implies that the numerical value of $|V_{ub}|$ determinations from inclusive B decays might become smaller. To make a conclusive statement it will be necessary to include subleading power corrections (and possibly higher-order corrections) to the predictions derived here. For future determinations we proposed to use the P_+ variable to discriminate against the charm background. A detailed study of the current theoretical uncertainties and the nature of the charm

background was also performed.

QCD-Factorization was proved to all orders in the coupling constant and to leading power for the exclusive $B^- \rightarrow \gamma l^- \bar{\nu}$ decay amplitude. This mode provides a clean and realistic environment in which to study the aforementioned methodology. We performed a detailed matching calculation $\text{QCD} \rightarrow \text{SCET}_{II}$. Large logarithms were resummed by first factorizing the hard-scattering kernel into a hard and a jet function. This is accomplished by matching in two steps $\text{QCD} \rightarrow \text{SCET}_I \rightarrow \text{SCET}_{II}$. While the first matching step gives rise to the hard function, the jet function arises in the second step. Sudakov resummation was then achieved by solving the RGEs of the hard function and the combined hard-scattering kernel. We found that the resummation effects enhance the amplitude (as opposed to a “Sudakov suppression”).

Finally we turned our attention to amplitudes that do not factorize. Form factors encode the exclusive decay amplitudes for $B \rightarrow P l^- \bar{\nu}$ and $B \rightarrow V l^- \bar{\nu}$ (P = light pseudoscalar meson, V = light vector meson). There are three different form factors for $B \rightarrow \pi$ and seven for $B \rightarrow \rho$ transitions. In the large recoil limit they obey approximate spin-symmetry relations (corrections of which factorize), leaving only three independent universal form factors. In our formalism, the proof of this statement was rather simple; however, our analysis revealed also that there exists a soft contribution to the form factors which cannot be factorized. In SCET_{II} this can be understood as the soft-collinear sector does not decouple. As a result, there exists a long-distance operator O_5 , which mixes into the short-distance operators under renormalization. Since the short-distance operators do not mix back into O_5 , the anomalous dimension of O_5 , which is identical to the one of heavy-to-collinear current operators, is also an Eigenvalue of the entire anoma-

lous dimension matrix. The matrix element of the corresponding “Eigenvector”, a linear combination of all operators, is endpoint-finite and contributes to the form factor without any suppression. In fact, the knowledge of the anomalous dimension Eigenvalue allows to control the short-distance dependence on the large recoil energy. We found that there is no sizable Sudakov suppression to the universal form factors. In summary, the spin-symmetric soft overlap exists, and dominates over the factorizable hard-scattering contributions that break spin-symmetry.

In light of these few examples of B decay processes, the power of the QCD-Factorization approach to strong-interaction effects with more than one relevant physical energy scale is apparent. While we are unable to solve QCD analytically, an approximation to leading power in the expansion parameter Λ_{QCD}/m_b can be of great help in our ability to predict Standard-Model processes. In some cases (e.g. inclusive decays) we are even provided with a framework in which corrections to the leading-power factorization formulae can be calculated systematically. In the future, we will be able to use such frameworks to improve the precision of theoretical input quantities necessary for the extraction of Standard Model parameters and for searches of New Physics effects. We shall mention here the important examples of flavor-changing neutral decay modes such as $B \rightarrow X_s \gamma$ and $B \rightarrow X_s l^+ l^-$, which are particularly sensitive to possible New Physics, but suffer from sizable QCD-uncertainties which can spoil valuable information. It will certainly be worthwhile to apply the general methodology presented in this Thesis and in the corresponding references to these processes, as well as to improve the accuracy of our results in both the power expansion and the coupling expansion to higher orders. On the exclusive side we have dealt with a few exemplary decay channels. It will be exciting to study how the lessons we learned are applicable to decay modes of bigger

phenomenological interest, such as the radiative $B \rightarrow K^*\gamma$, or the non-leptonic $B \rightarrow \pi\pi$ and $B \rightarrow K\pi$. As far as searches for New Physics effects are concerned, precision in Flavor Physics can provide us with valuable information. In both the experimental and theoretical community this fact is reflected in the ongoing discussion on the potential of a “Super B -factory”, that might complement the direct searches of New Physics at next-generation particle colliders.

APPENDIX A

LIST OF ABBREVIATIONS AND ACRONYMS

| | |
|------|-----------------------------------|
| c | - collinear |
| CKM | - Cabibbo, Kobayashi, Maskawa |
| CLCG | - Collinear Light-Cone Gauge |
| h | - hard |
| hc | - hard-collinear |
| HQET | - Heavy-Quark Effective Theory |
| NLO | - Next-to-Leading Order |
| NNLO | - Next-to-Next-to-Leading Order |
| pQCD | - perturbative QCD |
| QCD | - Quantum Chromo Dynamics |
| RG | - Renormalization Group |
| RGE | - Renormalization-Group Equation |
| s | - soft |
| sc | - soft-collinear |
| SCET | - Soft-Collinear Effective Theory |
| SLCG | - Soft Light-Cone Gauge |
| us | - ultrasoft |

BIBLIOGRAPHY

- [1] Courses include the Cornell quantum-field theory classes in 1998/99 by Philip Argyres and Henry Tye, the summer school “TASI 2002” at Boulder, Colorado, as well as the advanced courses by Csaba Csaki, Matthias Neubert, and Konstantin Matchev in the years 2002 through 2004 at Cornell.
- [2] For a review, see M. Neubert, “Heavy quark symmetry,” Phys. Rept. **245**, 259 (1994) [arXiv:hep-ph/9306320].
- [3] M. Beneke, G. Buchalla, M. Neubert and C. T. Sachrajda, “QCD factorization for $B \rightarrow \pi \pi$ decays: Strong phases and CP violation in the heavy quark limit,” Phys. Rev. Lett. **83**, 1914 (1999) [arXiv:hep-ph/9905312].
- [4] M. Beneke, G. Buchalla, M. Neubert and C. T. Sachrajda, “QCD factorization for exclusive, non-leptonic B meson decays: General arguments and the case of heavy-light final states,” Nucl. Phys. B **591**, 313 (2000) [arXiv:hep-ph/0006124].
- [5] M. Beneke, G. Buchalla, M. Neubert and C. T. Sachrajda, “QCD factorization for $B \rightarrow \pi K$ decays,” arXiv:hep-ph/0007256.
- [6] M. Beneke, G. Buchalla, M. Neubert and C. T. Sachrajda, “QCD factorization in $B \rightarrow \pi K$, $\pi \pi$ decays and extraction of Wolfenstein parameters,” Nucl. Phys. B **606**, 245 (2001) [arXiv:hep-ph/0104110].
- [7] C. W. Bauer, D. Pirjol and I. W. Stewart, “A proof of factorization for $B \rightarrow D \pi$,” Phys. Rev. Lett. **87**, 201806 (2001) [arXiv:hep-ph/0107002].
- [8] C. W. Bauer, S. Fleming and M. E. Luke, “Summing Sudakov logarithms in $B \rightarrow X/s \gamma$ in effective field theory,” Phys. Rev. D **63**, 014006 (2001) [hep-ph/0005275].
- [9] C. W. Bauer, S. Fleming, D. Pirjol and I. W. Stewart, “An effective field theory for collinear and soft gluons: Heavy to light decays,” Phys. Rev. D **63**, 114020 (2001) [hep-ph/0011336].
- [10] C. W. Bauer and I. W. Stewart, “Invariant operators in collinear effective theory,” Phys. Lett. B **516**, 134 (2001) [arXiv:hep-ph/0107001].
- [11] C. W. Bauer, D. Pirjol and I. W. Stewart, “Soft-collinear factorization in effective field theory,” Phys. Rev. D **65**, 054022 (2002) [hep-ph/0109045].
- [12] M. Beneke, A. P. Chapovsky, M. Diehl and T. Feldmann, “Soft-collinear effective theory and heavy-to-light currents beyond leading power,” Nucl. Phys. B **643**, 431 (2002) [arXiv:hep-ph/0206152].

- [13] M. Beneke and T. Feldmann, “Multipole-expanded soft-collinear effective theory with non-abelian gauge symmetry,” *Phys. Lett. B* **553**, 267 (2003) [arXiv:hep-ph/0211358].
- [14] R. J. Hill and M. Neubert, “Spectator interactions in soft-collinear effective theory,” *Nucl. Phys. B* **657**, 229 (2003) [hep-ph/0211018].
- [15] T. Becher, R. J. Hill and M. Neubert, “Soft-collinear messengers: A new mode in soft-collinear effective theory,” *Phys. Rev. D* **69**, 054017 (2004) [arXiv:hep-ph/0308122].
- [16] T. Becher, R. J. Hill, B. O. Lange and M. Neubert, “External operators and anomalous dimensions in soft-collinear effective theory,” *Phys. Rev. D* **69**, 034013 (2004) [arXiv:hep-ph/0309227].
- [17] M. Beneke and V. A. Smirnov, “Asymptotic expansion of Feynman integrals near threshold,” *Nucl. Phys. B* **522**, 321 (1998) [arXiv:hep-ph/9711391].
For a review, see V. A. Smirnov, “Applied Asymptotic Expansions In Momenta And Masses,” Springer tracts in modern physics. 177 (2002).
- [18] J. Charles, A. Le Yaouanc, L. Oliver, O. Pene and J. C. Raynal, “Heavy-to-light form factors in the heavy mass to large energy limit of QCD,” *Phys. Rev. D* **60**, 014001 (1999) [hep-ph/9812358].
- [19] G. 't Hooft and M. J. G. Veltman, “Regularization And Renormalization Of Gauge Fields,” *Nucl. Phys. B* **44**, 189 (1972).
- [20] M. Neubert, lectures on effective field theories, fall 2003, Cornell University.
See also D. J. Gross, “Applications Of The Renormalization Group To High-Energy Physics,” In *Les Houches 1975, Proceedings, Methods In Field Theory*, Amsterdam 1976, 141-250.
- [21] K. Hagiwara *et al.* [Particle Data Group Collaboration], “Review of particle physics,” *Phys. Rev. D* **66**, 010001 (2002).
- [22] J. Chay and C. Kim, “Collinear effective theory at subleading order and its application to heavy-light currents,” *Phys. Rev. D* **65**, 114016 (2002) [hep-ph/0201197].
- [23] R. J. Hill, T. Becher, S. J. Lee and M. Neubert, “Sudakov resummation for subleading SCET currents and heavy-to-light form factors,” arXiv:hep-ph/0404217.
- [24] S. W. Bosch, R. J. Hill, B. O. Lange and M. Neubert, “Factorization and Sudakov resummation in leptonic radiative B decay,” *Phys. Rev. D* **67**, 094014 (2003) [hep-ph/0301123].

- [25] G. P. Korchemsky and A. V. Radyushkin, “Renormalization Of The Wilson Loops Beyond The Leading Order,” Nucl. Phys. B **283**, 342 (1987).
- [26] A. F. Falk, H. Georgi, B. Grinstein and M. B. Wise, “Heavy Meson Form-Factors From QCD,” Nucl. Phys. B **343**, 1 (1990).
- [27] M. Beneke and T. Feldmann, “Factorization of heavy-to-light form factors in soft-collinear effective theory,” Nucl. Phys. B **685**, 249 (2004) [arXiv:hep-ph/0311335].
- [28] C. W. Bauer, M. P. Dorsten and M. P. Salem, “Infrared regulators and SCET_{II},” Phys. Rev. D **69**, 114011 (2004) [arXiv:hep-ph/0312302].
- [29] G. P. Lepage and S. J. Brodsky, “Exclusive Processes In Perturbative Quantum Chromodynamics,” Phys. Rev. D **22**, 2157 (1980).
- [30] B. O. Lange and M. Neubert, “Renormalization-group evolution of the B-meson light-cone distribution amplitude,” Phys. Rev. Lett. **91**, 102001 (2003) [hep-ph/0303082].
- [31] G. P. Korchemsky, “Sudakov Form-Factor In QCD,” Phys. Lett. B **220**, 629 (1989).
- [32] A. V. Manohar, T. Mehen, D. Pirjol and I. W. Stewart, “Reparameterization invariance for collinear operators,” Phys. Lett. B **539**, 59 (2002) [hep-ph/0204229].
- [33] A. G. Grozin and M. Neubert, “Asymptotics of heavy-meson form factors,” Phys. Rev. D **55**, 272 (1997) [hep-ph/9607366].
- [34] B. O. Lange and M. Neubert, in preparation.
- [35] M. Neubert, “QCD based interpretation of the lepton spectrum in inclusive anti-B \rightarrow X(u) lepton anti-neutrino decays,” Phys. Rev. D **49**, 3392 (1994) [hep-ph/9311325]; “Analysis of the photon spectrum in inclusive B \rightarrow X(s) gamma decays,” Phys. Rev. D **49**, 4623 (1994) [hep-ph/9312311].
- [36] S. W. Bosch, B. O. Lange, M. Neubert and G. Paz, “Factorization and shape-function effects in inclusive B-meson decays,” arXiv:hep-ph/0402094.
- [37] F. De Fazio and M. Neubert, “B \rightarrow X/u l anti-nu/l decay distributions to order $\alpha(s)$,” JHEP **9906**, 017 (1999) [hep-ph/9905351].
- [38] C. Balzereit, T. Mannel and W. Kilian, “Evolution of the light-cone distribution function for a heavy quark,” Phys. Rev. D **58**, 114029 (1998) [hep-ph/9805297].

- [39] A. G. Grozin and G. P. Korchemsky, “Renormalized sum rules for structure functions of heavy mesons decays,” *Phys. Rev. D* **53**, 1378 (1996) [hep-ph/9411323].
- [40] T. Mannel and M. Neubert, “Resummation of nonperturbative corrections to the lepton spectrum in inclusive $B \rightarrow X$ lepton anti-neutrino decays,” *Phys. Rev. D* **50**, 2037 (1994) [hep-ph/9402288].
- [41] A. L. Kagan and M. Neubert, “QCD anatomy of $B \rightarrow X/s$ gamma decays,” *Eur. Phys. J. C* **7**, 5 (1999) [hep-ph/9805303].
- [42] I. Bigi and N. Uraltsev, “On the expected photon spectrum in $B \rightarrow X + \text{gamma}$ and its uses,” *Int. J. Mod. Phys. A* **17**, 4709 (2002) [hep-ph/0202175].
- [43] A. F. Falk, M. Neubert and M. E. Luke, “The Residual mass term in the heavy quark effective theory,” *Nucl. Phys. B* **388**, 363 (1992) [hep-ph/9204229].
- [44] I. I. Y. Bigi, M. A. Shifman, N. G. Uraltsev and A. I. Vainshtein, “The Pole mass of the heavy quark. Perturbation theory and beyond,” *Phys. Rev. D* **50**, 2234 (1994) [hep-ph/9402360].
- [45] M. Beneke and V. M. Braun, “Heavy quark effective theory beyond perturbation theory: Renormalons, the pole mass and the residual mass term,” *Nucl. Phys. B* **426**, 301 (1994) [hep-ph/9402364].
- [46] I. I. Y. Bigi, M. A. Shifman, N. Uraltsev and A. I. Vainshtein, “High power n of $m(b)$ in beauty widths and $n = 5 \rightarrow \text{infinity}$ limit,” *Phys. Rev. D* **56**, 4017 (1997) [hep-ph/9704245].
- [47] M. Beneke, “A quark mass definition adequate for threshold problems,” *Phys. Lett. B* **434**, 115 (1998) [hep-ph/9804241].
- [48] I. I. Y. Bigi, M. A. Shifman and N. Uraltsev, “Aspects of heavy quark theory,” *Ann. Rev. Nucl. Part. Sci.* **47**, 591 (1997) [hep-ph/9703290].
- [49] D. Benson, I. I. Bigi, T. Mannel and N. Uraltsev, “Imprecated, yet impeccable: On the theoretical evaluation of $\Gamma(B \rightarrow X/c \ell \nu)$,” *Nucl. Phys. B* **665**, 367 (2003) [hep-ph/0302262].
- [50] G. Martinelli, M. Neubert and C. T. Sachrajda, “The Invisible renormalon,” *Nucl. Phys. B* **461**, 238 (1996) [hep-ph/9504217]; M. Neubert, “Exploring the invisible renormalon: Renormalization of the heavy-quark kinetic energy,” *Phys. Lett. B* **393**, 110 (1997) [hep-ph/9610471].
- [51] G. P. Korchemsky and G. Sterman, “Infrared factorization in inclusive B meson decays,” *Phys. Lett. B* **340**, 96 (1994) [hep-ph/9407344].

- [52] I. I. Y. Bigi, M. A. Shifman, N. G. Uraltsev and A. I. Vainshtein, “On the motion of heavy quarks inside hadrons: Universal distributions and inclusive decays,” *Int. J. Mod. Phys. A* **9**, 2467 (1994) [hep-ph/9312359].
- [53] J. Chay, H. Georgi and B. Grinstein, “Lepton Energy Distributions In Heavy Meson Decays From QCD,” *Phys. Lett. B* **247**, 399 (1990).
- [54] I. I. Y. Bigi, N. G. Uraltsev and A. I. Vainshtein, “Nonperturbative corrections to inclusive beauty and charm decays: QCD versus phenomenological models,” *Phys. Lett. B* **293**, 430 (1992) [Erratum-ibid. *B* **297**, 477 (1993)] [hep-ph/9207214];
 I. I. Y. Bigi, M. A. Shifman, N. G. Uraltsev and A. I. Vainshtein, “QCD predictions for lepton spectra in inclusive heavy flavor decays,” *Phys. Rev. Lett.* **71**, 496 (1993) [hep-ph/9304225];
 B. Blok, L. Koyrakh, M. A. Shifman and A. I. Vainshtein, “Differential distributions in semileptonic decays of the heavy flavors in QCD,” *Phys. Rev. D* **49**, 3356 (1994) [Erratum-ibid. *D* **50**, 3572 (1994)] [hep-ph/9307247].
- [55] A. V. Manohar and M. B. Wise, “Inclusive semileptonic B and polarized Lambda(b) decays from QCD,” *Phys. Rev. D* **49**, 1310 (1994) [hep-ph/9308246].
- [56] U. Aglietti, M. Ciuchini and P. Gambino, “A new model-independent way of extracting $|V(ub)/V(cb)|$,” *Nucl. Phys. B* **637**, 427 (2002) [hep-ph/0204140].
- [57] S. Moch, J. A. M. Vermaseren and A. Vogt, “The three-loop splitting functions in QCD: The non-singlet case,” *Nucl. Phys. B* **688**, 101 (2004) [arXiv:hep-ph/0403192].
- [58] For a recent discussion, see: I. I. Y. Bigi and N. Uraltsev, “A vademecum on quark hadron duality,” *Int. J. Mod. Phys. A* **16**, 5201 (2001) [hep-ph/0106346].
- [59] C. W. Bauer, M. Luke and T. Mannel, “Subleading shape functions in $B \rightarrow X/u \ell$ anti- ν and the determination of $|V(ub)|$,” *Phys. Lett. B* **543**, 261 (2002) [hep-ph/0205150].
- [60] M. Neubert, “Subleading shape functions and the determination of $|V(ub)|$,” *Phys. Lett. B* **543**, 269 (2002) [hep-ph/0207002].
- [61] C. W. Bauer, Z. Ligeti and M. E. Luke, “Precision determination of $|V(ub)|$ from inclusive decays,” *Phys. Rev. D* **64**, 113004 (2001) [hep-ph/0107074].
- [62] A. K. Leibovich, I. Low and I. Z. Rothstein, “Extracting $V(ub)$ without recourse to structure functions,” *Phys. Rev. D* **61**, 053006 (2000) [hep-ph/9909404].
- [63] M. Neubert, “Note on the extraction of $|V(ub)|$ using radiative B decays,” *Phys. Lett. B* **513**, 88 (2001) [hep-ph/0104280].

- [64] A. K. Leibovich, I. Low and I. Z. Rothstein, “A comment on the extractions of $V(ub)$ from radiative decays,” *Phys. Lett. B* **513**, 83 (2001) [hep-ph/0105066].
- [65] T. Mannel and S. Recksiegel, “Comparing $B \rightarrow X/u \ell \nu/\ell$ to $B \rightarrow X/s \gamma$ and the determination of $|V(ub)|/|V(ts)|$,” *Phys. Rev. D* **60**, 114040 (1999) [hep-ph/9904475].
- [66] M. Beneke and A. Signer, “The bottom \overline{MS} -bar quark mass from sum rules at next-to-next-to-leading order,” *Phys. Lett. B* **471**, 233 (1999) [hep-ph/9906475].
- [67] S. Chen *et al.* [CLEO Collaboration], “Branching fraction and photon energy spectrum for $b \rightarrow s \gamma$,” *Phys. Rev. Lett.* **87**, 251807 (2001) [hep-ex/0108032].
- [68] D. Cronin-Hennessy *et al.* [CLEO Collaboration], “Hadronic mass moments in inclusive semileptonic B meson decays,” *Phys. Rev. Lett.* **87**, 251808 (2001) [hep-ex/0108033].
- [69] A. H. Mahmood *et al.* [CLEO Collaboration], “Measurement of lepton momentum moments in the decay $\text{anti-B} \rightarrow X \ell \text{ anti-}\nu$ and determination of heavy quark expansion parameters and $|V(cb)|$. ((B)),” *Phys. Rev. D* **67**, 072001 (2003) [hep-ex/0212051].
- [70] B. Aubert *et al.* [BaBar Collaboration], “Measurement of the first and second moments of the hadronic mass distribution in semileptonic B decays,” hep-ex/0307046.
- [71] I. I. Y. Bigi, R. D. Dikeman and N. Uraltsev, “The hadronic recoil mass spectrum in semileptonic B decays and extracting $|V(ub)|$ in a model-insensitive way,” *Eur. Phys. J. C* **4**, 453 (1998) [hep-ph/9706520].
- [72] A. F. Falk, Z. Ligeti and M. B. Wise, “ $V(ub)$ from the hadronic invariant mass spectrum in semileptonic B decay,” *Phys. Lett. B* **406**, 225 (1997) [hep-ph/9705235].
- [73] M. Jezabek, T. Mannel, B. Postler and P. Urban, “Determination of $V(ub)$ from inclusive semileptonic B decays,” *Phys. Lett. B* **512**, 65 (2001) [hep-ph/0101330].
- [74] R. D. Dikeman and N. G. Uraltsev, “Key distributions for charmless semileptonic B decay,” *Nucl. Phys. B* **509**, 378 (1998) [hep-ph/9703437].
- [75] M. B. Voloshin, “Nonfactorization effects in heavy mesons and determination of $|V(ub)|$ from inclusive semileptonic B decays,” *Phys. Lett. B* **515**, 74 (2001) [hep-ph/0106040].

- [76] H. Kakuno *et al.* [Belle Collaboration], “Measurement of $|V(ub)|$ using inclusive $B \rightarrow X/u \ell \nu$ decays with a novel X/u reconstruction method,” hep-ex/0311048.
- [77] S. W. Bosch, B. O. Lange, M. Neubert and G. Paz, “Proposal for a precision measurement of $|V(ub)|$,” arXiv:hep-ph/0403223.
- [78] C. N. Burrell, M. E. Luke and A. R. Williamson, “Subleading shape function contributions to the hadronic invariant mass spectrum in anti- $B \rightarrow X/u \ell \text{anti-}\nu/\ell$ decay,” hep-ph/0312366.
- [79] C. W. Bauer and A. V. Manohar, “Shape function effects in $B \rightarrow X/s \text{ gamma}$ and $B \rightarrow X/u \ell \nu$ decays,” hep-ph/0312109.
- [80] T. Becher and M. Neubert, “Improved determination of $|V(ub)|$ from inclusive semileptonic B-meson decays,” Phys. Lett. B **535**, 127 (2002) [hep-ph/0105217].
- [81] A. H. Hoang, Z. Ligeti and A. V. Manohar, “B decay and the Upsilon mass,” Phys. Rev. Lett. **82**, 277 (1999).
- [82] N. Uraltsev, “Theoretical uncertainties in $\text{Gamma}(\text{sl})(b \rightarrow u)$,” Int. J. Mod. Phys. A **14**, 4641 (1999).
- [83] G. P. Korchemsky, D. Pirjol and T. M. Yan, “Radiative leptonic decays of B mesons in QCD,” Phys. Rev. D **61**, 114510 (2000) [hep-ph/9911427].
- [84] S. Descotes-Genon and C. T. Sachrajda, “Factorization, the light-cone distribution amplitude of the B-meson and the radiative decay $B \rightarrow \text{gamma} \ell \nu/\ell$,” Nucl. Phys. B **650**, 356 (2003) [hep-ph/0209216].
- [85] E. Lunghi, D. Pirjol and D. Wyler, “Factorization in leptonic radiative $B \rightarrow \text{gamma} e \nu$ decays,” Nucl. Phys. B **649**, 349 (2003) [hep-ph/0210091].
- [86] C. W. Bauer, D. Pirjol and I. W. Stewart, “Factorization and endpoint singularities in heavy-to-light decays,” preprint hep-ph/0211069.
- [87] M. Neubert, “Heavy meson form-factors from QCD sum rules,” Phys. Rev. D **45**, 2451 (1992).
- [88] A. V. Efremov and A. V. Radyushkin, “Factorization And Asymptotical Behavior Of Pion Form-Factor In QCD,” Phys. Lett. B **94**, 245 (1980).
- [89] B. O. Lange and M. Neubert, “Factorization and the soft overlap contribution to heavy-to-light form factors,” Nucl. Phys. B **690**, 249 (2004) [arXiv:hep-ph/0311345].

- [90] M. Beneke and T. Feldmann, “Symmetry-breaking corrections to heavy-to-light B meson form factors at large recoil,” Nucl. Phys. B **592**, 3 (2001) [hep-ph/0008255].
- [91] M. Beneke and T. Feldmann, “Spectator interactions and factorization in $B \rightarrow \pi l \nu$ decay,” preprint hep-ph/0308303.
- [92] A. Szczepaniak, E. M. Henley and S. J. Brodsky, “Perturbative QCD Effects In Heavy Meson Decays,” Phys. Lett. B **243**, 287 (1990).
- [93] G. Burdman and J. F. Donoghue, “Reliable Predictions In Exclusive Rare B Decays,” Phys. Lett. B **270**, 55 (1991).
- [94] R. Akhouri, G. Sterman and Y. P. Yao, “Exclusive Semileptonic Decays Of B Mesons Into Light Mesons,” Phys. Rev. D **50**, 358 (1994).
- [95] M. Dahm, R. Jakob and P. Kroll, “A Perturbative approach to B decays into two pi mesons,” Z. Phys. C **68**, 595 (1995) [hep-ph/9503418].
- [96] T. Kurimoto, H. n. Li and A. I. Sanda, “Leading power contributions to $B \rightarrow \pi, \rho$ transition form factors,” Phys. Rev. D **65**, 014007 (2002) [hep-ph/0105003].
- [97] Y. Y. Keum, H. n. Li and A. I. Sanda, “Fat penguins and imaginary penguins in perturbative QCD,” Phys. Lett. B **504**, 6 (2001) [hep-ph/0004004];
“Penguin enhancement and $B \rightarrow K \pi$ decays in perturbative QCD,” Phys. Rev. D **63**, 054008 (2001) [hep-ph/0004173].
- [98] For a critical discussion, see: S. Descotes-Genon and C. T. Sachrajda, “Sudakov effects in $B \rightarrow \pi l \nu/l$ form factors,” Nucl. Phys. B **625**, 239 (2002) [hep-ph/0109260].
- [99] V. L. Chernyak and I. R. Zhitnitsky, “B Meson Exclusive Decays Into Baryons,” Nucl. Phys. B **345** (1990) 137.
- [100] J. H. Kühn, A. A. Penin and V. A. Smirnov, “Summing up subleading Sudakov logarithms,” Eur. Phys. J. C **17**, 97 (2000) [hep-ph/9912503].